

Sources of moisture for Central America and transport  
based on a Lagrangian approach: variability, contributions  
to precipitation and transport mechanisms



UNIVERSIDADE  
DE VIGO

Ana María Durán Quesada  
Applied Physics Department  
Universidade de Vigo

Submitido para la obtención del grado de  
*Doutora pola Universidade de Vigo con Mención Internacional.*

February 2012





To my parents



## Acknowledgements

The financial support through a PhD grant provided by the Fundación Carolina (Agencia Española de Cooperación Internacional) and the University of Costa Rica that made possible the work developed during the PhD Programme in Applied Physics at the University of Vigo and that allowed the preparation of the thesis herein presented is greatly acknowledged. Additional financial support from the European Science Foundation, The National Research Council (UK) and the University of Vigo for attending conferences and summer schools during the four years of my PhD Programme is also acknowledged. My gratitude to my advisors Dr. Luis Gimeno Presa (UVigo) and Dr. Jorge A. Amador (UCR) as they encouraged the development of this work. To the ATMOS group at the Norwegian Institute for Air Research, specially Dr. Andreas Stohl, Dr. Harald Sodemann and Dr. Sabine Eckhardt who guided me during a short term scientific mission in their group and provided me with a basis on Lagrangian analysis. To the Energy and Environmental Modeling unit of the Italian National Agency for New Technologies, Energy and Sustainable Economic Development (ENEA) where I did a long term internship during 2010, I would like to thank the work group there for their encouraging help and advise, in particular to my advisor there Dr. Paolo Ruti, as well as UTMEA group members Dr. Sandro Calmanti, Dr. Alessandro dell' Aquila, Dr. Vincenzo Artale, Dr. Salvatore Marullo, Dr. Emanuele Lombardi and Ms. Ivana Berdini. I would expect to return back to the work we started on climate modelling and SST sensibility soon. I would also like to thank the colleagues at the EPhysLab who have helped me a lot during the development of this work, the IT group for their help with the data retrieving and for making megatron work and Alex Ramos who has been an excellent colleague with whom I have been happy to work with. To the great people I met during these years thanks for making my time here easier. To my family and friends thanks for the great support you have given me, specially during these four years when I have been away from home.



## Preface

The present work presents a detailed analysis on the sources that provide moisture to Central America based on a backward Lagrangian trajectories approach. As it is known many other regions in tropical America have been extensively analysed (e.g Amazon), Central America has been left aside in terms of extensive studies on climate processes in regard to moisture transport. Central America is a region well known for the vulnerability to natural hazards from which extreme precipitation episodes and drought can be mentioned to affect severely both socio-economics and biodiversity. In order to improve the knowledge on the regional processes that control precipitation, the study of the sources that provide moisture for that precipitation is a necessary. Under this motivation, an exploratory analysis of the sources of moisture was performed and results obtained encouraged the proposal of a more detailed analysis on the issue.

The aim of this work is to provide a comprehensive study of the regional component of the hydrological cycle that may improve the present knowledge on the regional climate processes, to study how different structures merge together to build up regional climate and to which extent processes ongoing on this region of the world may exert an influence on remote locations. The problem proposed was the identification of the sources of moisture for continental Central America in a Lagrangian framework, the analysis of the mean state of the sources and its time and space variability. To understand how important sources of moisture are for precipitation, the quantitative estimation of the contributions from the sources of moisture needed to be considered. To finally obtain an integral picture of the relation between the sources of moisture and precipitation over Central America, the analysis of the moisture transport process completes the mainframe of the work with a focus on the mechanisms that relate the components of the regional hydrological cycle.

## Contents

The development of this work is divided in three main parts. A first introductory part in which the state of the art of the water vapour distribution and role in the climate system is presented. The structure of atmospheric water vapour and the generalities of the components of the hydrological cycle are introduced. The main concepts on global sources of moisture, which are those regions and how are they related to continental precipitation pretends to situate a global background to a regional problem. Since the problem proposed may be of interest for people from a wide diversity of research interests that may not be familiar with the climate features of the region of interested, a brief introduction to the main features of the climate is presented in chapter 2: Climate and Variability in the Intra Americas Seas. In that chapter, key information on the regional climate is included. This to provide material that may be useful for following most of the discussions along this work. The problem of moisture availability and transport in the IAS is presented in chapter 3 which also contains a brief discussion on previous studies. The generalities on the use of Lagrangian methodologies is presented before introducing the formal proposal on the work that has been carried out. This first part closes with the description of the work proposed to solve the problem described. The main motivation and objectives of this work are indicated there.

Chapter 4 presents the data and analysis methodologies used. First, the FLEXPART model is introduced and the details on how the backward trajectories simulations were performed. The description of the method used for the identification of the sources of moisture is presented. Then the clustering methodology applied is introduced as well as the used datasets and indices. The general description of the main statistical methodologies used in this study is included, so that the reader may know how computations were made. The results and discussions of the Lagrangian identification of sources of moisture for continental Central America are presented in chapter 5. The mean state of the sources of moisture as well as the seasonal cycle is presented. The variability of the sources under the influence of selected variability modes is presented by describing the patterns of anomalies. At the end of the chapter, an introduction to the role that the transport of moisture from the sources of moisture may have is presented as a link with the following chapter. Chapter 6 presents the analysis of the relative contributions from the identified source to precipitation, following the introduction of the

contributions from previous chapter. Through chapter 6, the results of the quantitative estimates of the contributions of the sources to precipitation are presented. In the absence of a proper complete dataset on observed precipitation, the response of the contributions from the sources of moisture is carried out using observational data from few selected stations as explained in chapter 4. Once an analog to a validation/calibration of the results obtained using the Lagrangian approach, the interannual variability of the contributions to precipitation is analysed. The dynamics of the transport of moisture is presented in chapter 7, starting by the simplistic description of the origin of the air masses, following with the description of the three dimensional structure of the transport to finally explain the processes and structures involved in the transport of moisture through a conceptual model that describes the main features of the transport of moisture that precipitates over Central America. At the end of this part of results and analysis, in chapter 8 the special case of the CLLJ is analysed with detail along with the influence this structure exerts on regional climate and how this low level jet modulates the distribution and variability of regional precipitation. This part closes with the proposal of a simplified method for describing the structure of the sources of moisture as well as transport of moisture modulation and associated precipitation over Central America.

The presentation of this work closes with a third section in which the conclusions of the work are presented, the main results remarked and the problems found advertised in chapter 9. The last chapter 10 presents a list of scientific questions that merged from the work herein presented as future research lines that will be followed based on the results of this work and motivated by the useful concepts developed and described. Further information on the FLEXPART model, an introduction to the problem of drought in Central America and a brief description of the transport of moisture to another location of interest in the IAS to be the North American Monsoon System are included in separated appendices.

This work has been performed with the financial support of Fundacion Carolina from the Agencia Espanola de Cooperacion Internacional, Universidad de Costa Rica and Universidade de Vigo. Additional support for attending workshops and summer schools was provided by Universidade de Vigo, National Research Council (UK) and the WAVACS. A scientific mission held at the Norwegian Institute for Air Research

(NILU) was supported by the SSTM program of the European Cooperation in Science and Technology (COST). A long terms was done at the ENEA with the support of bolsas de viaje of Universidade de Vigo. Support for attending different conferences where some of the results were presented was provided by the Universidade de Vigo and Ttorch. Founded by the European Science Foundation.



## Resumen

Con el objetivo de proveer algunos conceptos básicos necesarios para seguir de la mejor manera este trabajo, una introducción a la distribución de vapor de agua, el ciclo hidrológico y las principales características del clima de la región de los mares Intra Americanos inicia el presente trabajo. De la distribución global del vapor de agua, la presencia de máximos valores es notable en la región tropical. Es de importancia la región que se extiende desde el extremo este del Atlántico tropical hasta el mar de China así como la región conformada por el mar Caribe y el Pacífico Tropical del Este (ETPac por sus siglas en inglés). La distribución del vapor de agua, determinada en parte por la radiación solar, es importante debido a su estrecha relación con el sistema climático como elemento clave del ciclo hidrológico. Basándose éste último en el balance entre la evaporación, precipitación y transporte de humedad. Aproximadamente el 80% del agua que se evapora globalmente proviene de los océanos, de ahí que sean éstos la principal fuente de humedad para la precipitación continental. La evaporación sobre los océanos está dada por la relación entre el viento y las variaciones de humedad. El resto de evaporación tiene lugar en las regiones continentales, donde la contribución de la evaporación local a la precipitación se denomina como 'recycling'. El recycling de humedad forma parte del acople entre la atmósfera y el suelo, así como de la liberación de vapor de agua y energía a la atmósfera. Por otro lado, la precipitación, resultado de la condensación del vapor de agua, tiene una distribución similar a la del vapor de agua. Los valores de máxima precipitación ocurren en las zonas tropicales donde se localizan las grandes zonas de convergencia en niveles bajos. Existen además, a nivel global, regiones caracterizadas por regímenes de precipitación abundante como resultado de circulaciones monzónicas. Tal es el caso de regiones como el Oeste de Africa, Asia, Australia e incluso América. El transporte de humedad completa el ciclo hidrológico, el cual tiene lugar desde las regiones oceánicas sobre las que se evapora el agua pero también desde zonas terrestres. El transporte de humedad en la atmósfera

puede aproximarse como el integrado total del flujo horizontal de vapor de agua en la columna atmosférica. De acuerdo al principio de conservación de masa, la tasa de cambio del 'water storage' debe ser balanceada por la integral de la divergencia del flujo de humedad y la diferencia entre evaporación y precipitación. De manera que para periodos largos de tiempo, el integrado de la divergencia del flujo de humedad es balanceado por el flujo de agua dulce en superficie (E-P). Esta aproximación permite

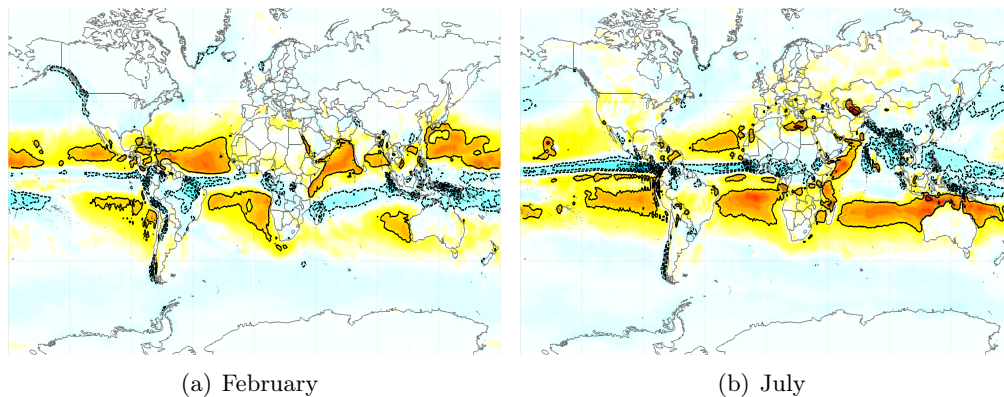


Figure 1: Climatological monthly mean of vertically integrated divergence of moisture flux computed from ERA-40 data for the 1980-1999 period in  $Kgm^{-2}s^{-1}$  for (a) February and (b) July. Note the regions where divergence is in average positive compared with the regions with more intense evaporation in figure 1.3. Those regions are featured to be importance sources of moisture, conversely to those regions featured by convergence where precipitation is known to be more intense, in agreement with the patterns of figure 1.4)

estimar las regiones fuente y sumideros de humedad. A nivel global, hay regiones que se caracterizan por ser importantes fuentes de humedad para la precipitación. De estas fuentes de humedad, nos interesa destacar el caso del mar Caribe, el cual contribuye a la humedad (y precipitación asociada en América Central). Fuentes de humedad para la precipitación en regiones determinadas del globo han sido ampliamente estudiadas, sin embargo en el caso de regiones como América Central, la cantidad de estudios al respecto es mucho menor comparada con regiones como la India o Amazonia. De esta forma se introduce la importancia y necesidad de estudiar América Central como una región de interés. Cabe destacar que la necesidad de analizar esta región proviene de las características que posee y de su ubicación en un entorno rico en procesos y fenómenos atmosféricos y oceánicos que favorece su importancia como sistema climático único. La

región comprendida por el mar Caribe y el Golfo de México, que baña la costa este de América tropical, es determinada como los mares Intra Americanos (IAS). Una amplia banda de flujos de calor latente, fuertes vientos del este, el sistema de altas presiones en el Atlántico Norte subtropical, temperaturas cálidas en la superficie del mar e intensa precipitación conforman el sistema climático de esta región. El IAS posee algunas estructuras características como la Piscina de agua cálida del hemisferio oeste (WHWP), definida por la isoterma de 28.5 y es el segundo cuerpo de agua cálida en extensión después de la region Indo-Pacífico. La WHWP tiene por componentes la porción norte del Pacífico este (ENP) y la región que comprende desde el oeste de América Central hasta el oeste del Atlántico Norte Tropical (TNA) y que se denomina comúnmente como la piscina de agua cálida del Atlántico (AWP). Existe un enlace importante entre las variaciones estacionales del calor en la troposfera y la humedad en la región de América tropical y el desarrollo de la WHWP. Siendo las desviaciones de la última de gran importancia para el desarrollo de la convección en los trópicos. La distribución de precipitación en la región está determinada por los procesos convectivos sobre el Caribe, la migración estacional de la zona de convergencia inter tropical (ITCZ), la temporada de huracanes y la existencia de un periodo seco durante el verano. Este periodo corresponde al denominado 'veranillo' (MSD) y es característico del patrón bimodal de la precipitación en la región de América Central y el Caribe. Esta distribución consiste de dos periodos de máxima precipitación durante los meses de mayo y octubre así como mínimos de precipitación durante los meses de invierno y verano (ver figura 2). Parte de la comprensión del régimen de precipitación requiere del conocimiento sobre el veranillo, que guarda una estrecha relación con el viento en los niveles bajos de la troposfera así como con la distribución de SST. Otra de las características de la precipitación en América tropical consiste de la presencia de circulaciones de tipo monzónico en ambos hemisferios. Por un lado el sistema del monzón de América del Norte (NAMS) que aporta más del 40% de la precipitación durante el verano en el oeste del sector sur de América del Norte y por otro el sistema del monzón de América del Sur (SAMS), importante por el marcado contraste en extremos de precipitación en el continente. El viento de bajos niveles, como elemento importante en el clima regional, se caracteriza por su procedencia este. A lo que se suma la presencia de una estructura de viento que se intensifica durante Febrero y los meses de verano. Dadas sus características, este

jet de bajo nivel del Caribe (CLLJ) posee un núcleo localizado 75 W entre 12 y 15 N aproximadamente en el nivel de 925hPa. Los reportes de vientos del este intensificados, identificados como un jet de bajo nivel se encuentran en la literatura de forma explícita a finales de la década del noventa. Debido a su importancia para el clima regional, los estudios sobre el CLLJ se han multiplicado en los últimos años con el objetivo de comprender su dinámica. Tales estudios han determinado una relación entre la intensidad del CLLJ con las variaciones de presión de la NASH (Sistema de Altas Presiones del Atlántico Norte) así como con las variaciones de SST, el gradiente de temperatura entre la región continental y la oceánica así como la topografía regional. El papel que desempeña el CLLJ es de gran importancia debido a su conexión con la distribución regional de precipitación. Esta está asociada a un potencial efecto modulador del transporte de humedad y la actividad convectiva. Lo anterior sumado a la relación entre el CLLJ con el proceso de ciclogénesis en el Caribe y la intensidad del NAM (Monzón de América del Norte). Los elementos mencionados determinan el estado estacional del clima en la región del IAS. No obstante, éste no es un estado estacionario sino que es sensible a significativas variaciones en la escala interanual. Modos como el ENSO (El Niño-Oscilación del Sur), NAO (Oscilación del Atlántico Norte), PDO (Oscilación Decadal del Pacífico) y MJO (Oscilación de Madden-Julian) son los principales forzantes de la variabilidad interanual del clima en la región a través de su efecto en las estructuras y sistemas anteriormente indicados. La variabilidad del clima en el IAS se ve afectada desde escalas menores como el caso de la MJO que puede caracterizarse como una onda tropical con un periodo de 30-60 días que se propaga hacia el este hasta variabilidad de una frecuencia menor como la PDO. Sin dejar de lado la influencia del ENSO conocido por su impacto a nivel global, que debido a la cercanía con la región del IAS tiene una fuerte influencia en el clima regional. Así como la NAO, que si bien es cierto afecta principalmente el Atlántico Norte durante el invierno, su influencia como principal modo de variabilidad de los campos de presión se asocia con un forzante de estructuras regionales afectadas por los cambios de presión. De lo anterior se desprende la importancia del viento en la región en relación con el transporte de humedad y consecuentemente con la precipitación. Que tal como se ha mencionado, ha sido relativamente poco estudiado para el caso de América Central. Estudios en el transporte de humedad en el IAS incluyen los trabajos de Hastenrath (1966) en los cuales se discute la importancia del

transporte en dirección oeste y del máximo del transporte por debajo de los 900hPa durante invierno. Destacando además el transporte con componente norte a través de los 20 N durante verano. Cuatro décadas más tarde, Mestas-Núñez et al (2005) publican un nuevo análisis del flujo de vapor de agua en el IAS, en el cual describen la estructura zonal del balance del flujo de humedad en la región. Sus resultados indican además el balance entre el transporte del Atlántico tropical norte y el vapor de agua evaporado del IAS con el transporte hacia el Pacífico tropical a través de México y América Central. De lo que se infiere la estructura del transporte análoga a la descrita por Hastenrath, de la que se extrae la presencia del CLLJ y su papel en el transporte asociado al flujo de humedad. No obstante, la importancia del transporte va más allá de la escala regional, ya que hay evidencias del transporte de humedad desde partes del IAS hasta las Grandes Planicies de América del Norte (Knippertz and Wernli, 2010). La escala del transporte de humedad es determinante para la distribución del vapor de agua pero además como forzante de procesos convectivos. Por lo anterior, considerando las principales características climáticas del IAS, un análisis completo del transporte de humedad y su influencia en la distribución regional de precipitación es necesario. Con esta motivación y con base en un estudio preliminar de identificación de fuentes de humedad, se propone un análisis de las fuentes de humedad para la región de América Central, su variabilidad, influencia sobre la precipitación regional así como los mecanismos de transporte involucrados. Debido a la complejidad de la región y la necesidad de conocer con cierto grado de precisión el comportamiento (historial) de las masas de aire, el análisis de tipo Lagrangiano se utiliza como principal herramienta. Esto debido a que la aproximación de tipo Lagrangiano permite conocer las características de elementos finitos de fluido en el tiempo más allá de proveer información del estado medio de un campo escalar, como lo hace la aproximación Euleriana. Como propuesta de trabajo se plantea un conjunto de objetivos generales: a) Generar una base de datos de retro-trayectorias Lagrangianas para un periodo de 20 años (1980-1999) con el modelo de dispersión Lagrangiano FLEXPART utilizando el reanálisis de ERA-40 como datos de entrada, b) Proveer un estudio completo de las fuentes de humedad para América Central, c) Estudiar la relación entre el aporte de humedad de las fuentes identificadas con la precipitación sobre América Central, d) Estudiar el transporte de humedad y e)

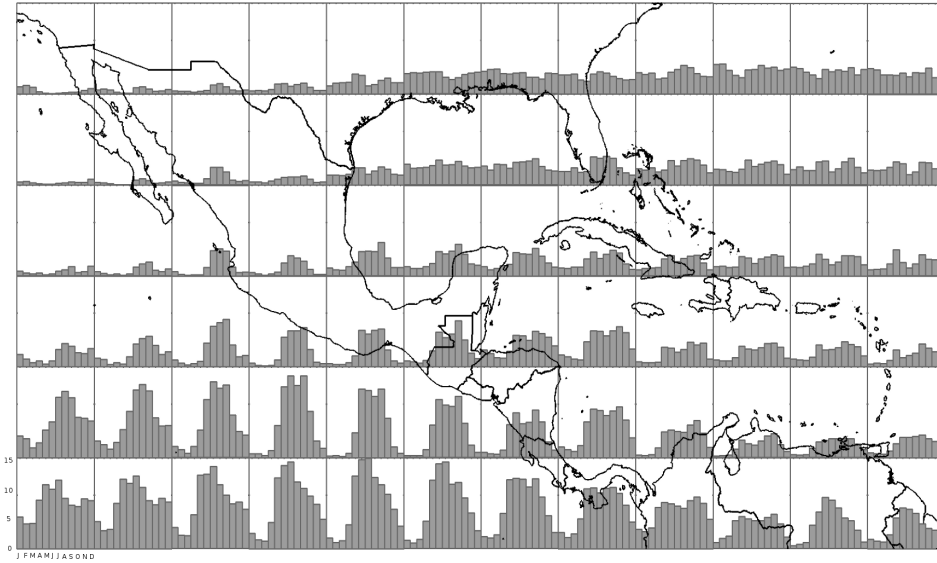


Figure 2: Climatological distribution of monthly mean precipitation ( $mmday^{-1}$ ) for contiguous 5 x 5 area boxes. Dataset and analysis period as in figure 1.3. Bars show the value of precipitation for each month, the scale is from zero to 15  $mmday^{-1}$

Analizar el papel del CLLJ en el transporte regional de humedad y la modulación de precipitación.

El modelo de dispersión Lagrangiano FLEXPART se utiliza para generar la base de datos de retrotrayectorias. La física de este modelo se describe a través de la parametrización de Hanna (1982) para las fluctuaciones de viento. La velocidad friccional se estima a través de la tensión de superficie mientras que el flujo de calor sensible es considerado en la parametrización de capa límite (el método del perfil se utiliza en ausencia de información de la velocidad friccional). Como datos de entrada para las simulaciones con FLEXPART se utiliza el Reanálisis de ERA-40 con una resolución horizontal de 1 en 61 niveles verticales. Dado que la resolución temporal es de importancia para la precisión de las trayectorias, información del análisis se usa cada 6 horas (0000, 0600, 1200 y 1800) mientras que para las horas intermedias se utiliza información del pronóstico (0300,0900,1500,2100). Las simulaciones se realizan bajo una configuración de dominio limitado en el que los flujos de masa se determinan en pequeñas celdas en los bordes del dominio. Se utiliza un total aproximado de 250000 partículas que

son distribuidas de manera uniforme en el dominio de las simulaciones. La selección del dominio de las simulaciones toma en cuenta la escala de los principales elementos moduladores en la región. Dado que el objetivo es el estudio de fuentes de humedad y precipitación, las simulaciones se realizan usando como trazador el vapor de agua. Las salidas del modelo se obtienen con la misma resolución espacial y temporal de los datos de entrada para las variables de posición, humedad específica, vorticidad potencial, densidad del aire, razón de mezcla y temperatura. Para la identificación de las fuentes de humedad se considera como región de análisis América Central continental, a diferencia del análisis exploratorio en el que se usa una caja, se toma como límite la región costera para evitar tomar en cuenta parte de agua para ser más precisos con el estudio de la precipitación sobre el continente. Siguiendo el balance del vapor de agua y el hecho de que la atmósfera puede dividirse en un conjunto de elementos de fluido homogéneos, la tasa de cambio de vapor de agua puede expresarse para aproximar la diferencia entre evaporación y precipitación (Stohl and James 2004). De manera tal que el integrado de los cambios sobre los elementos que forman parte de una columna atmosférica por unidad de área provee una estimación del flujo de agua dulce en superficie. Considerando que el tiempo de vida media del vapor de agua en la atmósfera y la escala de la interacción entre humedad y convección es del orden de 10 días, se analizan los integrados de  $(E - P)^{-n}$  en esa escala de tiempo. Se encuentra que la escala del máximo transporte de humedad y a la cual el valor de E-P converge es  $n=6$ . De manera que para el análisis se toman en cuenta los integrados a 6 días. Para estimar las contribuciones a la precipitación, se asume que la precipitación puede estimarse a través de la proyección sobre la región receptora de la humedad del cambio de humedad de las partículas de aire en el paso de tiempo previo a la llegada a la región (Stohl and James 2004). Esta aproximación tiene la desventaja de que no considera procesos microfísicos, sin embargo se considera una aproximación aceptable. Un refinamiento de esta estimación puede obtenerse considerando la totalidad de la trayectoria y analizando los cambios de humedad que ocurren dentro de la capa límite a través de la misma (Sodemann et al., 2008). Con el objeto de realizar el estudio del transporte de humedad y debido al volumen de trayectorias se utiliza un algoritmo de clasificación basado en clustering, que permite la reducción del total de trayectorias en conjuntos menores que representan las propiedades medias del conjunto total de datos. Se hace

uso de un algoritmo modificado basado en el método de Dorling y Davies (1992) para obtener haces coherentes de partículas que son representativos de las principales trayectorias seguidas por las partículas en su camino a la región de análisis. Para reducir la subjetividad en la clasificación de las trayectorias, se genera un conjunto de trayectorias madre con origen en el centroide de la región de llegada a modo de rayos en un plano cartesiano separados 6 grados unos de otros. Se utiliza como medida de similitud, la distancia euclídea media entre las trayectorias 'reales' de la base de datos y las trayectorias madre. Esto permite asignar a cada trayectoria madre el conjunto de trayectorias más cercanas, las cuales una vez agrupadas son promediadas entre sí. Este procedimiento es iterativo hasta lograr que el número de clusters o trayectorias equivalente sea convergente. El estudio del transporte asociado al CLLJ requiere de una clasificación adicional, en la que se seleccionan aquellas partículas que son influenciadas por esta estructura. Para lograrlo, se aplica (ya sea antes o después del clustering dependiendo de la aplicación) un criterio de selección en el cual se impone a las partículas transitar por la región de influencia del núcleo del CLLJ. El criterio más sencillo es considerar solo aquellas partículas que han transitado en alguna parte de su trayectoria por la región del núcleo del CLLJ, sin embargo esto deja por fuera partículas que pueden ser influenciadas por el gradiente de presión en la región cercana al núcleo. Por esta razón el criterio utilizado considera la región cercana al núcleo delimitada por la región en la que el cambio de presión entre las isobetas características del CLLJ tiende a cero. Esto permite aislar aquellas partículas que se mueven bajo la influencia de la estructura de interés. De forma adicional se definen índices para medir el cambio de geopotencial entre la zona de la NASH y el núcleo del CLLJ, así como de la diferencia de SST entre el Golfo de México y el mar Caribe y el ETPac y el mar Caribe, estos cambios se toman como la diferencia entre la magnitud del campo entre ambos puntos. Parte del análisis requiere del uso de parámetros adicionales, los cuales han sido extraídos del Reanálisis de ERA-40 para el periodo de estudio. Índices climáticos para ENSO, NAO, PDO y MJO han sido obtenidos a través del climate diagnostics center. Información sobre precipitación ha sido utilizada tomando la base de datos de CMAP así como observaciones de estaciones de precipitación en América Central. A estas estaciones de observación de precipitación, previamente se les ha aplicado un análisis de control de calidad, en el cual la cantidad de estaciones útiles se ha reducido de 386 a 46. El control de calidad



aplicado ha consistido de la identificación de outliers en el caso de las estaciones con información diaria así como test de homogeneidad. En el caso de datos faltantes, éstos han sido rellenados con un método simple de media de las muestras. El análisis realizado considera el uso de funciones ortogonales empíricas y composiciones así como la descomposición de la señal usando la técnica de wavelets.

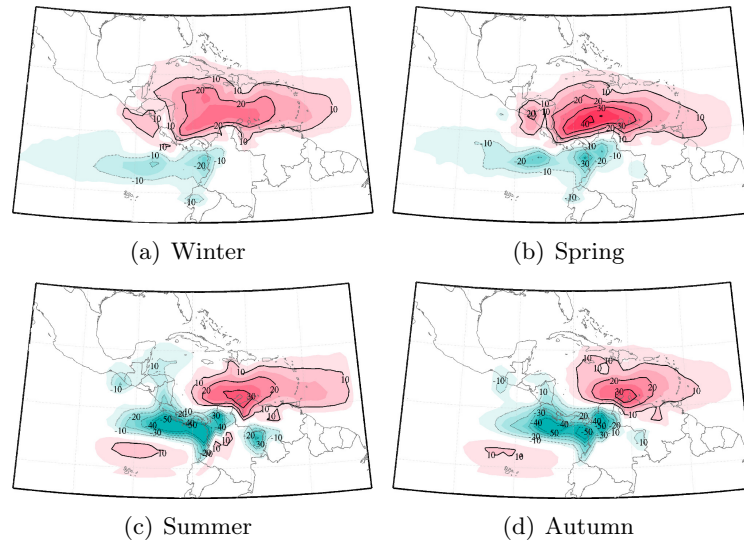


Figure 3: Long term seasonal means of the the conditional  $(E - P)^{-6}$  field in mm/day. Positive(red) and negative(green) contours indicated every 10mm/day starting in 10mm/day and  $-10$ mm/day respectively.

Los integrados  $(E - P)^{-6}$  permiten distinguir las regiones en las que domina la evaporación y por tanto la identificación de las fuentes de humedad evaporativas. Los resultados destacan el papel del mar Caribe como principal fuente de humedad así como la presencia de una fuente en el sector del ETPac. El análisis de la marcha mensual del campo de  $(E - P)^{-6}$  permite identificar además la importancia del recycling de humedad así como la presencia de una fuente en el sector norte de América del Sur. Las fuentes de humedad asociadas a la precipitación en América Central muestran un marcado comportamiento estacional. En el caso del Caribe, a pesar de que éste es una fuente permanente presenta variaciones en su estructura espacial así como en su magnitud. La fuente ETPS tiene actividad solo durante los periodos de verano y otoño. Mientras que CS presenta una reducción importante con la llegada del verano, asociada con la

intensificación de los vientos del este que transportan la humedad desde el Caribe distancias más largas, más allá de América Central. Durante el otoño el núcleo del CS se retira hacia el este, retomando su posición en la cercanía de la costa Centroamericana durante el invierno. Durante los meses de primavera, la fuente alcanza su mayor intensidad con un importante núcleo sobre los 12N. Esta intensificación corresponde al inicio del crecimiento de la magnitud del CLLJ durante estos meses, en los cuales se dan las condiciones óptimas para la evaporación y el transporte de la humedad. Como parte del IAS, el Golfo de México, a pesar de no tener una estructura bien determinada como fuente debe ser considerada por el efecto que tiene sobre el norte de América Central a través de la suma de pequeñas contribuciones. La fuente identificada en el norte de América del Sur, denominada como NSAS, esta fuente, con máximos valores sobre la zona de los llanos Venezolanos y la cuenca del río Magdalena es un aporte significativo al estudio del transporte de humedad en la región. Tanto como evidencia del transporte de humedad desde los llanos venezolanos, sugiriendo el acople entre la corriente en chorro sobre los llanos con el viento del este. Sugiere la interacción hidrológica entre América Central y la región más lluviosa del planeta. El ciclo estacional de la fuente sobre el río Magdalena guarda una estrecha relación con la precipitación observada, coincidiendo la máxima intensidad de la región como fuente de humedad con el periodo de disminución de la precipitación sobre la cuenca (Restrepo et al., 2006). La variabilidad de las fuentes

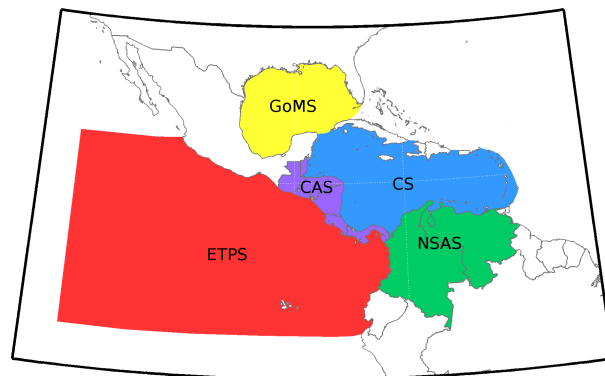


Figure 4: Representation of the sources of moisture for continental Central America identified in the previous chapter. Note that the area comprised by the ETPS is more extended in comparison with the regions where the positive values of the conditional (E-P)-6 field were found, this in order to account for the meridional movements of the source of moisture over this location which varies month to month.

de humedad es explorada a través de la técnica de EOFs, la que revela que el primer modo asociado con el flujo medio del viento del este en el Caribe y el flujo oeste sobre el ETPac explica el 16.2% de la variabilidad de las fuentes. Un segundo modo que explica el 10.5% de la variabilidad se vincula con las variaciones horizontales de CS, lo que remarca la importancia de la posición de la fuente ya sea cerca de la costa Centroamericana o retirada sobre las Antillas Menores. Los cambios en la posición meridional de la fuente CS (señal de la presencia del CLLJ) son también importantes, contando por un 9% de la variabilidad. Un modo relacionado con el contraste observado en la NSAS entre los grandes llanos Venezolanos y la cuenca del río Magdalena cuenta por un 5% de la variabilidad. El análisis de las componentes principales permite identificar la fuerte influencia de la variabilidad asociada a periodos en los que la señal de ENSO es fuerte para los 4 primeros modos mientras que señala la importancia de la variabilidad de baja frecuencia para NSAS. El análisis de los composites muestra que durante la fase positiva de ENSO el Caribe se intensifica como fuente de humedad. Durante el verano, el incremento de la fuente en el sector central del Caribe es muy marcado, así como su extensión sobre los llanos Venezolanos, en contraste con una disminución sobre la cuenca del Magdalena. Mientras que hacia fines del otoño la fuente del Caribe intensificada se extiende hasta el este de las Antillas Menores y la fuente ETPS disminuye su intensidad. La fase negativa de ENSO se caracteriza por el desplazamiento meridional de la zona de máxima intensidad de la fuente Caribe, la cual decrece conforme se desplaza hacia el sureste y aumenta hacia el oeste. Contrario al comportamiento en verano, durante el cual la fuente se intensifica sobre América Central y el ETPac mientras que disminuye sobre todo el sector Caribe. Tal efecto se mantiene hasta el periodo de otoño aunque el aumento de la intensidad de la fuente sobre el ETPac se reduce. La influencia de la NAO es notoria principalmente durante la primavera, periodo en que la importancia de la fuente Caribe disminuye durante la fase positiva a inicios de la primavera y pese a aumentos en el norte del Caribe las contribuciones de las fuentes oceánicas disminuyen ya que además decrece la fuente del ETPac. En los meses de verano el exceso de evaporación sobre el centro del Caribe es mayor, al igual que sobre NSAS, que además tiene un fuerte incremento durante Agosto. El comportamiento durante la fase negativa de NAO cambia y el incremento de la intensidad de la fuente Caribe se restringe al sector norte, con lo que las contribuciones del Golfo de México adquieren importancia,

así como el recycling local. La fuente del ETPac sigue presentando una disminución en su intensidad al igual que los llanos Venezolanos durante el verano. La influencia de la PDO se resume a la disminución (aumento) de la intensidad de la fuente Caribe (recycling local) durante invierno que precede una intensificación de la fuentes Caribe y NSAS en el verano. La fase negativa de la PDO favorece la intensificación de la fuente Caribe sobre las Antillas Menores, indicando un desplazamiento hacia el sureste en los meses de invierno así como la disminución de la fuente ETPac en primavera. El comportamiento de las fuentes bajo la influencia de esta fase cambia y durante el verano las fuentes continentales se reducen sustancialmente mientras que las fuentes oceánicas se intensifican. En el caso de la MJO, la fase definida como positiva está asociada con la disminución de la fuente Caribe durante el invierno mientras que durante la primavera aumenta junto con el recycling local en detrimento de la disminución de la fuente del ETPac. En verano, para la misma fase de la MJO, se incrementa el contraste del NSAS con un aumento de la fuente sobre el norte de Colombia y la disminución sobre los llanos Venezolanos. Para la fase negativa de la MJO, el Golfo de Mexico toma relevancia como fuente durante el invierno mientras que la disminución de la fuente en el extremo del ETPac en primavera es compensada por el aumento del recycling local, el norte del caribe y el Golfo de Mexico. Posteriormente en el verano, la fase negativa favorece la intensificación de las fuente CS y NSAS.

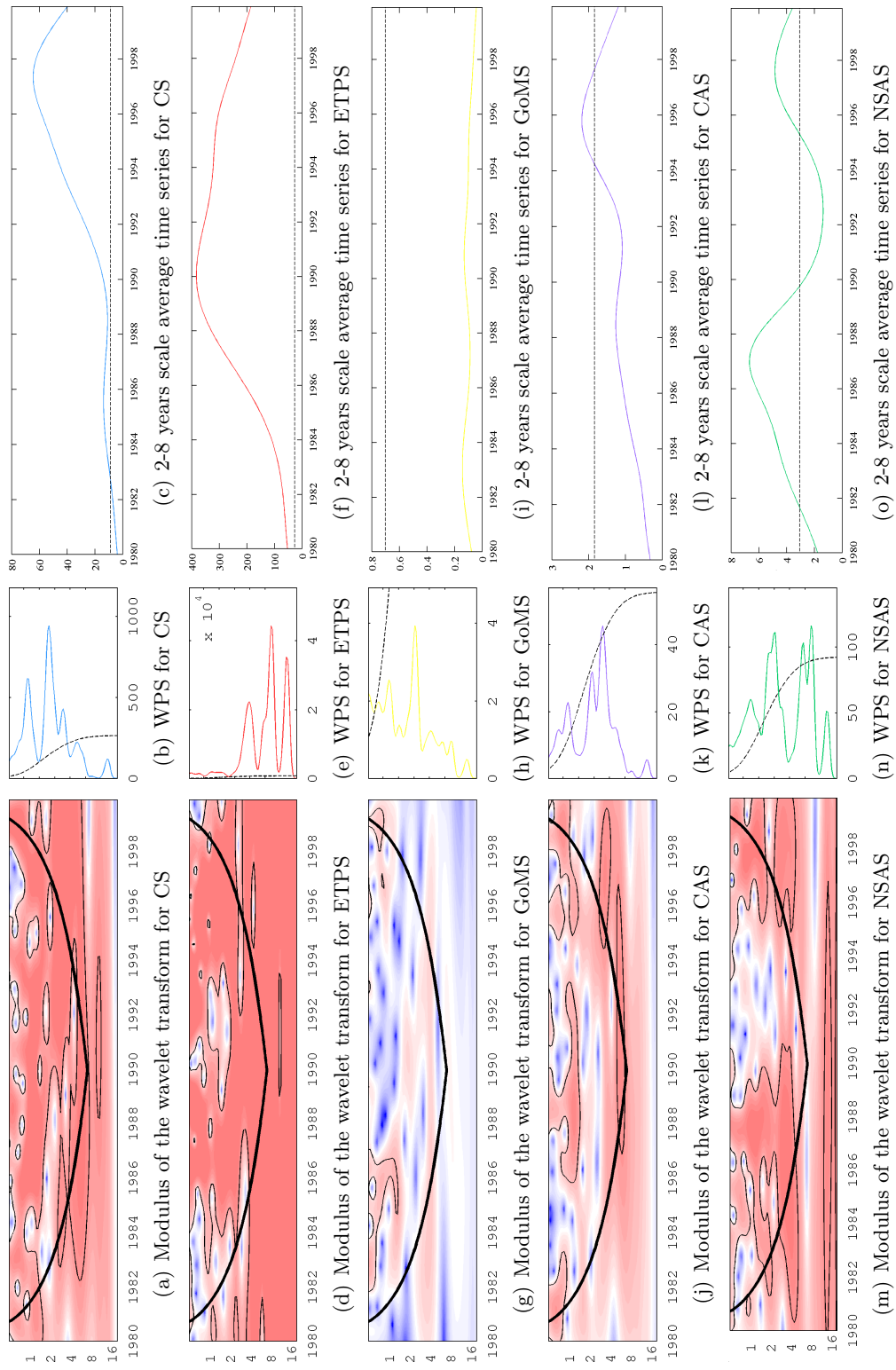


Figure 5: Modulus of the wavelet power spectrum for the time series the relative contributions to precipitation over Central America from a) CS, d) ETPS, g) GoMS, j) CAS and m) NSAS, the cone of influence is marked by a thick black line and the contours significant at 95% percent are enclosed by a black contour is indicated for the modulus of the wavelet transform. Average wavelet power spectrum for the same time series: b) CS, e) ETPS, h) GoMS, k) CAS and n) NSAS. Two- eight years average time series (variance) for the same time series: c) CS, f) ETPS, i) GoMS, l) CAS and o) NSAS, 95% significance level is indicated with black dotted line for the average wavelet power spectrum and 2-8 years scale average time series.

Las contribuciones a la precipitación desde las fuentes identificadas indican que durante el invierno, la humedad del mar Caribe contribuye mayoritariamente a la precipitación en el Golfo de México y sobre el ETPac. La humedad dejada a su paso por América Central favorece la contribución de la humedad del Caribe a la precipitación sobre esta zona y el oeste de Colombia. El aporte de humedad del Golfo de México tiene básicamente una influencia a la precipitación sobre el extremo norte de América Central. Por otro lado, la humedad del ETPS se pierde considerablemente debido a la presencia de la ITCZ sobre el océano, alcanzando apenas el extremo sur de América Central con muy poca influencia en el norte. Por tal motivo, la humedad del ETPS que contribuye a la precipitación se limita básicamente a la que se evapora en la cercanía de la costa. El recycling local tiene un ciclo estacional que sigue el patrón de la precipitación sobre la región de análisis, de acuerdo a lo esperado del recycling. En el caso de las contribuciones desde la fuente continental remota determinada como NSAS, éstas tienen un máximo sobre la cuenca de los ríos Magdalena y Orinoco sin embargo importantes contribuciones se observan sobre América Central, especialmente en el sector sur durante el verano. La distribución de las contribuciones a la precipitación sobre América Central muestran el dominio del mar Caribe durante todo el año. Sugiere la importancia del Golfo de México como fuente de humedad durante el invierno, al mismo tiempo que muestra el marcado pico de las contribuciones desde NSAS durante el verano. La evaluación de las contribuciones a la precipitación estimadas a través de la pérdida de humedad en el último paso de tiempo previo a la llegada de las masas de aire a las regiones consideradas para la evaluación, lo que indica que hay un bias en el rango de 23 a 46% dependiendo de la ubicación de la región. Tomando en cuenta datos de CMAP para América Central, el bias es del 29% , no obstante cabe mencionar que los estimados de precipitación del método Lagrangiano al no considerar procesos microfísicos no son comparables con la totalidad de la precipitación observada, sino como una parte de ésta. Esto implica que los biases pueden reducirse de forma considerable y por tanto las estimaciones de las contribuciones de las fuentes de humedad a la precipitación sobre el continente obtenidas con el método Lagrangiano constituyen una buena aproximación de las contribuciones relativas a la precipitación. Las series de tiempo de las contribuciones relativas de cada fuente indican que el mar Caribe provee la mayoría de la humedad que precipita sobre América Central, mostrando además la importancia de

las contribuciones de NSAS y en menor cantidad del recycling local y el Golfo de México. Muestran además que las contribuciones del ETPS son significativas, no obstante tienen un comportamiento en el tiempo muy diferenciado del resto de contribuciones, con saltos de intensidad importantes. El análisis de la variabilidad inter anual de las contribuciones revela que la mayor variabilidad de las fuentes se da en la banda de 2-8 años, que corresponde a la banda del ENSO (excepto en el caso del aporte del Golfo de México, ya que el resultado no es estadísticamente significativo). En el caso de las contribuciones desde el ETPac una fuerte señal de variabilidad es notoria también para frecuencias más bajas y se muestran claramente los picos de intensidad de 2-4, 4-8 y 8-16 años. En el caso de las contribuciones de NSAS, la variabilidad de bajas frecuencias también es importante aunque no tan intensa como para ETPS. De lo anterior se concluye que la señal que tiene un mayor impacto en las contribuciones a la precipitación es la del ENSO y que las fuentes ETPS y NSAS tienen una influencia importante de modos de muy baja frecuencia como lo puede ser la PDO. No obstante, cabe mencionar que la longitud del periodo de análisis puede no ser adecuada para dar conclusiones sobre el efecto total de la PDO, aunque sí permite señalar la potencial importancia de este modo de variabilidad, dada la evidencia de ser una forzante a considerar. El análisis de los composites para las fases positiva y negativa de los modos de variabilidad, así como de las condiciones neutras, permite determinar la influencia que tiene cada fase en las contribuciones a la precipitación. En el caso de ENSO, las diferencias entre las fases para el periodo de primavera muestran el contraste en las contribuciones desde el ETPS y el Golfo de México así como del NSAS. Ya que durante la fase negativa hay una disminución marcada de las contribuciones del ETPS que es compensada por el aumento de las contribuciones del Golfo de México, mientras que en la fase positiva las contribuciones del completan la distribución. Durante el verano, la fase negativa (positiva) se caracteriza por la disminución (aumento) de las contribuciones del ETPS en comparación a las condiciones neutras. La señal de la NAO tiene su mayor influencia en la variabilidad de las fuentes CS y ETPS, asociada en la primera parte de invierno con un aumento (disminución) de las contribuciones del Caribe (ETPS) durante la fase negativa. Durante la fase positiva el patrón se invierte pero las variaciones no son tan drásticas como para la fase negativa. La PDO se caracteriza por favorecer el incremento de las contribuciones desde NSAS durante la fase positiva a finales de otoño y del Golfo

de México durante parte del invierno y primavera. La fase negativa por el contrario está asociada a la marcada disminución de las contribuciones del Golfo de México y al aumento de las contribuciones del ETPS durante buena parte del año. Finalmente la MJO está asociada con la intensificación (disminución) de las contribuciones de GoM durante la fase positiva (negativa). Las variaciones de las contribuciones de GoM, son en este caso compensadas con las de CS, lo que sugiere un fuerte impacto de esta señal en el IAS. Es importante además, mencionar que el efecto de los modos de variabilidad en las contribuciones a la precipitación además de tener un componente inmediato, tiene un efecto a largo plazo, que normalmente es del orden de 6 meses para ENSO, NAO y de 6-9 meses para la MJO. (valores no significativos para PDO). Lo anterior es importante, ya que el efecto de los modos de variabilidad tiene la capacidad de modificar los patrones de precipitación en escalas de tiempo mayores a las de la propagación de la señal. Esto es el resultado de la modificación del transporte de humedad y de los cambios que éste tiene en el ciclo hidrológico en escalas espaciales más pequeñas. Un breve análisis del efecto de ENSO sobre las contribuciones de las fuentes de humedad y precipitación observada en las localidades de Costa Rica y Panamá permite comprobar los resultados obtenidos para el modo ENSO. Lo anterior a través del estudio de un periodo Niño, uno Niña y un ciclo ENSO quasi-completo. Mostrando que en general la fase cálida del ENSO se caracteriza por una disminución del aporte de humedad desde las fuentes, relacionado con la disminución en la precipitación observada. De los resultados obtenidos se puede concluir además, que la respuesta a ENSO depende de la ubicación de la región receptora de la humedad. En el caso del sur de América Central, incluso bajo el efecto de una fase positiva de ENSO no siempre hay una disminución en la precipitación observada, comportamiento que también se observa en las contribuciones de las fuentes de humedad. Lo que indica la importancia de análisis de carácter más regional a pesar de la pequeña extensión de América Central, ya que la respuesta a los modos de variabilidad es tan heterogénea como su distribución de precipitación.

La identificación de las fuentes de humedad permite conocer la procedencia de las masas de aire húmedo, no obstante es importante saber de qué forma se lleva a cabo el transporte de la humedad desde la fuente hasta la región receptora. Una gran ventaja de los métodos Lagrangianos es la posibilidad de reconstruir la historia de las masas de aire previa a su llegada a la región receptora. De esta manera es posible determinar



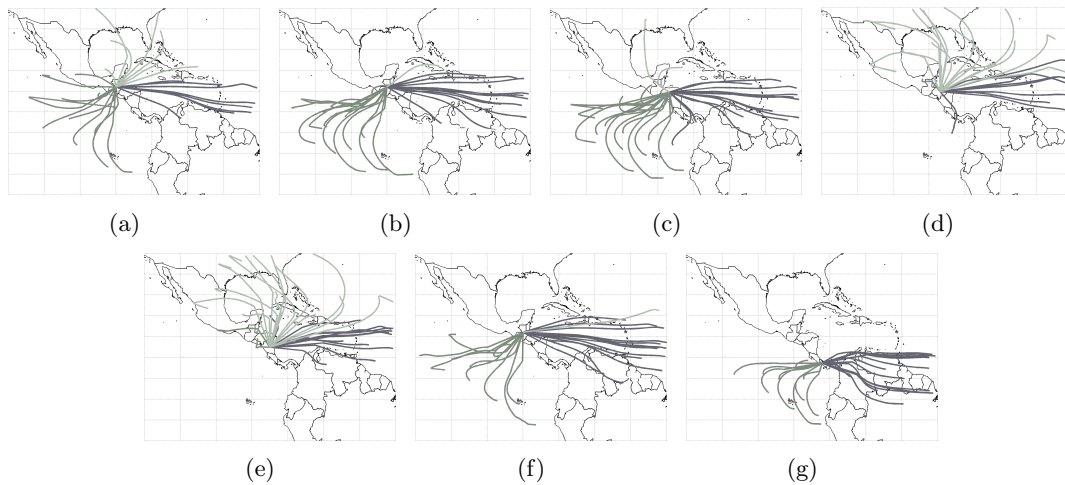


Figure 6: Mean climatological air streams for the trajectories losing moisture over different locations of Central America.

la forma en la que la humedad ha sido transportada. Tomando en consideración la heterogeneidad de la región de análisis, América Central ha sido seccionada en 4 partes: Guatemala-Belice (GB), Honduras-El Salvador (HS), Nicaragua (Nic) y Costa Rica-Panamá (CRP), con el objeto de que el análisis permita identificar las diferencias en el transporte que estén asociadas a las diferencias observadas en la distribución de la precipitación regional. Una revisión inicial de la distribución porcentual del origen de las masas de aire (su posición 6 días antes de que precipiten sobre América Central, ver ejemplo en la figura 6) indica que el aire viaja de 3 fuentes principalmente: a) GoM, b) ETPS y c) Caribe para las 3 subregiones ubicadas hacia el norte mientras que para Costa Rica-Panamá hay una componente importante que proviene del norte de América del Sur. Si bien es cierto y aire de esta región también llega al resto de las subregiones, la cantidad de partículas es menor al 10% del total de partículas de llegada y en su mayoría su posición es más cercana al Caribe que a la parte continental propiamente. Los resultados indican que la cantidad de masas de aire con procedencia del Caribe es mucho mayor que del resto de las regiones, excepto para el extremo sur, en el que la distribución es más equitativa. Lo anterior, tomando en cuenta los resultados de las estimaciones de contribuciones a la precipitación, además de indicar que la cantidad de humedad transportada desde el Caribe es mayor, indica que el contenido de humedad de las masas de aire del ETPac es alto. La evaluación de la estructura de las trayectorias de

las partículas remarca el papel que desempeña el viento en el transporte de la humedad, así como la estacionalidad del transporte. El análisis del contenido de humedad a lo largo de las trayectorias (de los clusters en este caso) permite comprobar que en efecto el contenido de humedad de las partículas del ETPac es muy alto, comparado con las otras fuentes. Además, es posible identificar las regiones en las que el contenido de humedad de las masas de aire se intensifica de forma significativa. Como se ha indicado, hay un incremento muy alto de humedad en la región del ETPac desde verano hasta otoño mientras que sobre el Caribe esta intensificación (durante los mismos periodos) se limita a las masas de aire que contribuyen con precipitación sobre la parte sur de América Central. Por otro lado, el aire que viaja desde el Golfo de México tiende a ser más seco. Puede notarse además como en el caso del aire que procede de NSAS presenta una tendencia a ganar humedad cerca de las regiones costeras en promedio. De la estructura vertical de los clusters se puede determinar con claridad la separación del flujo según la altura y su contenido de humedad. Siendo aire más húmedo el de los niveles más bajos, donde tanto la altura como la humedad tienen un marcado comportamiento estacional. En el caso de las subregiones ubicadas al norte, poco transporte de humedad ocurre durante el primer trimestre del año, aumentando con la llegada de la primavera e incrementando el contenido de la humedad transportada en los niveles más bajos durante el verano. Es importante destacar que el mayor incremento de humedad se da en las durante las 48 horas previas a la llegada de las masas de aire. Para CRP se nota un importante aumento del contenido de humedad a finales del invierno en los niveles más bajos, seguido de un periodo de transporte relativamente seco hasta que a finales de primavera hay un aumento en el contenido de humedad del aire que llega a la región, el cual decrece durante otoño. Se debe señalar que el incremento del contenido de humedad que se nota en verano es bastante menor que el que tiene lugar en el caso del aire que llega a la parte norte de América Central y que además en el caso de Nicaragua este es aún menor. La intensificación del transporte de humedad hacia el norte de América Central y su consecuente disminución hacia el sur corresponde con el ciclo estacional del CLLJ. Al analizar el destino de la humedad del Caribe durante el verano, se determina además que aún cuando aumenta el transporte hacia el norte, la mayor parte de éste sigue la ruta del Golfo de México con lo que a pesar del aumento en el transporte el resultado es una disminución de la precipitación en la zona. El proceso

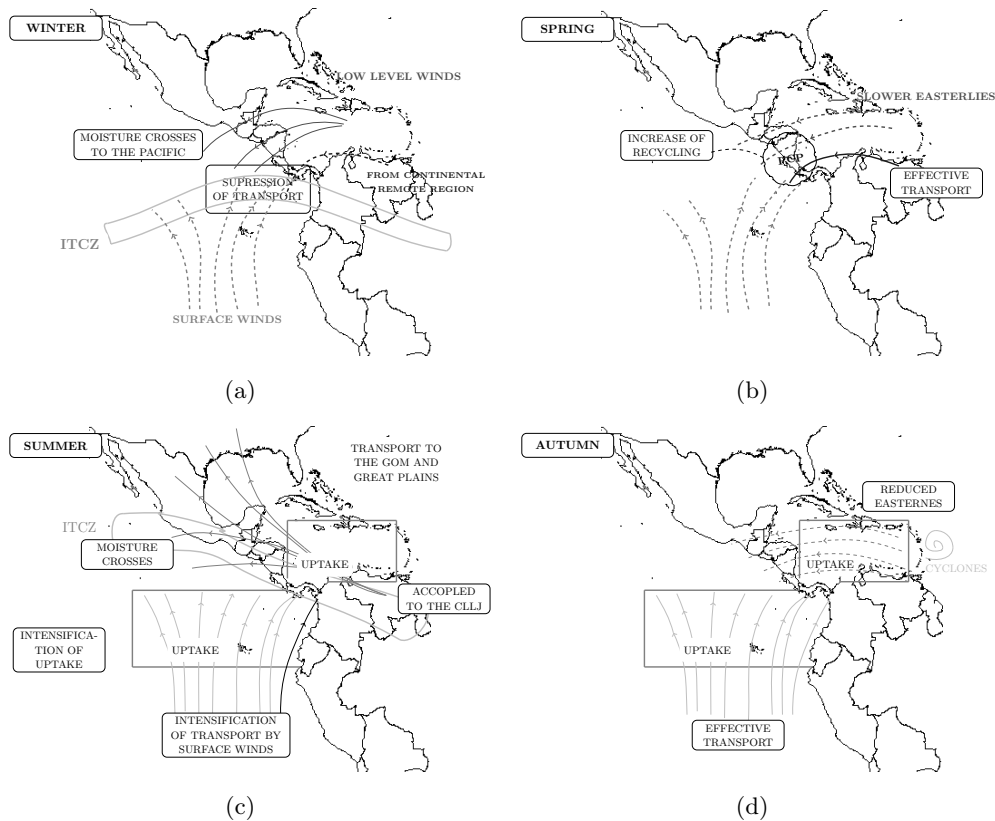


Figure 7: Diagramas de los mecanismos que intervienen en el transporte de humedad en la región de interés

de transporte de humedad hacia América Central desde las fuentes puede describirse en términos del viento en niveles bajos y el movimiento de la ITCZ, tal como lo ilustran los diagramas de la figura 7. Durante el invierno la intensidad de los vientos del este aumenta con una componente suroeste, lo que favorece el paso de humedad hacia el ETPac, dejando contribuciones sobre América Central. La intensidad del viento del este tiene la capacidad de frenar el avance del transporte desde el ETPac, dado principalmente a que la componente noreste es débil, con lo que el transporte desde el ETPac es disminuido. A esto se suma la posición de la ITCZ sobre el ETPac sur que contribuye al debilitamiento del transporte desde el ETPac al potenciar el aumento de precipitación sobre el océano. Las condiciones del viento del este sobre el Caribe durante la primavera favorecen el transporte hacia América Central. La presencia de vientos de

intensidad moderada está asociada al aumento de las precipitaciones durante los meses de primavera. De manera que en el verano, ante el máximo del CLLJ, los vientos del este (ubicados en alturas superiores) transportan parte de la humedad hacia el sector ETPac por medio de su rama suroeste. Al mismo tiempo que el desarrollo de una componente noreste lleva el resto de la humedad en dirección hacia el Golfo de México y las Grandes Planicies de América del Norte, con lo que sus contribuciones a la precipitación sobre América Central disminuyen. En este periodo, el incremento en la evaporación sobre el ETPac y la intensificación del viento son responsables de favorecer el transporte desde esta región hacia América Central. Dado que la mayor intensidad del viento del este tiene componente norte y que la ITCZ se encuentra en su posición más norte, no existe la supresión del transporte desde el ETPac. Existe además, a través del flujo de viento del este, un acomple entre el transporte de las masas de aire procedentes de NSAS (impulsadas por la corriente sobre los llanos venezolanos) con una debilitada componente suroeste del CLLJ, lo que permite el traslado de la humedad de esta fuente hacia América Central. En otoño, de forma similar a la primavera los vientos del este se reducen, la humedad apenas logra alcanzar distancia que le permiten llegar a América Central donde las contribuciones a la precipitación aumentan. El flujo de humedad del ETPac es también importante aunque el transporte proviene mayoritariamente del Caribe

El transporte de humedad desde el Caribe guarda una estrecha relación con el ciclo estacional del CLLJ debido al papel del viento en niveles bajos como elemento modulador del transporte. La evaporación sobre la superficie del Caribe aumenta con la intensidad del viento del este. Lo que implica que el CLLJ favorece el incremento en el contenido de humedad de las masas de aire al pasar por la zona de influencia del CLLJ. Es posible determinar cómo el transporte de humedad que contribuye a la precipitación sobre América Central responde al ciclo estacional del CLLJ. Durante el máximo secundario existe algún tipo de transporte a las diferentes regiones de América Central, sin embargo durante el máximo principal en verano se nota una clara disminución en el transporte debido al CLLJ que contribuye a la precipitación al desplazarse hacia el sur de América Central. Un aspecto importante del transporte debido al CLLJ es la influencia de su estructura vertical sobre la precipitación. Se ha mencionado que durante el máximo de verano el CLLJ alcanza alturas mayores comparadas con el máximo de invierno,

esto hace que durante el invierno el CLLJ tenga una mayor interacción con el sistema montañoso sobre América Central y por lo tanto contribuye al origen de precipitación topográfica. Mientras que al ser más alto durante el verano (y con mayor velocidad) pueda cruzar con mayor facilidad sobre América Central sin interactuar tanto con la topografía. Esto, junto con la estructura horizontal del CLLJ, explica su relación con la precipitación local (así como su interacción con otras características locales). Existe

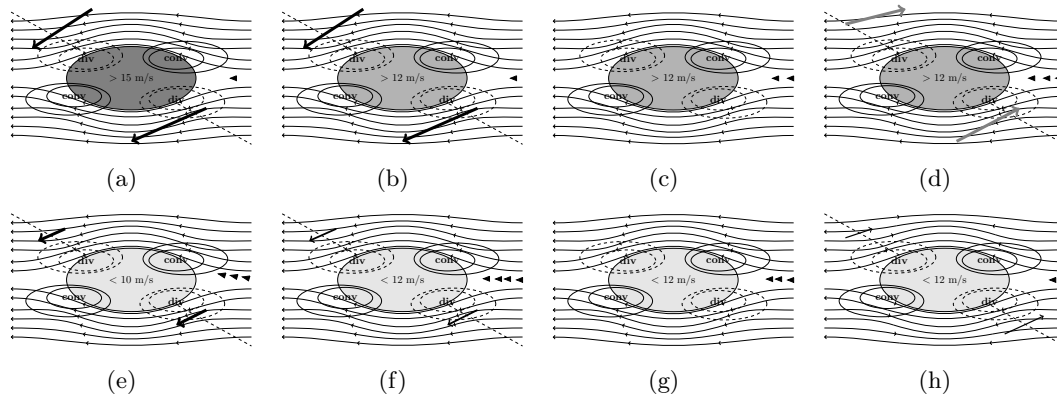


Figure 8: Sketch providing a summary of the conditions of the intensity of the CLLJ and the SST gradient between the Caribbean and ETPac that trigger the major changes in the transport of moisture from the Caribbean and associated precipitation.

además el forzamiento debido al gradiente de temperatura, ya que dada la posición de América Central, la región es muy sensible al gradiente de SST entre las cuencas Caribe y ETPac. La respuesta al gradiente de temperatura es la de una circulación inducida (tipo Gill, 1988), lo que está asociado al incremento o disminución del viento del este mayoritariamente y por tanto tiene un impacto en el transporte. Esto nos permite plantear un sencillo modelo para estimar las condiciones que favorecen o no el transporte de humedad hacia América Central y por tanto contribuyen a la precipitación en la región, como se ejemplifica con los diagramas de la figura 8:

- vientos muy fuertes (caracterizados por el máximo de verano del CLLJ) superiores a 15 m/s transportan la mayor part de la humedad al Pacífico, disminuyendo por lo tanto el aporte a la precipitación sobre América Central.
- vientos del este relativamente intensos acompañados de un gradiente de SST en el sentido del Pacífico resultan en vientos más fuertes que son equivalentes al caso

anterior.

- un CLLJ desarrollado con un gradiente muy pequeño de SST permite que parte de la humedad sea transportada a América Central.
- un CLLJ desarrollado con un Caribe más cálido resulta en una disminución de los vientos del este, con lo que se favorece el transporte de humedad.
- en ausencia de un CLLJ desarrollado (flujo débil desde el este) un Pacífico más cálido induce una circulación que intensifica moderadamente el flujo del este con lo que hay un leve favorecimiento del transporte.
- en un caso similar al anterior pero con una intensidad mayor de viento del este, el transporte se favorece y si las condiciones son apropiadas para la convección hay un aumento de la precipitación debido a la humedad del CS.
- un CLLJ no desarrollado en ausencia de un gradiente de SST deja el transporte limitado a la intensidad del viento zonal, con lo que el transporte se favorece si la intensidad del viento oscila entre 8 y 12 m/s.
- un viento entre 8 y 12 m/s con un Caribe más cálido es responsable de una reducción del transporte.

Tomando en cuenta estas consideraciones, es posible determinar el efecto de los modos de variabilidad en el transporte de humedad. Además, analizando la respuesta del CLLJ a estos modos se puede conocer las variaciones en los patrones de convergencia y divergencia asociados a la estructura del CLLJ que son también indicadores de las condiciones que favorecen la precipitación en la región. De los resultados obtenidos, se menciona como ejemplo el caso del ENSO (resultados en la figura 9) se nota como una fase positiva de ENSO debilita el máximo de Febrero y el patrón de convergencia a la izquierda del núcleo del CLLJ no se desarrolla. Como resultado de esto, el transporte de humedad disminuye y se favorece la divergencia con lo que se suprime la precipitación sobre América Central. La fase negativa por el contrario aumenta la intensidad del CLLJ, favorece la convergencia a la izquierda del núcleo con lo que sumado al aumento del transporte, favorece la precipitación sobre la costa Caribe y partes de América Central. El efecto durante el máximo de Julio es opuesto para la señal del ENSO, debido en

parte al desarrollo de la componente norte del CLLJ, el transporte y la convergencia disminuyen. La influencia de la NAO durante la fase negativa (positiva) debilita (intensifica) el CLLJ, modulando el transporte durante el invierno. No obstante el efecto de la NAO en la precipitación es más importante durante primavera, cuando la intensificación del viento del este en la fase negativa contribuyen al aumento del transporte desde el Caribe, que resulta en un aumento de las contribuciones a la precipitación (de acuerdo a los resultados del capítulo 6). La señal de la PDO sobre el Caribe es débil, sin embargo en invierno se asocia con divergencia sobre América Central y la costa Pacífica con la correspondiente disminución de precipitación. Durante Febrero, la fase positiva de la MJO favorece la intensificación del CLLJ mientras que durante Julio esto sucede para la fase negativa, siendo esta última asociada con la intensificación del patrón de divergencia. Durante los periodos en los que hay máximos del CLLJ, éste domina en el transporte. Los patrones de convergencia y divergencia asociados con el jet definen las condiciones que favorecen la precipitación y la intensidad del uptake y por tanto de las fuentes de humedad. Mientras que en los periodos en los que la actividad del CLLJ es mínima, el transporte de humedad desde el Caribe hasta América Central es forzado por el gradiente de temperatura entre el Atlántico y el Caribe. El análisis detallado del transporte de humedad durante fases extremas de los modos de variabilidad permite comprobar que el transporte de humedad cumple con bastante precisión el comportamiento descrito por el modelo. Además de que se termina que las variaciones en el transporte de humedad desde el Caribe está relacionado con periodos de sequía intensa en Nicaragua y que las mayores variaciones están relacionadas con ENSO. La estructura del CLLJ es responsable de la heterogeneidad de la distribución espacial de la precipitación en la región.

Se preparó para este trabajo una base de datos de retrotrayectorias para un periodo de 20 años (1980-1999) con una resolución espacial de un grado y temporal de 3 horas, con un total aproximado de 250000 parcelas de aire con el modelo de dispersión Lagrangiano FLEXPART con el objeto de realizar un estudio completo del transporte de humedad y precipitación en América Central. El método de análisis Lagrangiano, a diferencia de los métodos Eulerianos tradicionales, permite conocer la 'historia' completa de las parcelas de aire, con lo cual la identificación de los cambios de sus propiedades (tal como la humedad) facilita el estudio del transporte de humedad

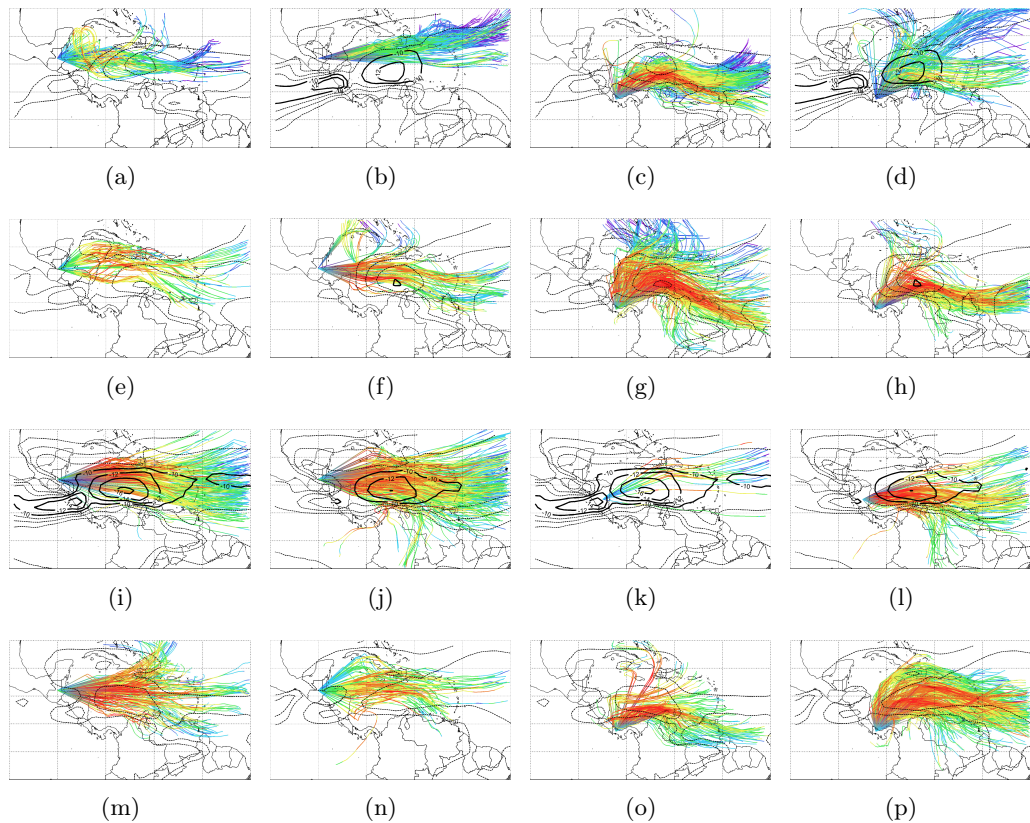


Figure 9: Analysis of transport of moisture for extreme ENSO.

(así como de otros trazadores). Si bien es cierto que la precisión de las trayectorias es dependiente de la precisión con que los Reanálisis representan las variables atmosféricas y oceánicas, la continua mejora en la resolución de éstos sumada a las crecientes facilidades computacionales nos permiten representaciones cada vez mejores del sistema climático. En el caso particular de América Central, al ser una zona tradicionalmente poco estudiada y no muy bien representada en muchos de los modelos, los resultados obtenidos constituyen un aporte importante a la comprensión de la dinámica local. Lo anterior es de gran relevancia al tomar en cuenta la importancia que tiene la lluvia en el desarrollo regional además de la sensibilidad que tiene a fenómenos como sequías e inundaciones causadas por precipitaciones extremas. El análisis realizado ha permitido además de una fiel identificación de las fuentes de humedad asociada a la precipitación en la región, el estudio del aporte que hacen las fuentes identificadas a la lluvia sobre



el Istmo. Más allá de describir los resultados generales, se ha realizado un estudio detallado del ciclo anual de la distribución espacial de las fuentes de humedad así como de la variabilidad inter anual y la respuesta que tienen al forzamiento de modos de variabilidad de baja frecuencia. Por otro lado se ha presentado un análisis cuidadoso de la variabilidad del aporte de humedad a la precipitación de cada una de las fuentes de humedad, así como un estudio del recycling de humedad que ocurre en la región. Una vez conocida la variabilidad del aporte de humedad de las fuentes a la precipitación se realizó un estudio de la estructura tridimensional del transporte de humedad desde las regiones fuentes hasta América Central. Para tomar en cuenta la heterogeneidad de la distribución espacial de la precipitación en la región, se hizo el estudio para 4 subregiones, con el objetivo de realizar un estudio que contemplara las principales diferencias en el régimen de precipitación regional. El estudio de la estructura del transporte permitió identificar características importantes del transporte que no han sido documentadas y que además muestran la importancia de analizar con detalle esta región. Se analizó además del comportamiento medio de la estructura del transporte, sus variaciones bajo los modos de variabilidad, donde se encontró que el transporte desde cada región puede compartir características comunes ante el mismo modo o ser totalmente distinto. Este resultado supuso un reto grande para la interpretación de los resultados obtenidos ya que denota la complejidad del sistema. Se propuso un modelo conceptual para explicar los mecanismos de transporte de humedad y la forma en la que los mismos interactúan para modular tanto el transporte de varias fuentes como la distribución espacial de precipitación. Finalmente se realizó un estudio minucioso de la estructura del CLLJ y su importancia como mecanismo modulador de transporte en diferentes escalas de tiempo. Los resultados permitieron mostrar la gran sensibilidad de esta estructura a la variabilidad y como esto causa un impacto directo en la precipitación local. Se propuso para el caso del CLLJ otro modelo conceptual en el que se explica la forma en la que esta estructura puede modular la precipitación en la región. La metodología aplicada se perfila de gran utilidad para el estudio de procesos de transporte, por lo que a partir de los resultados obtenidos, un conjunto de actividades de investigación derivadas de los resultados de esta tesis han sido propuestos, sobre algunos de los cuales ya se ha iniciado el trabajo. Se espera que el trabajo realizado permita mejorar la comprensión

de la dinámica del transporte de humedad en la región y que este estudio motive la aplicación de estas metodologías a otros tipos de análisis.

# Contents

<b>List of Figures</b>	<b>vii</b>
<b>List of Tables</b>	<b>xiii</b>
<b>I Introduction</b>	<b>1</b>
<b>1 Water Vapour in the climate system</b>	<b>3</b>
1.1 The structure of the distribution of moisture and moisture availability . . .	4
1.2 Water vapour and the water cycle . . . . .	5
Components of the water cycle . . . . .	5
1.3 Sources of moisture and precipitation around the globe . . . . .	10
Main global sources of moisture . . . . .	11
<b>2 Climate and variability in the IAS</b>	<b>15</b>
2.1 Climate in the IAS region . . . . .	16
Western Hemisphere Warm Pool . . . . .	16
Distribution of precipitation . . . . .	18
The Mid-Summer Drought . . . . .	19
2.2 The American Monsoon System . . . . .	21
North American Monsoon System . . . . .	22
South American Monsoon System . . . . .	24
2.3 The Caribbean Low Level Jet . . . . .	26
Structure . . . . .	26
Importance for regional climate . . . . .	27
2.4 Principal modes of variability . . . . .	29

EL Niño-Southern Oscillation . . . . .	30
North Atlantic Oscillation . . . . .	31
Madden-Julian Oscillation . . . . .	31
Pacific Decadal Oscillation . . . . .	32
Multi Decadal Oscillation . . . . .	33
<b>3 Moisture availability and transport in the IAS</b>	<b>35</b>
3.1 Importance and previous studies . . . . .	37
3.2 The problem of analysing moisture sources and transport in the IAS region	39
3.3 Lagrangian methodologies as an alternative . . . . .	40
Back trajectory analysis in the region as part of the Water Cycle Research	
Programme of the NSF . . . . .	42
3.4 The proposal . . . . .	44
Motivation . . . . .	44
Objectives . . . . .	46
<b>II Lagrangian analysis of sources of moisture and transport processes in the IAS</b>	<b>49</b>
<b>4 Data and Methods</b>	<b>51</b>
4.1 The backward Lagrangian trajectories dataset . . . . .	52
The FLEXPART model . . . . .	52
Input data and simulations . . . . .	53
Output data . . . . .	54
Identification of sources of moisture . . . . .	55
Estimation of contributions to precipitation . . . . .	56
4.2 Clustering method applied . . . . .	58
Selection of the particles of interest . . . . .	59
The clustering . . . . .	59
4.3 Indices for the intensity of the CLLJ and the SST gradient . . . . .	61
4.4 Additional Reanalysis variables, climate indices and precipitation data .	62
ERA-40 data . . . . .	62

Precipitation . . . . .	64
Climate Indices . . . . .	66
4.5 Used statistical methodologies . . . . .	67
Empirical Orthogonal Functions . . . . .	67
Composites . . . . .	68
Wavelet analysis . . . . .	70
<b>5 Lagrangian identification of sources of moisture for continental Central America</b>	<b>75</b>
5.1 Identification of moisture sources . . . . .	75
The mean climatology and seasonal cycle . . . . .	77
5.2 Variability of the sources of moisture . . . . .	81
ENSO . . . . .	84
NAO . . . . .	87
PDO . . . . .	89
MJO . . . . .	93
5.3 Chapter highlights . . . . .	96
<b>6 Relative contributions to precipitation</b>	<b>99</b>
6.1 Estimation of moisture lost over Central America . . . . .	100
6.2 Relative contributions to precipitation from the sources of moisture . . .	105
6.3 Evaluation of the response of the contributions from the moisture sources using observational data . . . . .	107
6.4 Long term time series of contributions to precipitation and associated variability . . . . .	108
The mean picture of the variability . . . . .	108
Evolution of the anomalies of the contributions to precipitation . . . . .	112
6.5 Variations under the influence of main variability modes . . . . .	114
ENSO and contributions to southern CA . . . . .	121
6.6 Variability of local recycling of moisture . . . . .	124
6.7 Chapter highlights . . . . .	126

<b>7</b>	<b>Dynamics of transport</b>	<b>131</b>
7.1	Origin of air masses . . . . .	132
7.2	The structure of transport . . . . .	139
	The horizontal structure of the mean airflow . . . . .	140
7.3	The content of air moisture along the trajectories . . . . .	141
	Vertical structure of the air streams . . . . .	147
7.4	Dynamics of transport . . . . .	152
	A conceptual model for the modulation of moisture transport . . . . .	157
7.5	Chapter highlights . . . . .	159
<b>8</b>	<b>Role of the CLLJ in the modulation of the transport of moisture</b>	<b>161</b>
8.1	The climatological structure of the transport of moisture from the Caribbean	162
8.2	A reduced model for the role of the CLLJ as a modulator structure . . .	166
8.3	The CLLJ as moisture transport and precipitation patterns modulator .	170
8.4	Modulation of the moisture transport, CLLJ and variability modes . . .	175
	ENSO . . . . .	176
	Precipitation associated to the transport of moisture, role of the CLLJ and response to variability modes . . . . .	182
8.5	Chapter highlights . . . . .	190
<b>III</b>	<b>Final remarks</b>	<b>193</b>
<b>9</b>	<b>Conclusions</b>	<b>195</b>
9.1	Lagrangian approach . . . . .	196
9.2	Sources of moisture and contributions to precipitation . . . . .	196
9.3	Moisture transport and associated mechanisms . . . . .	199
9.4	Role of the CLLJ in moisture transport and distribution of precipitation	200
<b>10</b>	<b>Further research lines</b>	<b>205</b>
10.1	Transport of moisture to and from additional structures . . . . .	206
	Moisture transport processes related with the South Pacific Convergence Zone . . . . .	206
	Monsoon-like circulations . . . . .	206

Transport of moisture associated to cyclonic structures . . . . .	207
Moisture and energetics for extreme hurricanes . . . . .	207
10.2 Vertical structure of the transport of moisture . . . . .	209
Short range transport and orographic convection . . . . .	209
Long range transport and the extra-tropical connection . . . . .	210
Vertical transport of moisture to higher altitudes . . . . .	210
10.3 Response of the sources of moisture to conditional forcing . . . . .	212
Warming . . . . .	212
Atlantic SST forcing . . . . .	212
Extreme events . . . . .	213
10.4 CLLJ related aspects . . . . .	214
air-sea interaction . . . . .	215
<b>A Brief introduction to FLEXPART</b>	<b>217</b>
A.1 Computing . . . . .	218
A.2 Input data . . . . .	218
A.3 Physics of the model . . . . .	219
Parameterizations . . . . .	219
More useful information . . . . .	223
<b>B Monthly march of (E-P)-6</b>	<b>225</b>
<b>C Sources of moisture for the NAMS</b>	<b>227</b>
C.1 Moisture sources analysed from backward trajectories . . . . .	228





## List of Figures

1	Climatological VIDMF . . . . .	L
2	Annual cycle of precipitation . . . . .	P
3	Seasonal mean of the $(E - P)^{-6}$ field . . . . .	S
4	Identified sources of moisture . . . . .	T
5	Wavelet analysis of the relative contributions to precipitation over Central America from the identified sources of moisture . . . . .	W
6	Mean climatological air streams for the trajectories losing moisture over different locations of Central America. . . . .	
7	Diagramas de los mecanismos que intervienen en el transporte de humedad en la regi3n de inter3s . . . . .	
8	Sketch providing a summary of the conditions of the intensity of the CLLJ and the SST gradient between the Caribbean and ETPac that trigger the major changes in the transport of moisture from the Caribbean and associated precipitation. . . . .	
9	Analysis of transport of moisture for extreme ENSO. . . . .	
1.1	Specific humidity profiles . . . . .	4
1.2	The hydrologic cycle . . . . .	6
1.3	Climatological evaporation . . . . .	7
1.4	Climatological precipitation . . . . .	9
1.5	Climatological VIDMF . . . . .	11
1.6	Schematical representation of the main sources of moisture and associated sink locations for (a) February and (b) July, adapted from figure 1 of ? . . . . .	12
2.1	Seasonal climatological SST . . . . .	17
2.2	Climatological mean precipitation . . . . .	20

2.3	Annual cycle of precipitation . . . . .	21
2.4	Climatological conditions during NAMS . . . . .	23
2.5	Climatological conditions during SAMS . . . . .	25
2.6	Vertical profile of zonal wind nearby the CLLJ core . . . . .	26
2.7	Mean zonal wind at 925hPa . . . . .	27
2.8	Mean vertical structure of the CLLJ core . . . . .	28
3.1	Comparison between water vapour flux studies by Hastenrath, 1996 and Mestas-Núñez et al., 2006 . . . . .	36
3.2	Lagrangian interpretation schematic representation . . . . .	41
3.3	Summary of results of the quasi-isentropic analysis of vapour origin for precipitation events by Dirmeyer and Brubaker (2006) . . . . .	43
3.4	Summary of results shown by ? . . . . .	44
4.1	Simulations domain . . . . .	55
4.2	Schematic representation of the specific humidity variations that undergo an air particle . . . . .	56
4.3	Schematic representation of the integration method . . . . .	57
4.4	Schematic representation of the criteria used for the particles selection . . . . .	58
4.5	Clustering algorithm schematic representation . . . . .	60
4.6	Selected points for computing additional indices . . . . .	61
4.7	Location of rain gauges . . . . .	65
5.1	Vertically integrated divergence of moisture flux . . . . .	76
5.2	Long term mean $(E - P)^{-6}$ field . . . . .	77
5.3	Seasonal mean of the $(E - P)^{-6}$ field . . . . .	79
5.4	Long term seasonal means of the $(E - P)^{-n}$ field. . . . .	81
5.5	First 5 modes of the non rotated EOF pattern for the of $(E - P)^{-6}$ field . . . . .	82
5.6	Warm ENSO anomalies composites . . . . .	85
5.7	Cold ENSO anomalies composites . . . . .	86
5.8	ENSO and zonal wind regression maps onto El Niño 3.4 index . . . . .	87
5.9	Positive NAO anomalies composites . . . . .	88
5.10	Negative NAO anomalies composites . . . . .	89

5.11	Regression maps of onto NAO index . . . . .	90
5.12	Positive PDO anomalies composites . . . . .	91
5.13	Negative PDO anomalies composites . . . . .	92
5.14	Regression map of E-P and zonal wind onto PDO index . . . . .	93
5.15	Positive and Negative MJO anomalies composites . . . . .	95
5.16	Regression maps of the E-P field and zonal wind regressed onto the MJO index . . . . .	96
6.1	Identified sources of moisture . . . . .	100
6.2	Forward conditional ( $E - P$ ) for the CS . . . . .	102
6.3	Forward conditional ( $E - P$ ) for the GoMS . . . . .	103
6.4	Forward conditional ( $E - P$ ) for the ETPS . . . . .	104
6.5	Forward conditional ( $E - P$ ) for the NSAS . . . . .	105
6.6	Annual cycle of contributions to precipitation and distribution . . . . .	106
6.7	Correlations between observed precipitation and relative contributions to precipitation . . . . .	108
6.8	Time series for precipitation and estimated contributions to precipitation from the sources of moisture . . . . .	109
6.9	Wavelet analysis of the relative contributions to precipitation over Cen- tral America from the identified sources of moisture . . . . .	111
6.10	Hovmoller plots for the relative contributions to precipitation . . . . .	113
6.11	ENSO composites of the distribution of contributions to precipitation . .	115
6.12	NAO composites of the distribution of contributions to precipitation . .	116
6.13	PDO composites of the distribution of contributions to precipitation . .	117
6.14	MJO composites of the distribution of contributions to precipitation . .	119
6.15	Lagged cross-correlation between contributions from the sources and se- lected variability modes indices . . . . .	120
6.16	Time series for averaged observed precipitation over Costa Rica and Panama (black line) and the sum of the estimates of relative contributions to precipitation from the identified sources (gray line) for the analysis period. . . . .	122
6.17	Cross-correlation function for the contributions from the sources and observed precipitation.	123
6.18	. . . . .	125

6.19 Response of regional recycling to MJO . . . . . 127

6.20 Response of regional recycling to NAO . . . . . 128

6.21 Response of regional recycling to PDO . . . . . 128

7.1 vertically integrated divergence of moisture flux (VIDMF) field (shaded contours) and vertically integrated water vapour flux vector. . . . . 134

7.2 Mean climatological air streams for the trajectories losing moisture over different locations of Central America. . . . . 140

7.3 Mean climatological air streams for the trajectories losing moisture over GB and associated moisture content. . . . . 142

7.4 Mean climatological air streams for the trajectories losing moisture over HS and associated moisture content. . . . . 143

7.5 Mean climatological air streams for the trajectories losing moisture over Nic and associated moisture content. . . . . 145

7.6 Mean climatological air streams for the trajectories losing moisture over CRP and associated moisture content. . . . . 146

7.7 Vertical structure of transport of moisture to CRP . . . . . 148

7.8 Vertical structure of transport of moisture to Nic . . . . . 150

7.9 Vertical structure of transport of moisture to HS . . . . . 151

7.10 Vertical structure of transport of moisture to GB . . . . . 153

7.11 Climatological seasonal wind at 850hPa for the 1980-1999 period from ERA-40 Reanalysis . 154

7.12 Significant correlation pattern between the intensity of the  $(E - P) - 6$  field for Central America and the surface wind field . . . . . 156

7.13 Significant correlation pattern between the intensity of the  $(E - P) - 6$  field for Central America and the surface wind field . . . . . 157

8.1 Zonal and vertical structure of the moisture transport. . . . . 163

8.2 Significant correlation pattern between the intensity of the  $(E - P) - 6$  field for Central America and the surface wind field. . . . . 164

8.3 Significant correlation pattern between the intensity of the  $(E - P) - 6$  field for Central America and the surface wind field. . . . . 165

8.4 Significant correlation pattern between the intensity of the  $(E - P) - 6$  field for Central America and the surface wind field . . . . . 167

8.5	Significant correlation pattern between the intensity of the $(E-P)^{-6}$ field for Central America and the surface wind field. . . . .	168
8.6	Sketch providing a summary of the conditions of the intensity of the CLLJ and the SST gradient between the Caribbean and ETPac that trigger the major changes in the transport of moisture from the Caribbean and associated precipitation. . . . .	169
8.7	Analysis of transport of moisture for ENSO. . . . .	171
8.8	Analysis of transport of moisture for NAO. . . . .	171
8.9	Analysis of transport of moisture for PDO. . . . .	172
8.10	Analysis of transport of moisture for MJO. . . . .	173
8.11	Indices for the intensity of the CLLJ, SST gradient and conditional (E-P)-6 over the Caribbean Sea for the positive and negative phases of ENSO, NAO, PDO and MJO. . . . .	174
8.12	Analysis of transport of moisture for extreme ENSO. . . . .	177
8.13	Analysis of transport of moisture for extreme NAO. . . . .	178
8.14	Analysis of transport of moisture for extreme PDO. . . . .	180
8.15	Analysis of transport of moisture for extreme MJO. . . . .	181
8.16	Scatter plots of the linear relation between transport of moisture, relative contributions to precipitation and the CLLJ under the influence of ENSO	184
8.17	Scatter plots of the linear relation between transport of moisture, relative contributions to precipitation and the CLLJ under the influence of MJO	186
8.18	Scatter plots of the linear relation between transport of moisture, relative contributions to precipitation and the CLLJ under the influence of NAO	187
8.19	Scatter plots of the linear relation between transport of moisture, relative contributions to precipitation and the CLLJ under the influence of PDO	188
8.20	Scatter plots of the linear relation between transport of moisture, relative contributions to precipitation and the CLLJ under the influence of WHWP	189
8.21	Sketch of the mechanisms in which the CLLJ plays a role for the regional water cycle . . .	191
10.1	Hurricane Mitch vertical velocity (shaded) and relative humidity (line contours) used to approximate the hurricane horizontal extension, as indicated by the gray dots. . . . .	208
10.2	Seasonal $(E - P)^6$ fields for the Caribbean Sea (a) winter, (b) spring, (c) summer and (d) autumn in mm/day. . . . .	211

10.3	Seasonal $(E - P)^6$ fields for the Caribbean Sea (a) winter, (b) spring, (c) summer and (d)autumn in mm/day. . . . .	211
10.4	Seasonal $(E - P)^6$ fields for the Caribbean Sea (a) winter, (b) spring, (c) summer and (d)autumn in mm/day. . . . .	213
10.5	Seasonal $(E - P)^6$ fields for the Caribbean Sea (a) winter, (b) spring, (c) summer and (d)autumn in mm/day. . . . .	214
10.6	Seasonal $(E - P)^6$ fields for the Caribbean Sea (a) winter, (b) spring, (c) summer and (d)autumn in mm/day. . . . .	215
10.7	Seasonal $(E - P)^6$ fields for the Caribbean Sea (a) winter, (b) spring, (c) summer and (d)autumn in mm/day. . . . .	216
B.1	Mean climatological air streams for the trajectories losing moisture over different locations of Central America. . . . .	226
C.1	Long term mean of vertically integrated moisture flux divergence (shaded contours) and vertically integrated moisture flux (vector) . . . . .	229
C.2	Caption of subfigures (a), (b) and (c) . . . . .	231
C.3	Mean contributions from each source of moisture (in mm/day) for the composites computed, black presents the mean of the neutral composites. . . . .	232
C.4	Mean contributions from each source of moisture (in mm/day) for the composites computed, black presents the mean of the neutral composites. . . . .	233

## List of Tables

1.1	Main global sources of moisture and associated sink regions . . . . .	13
4.1	Output variables . . . . .	55
4.2	Additional variables retrieved from ERA-40 dataset . . . . .	63
4.3	Stations used for the evaluation of the estimations of precipitation from the Lagrangian approach. . . . .	66
4.4	ENSO Phases . . . . .	69
4.5	MJO Phases . . . . .	70
4.6	NAO Phases . . . . .	71
4.7	PDO Phases . . . . .	72
4.8	WHWP Phases . . . . .	73
7.1	February Month . . . . .	135
7.2	May Month . . . . .	136
7.3	July Month . . . . .	137
7.4	October Month . . . . .	138
A.1	Input data required to execute the FLEXPART model . . . . .	218





Part I  
Introduction



# 1

## Water Vapour in the climate system

The water vapour is a main element of the climate system that plays a direct role via radiative effects and indirectly through cloud, aerosols and chemical feedbacks (Gaffen et al., 1991). It has a relatively large heat capacity and is related with the storage of large amounts of energy. Moisture is key for driving the circulation in the atmosphere. The availability of water vapour is part of the closed cycle that links the radiative transfer and the circulation. The distribution of moisture in the atmosphere depends on temperature, evaporation and precipitation. The general known features of the distribution of moisture in the atmosphere are a) its decrease with height and b) the excess of water vapour in the tropics compared to higher latitudes (Peixóto & Oort, 1984). A brief description of the distribution of atmospheric moisture is presented followed by a review of the main details of the key components of the hydrological cycle. Since the hydrological cycle can be understood in terms of the balance between evaporation and precipitation with the transport of moisture, therefore, associated with sources and sinks of moisture, the general picture of the global moisture sources and sinks is presented.

## 1.1 The structure of the distribution of moisture and moisture availability

The mean distribution of moisture in the atmosphere is depicted in figure 1.1, specific humidity is maxima in the tropics (figure 1.1.a) and the major part of the moisture content is trapped in the lower levels (figure 1.1.b). The sharp difference between the moisture content in the tropics and the poles is due to the fact that cold air can only hold very little water vapour. ? This particular distribution highlights the importance of the tropical regions, where most of the global moisture is contained. The monitoring of the distribution of atmospheric water vapour is complex and has been favoured by the satellite era<sup>1</sup>.

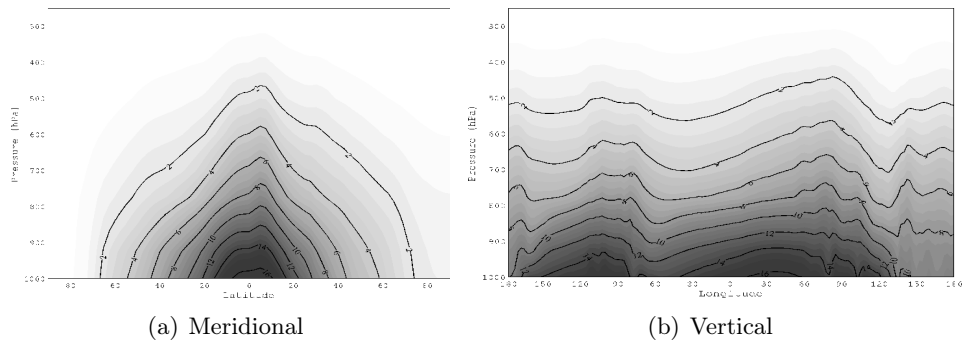


Figure 1.1: Average profiles of specific humidity in  $g/Kg$  from ERA-40 Reanalysis data for the 1980-2000 period

From the meridional average of specific humidity shown in figure 1.1.a two regions are highlighted. First, the region extending from the easternmost portion of the tropical Atlantic to the region enclosed by the China Sea. North Africa, the Mediterranean Sea, Middle East and China (and surrounding water bodies) are the components of this region. Processes involving large amounts of moisture and important convection are known to occur in these locations. The global distribution of water vapour has a strong relation with the regions associated as large sources of moisture for determined regions. Consider for example the case of the Mediterranean Sea, which is known to be an important source of moisture for weather systems affecting Europe and North Africa.

<sup>1</sup>satellites are of particular importance for estimating water vapour (among other parameters) in the upper levels, where measuring is complex and very expensive

Meanwhile, the Red and Arabian Seas have been also found to be important moisture suppliers to Middle East and from central to eastern Eurasia (Gimeno et al., 2011; see their figure 1.b). The second region that exhibits a maxima in specific humidity is the one comprised between the Caribbean Sea and the Eastern Tropical Pacific. This region is extremely important since it includes the elements of the IAS, the WHWP and a portion of the tropical Pacific featured to be a region of important evaporation (Amador et al., 2006).

## 1.2 Water vapour and the water cycle

The relationship between the distribution of moisture and the surface energy balance implies a link between moisture and temperature. As any other substance, phase changes of water are strongly related with the temperature. In fact, for water vapour, the saturation vapour pressure can be approximated as an exponential function of the temperature (Clausius-Clapeyron relationship). The Sun provides the energy required to evaporate water from the ocean surface, which is transported in all directions and approximately one third of this evaporated water precipitates over land areas (Hartmann, 1994 ). In agreement with the distribution of water vapour, the convergence of meridional flux of water vapour peaks at the tropics. Within the water cycle, evaporation and recycling provide the moisture that precipitates over the globe and is redistributed by transport processes. The diagram of figure 1.2 shows an adaptation of figure 1 from ? in which the global and local water cycles are represented. Several studies on the global and regional water cycle have been carried out in terms of the atmospheric water budget. From diagram in figure 1.2, the balance between evaporation, precipitation, recycling and transport of moisture is important at different spatial scales

### Components of the water cycle

#### Evaporation

The evaporation simply said, is the conversion of water into air. In the air-water interface it can be estimated in terms of a turbulent exchange coefficient  $c_e$ , wind speed  $U$ , the saturation specific humidity at the sea surface  $q_s$ , near surface atmospheric specific humidity  $q_a$  (function of air temperature  $T_{air}$  and relative humidity  $RH$ ) and

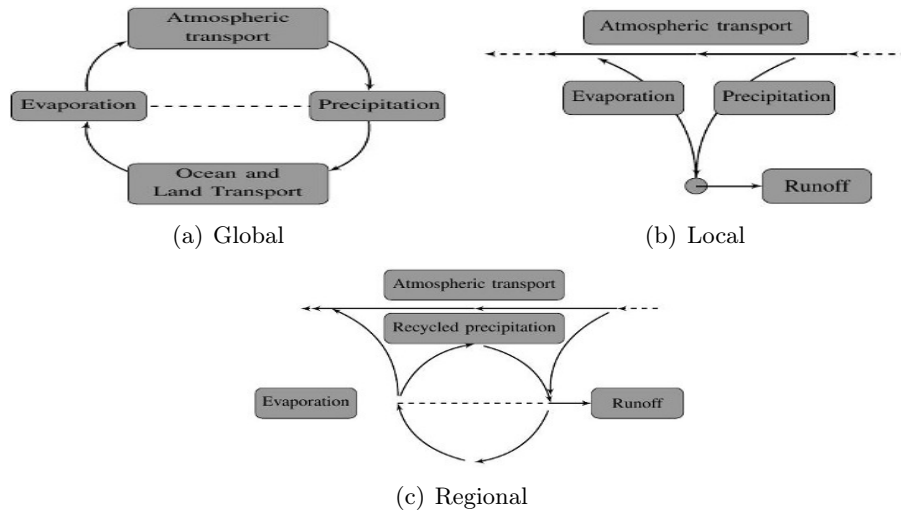


Figure 1.2: A representation of the (a) Global, (b) local, and (c) regional hydrologic cycles adapted from ? is presented.

$dq = q_s - q_a$  as described by (Fairall et al., 2003) (see equation 1.2). As part of the hydrological cycle, evaporation from the ocean surface is of main interest since it provides approximately an 80% of the total evaporated water from the globe (Trenberth, 2007). ? indicates heat energy, air-sea humidity differences and wind as main requirements for evaporation to occur. The first to break the hydrogen bonds, the second to set up a threshold for which evaporation may undergo or not and the third to maintain the vertical air-sea humidity gradient. From the dependence of evaporation on temperature it follows the role of SST patterns in the distribution of evaporation. Therefore, evaporation is also a function of the radiative energy balance and present a similar pattern to those of incoming solar radiation and SST distribution. Estimation of evaporation is quite complex and biases are large since calculations require surface fluxes that are not easy to measure systematically for the entire globe. Traditional bulk parameterizations (Liu et al., 1979) and current satellite facilities (Schlosser and Houser, 2007) enable the computation of global datasets of reasonable accuracy. The OAFflux<sup>2</sup> products (Yu & Weller, 2007) are widely used for different applications requiring surface fluxes and evaporation data. Figure 1.3 shows the climatological mean of evaporation for a) February and b) July, showing the most important regions of oceanic evaporation to be the

<sup>2</sup><http://oafux.whoi.edu/>

tropical regions and the western boundary currents.

$$E = c_e U (q_s(SST) - q_a(T_{air}, RH)) \quad (1.1)$$

$$E = c_e U dq \quad (1.2)$$

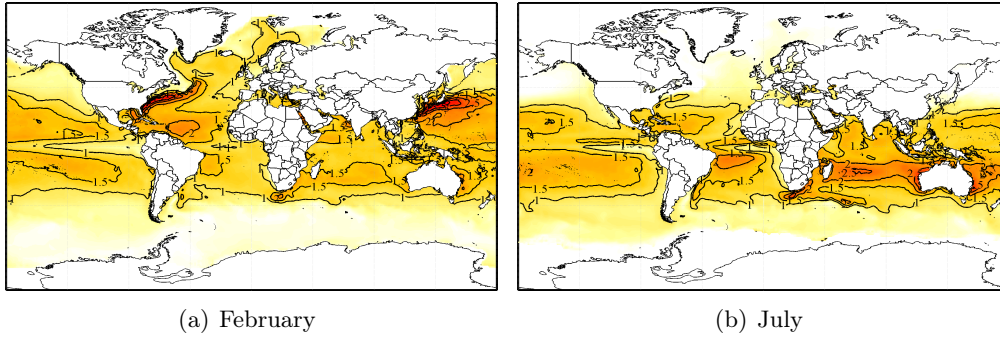


Figure 1.3: Climatological monthly mean of evaporation based on OAFUX data for the 1980-1999 period in  $m$  for (a) February and (b) July. Data was retrieved from the OAFUX project website

## Recycling

Recycling is the contribution of local evaporation to local precipitation (Trenberth, 1998). Over land, this is basically the contribution of evaporation from the land surface. Recycling helps to understand the land-atmosphere coupling and supply of water vapour and latent energy to the atmosphere, leading variables in the formation of precipitation (B. & L., 1996). Recycling has a significant contribution to the heat and moisture budgets of the clouds (Worden et al., 2007). Precipitation recycling is an important moisture supplier for large regions such as the Amazon basin (B. & L., 1996) and Europe (Bisselink & Dolman, 2008). Determinant factors for the modulation of precipitation recycling are winds, topography and land cover (J. et al., 2010). The theoretical framework for its quantification was set after Budyko and Drosdov (1953) and later in English by Budyko (1974). The analytical model of Budyko to estimate recycling assumes: a) a well mixed atmosphere and b) that the change in storage of water vapor is smaller compared to the fluxes of atmospheric water vapour at long timescales. Thus model has been extended to two dimensional models. ? and ? presents a recycling

formulation in terms of the intensity of the hydrological cycle, from which large recycling is noticed over the main river basins and transport of moisture shows a determinant role.

## **Precipitation**

The global picture of precipitation follows a similar distribution to that of humidity in the air, with larger values over the tropical belt where low level convergence is a maximum. Observing global precipitation is not easy, mainly because the distribution of rain gauges is not homogeneous<sup>3</sup> over the globe and measuring precipitation over the oceans is not straightforward. As with water vapour content and estimation of evaporation, satellites become very useful to overcome the issue of observing precipitation at a global scale. Merging observations with satellite retrievals provide reasonable reanalysis of global precipitation (even when biases are large). ? present in their figure 4 a comparison between different global precipitation datasets. Despite the differences among them, the pattern is almost the same, with a marked intensification of precipitation over some regions during summer. Figure 1.4 shows the climatological mean of precipitation from CMAP data (Xie and Arkin, 1997). There are regions in which precipitation is significantly more intense as a result of monsoon circulations. These regions are West Africa (Janicot et al., 2009), Asia (Kang et al., 1999), Australia (Taschetto et al., 2010) and the Americas (Vera et al., 2006).

It is also important to mention that moisture is a requirement for precipitation to occur in terms of microphysical processes. ? point out that the upper level clouds in the tropics, enhanced by deep convection, generate precipitation that falls through a sub-saturated environment. Therefore, the importance of water vapour associated to precipitation is also related with stability, convection and the transport of moist air. The latter is important in the case of deep convection since it enhances the transport of saturated air into the upper troposphere acting as a source of moisture (Salathé & Hartmann, 1997).

---

<sup>3</sup>historically, the observing systems have been located in the northern hemisphere



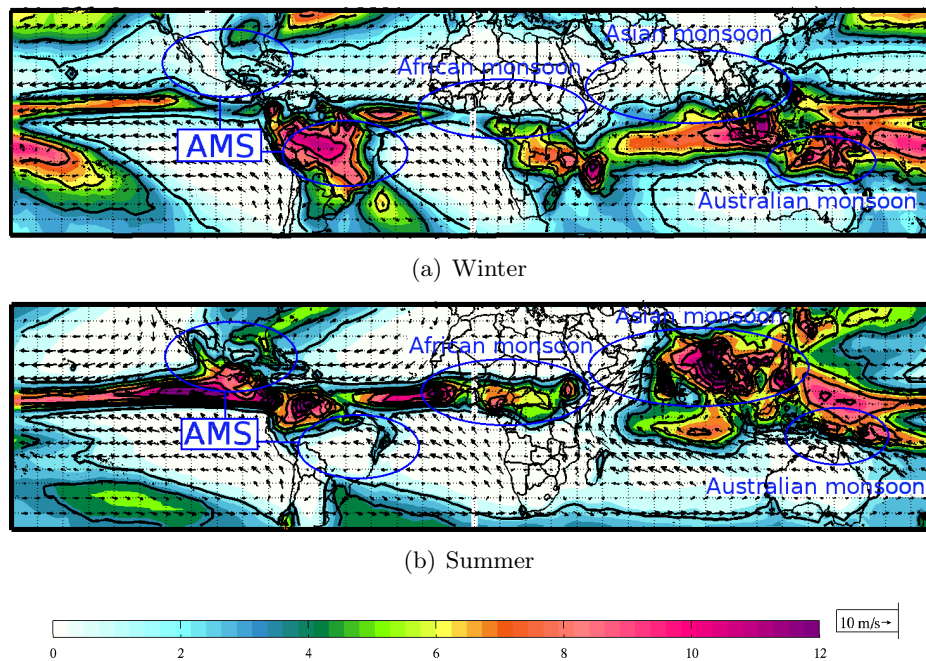


Figure 1.4: Climatological monthly mean of precipitation based on CMAP data for the 1980-1999 period in  $mm/day$  and wind vector at 850 hPa from ERA-40 Reanalysis for (a) Winter and (b) Summer. Worth is to notice the largest intensity of precipitation over the tropical belt, from which the ITCZ and the monsoon circulation regions are noticeable as the main large scale features of global precipitation

### Transport of moisture

The role played by the transport of moisture is a fundamental element of the water cycle as shown in figure 1.2. Moisture is transported by winds, mainly from the oceans to continental regions but also from other continental areas. Seasonality of precipitation is strongly associated with the circulation by means of the winds. Consider e.g. the case of the monsoon circulation associated with heavy rainfall as mentioned previously. Moisture can be transported at different scales, the most efficient is the regional transport in which most of the moist content of the air can be transferred between nearby locations. However, transport at larger scales has been found to be important, as is the case of the transport between tropics and extratropics. In this, moisture can be transported long distances, providing a connection between processes in the tropics with extratropical precipitation as the case of the 'pineapple express' (Peter & Heini,

2010). Since moisture availability is larger in the lower troposphere, low level winds are expected to carry most of the moisture. Nevertheless, the vertical transport of moisture is also important in terms of convection. The vertically integrated total horizontal flux of water vapour provides an approximation to the transport of moisture in the atmosphere. Let  $\Theta$  be the transport of moisture,  $P$  the pressure,  $q$  the specific humidity,  $V_{x,y}$  the horizontal wind field and  $g$  the acceleration of gravity, the transport can be estimated as:

$$\Theta = \frac{1}{g} \int_{sfc}^{top} q V_{x,y} dp \quad (1.3)$$

The principle of conservation of mass states that the rate of change of water storage  $W$  must be balanced by the vertically integrated moisture flux divergence  $\nabla \cdot \Theta$  and the difference between evaporation "E" and precipitation "P" when the balance water residual is small, so that equation 1.3 becomes.

$$\frac{dW}{dt} = (E - P) - \nabla \cdot \Theta \quad (1.4)$$

when the averaging time period is large (several years), the water vapour storage term becomes small and can be neglected so that the vertically integrated moisture flux divergence balances the difference between evaporation and precipitation.

$$\nabla \cdot \Theta = E - P \quad (1.5)$$

This expression is very useful in the interpretation of the presence of sources and sinks of moisture, since it provides an estimate of the fresh water flux balance at the surface from the divergence of the moisture transport flux.

### 1.3 Sources of moisture and precipitation around the globe

If water evaporated from the oceans is transported to the continents where it accounts for precipitation, the oceans are a determinant moisture supply for continental precipitation. Figure 1.5 shows the mean divergence of the vertically integrated moisture flux. According to the balance equation, regions in which evaporation exceeds precipitation can be considered sources of moisture. Therefore, those regions in which the divergence of moisture flux is negative are sinks of moisture. The conditions of these sources and sinks of moisture are sensitive to the seasonal variations of the moisture availability in

the atmosphere as well as to circulation. As is natural, from the figure 1.5 it can be followed that the oceanic regions represent important sources of moisture whereas the regions associated with strong convergence are large moisture sinks (as is the case of the ITCZ). To determine which source contributes with moisture for precipitation over determined regions, the source-sink relationship is extremely useful. Several studies focus on the study of the sources of moisture associated with precipitation in regions of specific interest.

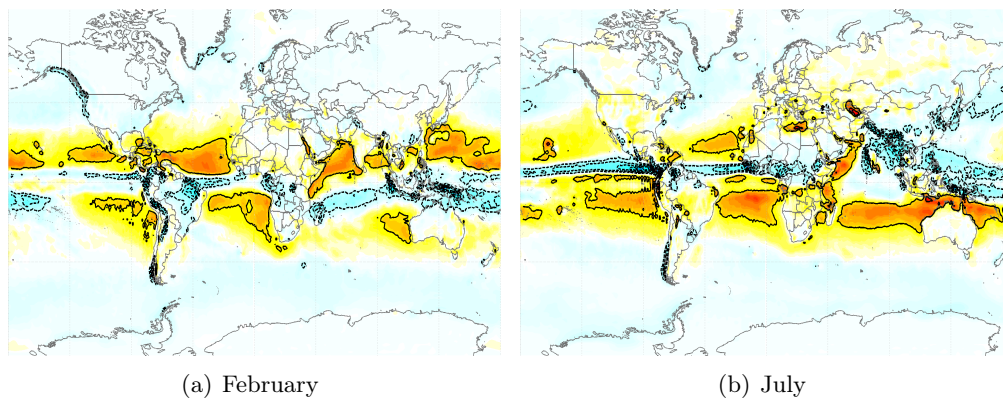


Figure 1.5: Climatological monthly mean of vertically integrated divergence of moisture flux computed from ERA-40 data for the 1980-1999 period in  $Kgm^{-2}s^{-1}$  for (a) February and (b) July. Note the regions where divergence is in average positive compared with the regions with more intense evaporation in figure 1.3. Those regions are featured to be importance sources of moisture, conversely to those regions featured by convergence where precipitation is known to be more intense, in agreement with the patterns of figure 1.4)

### Main global sources of moisture

From figure 1.5, the large evaporation regions correspond to the oceans, which are the main sources of moisture for continental precipitation (Gimeno et al., 2010). One of the most important oceanic sources of moisture is the Atlantic ocean (AO). The tropical AO is known to be a source of moisture for the IAS system and the Amazon region (Marengo, 1992). While the North-Atlantic Ocean is able to provide moisture for several regions as Mexico, USA, British Isles, Mediterranean and Central Europe (Gimeno et al., 2010). The South Atlantic Ocean is well known to contribute to the northeastern part of Brazil (Yoon & Zeng, 2010), as well as for providing moisture for

the development and maintenance of major cyclones in South America (Reboita et al., 2010). In the vicinity of the tropical Atlantic, the Caribbean Sea as part of the IAS system has been determined to be the main source of moisture for Central America (Durán-Quesada et al., 2010), the Gulf of Mexico (Mestas-Núñez et al., 2005) and even the extratropics (Peter & Heini, 2010). The Pacific Ocean, characterised by the presence of the largest warm pool contributes to Eurasia, west coast of North America. The Indian Ocean (IO) is also an important source despite is not active all year round as is the Atlantic. The IO is a key source of moisture for the development of the Indian monsoon and it also contributes to Africa, Australia and southern Asia. Other water bodies rather than the oceans account importantly as sources of moisture as is the case of different seas and rivers (Stohl & James, 2005).

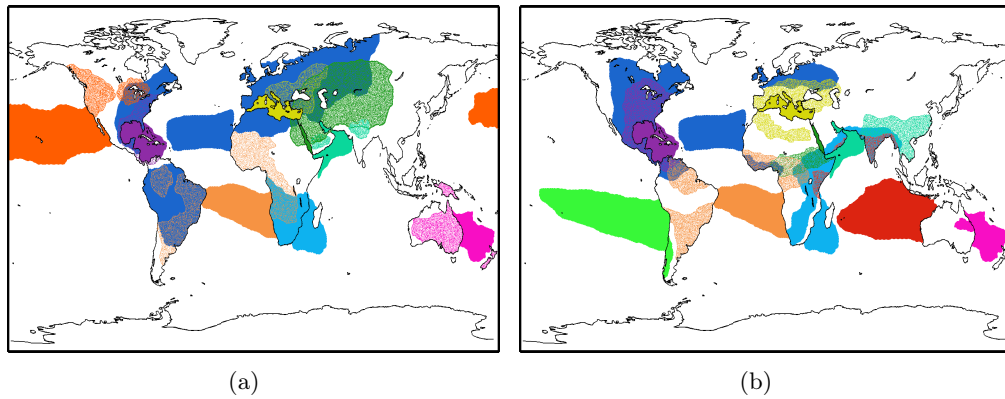


Figure 1.6: Schematical representation of the main sources of moisture and associated sink locations for (a) February and (b) July, adapted from figure 1 of ?

Evaporation also occurs over land, so that the continental regions themselves are also sources of moisture due to recycling. The Amazon has been shown to be an important source of moisture due to this process as the NAM region. Table 1.1 provides a summary of the mean global sources of moisture and figure 1.6 shows a summary of the main sources of moisture and the associated continental region to which they contribute to show the seasonal behaviour of the sources os moisture and their sinks.

<b>SOURCE</b>	<b>INFLUENCE REGION</b>	<b>REFERENCES</b>
<b>CONTINENTAL SOURCES</b>		
EEEV	China	?
	Siberia	?
USEV	Northeastern USA, Europe	?
NAM	North America	Dominguez et al. (2010)
SA	South America	?
Waf	West Africa	?; ?
SAf	West Africa	?; ?
EAF	West Africa	?; ?
	Congo	?
Congo	Sahel	?
<b>OCEANIC SOURCES</b>		
NAtl	Continental and ECNA	?
	Western Europe, British Isles	?
CS	Caribbean Islands, Central America	?
	Gulf of Mexico	?
SA	South American east coast	?;?
SA	Antartica	?
NP	Eurasia, North America west coast	?
SP	South America west coast	?
	Australia, Indonesia and Antartica	?
IO	East Africa, Australia and Southern Asia	?
	South Africa	Stohl & James (2005)
MS	Iberian Peninsula, North Africa	?
RS	Gulf of Guinea, Indochina	?
	African Great Lakes and Asia	?

Table 1.1: A summary with the main sources of moisture with their correspondent sink regions is provided, note that the list aims to provide a general idea and is not an exhaustive list of source/sink regions and related works



# 2

## Climate and variability in the IAS

The Intra Americas Sea (IAS) comprised by the Gulf of Mexico and the Caribbean Sea, is fundamental for the regional climate system. Its particular location makes it sensible to the effect of both regional and large scale dynamical systems acting in its vicinity. A belt of large latent heat fluxes, strong easterly winds, a developed pressure system defined as the NASH (North Atlantic Subtropical High), warm SSTs and intense precipitation build up the general picture of regional climate and variability (Wang et al., 2008). The Caribbean Sea as a component of the IAS is significant due to its importance as a cyclone-genetic activity region. The region is located under the Inter Tropical Convergence Zone (ITCZ), enhancing the importance of precipitation regimes jointly with the Mid Summer Drought (MSD) which is another feature of regional precipitation (Magaña et al., 1999). Local intensification of the easterly winds is a remarkable feature of the region associated to the Caribbean Low Level Jet, CLLJ, (Amador, 1998). The wide variety of processes and structures leading climate and its variability in the IAS is of importance for the region but also for the extra-tropics. To provide the basis of the general processes that take place in the analysis region, a brief introduction to the main features of climate in the IAS and the major modes leading variability are described along this chapter.

## 2.1 Climate in the IAS region

The location of the IAS enables the entrance of large amounts of net radiant flux of energy into surface, while the heat capacity of regional water bodies favours the energy storage. The main features of the IAS climate include pressure systems, precipitation patterns over Central America, the Caribbean Sea and the Gulf of Mexico and the hurricane season. The presence of a warm water body and the particular distribution of precipitation are of importance for the discussions provided through this document.

### Western Hemisphere Warm Pool

As already mentioned, the tropical belt is known for a maximum of incoming solar radiation (of the order of  $240 \text{ W m}^{-2}$ ) and SST is particularly warm in the vicinity of the Caribbean Sea and the Gulf of Mexico. The Western Hemisphere Warm Pool (WHWP) has been defined as enclosed by the  $28.5 \text{ C}$  isotherm. It corresponds to the second largest warm water body after the Indo-Pacific Warm Pool (Wang & Enfield, 2002). The WHWP has a defined seasonal cycle in which warmer temperatures are dislocated from the Eastern North Pacific (ENP) and west of Central America to the IAS. The structure extends along the western Tropical North Atlantic (TNA) following the description by ? (see details in figure 2.1). According to ?, ?, there is an important link between seasonal variations in tropospheric heat and moisture over tropical Americas and the development of the WHWP. Moreover, the WHWP anomalies may have a significant impact for the development of tropical convection.

The east component of the WHWP defined as the Atlantic Warm Pool (AWP) has been shown to be important for the IAS in both seasonal and inter-annual scales (Wang et al., 2006). The importance of the AWP relies on its potential role to influence local winds, precipitation and hurricanes (Wang & Sang-Ki, 2007). SST gradients enhanced by the AWP may be partially responsible to force low level winds and convergence in the region, through mechanisms as the one proposed by ?. A similar reasoning involving the influence of the NASH is followed by ? to study the role of the AWP in the forcing of the CLLJ and associated zonal moisture transport.



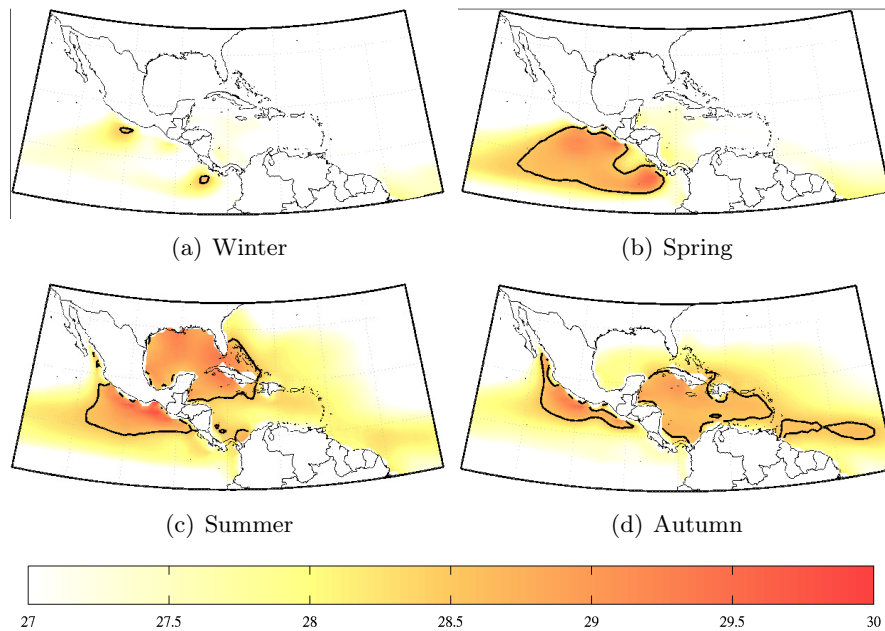


Figure 2.1: Seasonal climatological SST for the analysis region based on ERA-40 Reanalysis monthly data for the 1980-1999 period. SST larger than 28.5 C is contoured from orange to reddish colors in order to highlight the area comprised by the WHWP as defined by Wang and Enfield (2001). Data were retrieved from the ECMWF MARS server.

Based on observations, ? showed a relationship between variations in the AWP and the vertical wind shear that may affect the Atlantic hurricane activity. The period between summer and autumn is of particular importance since the AWP is fully developed. The influence exerted by the AWP on the vertical wind shear seems to be restricted to the transition between summer and autumn. In this period, the AWP dislocates southward and extends into the Atlantic sector (see figure 2.1) as highlighted by ?. Variability of the AWP is constrained by the major modes of variability influencing primarily the NASH, being ENSO the most important for regional variability. The importance of the AWP for climate in the IAS as well as interactions with the CLLJ and convective systems have been extensively studied. The role of the AWP for the climate system goes beyond regional interactions since atmospheric circulation cells have been proposed to be affected by Atlantic variability (Wang & Enfield, 2002). It is important to point out that the WHWP is of importance regarding moisture availability due to the enhancement of evaporation as well. At the same time that the relation between

warmer SSTs and regional winds is key for moisture transport processes.

### **Distribution of precipitation**

The distribution of precipitation in the IAS is determined by convective processes over the Caribbean, the seasonal migration of the ITCZ, the hurricane season and the MSD among other systems such as cold fronts.. The IAS is sensible to intense rainfall events and severe floods which affect mainly the Caribbean Isles and Central America. In general terms the distribution of precipitation over this region is bimodal. A significant reduction of precipitation during July-August is the main feature of the dry spell that affects Central America, specially the Pacific slope and some parts of the Caribbean. Even when precipitation patterns for Central America and the Caribbean may look similar, there are remarkable differences between different locations (see figure 2.2 for details on monthly precipitation patterns in the IAS). Precipitation in Central America is the result of the junction of various systems. The ITCZ, local winds and topography play a major role leading the observed precipitation distribution.

The climatologies of precipitation show the presence of the ITCZ as a well determined band. Precipitation in the Pacific slope is partly under the influence of the seasonal migration of the ITCZ. The Caribbean slope is mainly triggered by the transport of moisture from the Caribbean Sea, local topography and cyclonic systems developing in the Atlantic (Amador et al., 2003). Early descriptions of precipitation distribution in Central America have been given by Portig (1965) and Hastenrath (1966). A general overview is provided by figures 1 and 9 of Portig (1965) and Hastenrath (1966) respectively, where both authors remark the presence of a dry spell during mid-Summer. Hastenrath (1966) discusses the main features of the precipitation distribution in terms of the dynamics and focuses on the importance of regional climate variability, pointing out the role of the easterly waves in the trades inversion and its effect on regional precipitation.

Precipitation in Central America is described by two rainfall maxima in May-June and September-October with a marked dry spell in July-August. Winter and early Spring are normally dry periods with even drier conditions in the Pacific slope on average, as described by Alfaro (2002). The dry period between the two rainfall maxima is known

as the MSD (Magaña et al., 1999) and will be discussed later on. Precipitation distribution over Central America has been also found to be of importance related to storm activity in the eastern Pacific as pointed out by ?. Other studies are based on reanalysis and supported by observations on some Caribbean Isles to analyse the annual cycle of precipitation in the Caribbean as well as its variability (Gamble et al., 2008; Giannini et al., 2000). The use of statistical and numerical modelling has been also an alternative to study different aspects related to precipitation and variability in the Caribbean for forecasting (Ashby et al., 2005; Curtis & Gamble, 2007; Martínez-Castro et al., 2006). However, some important biases are caused primarily by physical parametrizations. Great efforts have been put in ongoing research to overcome this difficulty (Biasutti et al., 2006). The assimilation of observations has been found to solve significantly the biases, see for example recent NCEP Climate Forecast System Reanalysis dataset (Saha et al., 2010). Dynamically, Caribbean rainfall is influenced also by the Pacific ocean because of the location of the Central American Isthmus. The influence of these two water bodies determine some of the fluctuations observed in the rainfall rates (Chen & Taylor, 2002; Taylor et al., 2002). A dry season in the Caribbean occurs during winter, followed by a sharp increase in precipitation after March. A kind of MSD is also present in the Caribbean and after September precipitation increases again, influenced by the onset of the hurricane season (Angeles et al., 2010; Mestas-Nuñez et al., 2005). The mean climatological distribution of precipitation can be observed in figure 2.2, from which similarities and differences with respect to precipitation in Central America can be noticed. It is also important to remark that precipitation in the Caribbean has been shown to be related with large-scale disturbances as ENSO and NAO (Giannini et al., 2000; Mapes et al., 2005; Amador & Magana, 1999).

### **The Mid-Summer Drought**

This feature of Central American and Caribbean distribution of precipitation is referred to a decrease in precipitation from July to August. There is a dry period during winter and early spring, followed by a peak in precipitation during the rest of spring and autumn with a dry period in-between. This dry period is popularly known as 'canícula' or 'veranillo' and has been used by local farmers to determine the crop season for some products. This MSD is a permanent feature of regional precipitation and is extremely

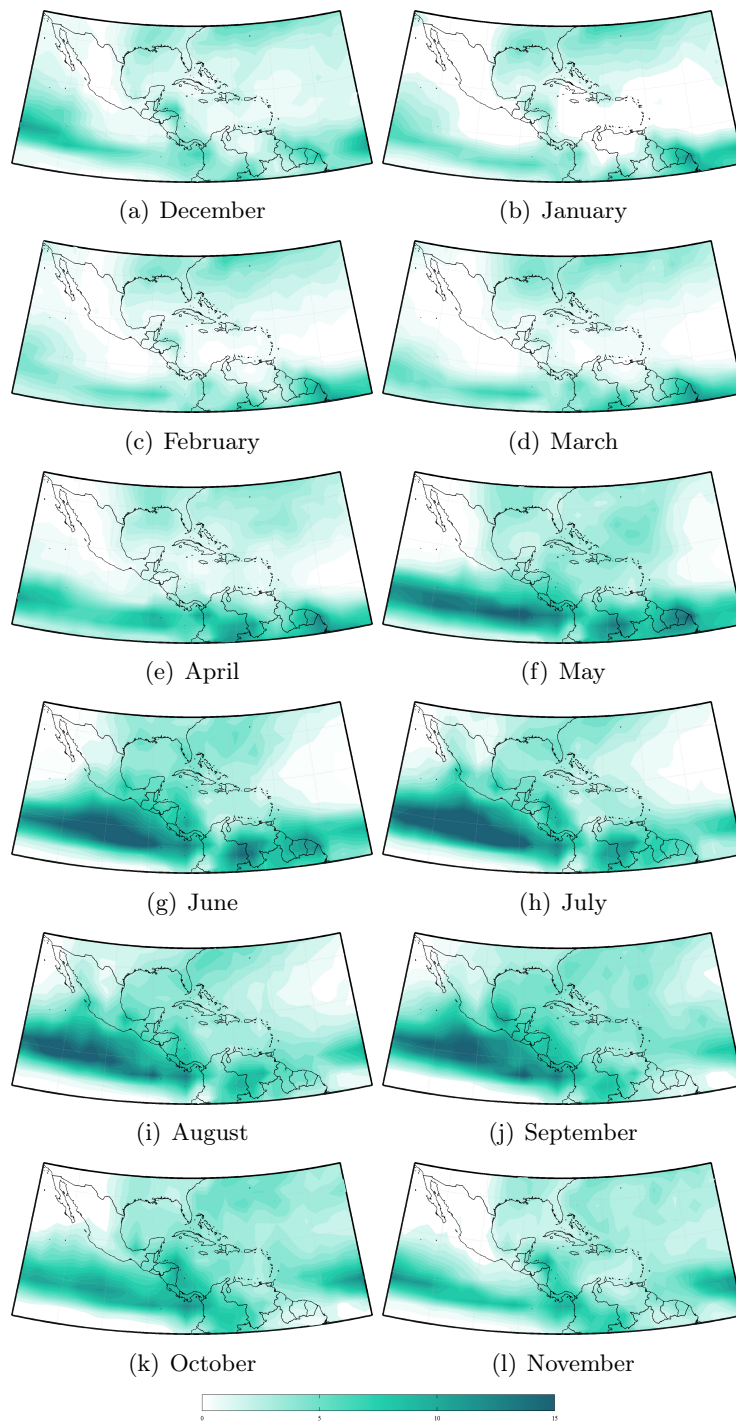


Figure 2.2: Climatological monthly mean precipitation for the 1980-1999 period from the Climate Prediction Center Merged Analysis of Precipitation (CMAP) dataset, units are in  $\text{mmday}^{-1}$ . Data was retrieved from the CMAP website <http://www.esrl.noaa.gov/psd/data/gridded/data.cmap.html>.

related with low level winds and the AWP (Magaña et al., 1999; Wang & Enfield, 2002). The link between the MSD and SST anomalies over warm water bodies is explained by variations in convective activity (Magaña et al., 1999). The SST is not the only field involved, the presence of the CLLJ has been also related to the intensity and variability of the MSD (Amador, 2008). The MSD is then, associated with changes in convective activity linked to SST distribution, incoming solar radiation and the seasonal cycle of the easterly wind flow (Magaña et al., 1999).

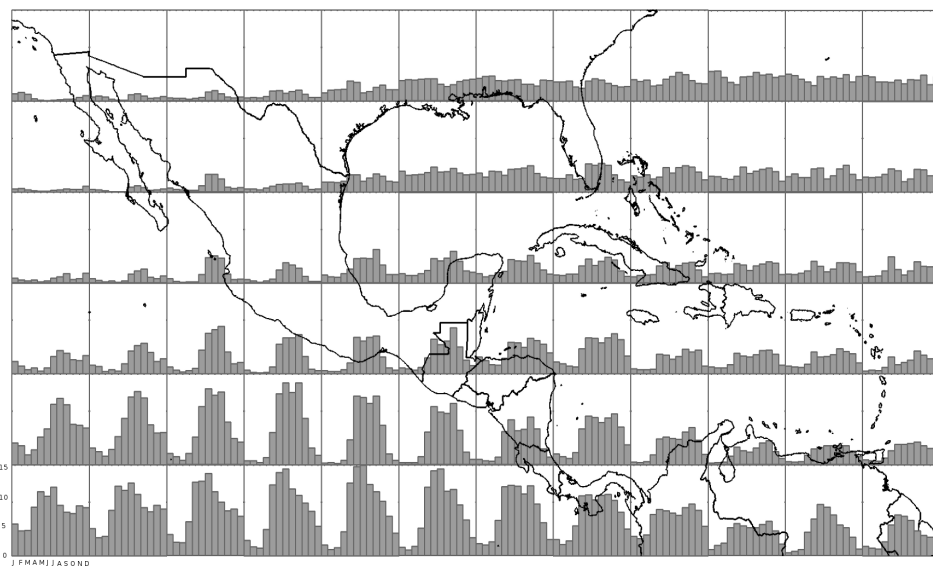


Figure 2.3: Climatological distribution of monthly mean precipitation ( $mmday^{-1}$ ) for contiguous  $5 \times 5$  area boxes. Dataset and analysis period as in figure 1.3. Bars show the value of precipitation for each month, the scale is from zero to  $15 mmday^{-1}$

## 2.2 The American Monsoon System

The IAS has been found to be important for climate processes in Central America and the Caribbean. However, the configuration of the IAS is of remarkable importance for climate in the surrounding extra-tropics. As an example, the distribution of precipitation in southern North America and central South America is modulated by processes

that take place within the IAS. The large amounts of energy stored in the IAS and the ocean-land distribution enable monsoon-like circulations to be fed by local moisture transport processes (Amador, 2006). Seasonal surface pressure distribution and low-level inflow of oceanic moisture in the Americas exhibit a monsoon-type pattern (Mechoso et al., 2004). Precipitation distribution with significant maxima over some locations in the Americas is also an indicator of such monsoon-like circulations in the region (Vera et al., 2005). Such circulations and precipitation distributions associated has been identified as a regional monsoon system known as the American Monsoon System (AMS).

The AMS is composed by two individual systems located in the northern and southern hemispheres of America. The North American Monsoon System (NAMS) is featured by intense precipitation over some locations in Mexico and south-west United States. Meanwhile, the South American Monsoon System (SAMS) is featured by intense precipitation over Central Brazil and Bolivia (Mechoso et al., 2004). The AMS is influenced by the continental distribution and alignment, topography and meteorological fields (e.g SST, SLP and winds). The presence of low level jets transporting moisture that favours the development of the monsoon circulation and enhance the intensification of precipitation is a common feature of both systems (SAMS and NAMS). The dynamics underlying the onset of the NAMS and the SAMS has been an important subject of study and field campaigns have been implemented to improve the knowledge of these structures. A brief description of both NAMS and SAMS is provided, focused on the main features of the structures, their seasonal cycle and mechanisms involved in it.

### **North American Monsoon System**

The NAMS accounts for approximately over 40 % of the summer rainfall for western Mexico and southern United States. ? point out that in some regions of Mexico, rainfall associated to the NAMS can contribute up to the 70% of annual rainfall (see figure 2.4 for an overview of precipitation distribution over North America during Summer). There is a relationship between the rainfall observed during the monsoon and the ITCZ movement. The meridional thermal contrast also accounts for an important component of the monsoon over water (Ropelewsky et al., 2004). The Gulf of Mexico, Pacific Ocean and the Gulf of California are the major oceanic components playing a

role for the NAMS onset. Complex orography over the region is the counterpart over land (Rocky Mountains and Sierra Madre) which indeed influences the evolution of the circulation patterns of the NAMS in the upper levels.

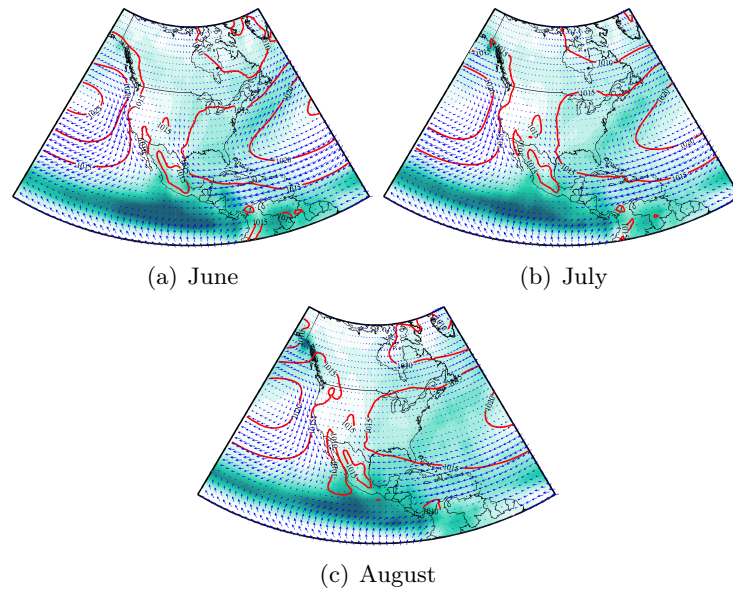


Figure 2.4: Climatological values for mean precipitation (green shaded contours) from CMAP dataset, SLP (red line contours) and surface wind (vectors) from ERA-40 Reanalysis dataset for the period of active NAMS: a) June, b) July and c) August.

Low level circulation during the pre-development of the NAMS, is characterised by the importance of easterly and south-easterly flow in the Gulf of Mexico and linked to the Great Plains Low Level Jet (GPLLJ). Due to the rainfall amount associated to the NAMS and in order to understand the dynamics and variability of the NAMS it is determinant to know the sources that provide moisture to the NAMS. Previous studies have suggested that the moisture source to the NAMS is located eastward, particularly the Gulf of Mexico as indicated by ?. Observations, reanalysis and modelling studies have been used to determine the origin of the moisture of the NAMS (Castro et al., 2001). According with those studies, the dominant sources of monsoon precipitation associated to the NAMS are the result of local continental evaporation and transport from adjacent oceanic regions. The North American Monsoon Experiment (NAME)

(Mesinger et al., 2006; Higgins et al., 2006) provided a large dataset of observations to study specific components of the NAMS. The modelling strategy has been useful in the improvement of the ability in the simulation and prediction of the monsoon precipitation.

The importance of moisture transport from the Gulf of Mexico and the Caribbean Sea (Mo et al., 2005; Wang, 2007; Mestas-Nunez et al., 2007) has been highlighted. Moisture transport from the Caribbean Sea and the related transport mechanisms are then crucial to understand the evolution of the NAMS. This evidences the importance of studying the interactions between regional systems that may trigger the transport of moisture. The relation of the GPLLJ and the NAMS regarding moisture transport from the Gulf of Mexico and the Caribbean Sea has been indicated in some of the above mentioned works. Furthermore, it has been proposed a connexion between the GPLLJ, the transport of moisture and the CLLJ. The general picture acquires complexity while trying to have an integral overview of the climate system in the IAS. Different scientific questions merge regarding mechanisms and processes. In this framework, a key element must be highlighted: moisture. Questions of remarkable interest to understand one of the components of the NAMS are where does the moisture come from? and, how does the moisture is transported to the NAMS?

### **South American Monsoon System**

Precipitation regime in South America is lead by the Andes, the Bolivian High , the Chaco Low and the South America Convergence Zone (SACZ) (Y., 1992). This region is well known for the variations from extreme rainfall to severe droughts. Intense rainfall has been documented to be a permanent feature of the seasonal cycle in some locations, i.e the Amazon (Houze & Betts, 1981; Czikowsky & Fitzjarrad, 2009; Petersen et al., 2002). Conversely, there are some periods marked by severe droughts in North-east Brazil (Hastenrath, 2006). The transition between dry and wet seasons has been explored in terms of thermodynamic and dynamical variations of the troposphere (Marengo et al., 2001). the seasonal distribution of precipitation and the sharp contrast between dry and rainy seasons are what defines the SAMS as the counterpart of the NAMS in South America (Vera et al., 2006; and references therein). Figure 2.5 shows



the distribution of precipitation during austral Summer, period in which a monsoon-like precipitation pattern is identified.

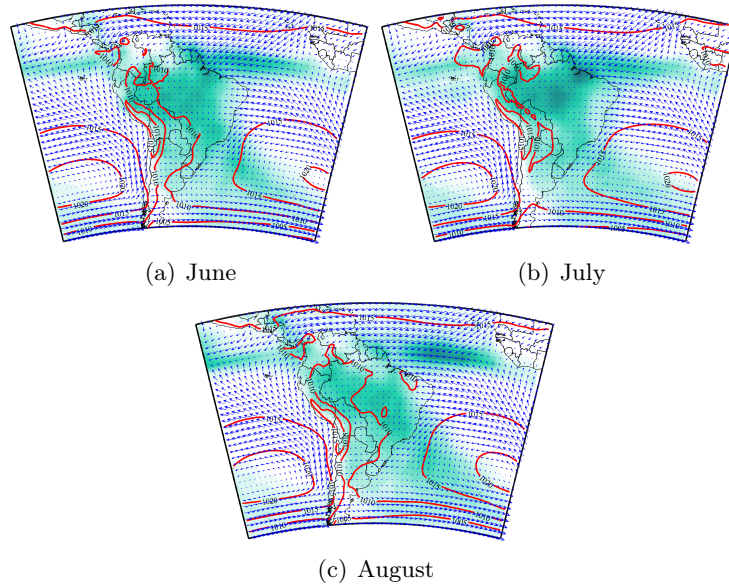


Figure 2.5: Climatological values for mean precipitation (green shaded contours) from CMAP dataset, SLP (red line contours) and surface wind (vectors) from ERA-40 Reanalysis dataset for the period of active SAMS: a) December, b) January and c) February.

The intensification of precipitation is related to the presence of strong low level winds and intense moisture convergence. This latter is related to the interaction between the Chaco Low (note pressure contours in figure 2.5) and the trade winds from the north-east (vectors in figure 2.5) as indicated by ?. Despite the enhancement of the development of the wet season in South America by synoptic systems, the vertical thermodynamic structure is fundamental. Variations in this structure are linked to the moistening of the lower levels as highlighted by ?. The temporal evolution of the SAMS has been indicated to start with an increase of the westerly wind flow of the upper troposphere in late austral Spring (Zhou & Lau, 1998). The following development of a vortex to the south-east of the Altiplano is associated to an increase in precipitation over subtropical eastern Brazil. According to ?, during the mature phase of the SAMS, there is a displacement of the intense rainfall core to the southernmost Brazilian highlands. Finally, during late austral summer the withdrawal of the SAMS is related to the

decrease of the moisture supply by the low level north-westerly flow. This moisture supply from low levels corresponds to the moisture transport due to the South American Low Level Jet (SALLJ). Significant moisture variations has been determined to occur in the boreal Summer based on observations during the South American Low Level Jet Experiment (SALLJEX) as indicated by ?. ? has found evidence of the presence of atmospheric disturbances remotely produced during warm phases of ENSO in the early monsoon season.

## 2.3 The Caribbean Low Level Jet

Amador (1998) reported the presence of a structure featured by intensified easterlies with a core located approximately at 75W between 12 and 15N at the 925hPa level and suggests the structure to be barotropically unstable and related with local SST gradients. ? propose this low level jet-like structure to be implicated in the seasonal distribution of moisture over Central America and Mexico and recently, Amador (2008) provides a review on the CLLJ.

### Structure

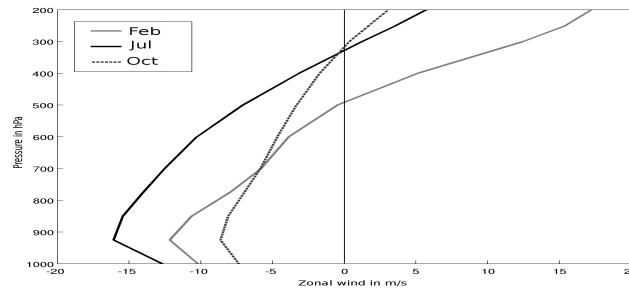


Figure 2.6: Climatological mean vertical profile of the zonal wind at 75W for the maximum and minimum intensity of the CLLJ based on ERA-40 Reanalysis data for the 1980-1999 period.

The climatological zonal wind speed at different levels is evaluated from ERA-40 Reanalysis data, the level is found to present the strongest westward winds over the Caribbean. The zonal wind field in figure 2.6 shows the presence of this low level jet structure as intensified easterlies as described by Amador (1998). Following the criteria

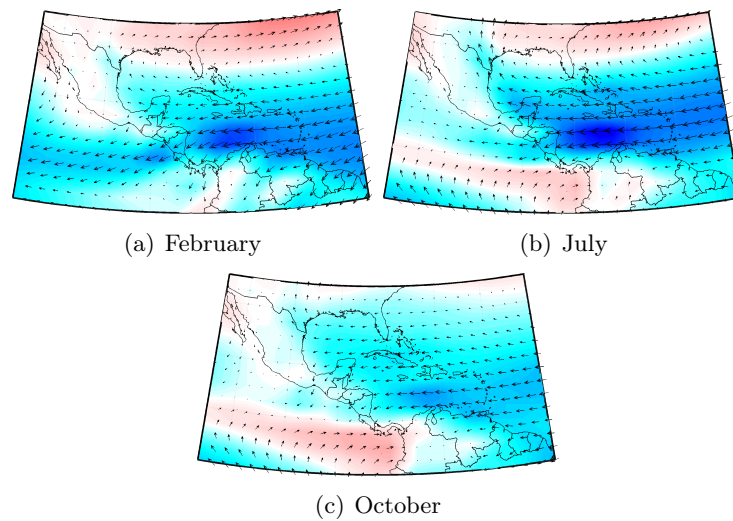


Figure 2.7: Mean zonal wind in  $ms^{-1}$  at 925hPa for a) February, b) July and c) October from ERA-40 Reanalysis dataset for the period 1980-1999.

of identification of a low level jet structure, the vertical profile of zonal wind speed in the vicinity of the region where the CLLJ core is located. The peak shown below the  $900hPa$  level shows the structure of these intensified winds that meet the criteria to be considered as a low level jet. As pointed out by different authors, the CLLJ is real and not an artifact of reanalysis data. The CLLJ does not have a single peak but two, it reaches the highest wind speeds in July but a secondary peak of intensity occurs by (February). Figure 2.7 shows the monthly mean of the structure of the wind during July and February (when maximum occurs) and October (when its intensity is almost vanished). The seasonality of the CLLJ makes it particularly interesting for the discussion of the distribution of precipitation as will be briefly commented. In the last years different groups have focused some attention to the study of this structure, mainly because of its importance as a regional climate modulator which is clear despite the dynamics of the CLLJ is still an open problem.

### Importance for regional climate

Wang (2007) finds an association between the maximum intensity of the CLLJ during summer, a maximum of SLP, the MSD and a minimum of cyclogenesis in the Caribbean Sea. Using an index to measure the intensity of the CLLJ, he studies the relation of the

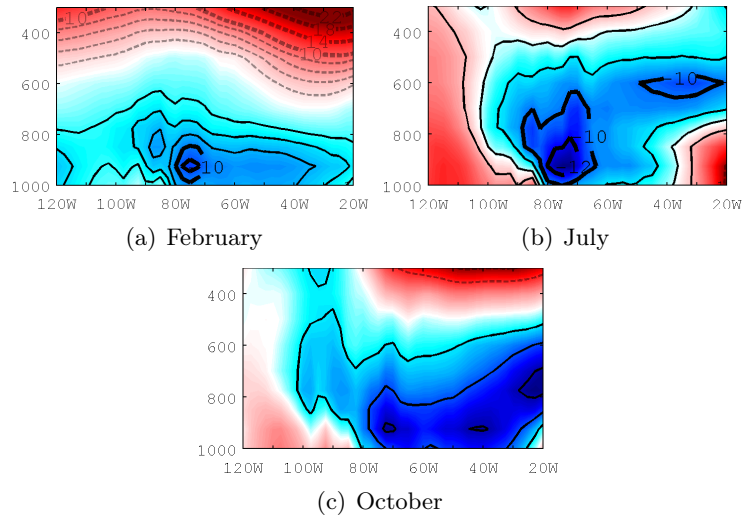


Figure 2.8: Mean meridional cross section of the vertical profile of the zonal wind at 12N a) February, b) July and c) October from ERA-40 Reanalysis dataset for the period 1980-1999. Showing the vertical structure of the wind field in the CLLJ core.

CLLJ with the SST and SLP fields. According to his results, during winter the CLLJ is related with the strengthening of the NASH and the weakening of the wintertime Auletian Low. Meanwhile during summer the intensified (decreased) intensity of the CLLJ is due to positives (negatives) SLP anomalies near the NAM region. This result implies that a strong (weak) CLLJ is associated with a weak (strong) summer monsoon. The mechanism for this to occur finds an explanation in the role of the AWP modulating the CLLJ as a result of a Gill type response (Wang et al., 2008; Magaña et al., 1999). Regarding SST, the results of ? indicate that warm (cool) anomalies of the Caribbean SST are related with weak (strong) conditions of the CLLJ.

? present a study on the features of the CLLJ with a correspondent characterisation of the structure. They find the CLLJ to be the first EOF mode of the zonal wind during July, accounting for that period for a 40% of the variability. The authors focus the study on the SST gradients and propose the intensification of the CLLJ to be modulated by a Pacific (warm) an Atlantic (cool) SST gradient (see their figure 5). They also suggest that the El Niño triggers the CLLJ, which may be used to assess forecasting since strong CLLJ is associated with a wet Central American coastline, as the authors suggest. Muñoz et al (2007) analyse the structure of the CLLJ during its peaks and

describes the CLLJ as an extension of the Bermuda High with an intensity modulated by temperature and orographic influences. They suggest that the strengthening of the CLLJ during late Spring is a result of the east-west gradient of diabatic heating between Central America and the Caribbean. A detailed study on the hydrodynamics of the CLLJ was published by ? in which the authors consider the geopotential gradient to explain the seasonal cycle of the CLLJ. They point out that this gradient tightens in July due to the NASH and in February due to the heating of northern South America, as has been proposed by Amador (2008). They suggest that the minimum of the CLLJ during October is a result of the increase of SST and a well developed PBL that debilitates the geopotential gradient. The role of Central American topography is also proposed as an element that may modulate the intensity of the CLLJ. ? analyses its variability and relation to climate and finds (as suggested by Magaña et al., 1999) a relation between the CLLJ and the MSD. The author proposes the increase of the moisture flux divergence over the Caribbean due to the presence of the CLLJ as a mechanism to suppress convection, reduce precipitation and suppress the formation of cyclones. Moreover, Wang (2007) mentions that the vertical wind shear during the intense phase of the CLLJ during summer may be related with the inhibition of the organisation of deep convection and as a result, the reduction of rainfall. Muñoz et al. (2008), Amador et al. (2003), Amador (2008) , Amador et al. (2000) and ? conclude that the CLLJ contributes to the generation of orographic precipitation over the Central American Caribbean basin at the same time that enhances the eastward divergence of the moisture flux, causing a minimum of precipitation over the Caribbean. The role this vertical wind shear associated to the CLLJ is also analysed by Wang & Sang-Ki (2007) regarding its potential impact on the Atlantic hurricanes activity.

## **2.4 Principal modes of variability**

Some of the most representative features of climate in the IAS have been indicated. The MSD has been mentioned to be a permanent feature of the distribution of precipitation. Its relation with other structures such as the NASH and the CLLJ has been indicated. The components of the AMS are, similarly, sensible to variations due to the forcing of external signals. In the previous sections, the seasonal behaviour of the components of the IAS climate system has been stated. The ENSO is known to affect inter-annual

climate variability in the IAS but it is not the only mode exerting an influence on regional climate. In addition the Pacific Decadal Oscillation (PDO) is quite important for describing the variability of climate in the tropical Pacific. The NAO has been found to be associated with the variability of the WHWP while the MJO is the most important intraseasonal global signal. Both, ENSO and NAO are related with modifications in the easterly winds and for instance play a role leading variability of the transport of moisture and regional precipitation patterns.

### **EL Niño-Southern Oscillation**

The ENSO is a two-component physical mechanism that describes the coupling of SST anomalies in the tropical Pacific Ocean (El Niño) and a pressure gradient in the southern Pacific (Southern Oscillation). Pioneer work on the ENSO was carried out mainly by Walker (1932, 1937) and ???. Bjerknes works set the fundamentals for the recognition of the link between the two components (Cane et al., 1986). Even when the effect of the ENSO is of global scale, just the highlights on the importance for the IAS region are herein given. A decrease in the intensity of the Atlantic hurricane season has been identified during warm ENSO events (Goldenberg & Shapiro, 1996). Inter-annual variability of the cyclone-genetic activity in the tropical Atlantic has been widely studied (Bell and Bell & Chelliah, 2006; Chen and Taylor, 2002). These studies suggest that the ENSO forcing variations in the SST field and vertical wind shear triggers this variability. Moreover, the ENSO effect on precipitation has been globally documented. Cold ENSO phases have been identified to be characterised by an increase in rainfall while the warm phase is featured by a reduction in observed precipitation (Dai & Wigley, 2000). ? highlight the intense inter-annual variability of precipitation over the Caribbean. An increase (decrease) of precipitation has been associated with ENSO cold (warm). Variability of the surface winds has been also observed related to ENSO. The strengthen of the easterly wind flow over surface has been found to occur during El Niño events while a reduction occurs in the opposite phase. This variations in the wind field has been mentioned to influence the vertical wind shear and then cyclone-genetic processes (Wang & Sang-Ki, 2007). It can be followed that ENSO is able to affect precipitation distribution by modulating two different mechanisms: a) evaporation variability linked

to SST and surface drag variations and b) transport of moisture due to wind flow modulation.

### **North Atlantic Oscillation**

The NAO has been indicated to be the main variability mode in the SLP field (W., 1996) can be defined as the pressure difference between the Azores High and the Icelandic Low (Rogers, 1984). Interesting features linked to the NAO are the regions characterised by SST anomalies in the East/South-east of Greenland. Negative anomalies during the NAO positive phase and vice-versa with contrasting SST anomalies in North America. A remarkable feature of the NAO is the well determined relationship between the SST gradients and the pressure patterns. For the IAS region, the effect of the NAO is noticeable from the anomalous systems developed over the Atlantic. One to the north and one westward of the African coast (and linked to the local pressure gradients). Since the NAO is related with the trade winds and easterly winds affect the circulation in the IAS, the impact of the NAO is expected to be associated with the climate features of the IAS. On the other hand, the NAO has been shown to play a role in the variability of the storms in the Caribbean. According to ?, the NAO has important seasonal variations, which may be reflected in its influence on the IAS easterly winds and precipitation patterns. The impact of the NAO on the distribution of precipitation in some locations of the IAS has been determined as is the case of Puerto Rico. ? found that during boreal Summer the NAO index has an inverse relation with the observed precipitation patterns. The relation between the NAO and the regional winds suggests the NAO to affect the variability of moisture transport and then, regional precipitation distribution.

### **Madden-Julian Oscillation**

In 1971 Roland Madden and Paul Julian found a 40-50 days oscillation in zonal wind anomalies in the tropical Pacific, after them named as the Madden-Julian Oscillation (MJO). It is a tropical wave with a 30-60 days period featured as a low-level convergence and convection region that propagates eastward (Madden & Julian, 1994). A detailed review on the MJO basics can be found in ?. An interesting analysis of the ocean-MJO relationship is provided by a recent study by ?. This high frequency oscillation is known for its effects on the tropical troposphere and strong impact on tropical convection. A

significant interaction between the MJO and ENSO has been also found (Tang and Yu, 2008 ; Moon et al., 2011). The importance of the MJO for the monsoons systems is well documented. According to ?, the MJO-related zonal wind anomalies in the ETPac region might be associated with the increase of rainfall in the NAM region. The authors point to the amplification of easterly waves as a trigger of gulf surges development that may be related with the variability of the moisture sources that feed the NAMS. Moreover, they also suggest the westerly phase of the MJO to be associated with the enhancement of favourable conditions for MCS development in the region. ? study the strength of the MJO during Autumn in terms of the MJO signal in the ETPac. ? analyse the impact of the MJO on precipitation over Mesoamerica based on stations data. Their findings suggest positive (negative) phases of the MJO to be associated with the increase (decrease) of precipitation in the region. Recently, ? published their analysis on the role of the MJO as a modulator of Caribbean precipitation. From their results, a link between the intensity of the CLLJ and the MJO is suggested to lead changes in precipitation. Both studies of Barlow and Salstein (2006) and ? find some relation between the occurrence of extreme events and the MJO phase.

### **Pacific Decadal Oscillation**

According to Zhang et al., (1997), the Pacific Decadal Oscillation (PDO) is a long-lived El Niño-like pattern of the variability of the Pacific climate. The PDO was determined through independent studies by ? to be the dominant pattern of Pacific Decadal Variability (PDV). Even when the PDO is referred as an El Niño-like pattern, it differs from ENSO in a) the time scale of the persistence of events and b) its fingerprint is more noticeable in the extratropics rather than the tropics (Mantua & Hare, 2002). These authors point out that the pattern of a warm PDO phase is featured by cooler than normal SSTs in the central North Pacific and warmer than normal SSTs along the west coast of the Americas. Symmetry in SSTAs patterns between northern and southern hemispheres exhibited by the PDO has been determined by ?. The mechanisms of the PDO are complex and still an open issue, however some studies suggest the importance of the tropical coupling for the existence of the PDO (Feng et al., 2010). Schneider and Cornuelle (2005) propose the PDO to evolve from a composition between the forcing due to El Niño 3.4, and the changes of the Aleutian low (in terannual frequencies) and the



Kuroshio-Oyashio Extension (decadal time scales). The importance that the PDO may have for global climate is related with a correlation between the PDO index (Mantua et al., 1997) and precipitation anomalies. Warm PDO phases have been found associated with anomalously dry periods in the eastern coasts of Eurasia, Northwest Pacific of USA, Central America and northern South America. While the same phase seems to be related to wetter than normal conditions in the Gulf of Alaska, South-west USA and Mexico, South-east Brazil, South central South America and western Australia.

### **Multi Decadal Oscillation**

Folland et al. (1986) detected the presence of a multidecadal mode in SST and later Schlesinger and Ramankutty (1994) isolated this mode which and suggested it has a 70-yr cycle. This cycle has been confirmed by a significant peak around 70 years found through spectral analyses of climate time series by Delworth & Mann (2000). The low frequency variability signal has been found in different modelling analysis (Delworth et al., 1993; Latif et al., 2004; Delworth & Greatbatch, 2000). The multidecadal pattern was identified as the first rotated North Atlantic SST EOF by Mestas-Nuñez & Enfield (1999). The low frequency mode featured by changes in the SST of the North Atlantic Ocean was named as Atlantic Multidecadal Oscillation (AMO) (Kerr, 2000). An index of SSTs in the North Atlantic (0 and 70N) is used to define the AMO (Enfield et al., 2001). The AMO signal has been found to be important as it modulates precipitation variations in different regions such as Africa (Fontaine and Janicot, 1996), Europe (Rodwell et al, 1999), the Caribbean (Giannini et al., 2003) and South America (Carton et al., 1996). In the IAS region, the signal of AMO has been found to be related to precipitation (Gianinni et al., 2003). Curtis (2008) reported positive AMO to be linked with a reduction of the transport of moisture from the Gulf of Mexico to northwestern Mexico which may be related with a decrease in precipitation. Meanwhile wetter (drier) conditions over Central America (north-east Brazil) during JJA (DJF) were found by Zhang and Delworth (2006). AMO has been also determined to be of importance modulating the impact of ENSO on drought (Mo et al., 2009). The regional impact of AMO is also related to its relationship with . Connection between AMO and other regional features such as the AWP has been also studied. Wang et al. (2008) show that warm (cool) phases of the AMO are associated with repeated large (small) AWP,

suggesting the relationship between the AMO and Atlantic tropical cyclones. The latter in agreement with results that indicate the presence of multidecadal variations in hurricane activity due to the Atlantic SST (see e.g. Gray, 1990; Landsea et al., 1999; Goldenberg et al., 2001). AMO is then of importance related to the low frequency variability of precipitation as it modulates the distribution of moisture and extreme rainfall events.

# 3

## Moisture availability and transport in the IAS

The importance of water vapour in the climate system has been introduced to some detail in chapter 1, addressing the role it plays in the different components of the hydrological cycle. The availability of moisture in the atmosphere was described in terms of the main fields, to be evaporation and precipitation. The transport of moisture was expressed in terms of the water vapour balance equation for long term averages. Using that expression, the vertically integrated divergence of moisture flux was shown for characteristic months when precipitation is particularly important. The latter, to be associated with regions that may be determined as sources of moisture. A general summary of the main global sources of moisture was listed in a table 1.1 and accompanied by figure 1.6 from previous chapter in which the sources and associated sinks can be observed. Then, along chapter 2, the main features of climate in the IAS were introduced. As could be followed from chapter 1, the study of sources of moisture for specific locations in the world have been focused on defined locations of interest. However, despite the richness of processes in which moisture is involved in the IAS region, the study of transport of moisture has been mainly addressed for those regions in which a monsoon like circulation has been found to develop. Therefore, regions like Central America, with such important precipitation patterns have been poorly studied.

To our knowledge, few published studies have been focused in the transport of moisture over this region. Moreover, there were no direct studies on the identification of the sources of moisture for Central America, their variability and how do they impact regional precipitation until the publication of ?. Here we aim to introduce the importance of the problem of moisture availability and transport for Central America. Here we present a proposal of the study of the sources of moisture, transport, associated precipitation, variability and mechanisms using a Lagrangian approach.

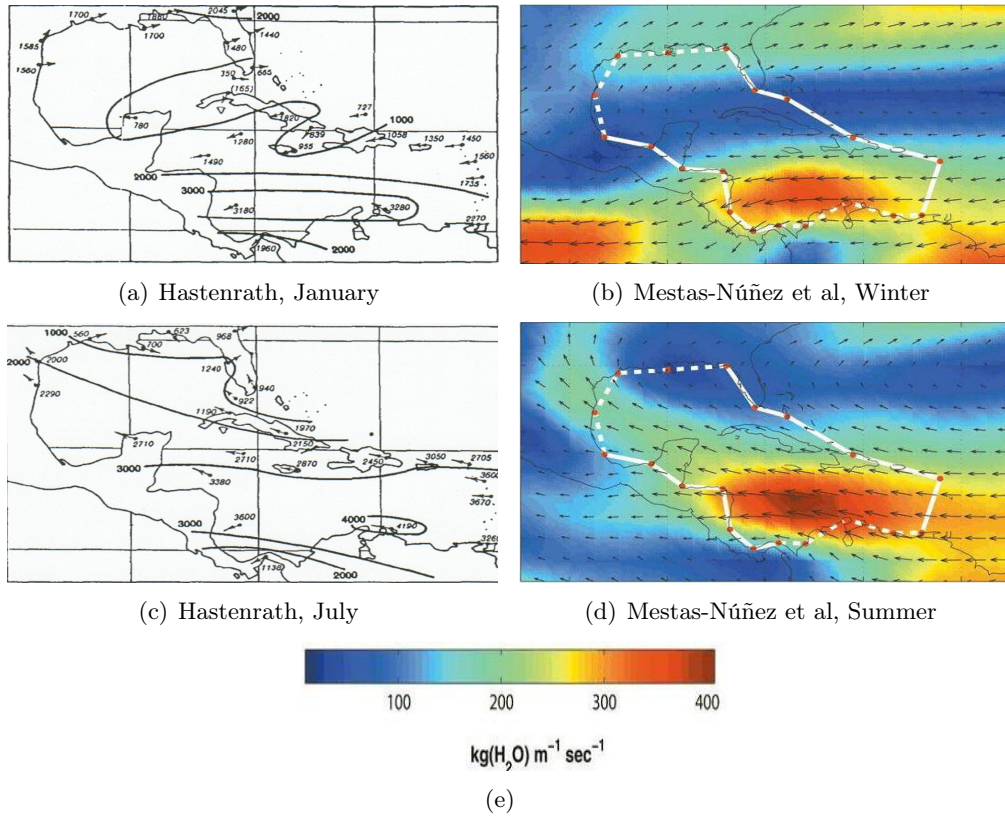


Figure 3.1: (a) Vertically integrated total flux of water vapour January (figure 4 from Hastenrath 1966), (b) December-March average of monthly vertically integrated water vapour flux (figure 3.a of Mestas-Núñez et al., 2006), (c) As a but for July (figure 8) and (d) as b but for June-September (figure 3.b)

### 3.1 Importance and previous studies

Moisture in the atmosphere is transported by several mechanisms and water vapour fluxes have been used as a traditional method to study this process. Water vapour is transported upward from the boundary layer and jointly with evaporation, transport provides moisture to moist-convective regions (Emanuel & Pierrehumbert 1995). The study of the water vapour fluxes facilitates the understanding of the processes involved in the transport of moisture, interaction of transport with other structures and their role on precipitation. The classification of air fluxes into the contributions from mean flows, stationary eddies and transient perturbations was the traditional way to study the transport of moisture (Rosen et al., 1979; Peixóto & Oort, 1984). Different approaches have been proposed, the concept of atmospheric rivers was introduced by Newell et al., (1992) on the basis that the transport of water vapour in the troposphere has a filamentary structure (Zhu & Newell, 1994; Zhu & Newell, 1998) which is also known as conveyor belt (Hane et al., 1993). This approach is useful in the analysis of the transport of moisture that undergo determined weather events such as cyclones and cold fronts.

Studies of Lagrangian transport yield to the relatively accurate representation of the transport of air moisture (Galewski et al., 2005). ? provide a climatological analysis based on isentropic coordinates from which suggest the balance between the drying into the extratropics with the moistening from the tropics into regions of relative humidity minima by eddy transport (in both directions). These two studies set up a good background for the role of transport of moisture between the tropics and the extratropics. Recently, ? have also addressed this relation and the importance of associated transport of moisture. Regional studies of the transport of moisture Considering the importance of moisture for enhancing the occurrence of precipitation in (and outside) the tropics, the transport of moisture is key to understand the patterns of precipitation over determined locations. Transport of moisture occurs at different scales, large scale transport, for example, is more associated with stronger low level winds and the modulation of the distribution of water vapour (Emanuel and Pierrehumbert, 1996). Large scale moisture transport is of particular importance since it is involved with the triggering of convection (Sherwood, 1996; Sherwood et al.m 2010).

Several studies on the transport of moisture from the main global sources of moisture have been carried out. In the case of America, studies on the transport of moisture have been mostly focused in the Amazon region (Rao et al., 1996; Marengo, 1992) and North America (Rasmusson, 1966; Trenberth et al., 1996; Douglas et al., 1993; Schmitz and Mullen, 1996; Bosilovich et al., 2001; Hu & Feng, 2001; among many others). In the case of Central America few studies have been done in comparison to other locations in the Americas such as the Great Plains of North America and the Amazon. Pioneer work was done in the mid sixties by Hastenrath (1966a). In those firsts works, the role of the transport of moisture from the Caribbean Sea and the Gulf of Mexico was highlighted in association with local winds and the regional distribution of precipitation. Hastenrath discusses that 'the westward direction of transport has its maximum below the 900 hPa level, and its core is clearly situated over the southern Caribbean Sea'. Hastenrath addresses the presence of 'a northward transport of moisture across the 20N latitude circle' and also remarks the southward shift of the minimal transport of moisture during boreal autumn. In this paper and a companion work on the analysis of rainfall in Central America (Hastenrath, 1966b) the author focused on the main details of the transport of moisture and the distribution of precipitation that are still being studied.

Forty years later, ? published an analysis on the water vapour fluxes over the Intra Americas Seas. Their results reveal a zonal structure of the moisture flux balance over the IAS and the balance between moisture exports from the tropical North Atlantic and evaporated locally and the transport toward the Pacific over Mexico and Central America. This result of the mostly zonal conditions of transport can be interpreted as an analogue to what Hastenrath (1966a) called as westward direct transport. The increase of the meridional transport found by ? which they suggest as consistent with the seasonal cycle of the CLLJ is no more than the northward transport mentioned in Hastenrath works of 1966. Notice that a first notion of strengthen of the easterlies over the Caribbean can be considered the work by Wirtky (1965) and is therefore not available at the time Hasterath wrote his analyses. However, in the absence of that evidence, he identifies with good accuracy that the transport conditions over the Caribbean must be related with the winds as he uses a calculation of the water vapour transfer in terms of a wind vector. A comparison of the results found by Hastenrath in

1966 and ? is presented in figure 3.1, in which both works are interested in the analysis of the water vapour fluxes over the region formed by the Caribbean Sea and the Gulf of Mexico (IAS) . To contrast these two studies is very helpful to illustrate how slow has been the advance in the understanding of the regional hydrological cycle over Central America and the scarcity of specific studies on this issue for the region. Fortunately the interest of studying the IAS region has increased as a result of interest in the analysis of the North American Monsoon system. Therefore the number of studies focused on the distribution of precipitation over the Caribbean and Central America has grown and the scientific community is little by little turning into the importance of studying this region not only for its specific features but also for its importance for climate in other scales.

### 3.2 The problem of analysing moisture sources and transport in the IAS region

Within the IAS system, the study of the sources of moisture and transport to two determined locations is of special interest. On one hand, the most studied of the two, the case of the sources of moisture that may be of importance for feeding the NAMS and thus maintaining the summer monsoon over North America. On the other, the moisture sources for Central America and correspondent transport, which has been poorly studied. The nature of precipitation over both regions differs, however, as part of a system being influenced by the IAS, it is important to understand the dynamic of the common elements they have. The general picture described in the previous section may suggest that the system is basically under the influence of the moisture transported by the wind regime. This statement may sound quite simplistic, however it encodes a very complex meaning since the regional dynamics is very rich as shown in the summary of the climate in the IAS provided in chapter 2.

Studying the sources of moisture and associated transport in the IAS region represents a problem from the logistic point of view. First of all, the regions of interest have received, traditionally, very different attention and the available resources for research are

---

<sup>2</sup>Note that units in figures from Hastenrath 1966 are  $g H_2O cm^{-1}s^{-1}$  while for those from Mestas-Núñez et al., 2007 are  $Kg H_2O m^{-1}s^{-1}$  so that a factor of 10 must be taken into account for direct comparisons

quite inhomogeneous for them. Therefore, information available for Central America differs enormously from that for North America. There are few complete records of precipitation observations over Central America so that the scarcity of long term observations of the main variables required for such studies is large and availability limited. Resolution is another problem, since Central America is a small continental region surrounded for large water bodies. Until the last years, the resolution of analysis products was not enough to appropriately resolve key processes in which moisture availability and transport are involved. Few points of the grid are actually representing the complete continental region and higher resolution is a demand. Higher resolution datasets are often not global and in some cases do not cover Central America and even if so, the access is not always public (even for research purposes<sup>1</sup>). In the absence of a complete analytical solution and long term and high resolution observations, recent higher resolution reanalyses and numerical models are the most suitable solution to assess the problem of moisture sources and transport in the IAS, particularly over regions that deserve special attention as Central America.

### **3.3 Lagrangian methodologies as an alternative**

The study of the sources of moisture can be treated as a source-receptor relationship problem, and reanalyses products can be used in two different ways to establish such relationship. One of the alternatives to these studies is the use of numerical water vapour tracers (WVT) which offer a good tool for tracking the origin of precipitable water vapour. This method can be divided in two different groups which are Eulerian and Lagrangian. For the present analysis the Lagrangian methodology was selected to be used. First of all, it is important to remember that the Lagrangian formulation basically follows an element of fluid along its trajectory. The atmosphere, can be considered as composed by a finite number of homogeneous elements of fluid from which position and other properties are known at every time (see diagram in figure 3.2). Lagrangian methods allow the study of the source-receptor relationship using a coordinate system in which the three dimensional position of a particle (air mass) is considered at any time. Conditions at every time are given by meteorological fields so that the movement

---

<sup>1</sup>Fortunately, several research centers are improving the resolution of the datasets they made public for research purposes



of the particles is represented by relatively accurate atmospheric conditions. In such models, turbulent fluxes play a key role in the processes in which sources and sinks are involved (Sawford, 1985; R., 1989). The importance of these models is that they provide valuable information for the complete transport history of the air parcels (Sodemann et al., 2008). The accuracy of the results obtained with these models depends on how proper is the representation of the meteorological conditions and the chemistry involved<sup>2</sup>. Better parametrisation schemes, higher resolution datasets and the assimilation of observations improve significantly the performance of the models. Lagrangian dispersion models are used to study the source-receptor relationship under different methodologies. In particular, back trajectories are used to determine potential source regions and associated contributions to receptor locations through different approaches. Which include flow climatologies (Katsoulis & Whelpdale, 1993), classification of trajectories by cluster analysis (R. et al., 1992; Stohl et al., 1996) and source-receptor matrix calculation (Seibert & Frank, 2003).

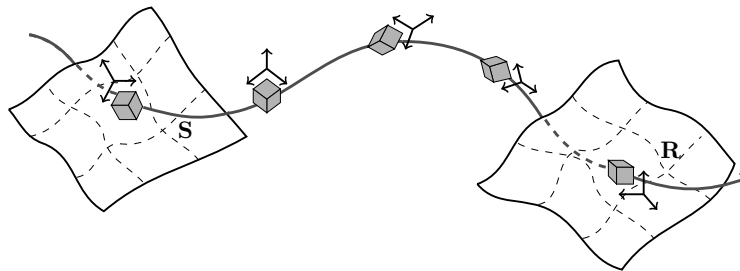


Figure 3.2: Schematic representation of the Lagrangian interpretation of a finite element of fluid

Lagrangian models can be used both in forward and backward modes to determine concentration fields. Alternative methods have been recently addressed in the literature such as the determination of sources through Bayesian inference (Andrew et al., 2007). Since Lagrangian approaches offer important information on the composition, content and history of air parcels, their use for moisture sources studies has increased. A wide

---

<sup>2</sup>particularly important depending on the tracers used

variety of studies using Lagrangian approaches for assessment of the source-receptor relationship related to moisture sources can be found in the literature (e.g Stohl & James, 2004; Sodemann et al., 2006, 2008; Gimeno, DQ2010). The use of Lagrangian analysis methods has become very useful for studying the hydrological cycle from general aspects to extreme events (Stohl & James, 2004; James et al., 2004). Lagrangian methods have been also used in the study of moisture sources and transport during monsoonal circulations (Joseph & Moustaoi, 2000). Other studies present a Lagrangian diagnosis of the variability of moisture sources associated with precipitation under forcing of determined atmosphere signals (Sodemann et al., 2008).

### **Back trajectory analysis in the region as part of the Water Cycle Research Programme of the NSF**

A quasi-isentropic backward trajectory analysis was applied for the 'Characterizing Land Surface Memory to Advance Climate Prediction' collaborative research developed as part of the Water Cycle Research Programme (WCR) of the National Science Foundation (NSF) at the Center for Ocean-Land-Atmosphere Studies (COLA) (Dirmeyer and Brubaker 2006, a and b for details ). In the datadabse of the WCR<sup>3</sup> the information of the evaporative sources of moisture that contributes to precipitation events can be found by nations and basins. Results of the identification os the sources of moisture by Dirmeyer and Brubaker (2006.a, 2006.b) for the former nations of Central America are shown in figure 3.3. Their results suggest the main source of moisture associated to precipitations event to be the Caribbean Sea, with an extension over northern South America and the ETPac region. The results by Durán-Quesada et al (2010) are in good agreement with the spatial structure of the sources of vapour as identified by Dirmeyer and Brubaker (2006a, b), however, important differences arise when comparing the seasonal climatologies shown by them and the seasonal results of the Lagrangian analysis. This because the quasi-isentropic methodology used do not fully represent the losses of moisture along the trajectories. The latter results in the interpretation of the origin of the air masses and not strictly the origin of moisture, as air is identified to come from a region even when moisture may be lost before precipitating over a target location.

---

<sup>3</sup>available at <http://www.iges.org/wcr/>

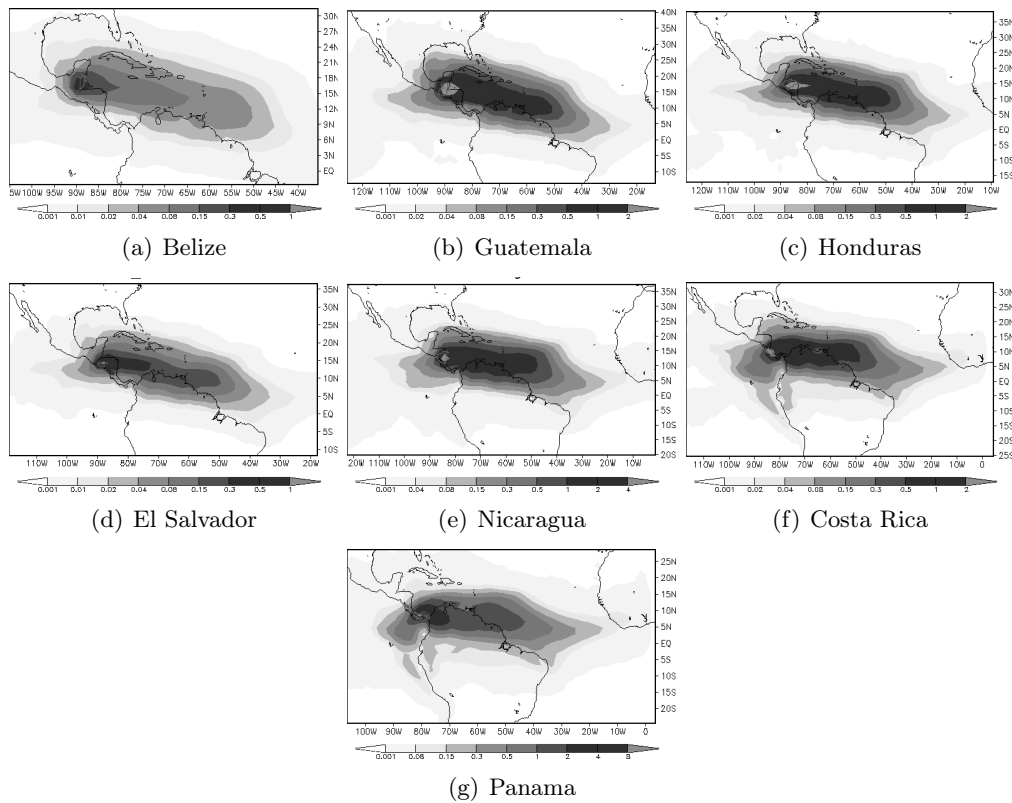


Figure 3.3: The results of the climatological evaporative sources of vapour for precipitation events for the former nations of Central America are shown as retrieved from the WCR database through their webpage. Units are in  $\text{Kg}/\text{m}^2/\text{month}$

The database of Dirmeyer and Brubaker offer anyway a good global dataset with the identification of the origin of air masses associated with precipitation events but not directly of moisture, as the complete history of the air parcels is missed. The main differences found between results from Durán-Quesada et al (2010) and Dirmeyer and Brubaker (2006) are more important for the source over the ETPac region, as the quasi-isentropic method does not account for moisture losses due to the presence of the ITCZ which modulates the moisture transport from the ETPac to Central America. Moreover, the method applied by Durán-Quesada et al (2010) uses the one degree resolution ERA-40 dataset as input for the generation of the backward trajectories whereas Dirmeyer and Brubaker use 1.875 by 1.9 degrees resolution NCEP NCAR reanalysis for the lowest 16 sigma levels while Durán-Quesada et al (2010) use the full 61 vertical levels of the

ERA40 Reanalysis. Here we aim to provide a complete inter-annual variability study of the sources of moisture associated with precipitation over Central America under similar conditions as those used by Durán-Quesada et al (2010).

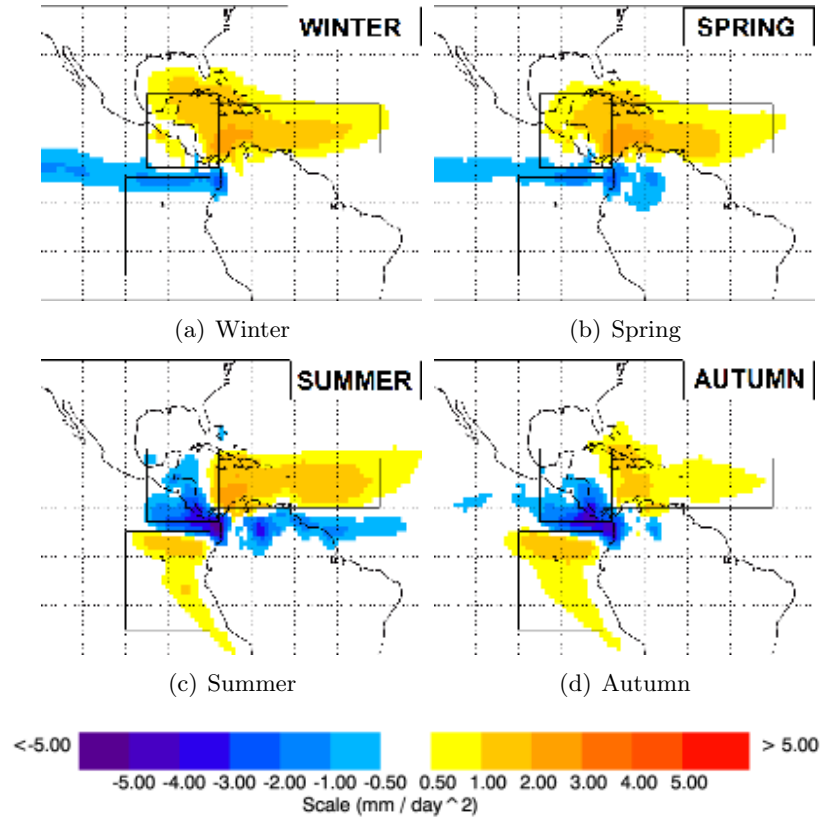


Figure 3.4: Results for the sources of moisture identification from ?. Note that the box domain used for Central America contains important parts of water compared to that of land

### 3.4 The proposal

#### Motivation

In a previous work (DQ2010), an exploratory analysis of the sources of moisture for Central America was performed using a Lagrangian backward trajectories dataset for the five years period 2000-2004. The skills of a Lagrangian approach to analyse the region were evaluated and the main findings of that work can be summarised as:

1. Two sources of moisture of oceanic origin for Central America were identified to be the Caribbean Sea (CS) and the Eastern tropical Pacific (ETPS).
2. The CS was determined to be the most important in terms of intensity in comparison the the ETPS.
3. The horizontal extent and intensity of the sources of moisture has a marked seasonal cycle. The CS has an important activity all year with a slight displacement towards the Gulf of Mexico during winter. In contrast, the ETPS shows significant variation throughout the year, as it disappears during winter and spring.
4. The transport of moisture was attributed to the effect of regional low level winds and the seasonal displacement of the ITCZ (however a complete discussion on the mechanisms was not provided). Further associations between the sources of moisture and relative contributions to precipitation were established between the seasonality of the sources and regional climate features.

The importance of the CS as the main source of moisture became a natural result of the regional climate, however, the presence of the ETPS required more attention. Even when the ETPS is supported by the findings of Lachiet et al. (2007) using isotope analysis, the intensity of the ETPS is small and since few evidence on the dynamics of this source exist explicitly a longer time span was required in order to be conclusive. This addresses the need of using longer datasets, because the use of short time series does not enable the assessment of the impact of variability modes, which are well known to affect the region. The work of the identification of the sources of moisture for Central America and the need of providing more evidence on the presence and features of the ETPS put on the table the need of: Providing a long term analysis of the mean state of the sources of moisture for Central America, but only accounting for the continental region, since the exploratory analysis defined Central America as a box that contained an important portion of water. Moreover, that enable a more complete identification of moisture sources, since due to the short time period used the structure of other sources could be lost. And at the same time answer the next questions:

1. Which are the main sources that provide moisture to continental Central America?

2. Which is the response of the sources of moisture to the forcing of the atmospheric signals that influence the IAS region?
3. What are the contributions from the sources to precipitation over continental Central America?
4. How the variability of the sources of moisture impact the regional precipitation through modulation of the contributions from the sources?
5. Which are the mean trajectories followed by the air parcels in their transit from the sources to continental Central America?
6. Which are the main structures associated with the regional transport of moisture and how do they respond to the local variability.
7. Based on the importance of the CLLJ as a regional climate feature, what is its role in the dynamics of transport and which is its effect on the modulation of precipitation over Central America.

## **Objectives**

Motivated by these questions merged from the exploratory analysis on the sources of moisture, a complete study of the sources of moisture within the IAS region is proposed. A set of main objectives were proposed with the aim of providing some answers:

1. Generate a new backward trajectories dataset that enable the study of the sources of moisture to Central America for a longer time period.
  - (a) The 1980-1999 time period was selected for the analysis due to availability of ERA-40 data with one degree of resolution to be used as input for the LDM FLEXPART to generate the trajectories dataset.
  - (b) Using a domain centred in Central America, the trajectories dataset was generated with output every three hours (further details can be found in chapter 4).
2. Provide a complete study of the sources of moisture for continental Central America.

- (a) Obtain a new climatology of the sources of moisture for continental Central America using a longer time span.
  - (b) Determine with a major accuracy the seasonal behaviour of the sources of moisture
  - (c) Analyse the interannual variability of the sources of moisture (intensity and horizontal extent) and evaluate the impact of the major modes of variability.
3. Study the relationship between the contributions from the identified sources of moisture and precipitation falling over continental Central America.
- (a) Determine the relative contributions to precipitation from the sources and analyse their seasonal cycle in comparison with the known seasonal cycle of precipitation over Central America
  - (b) Evaluate at some extent the estimation of contributions to precipitation using available observations data of precipitation.
  - (c) Evaluate the behaviour of the contributions from the sources of moisture during the presence of the MSD
  - (d) Study the inter annual variability of the contributions from the sources and associated precipitation to identify which modes force the major variations in precipitation.
4. Study the transport of moisture.
- (a) Determine the preferred path followed by the air in their transit from the sources to Central America. Provide a complete analysis of the mean air streams from the sources to Central America by considering the differences between different locations within Central America.
  - (b) Identify regions of significant variations in the air moist content along the trajectories.
  - (c) Analyse the correspondence between the mean air streams and regional climate structures that may act as moisture conveyors.
  - (d) Establish a conceptual model of the regional transport of moisture.

5. Analyse the role of the CLLJ in the process of regional transport of moisture
  - (a) Identify from the trajectories the mean structure of the CLLJ.
  - (b) Determine how much of the moisture that contributes to precipitation over Central America is transported by the CLLJ.
  - (c) Propose the mechanism through which the CLLJ may be able to modulate precipitation over Central America and the Caribbean.



## Part II

# Lagrangian analysis of sources of moisture and transport processes in the IAS



# 4

## Data and Methods

The analysis of the sources of moisture, precipitation and transport was proposed based on the skills of a Lagrangian approach developed by Stohl and James (2004, 2005) and whose application for Central America was evaluated in the preliminar study of Durán-Quesada et al (2010). A dataset of Lagrangian backward trajectories was generated as is explained in this chapter. The key details of the method used for the identification of the sources of moisture is presented as well as the assumptions made to estimate the relative contributions of the sources to precipitation. A clustering algorithm based on Dorling and Davies (1992) was implemented to reduce the huge dataset of trajectories into representative air streams. It was based on a non-hierarchical clustering method that is herein describe, the clustering algorithm was modified to be used to create composites of clusters as well. In order to study the transport due to the CLLJ, trajectories under the influence of this structure were isolated for an specific analysis. Additional datasets used for this study are indicated. A brief description of the observations dataset used for the evaluation of the estimations of the relative contributions to precipitation is included. Finally, some details on how the computations were made for processing the data are indicated.

## 4.1 The backward Lagrangian trajectories dataset

The aim of this work is to improve the comprehension of the processes involved in the transport of moisture in the IAS region, their relation with the local precipitation and associated variability. An accurate knowledge on the history of the air masses is required in order to accomplish the proposed study. For this reason, a Lagrangian approach is proposed instead of any other traditional Eulerian method. As already mentioned, this work is based on a backward Lagrangian trajectories dataset generated with a Lagrangian Dispersion Particle Model (LDPM). A LPDM is a three-dimensional model that includes both three-dimensional wind and turbulence (Seibert & Frank, 2003). In this section, a very brief introduction of the FLEXPART model is presented, followed by the description of the input data used and an explanation of some details of the performed simulations and a description of the generated dataset.

### The FLEXPART model

Some details of the FLEXPART model are highlighted, it is not intended to present a complete description of the model which can be found in the FLEXPART technical note by Stohl et al., (2005). FLEXPART is a LPDM developed originally for air pollutant dispersion calculations and is now used as a tool for atmospheric transport modelling and analysis in a wide variety of applications (Stohl et al., 2005). The model is written in standard Fortran 77 code<sup>1</sup> and is freely available through the FLEXPART homepage (<http://transport.nilu.no/flexpart>). The main reason for using FLEXPART instead of other available Lagrangian models is its robustness, supported with a large list of peer-reviewed publications in which the model is applied as well as validated. Since the interest region of the present work is located in the tropics, convective processes are of importance and most LPDM do not take into account the effects of convection while FLEXPART does. The structure of the model and implemented parametrisations allows its use for receptor-oriented transport studies. Those are of particular importance for determining the contribution from identified sources of moisture to precipitation over a receptor region.

The physics of the FLEXPART model is described by the zero acceleration scheme

---

<sup>1</sup>a version in Fortran 90 is currently available

and a set of parametrisations. Hanna (1982) parametrisation scheme is used for wind fluctuations. Frictional velocity computed using surface stresses and sensible heat fluxes is considered in the boundary layer parametrisation. Meanwhile the profile method (Berkowicz & Prahm, 1982) is applied in absence of frictional velocity information. Turbulent motion is parametrised considering a Markov process based on the Langevin equation (Thomson, 1987). Emanuel and Zivkovic-Rothman (1999) one-dimensional convection model is used as convection scheme. Radioactive decay as well as dry and wet deposition are also considered in the physics of the model.

## Input data and simulations

### Input data

FLEXPART model can be initialised with different datasets. In the case of the present work, ERA-40 Reanalysis (Uppala et al.) data have been used with one degree of horizontal resolution in 61 vertical levels. Analyses were used every 6 hours (0000, 0600, 1200 and 1800) and three hours forecasts for the intermediate hours (0300, 0900, 1500, 2100). This due to the importance of temporal resolution for accuracy of the trajectories as is pointed out by Stohl et al. (2004 and 1995). ERA-40 was used instead of ERA-INTERIM because of high resolution data availability for the twenty-year proposed analysis time period at the moment this study began <sup>2</sup> FLEXPART requires five three-dimensional fields: horizontal and vertical wind components, temperature and specific humidity. Additional two-dimensional fields are also required: surface pressure, total cloud cover, 10 m horizontal wind components, 2 m temperature and dew point temperature, large scale and convective precipitation, sensible air heatflux, east/west and north/south surface stress, topography, land-sea-mask and subgrid standard deviation of topography. ERA-40 data with three hours temporal resolution have been retrieved in GRIB format through the MARS server. A landuse inventory in which categories are related with Leaf Area Index and roughness length is used (ú et al.,1999). Similarly, an inventory which contains some characteristics of different chemical species/radionuclides is used.

---

<sup>2</sup>No attempts were made in order to use MM5 or WRF models to generate higher resolution datasets through dynamic downscaling as input for FLEXPART

### **Model configuration**

Version 8.1 of the FLEXPART model was installed on a NUMALink Blade System with 16 Itanium 2 core processors with a performance of 106 GFLOPS. Due to the relatively large time span of the simulations and in order to optimise the usage of computational resources, it was decided to use a limited domain instead of a global domain for the simulations. In the case of limited domain runs: a) the domain set up is based on the coordinates specified for the first release, b) mass fluxes are determined in small grid boxes at the boundary of the domain, c) mass fluxes are accumulated over time and new particles are released at random positions at the boundaries of the domain whenever the accumulated mass exceeds the mass of a particle and d) particles are terminated at the outflowing boundaries. A total of 250000 particles were uniformly distributed in the domain with each receiving the same mass. Notice that the number of particles can vary throughout the simulation as a result of the variations of the mass of the atmosphere and numerical effects. A numeric label is assigned to each particle so that it is unique and when new particles are released they do not replace any existing particle. The selection of the domain (see figure 4.1) for the simulations considered the horizontal extension of the main structures involved in the regional climate processes. The domain includes the ETPac region, the IAS (Gulf of Mexico and the Caribbean Sea). The longitude of a typical African Easterly Wave (AEW) was used as criteria for the selection of the easternmost boundary. Since we were interested in the analysis of moisture, tracer used was water vapour and the simulations were performed for the complete analysis period in backward mode using the convection and subgrid terrain effect parametrisations.

### **Output data**

Output for a set of twenty-years backward Lagrangian trajectories every three hours (00, 03, 06, 09, 12, 15, 18 and 21) was obtained from the simulations performed with FLEXPART. For every one of approximately 250000 particles, 13 variables were stored at every output time step (see table 4.1).

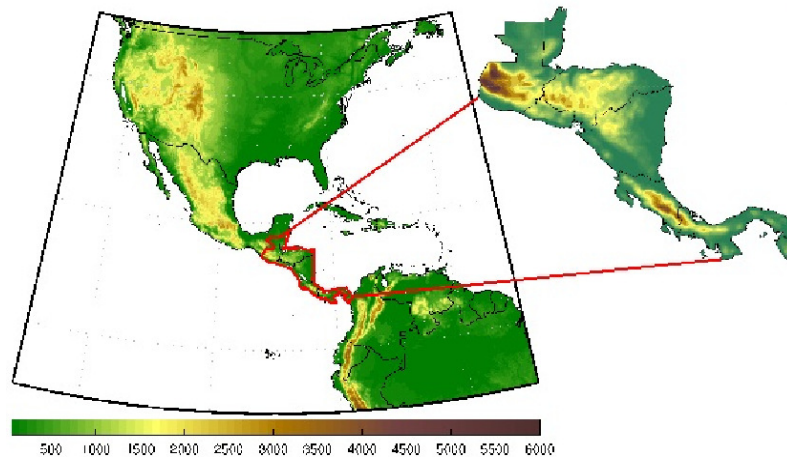


Figure 4.1: Domain used to generate the trajectories dataset. A zoom view of the analysis region indicated by the red lines is detailed. Topography height in  $m$  is shaded.

Variable	Symbol	Units
Latitude	lat	
Longitude	lon	
Height	H	m
Topography height	TH	m
Potential Vorticity	PV	$10^{-6}$ ( $m^2K/sKg$ )
Specific Humidity	q	g/Kg
Air density	$\rho_{air}$	$Kg/m^3$
Mixing height	Hmixi	m
Temperature	T	K

Table 4.1: Output variables

### Identification of sources of moisture

As known from the Lagrangian point of view, a fluid can be represented by a discrete number of finite elements of volume, for which position and several properties are known every time step. The FLEXPART model divides the atmosphere in a discrete number of  $N$  homogenous 'air particles' of mass  $m$  (see figure insert). This representation is very useful since, as followed from Stohl & James (2004), the net rate of change of water

vapour of an air particle can be expressed as

$$e - p = m \frac{dq}{dt} \quad (4.1)$$

so that over an area  $A$ , the surface freshwater flux results from the sum of the changes in moisture for all the particles and then can be written as

$$E - P \approx \frac{\sum_{i=1}^N (e - p)}{A} \quad (4.2)$$

where changes of moisture along the trajectory are related with evaporation and precipitation, as indicated in diagram of figure :

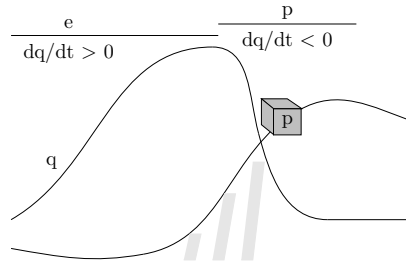


Figure 4.2: Schematic representation of the evaporation-precipitation cycle for a finite element of fluid, adapted from figure 1 of Stohl & James (2004).

$$e \text{ if } \frac{dq}{dt} < 0 \text{ p if } \frac{dq}{dt} > 0 \quad (4.3)$$

This can be used as a Lagrangian approximation of the balance equation (equation 1.4). Those particles arriving to a target location (Central America) that are featured by a loss of moisture during the last time step are then traced backward a determined number of days and then integrated over the atmospheric column (equation 4.2). (see figure 4.3).

### Estimation of contributions to precipitation

Estimating precipitation is complex, numerical models are under constant improvements in order to reduce the biases associated with this variable. In a simplistic approximation,



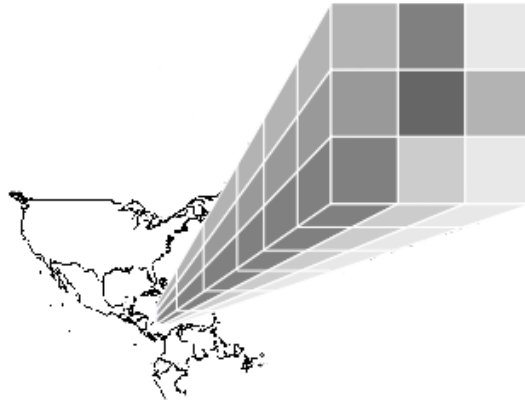


Figure 4.3: Schematic representation of vertical integrate of the changes of specific humidity of the contributing particles used to compute the conditional  $E - P$  field following equation 4.2.

precipitation can be assumed to be approximated by projection onto the receptor region of the decrease of specific humidity in the last time step before arriving to the receptor region (Stohl & James, 2004). For those air particles for which  $dq/dt < 0$  for the last time step it was assumed that the moisture decrease was due to precipitation that fell immediately over the surface. Therefore, the estimation of precipitation over the receptor region due to the contribution from air parcels coming from a determined source were computed by integrating those decreases in specific humidity. Let  $g$  be the acceleration of gravity,  $\Delta q_k^0$  the change of specific humidity for the last time step to the arrival to the receptor,  $\Delta h$  the vertical extent of the air column. Precipitation  $P$  can be approximated, for a determine time interval, by integrating the change of specific humidity for those particles for which  $dq/dt < 0$  for the last time step (see figure 4.5) as:

$$P \approx -\frac{1}{g} \sum_{i=1}^N \Delta q_k^0 \cdot \Delta h \quad (4.4)$$

This approximation may be considered bold since it does not consider different processes in which air particles can be involved (e.g microphysical processes). However as a first guess approximation it is considered to be acceptable. More detailed estimates use the evaluation of the moisture content of the air particles along the trajectory (see e.g. Sodemann, 2008).

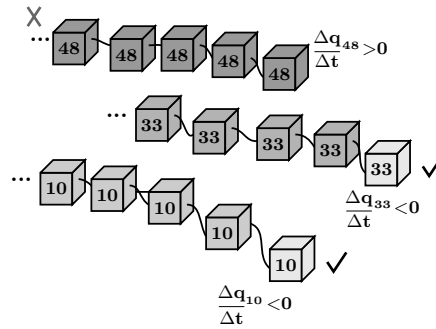


Figure 4.4: Representation of the criteria used for selecting the air particles that contribute to precipitation over a receptor location.

## 4.2 Clustering method applied

Clustering is a multivariate statistical technique that aims to explore structures in a given dataset (Everitt, 1980). In atmospheric science studies, the result of clustering is analogous to a flow climatology and allows the grouping of trajectories that have similar characteristics (e.g length and curvature) (Harris & Kahl, 1990). Due to the large amount of trajectories obtained, to explore the structure of the air flow, using mean air streams from the backward trajectories dataset instead of the total of trajectories is better for climatological purposes. One of the non hierarchical clustering methods is known as the of Centroid method, in which clusters with the smallest distance between the centroids are fused and the measure of similarity is then defined as the squared Euclidean distance (equation 4.1) (Everitt, 1980). Herein, we used a clustering algorithm applied based on the Dorling method (Dorling et al., 1992). The clustering process consisted of steps in which first of all, the particles reaching determined target regions were selected and an iterative clustering procedure following Dorling et al. (1992) was then applied. Once the set of trajectories was separated into a determined number of representative clusters, the identification of the clusters was performed.

$$D = \sqrt{\sum_{i=1}^N (x_i - y_i)^2} \quad (4.5)$$

### **Selection of the particles of interest**

From the complete dataset not all the particles circulated over the analysis regions and not all of them precipitated over the target. For this reason the first step was to select only those particles in order to speed up the calculations. From each selected analysis receptor region, all the particles that have circulated over the region and that lost moisture in the last time step previous to the arrival were selected and then tracked ten days backwards. This first classification reduces significantly the volume of trajectories and creates a new dataset in which only the interest particles and their trajectories are stored. Since the objective is the analysis of moisture transport in the lower levels of the troposphere, those particles that along their trajectories were above the tropopause level were discarded. Criteria for the height of the tropopause was based on the monthly means of tropopause height from the ERA-40 Analysis.

### **The clustering**

A non-hierarchical clustering algorithm following Dorling et al. (1991) was applied, the algorithm consisted of a set of steps described as follows.

1. In order to avoid introducing a subjective criteria for selecting the structure of the clusters and to make sure that all the possible directions are considered in the determination of the initial trajectories, a set of 'seed' trajectories were defined in a Cartesian plane as rays pointing out of the origin<sup>3</sup> with a separation of 6 degrees among them. This distribution gives a total of 60 'seed trajectories' covering the totality of horizontal space (see figure 4.3) to initialise the clustering.
2. The squared Euclidean distance (equation 4.4) is used as the similarity measure between each 'real trajectory' from the dataset and the 'seed trajectories', each 'real trajectory' is assigned its nearest neighbor 'seed trajectory'.
3. Once each 'real trajectory' is paired with a 'seed', a new set of 'seed trajectories' is calculated as the centroid of the correspondent set of 'real trajectories' paired with each initial 'seed'. Each new 'seed trajectory' being the equivalent average trajectory between the elements assigned to the initial seeds. This step is iteratively repeated until the number of clusters converges.

---

<sup>3</sup>the origin is considered as the centroid of the target area

4. Finally a set of clusters is obtained so that the particles trajectories have been classified into groups sharing a common basic spatial structure.

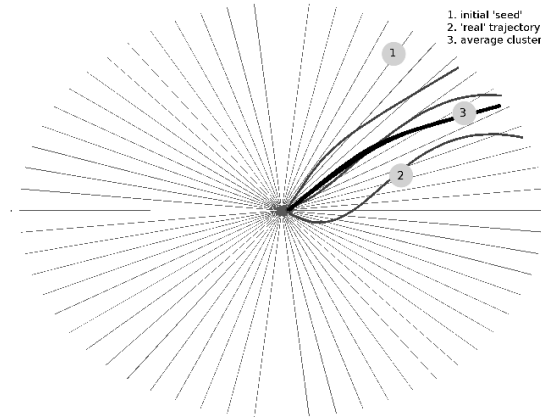


Figure 4.5: Schematic representation of the clustering algorithm used based on the algorithm developed by Dorling & Davies (1992). The thinner gray lines represented the initial seed trajectories, thick gray lines the 'real trajectories' and thicker black the cluster generated as the average of the real trajectories belonging to a seed trajectory.

With this procedure we are able to reduce large amounts of trajectories to more manageable smaller sets which represent the mean structure of the complete datasets. This is very useful to determine the regions from which air parcels that precipitate over a receptor region come <sup>4</sup>. However, apart from the problem of transport we are interested in the problem of transport due to determined structures. To accomplish the identification of atmospheric moisture transported by the CLLJ, additional selections and assumptions were made.

In order to select those particles that were moved within the CLLJ, two main conditions were imposed. The first was that the air particles must remain along the trajectory below the 3000m and second that they must flow inside the area of influence of the CLLJ. To determine this area of influence the effect of the pressure gradient was considered. Under the assumption that a boundary layer separates the airflow in two parts inside and outside the influence area of a pressure gradient, a separation between the jet current and the mean flow was established as the point in which the pressure gradient

---

<sup>4</sup>note that this procedure is quite flexible to be used for reducing datasets and obtaining information on more processes than precipitation

tends to zero. All those particles that circulate under the influence of the jet, were then separated from the rest of particles. The position of the flow in which the gradient becomes zero was determined from the correspondent analysis geopotential height at 850hPa.

### 4.3 Indices for the intensity of the CLLJ and the SST gradient

In order to have a sort of measure of the intensity of the CLLJ and of SST gradients that are of importance for further analysis, three indices related to low level winds, SST and Geopotential height gradients were defined to be used in this study. An index to quantify the intensity of CLLJ zonal wind defined similar to a previous work by Wang (2007) and Amador et al. (2010) by averaging the zonal wind speed at 850hPa over a box defined between  $(12 - 18)N$  and  $(80 - 70)W$  (see box in figure 4.3), anomalies for the  $CLLJ_{index}$  were computed in order to be used as a measure of the variability of the intensity of the CLLJ.

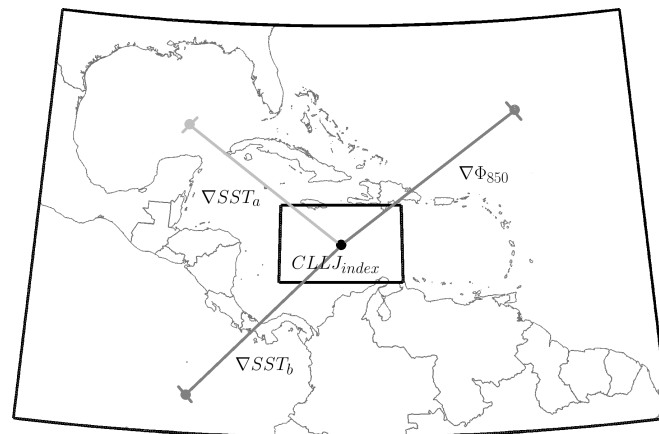


Figure 4.6: Representation of selected points for computing additional indices. The box is the area selected to compute the average of the zonal wind to define the CLLJ intensity index, black spot marks the CLLJ core location, dark and light gray the points selected to compute the SST difference between the CLLJ core and the ETPac and Gulf of Mexico respectively while dark gray on the right shows the point selected to compute the geopotential difference between a point of the NASH and the CLLJ

$$CLLJ_{index} = -(\bar{U}_{x,y}) \quad (4.6)$$

A geopotential height difference was estimated as the difference between the centre of the CLLJ core and a point nearby the mean centre of a developed NASH.

$$\Delta\Phi_{850} = \Phi_{850}(15N, 75W) - \Phi_{850}(25N, 60W) \quad (4.7)$$

Analogously, SST difference between the centre of the CLLJ core and the Gulf of Mexico and the ETPac region were computed.

$$\Delta SST_a = SST(15N, 75W) - SST(24N, 88W) \quad (4.8)$$

$$\Delta SST_b = SST(15N, 75W) - SST(3N, 87W) \quad (4.9)$$

A representation of the locations at which the values of  $U_{x,y}$ ,  $\Delta\Phi_{850}$  and  $SST$  were taken for computing the indices is shown in figure 4.6.

#### 4.4 Additional Reanalysis variables, climate indices and precipitation data

In order to support the Lagrangian trajectories dataset and provide a proper interpretation of the results, additional datasets have been used in the development of this work. Reanalysis data for variables of interest regarding the content of moisture as well as transport and energy were used. Since studying the relation between the transport of moisture and precipitation was part of the objectives of this work, CMAP precipitation data was also used.

##### ERA-40 data

As mentioned, information of additional variables was required to provide a robust analysis of the results and improve their interpretation. This extra information was basically related to winds, atmospheric content of moisture and transport. A set of variables from the high resolution ERA-40 Reanalysis both in surface and vertical levels depending on

---

<sup>5</sup>data from ERA40 Reanalysis was used for computing these indices

availability were retrieved. These variables were used to analyse the mean fields and variability, perform composite analysis to study the effect of determined atmospheric signals among other applications that will be indicated through the document. All data was retrieved for a global domain in a monthly basis with one degree of horizontal resolution and vertical resolution determined depending on the specific required application of the data. Table 4.2 presents a summary of the retrieved variables, corresponding units and resolution.

Variable	Symbol	Units
Pressure levels: 500, 600, 700, 775, 850, 925, 1000		
Divergence	DIV	$\text{s}^{-1}$
Potential Vorticity	PV	$\text{K m}^2 \text{kg}^{-1} \text{s}^{-1}$
U component of wind	U	$\text{m s}^{-1}$
V component of wind	V	$\text{m s}^{-1}$
vertical pressure velocity	OMEGA	$\text{Pa s}^{-1}$
Geopotential height	OMEGA	$\text{Pa s}^{-1}$
Pressure levels: 100, 150, 200, 250, 300, 400, 500, 600, 700, 775, 850, 925, 1000		
Specific Humidity	Q	$\text{kg kg}^{-1}$
Temperature	T	K
Surface		
Mean Sea Level Pressure	MSLP	Pa
Total column water vapour	TCWV	$\text{kg m}^{-2}$
Vertical integrals		
Vertical integral of divergence of moisture flux	VIDMF	$\text{kg m}^{-2} \text{s}^{-1}$
Vertical integral of eastward water vapour flux	VIEWVF	$\text{kg m}^{-1} \text{s}^{-1}$
Vertical integral of northward water vapour flux	VINWVF	$\text{kg m}^{-1} \text{s}^{-1}$
Vertical integral of total column water vapour	VITCWV	$\text{kg m}^{-2}$

Table 4.2: Additional variables retrieved from ERA-40 dataset

## Precipitation

### CMAP data

Precipitation is fundamental for the analysis herein presented, in particular regarding the analysis of the source-receptor relationship and extreme events. In the case of this work, the use of precipitation information is particularly complex since the representation of regions like Central America in the global datasets is poor due to the coarse resolution of the General Circulation Models (GCM) that perform the reanalysis. In addition, the availability of observational data in these regions is scarce. So it was decided to use CMAP dataset. Monthly data for the 1980-1999 time period was extracted from the global CPC Merged Analysis of Precipitation (CMAP) which has a resolution of 2.5 degrees. The CMAP data is produced using information from raingauges and satellite-based estimations (which are not constant in time due to the availability of information). The merging technique used to generate the CMAP consists of a reduction of random errors based on the maximum likelihood method used to obtain linear combinations of the satellites estimates and further use of Reynolds (1988) blending technique. Raingauges information of surrounding areas is used to determine the errors over global land areas while information over the Pacific atolls is used to estimate the random error over oceans. A complete description of the datasets and computation methodology can be found in Xie & Arkin (1997).

### Observations

Due to the nature of this study and the contribution it may represent for further studies on precipitation, moisture transport and the hydrological cycle in general over Central America and the possibility of evaluating the results using long term observations was an ideal portrait. However, the availability of long term complete datasets that meet the criteria of good quality data is quite poor, since most of the observations are distributed along the different regional institutions (and particular companies and owners) and the effort of merging these data is a recently ongoing process <sup>5</sup>. Due to the importance of evaluating at some point the results, an additional effort was made in the attempt of using observations. Data for a total of 386 stations was facilitated by the Center for

---

<sup>5</sup>as part of the projects of the Comote Regional de Recursos Hidraulicos CRRH



Geophysical Research (University of Costa Rica) with daily and monthly mean values ranging from the late forties to 2004 (see distribution of the stations in figure number 4.7.a). First of all, those stations for which data for the 1980-1999 period was not available at all were discarded. Unfortunately, due to the political conflict in Central America during the 80s and 90s most of the stations have more than 75% of missing data for those years. For a reduced number of stations, listed in table 4.3, a basic quality control procedure was applied the data based on the identification of outliers and homogeneity test. The Standard Normal Homogeneity Test (Alexander, 1986) was applied using as reference station a weighted average of the regional time series. After neglecting those stations that did not meet the homogeneity criteria, 42 stations located over Belize, El Salvador, Costa Rica and Panama were found to be usable (see distribution in figure 4.7.b). The criteria can be considered as very restrictive. However, it was decided that it was better to use well proven quality data for less number of stations than using more stations and increase the biases since the objective was to use averaged values (so homogeneity is determinant). Missing data was filled using an imputation of the sample mean method which consists of simply filling in the gaps using the sample mean of the series (Allison, 2001) due to its simplicity. Because of the availability of observations, a simple sort of evaluation was performed but only for those locations for which reliable quality observations data was available.

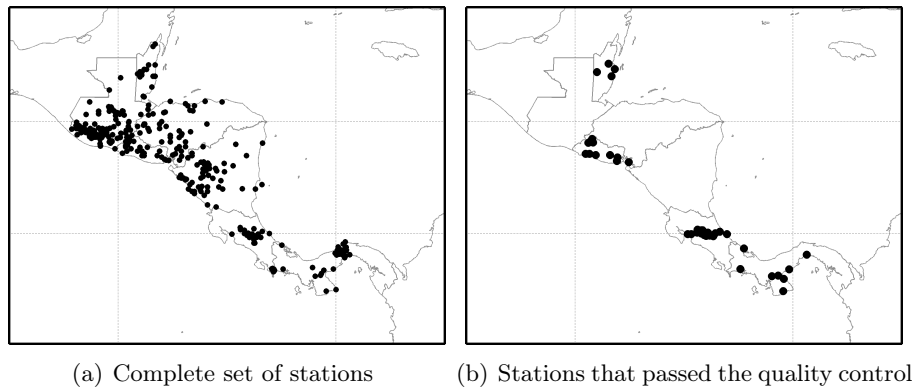


Figure 4.7: Location of a) complete set of raingauges considered for the quality control analysis and b) raingauges that met the quality criteria for the analysis and for which the imputation method was applied to fill the gaps of missing data to be used for the analysis.

Station	%	Station	%	Station	%
Belmopan	77.08	Sesuntepeque	97.50	Rosemont	99.58
Central Farm	93.33	Juan Santamaria	100.00	San Josesito Heredia	100.00
Melinda	90.83	San Jose	80.00	San Vicente	100.00
Pswgia	98.75	Avance 3 Rios	100.00	Zarcero	95.00
Ahuanchapan	99.17	Barrio Mexico	98.33	Cerro Prec	100.00
Candelaria de la Frontera	99.17	CATIE	95.42	Linda Vista	100.00
Guija	99.17	Guadalupe Esparza	100.00	Aton	100.00
La Hachadura	98.33	Diamantes	95.42	David	100.00
La Union	100.00	Laguna Fraijanes	98.33	Divisa	100.00
Nueva Concepcion	100.00	La Lola	95.00	Los Santos	100.00
Planes de Montecristo	96.25	Limon	100.00	Santiago	100.00
San Francisco Gotera	99.17	Pacayas	100.00	Tocumen	100.00
El Papalon	99.17	Puntarenas	100.00	Tonosi	100.00
Santa Ana El Palmar	99.17	Rancho Redondo	100.00	Bocas del Toro	100.00

Table 4.3: Stations used for the evaluation of the estimations of precipitation from the Lagrangian approach.

## Climate Indices

As part of the analysis, different indices were used to identify the presence of strong signals during 1980-1999 period, in particular ENSO, NAO, PDO and MJO. All climate indices used were retrieved from the Climate Prediction Center (CPC) from the website <http://www.esrl.noaa.gov/psd/data/climateindices>

**ENSO** An El Niño 3.4 index defined as the SST anomalies for the Niño region 3.4 which is bounded by  $(120 - 170)W$  and  $5S - 5N$  (Trenberth, 1997) was used since the analysis region is mainly influenced by the Niño region 3.4 to which is closer.

**NAO** NAO index (Hurrell, 1995; Jones et al., 1997) index from the UK Climate Research Unit (CRU) was retrieved through its website <sup>6</sup>. The NAO index available from the CRU Pressure and Circulation Indices is calculated using the normalized

<sup>6</sup><http://www.cru.uea.ac.uk/cru/data/>

pressure difference between one station on Gibraltar and one on Iceland. Information available from the CRU site includes data for SW Iceland (Reykjavik), Gibraltar and Ponta Delgada (Azores).

**PDO** PDO index from Mantua dataset (Mantua et al., 1997) was extracted for the 1980-1999 period. This PDO index is derived as the leading principal component of monthly SST anomalies in the North Pacific Ocean (poleward of 20 N). SST data used to compute the anomalies is from UKMO Historical SST data set, version 1 of Reynold's Optimally Interpolated SST.

**MJO** Using daily MJO index 7 (40W) from CPC (interpolated from pentads to daily values), two annual cycles were computed monthly anomalies were computed with respect to the annual cycle to compute an estimated monthly MJO index.

**WHWP** The WHWP index defined by Wang & Enfield (2001) as the monthly anomaly of the ocean surface area Ocean region enclosed by the 28.5 isotherm in the Atlantic and eastern North Pacific was used for evaluate the influence the presence of the WHWP may have in the regional moisture availability and transport.

## 4.5 Used statistical methodologies

### Empirical Orthogonal Functions

Described by Pearson (1902) and introduced in fluid dynamics by Edward Lorenz in 1956, EOF is a technique that aims to provide a description of the spatial and temporal variability of a time series in terms of orthogonal functions often referred as statistical modes. So it is an useful tool for the identification of variation patterns (von Storch and Zwiers, 2003). An EOF corresponds to a spatial pattern that is used to represent the statistical modes associated with the signals detected in a dataset. The computation of the EOFs can be performed by the construction of a covariance matrix of the given timeseries and its decomposition into eigenvalues and eigenvectors. For computing EOFs for a Field  $F$ , a spatial covariance matrix  $X_F$  must be derived

$$X_F = F * F^T \quad (4.10)$$

$$X_F * E = E\Lambda \quad (4.11)$$

where  $\lambda_m$  are the corresponding eigenvalues

$$\Lambda = \begin{vmatrix} \lambda_1 & 0 & \cdots & 0 \\ 0 & \lambda_2 & \cdots & 0 \\ \cdots & \cdots & \cdots & \cdots \\ 0 & 0 & \cdots & \lambda_m \end{vmatrix} \quad (4.12)$$

$$E = \begin{vmatrix} E_1^1 & E_1^2 & \cdots & E_1^m \\ E_2^1 & E_2^2 & \cdots & E_2^m \\ \cdots & \cdots & \cdots & \cdots \\ E_m^1 & E_m^2 & \cdots & E_m^m \end{vmatrix} \quad (4.13)$$

Here the  $E_m^k$  are the eigenvectors associated with each  $\lambda_m$  eigenvalue since the matrix  $E$  meeting the orthogonality criteria  $E * E^T = E^T * E = I$  ( $I$  is the identity matrix).

The temporal evolution of the  $k^{th}$  EOF is given by a series  $G$  obtained by projecting the original series  $F$  onto  $E_m^k$  such that

$$G_k(t) = \sum E_m^k F_m(t) \quad (4.14)$$

so that

$$G = E^T * F \quad (4.15)$$

Note that each eigenvalue  $\lambda_m$  is proportional to the percentage of variance of  $F$  that accounts for the  $k^{th}$  mode.

## Composites

Despite the simplicity of composite analysis, it is a powerful tool to be used in the construction of an estimate of the mean state of a given variable conditioned by the value of an external index. Composites were constructed for positive and negative phases of the main variability modes (ENSO, NAO, PDO and MJO). To select the basis for compositing, the climate indices for each mode (described in section bla) were used. The categories were set to be positive, negative and neutral condition depending if the negative and positives values of each index were larger or smaller than a threshold

defined as  $\pm 0.75STD$  from the mean series. Values relying in between were classified as neutral, all in a monthly basis. The means were computed for the used fields following the classification shown in tables 4.4 to 4.7, following von Storch and Zwiers (2003) as in equation 4.16, where the sets (composites)  $\Gamma$  of a field  $\mathbf{X}$  conditioned by an index  $\mathbf{n}$  for a number of observations  $i$  are given as:

$$\hat{\mathbf{X}}_{\Gamma} = \frac{1}{i} \sum_{j=i}^i \mathbf{x}_{ti} \quad (4.16)$$

A non parametric test (Mann and Whitney, 1947) was used to determine the evaluate the statistical significance at the 95% of confidence. Depending on the specific purpose of the analysis, the difference between the values of the fields for the positive/negative phase and the values for the neutral conditions was also computed to express the results in terms of the anomalies.

Phases	Winter DJF	Spring MAM	Summer JJA	Autumn SON
Positive	Jan 83	-	Jul 97	Sep 97
	Feb 83		Aug 97	Oct 97
				Nov 97
Negative	-	-	-	-
Neutral	Dec 80, 81, 85, 89	Mar 80, 81, 82, 88	Jun 81, 86, 90, 92	Sep 80, 81, 83, 84
	Dec 90, 92, 93, 96	Mar 90, 91, 93, 94	Jun 94, 95, 96	Sep 90, 91, 92, 93
	Jan 80, 81, 82, 88	Mar 95, 97	Jul 80, 83, 86, 90	Sep 94, 96
	Jan 90, 91, 93, 94	Apr 80, 82, 90, 91	Jul 92, 93, 94, 95	Oct 80, 81, 85, 89
	Feb 80, 82, 84, 88	Apr 94, 95, 97	Jul 96	Oct 90, 92, 93, 96
	Feb 90, 91, 93, 94	May 80, 90, 94, 95	Aug 80, 83, 84, 85	Nov 80, 81, 85, 89
	Feb 97		Aug 86, 89, 90, 92	Nov 90, 92, 93, 96
			Aug 93, 95, 96	

Table 4.4: ENSO Phases

Phases	Winter DJF	Spring MAM	Summer JJA	Autumn SON
Positive	Dec 82, 86, 87, 91	Mar 83, 87, 92, 98	Jun 82, 83, 87, 91	Sep 82, 86, 87, 97
	Dec 94, 97	Apr 83, 87, 92, 93	Jun 92, 93, 97, 98	Oct 82, 87, 91, 93
	Jan 83, 87, 88, 92	Apr 98	Jul 82, 83, 87, 91	Oct 94, 97
	Jan 95, 98	May 83, 87, 92, 93	Jul 93, 97	Nov 82, 87, 91, 94
	Feb 83, 87, 92, 98	May 97, 98	Aug 82, 83, 87, 97	Nov 97
Negative	Dec 88, 99	-	Jul 88	Sep 88
	Jan 89, 99		Aug 88	Oct 88
	Feb 89, 99			Nov 88, 98
Neutral	Dec 80, 81, 83, 85	Mar 81, 82, 84, 86	Jun 81, 84, 85, 86	Sep 80, 81, 83, 84
	Dec 89, 90, 96	Mar 88, 91, 94, 96	Jun 89, 90, 96	Sep 89, 90, 92, 95
	Jan 81, 82, 84, 86	Mar 97	Jul 81, 84, 85, 86	Sep 96
	Jan 90, 91, 94, 97	Apr 82, 84, 85, 86	Jul 89, 90, 95, 96	Oct 80, 81, 83, 84
	Feb 81, 82, 84, 86	Apr 88, 90, 91, 94	Jul 99	Oct 85, 89, 90, 95
	Feb 90, 91, 94	Apr 95, 96, 97	Aug 80, 81, 84, 85	Oct 96
		May 81, 82, 84, 86	Aug 89, 90, 95, 96	Nov 80, 81, 83, 84
		May 88, 89, 95, 96	Aug 98	Nov 85, 89, 90, 95
			Nov 96	

Table 4.5: MJO Phases

### Wavelet analysis

The analysis of time series sometimes finds a problem in their non-stationary nature and wavelet analysis solves this issue by estimating the spectral characteristics of a given time series as a function of time (Torrence & Compo, 1998). Wavelet can be used as a method to detect climate-induced patterns. An advantage on the usage of wavelet analysis is that the wavelet transform decomposes a signal over functions (named wavelets). This leads a good trade-off for the time scale resolution. Which is ideal to allow a good localisation in both time and frequency (Lau & Weng, 1995). A complete description of the wavelet analysis and the correspondent mathematical treatment can be found in Daubechies (1992). For the present work, the analysis was performed following the guide of Torrence & Compo (1997) from which follows that using a mother wavelet  $\Psi$ , the continuous wavelet transform of a time series  $x_n$  is given by

Phases	Winter DJF	Spring MAM	Summer JJA	Autumn SON
Positive	Dec 82, 93, 94, 99	Mar 86, 89, 90, 94	Aug 83	Sep 82, 89
	Jan 83, 84, 93	Mar 95, 97		Oct 86
	Feb 89, 90, 97	Apr 87, 90, 92 May 92		Nov 82, 86, 93
Negative	Dec 95	-	Jun 87, 98	Sep 98
	Jan 85		Jul 93	Oct 80, 92, 97
			Aug 80	
Neutral	Dec 81, 83, 84, 85	Mar 80, 84, 85, 87	Jun 80, 81, 84, 89	Sep 84, 85, 91, 92
	Dec 87, 90, 91, 92	Mar 88, 91, 96, 99	Jun 90, 92, 95	Sep 95
	Jan 81, 92, 96, 98	Apr 81, 82, 84, 85	Jul 80, 81, 84, 86	Oct 84, 87, 89, 90
	Feb 80, 96, 98	Apr 89, 91, 96	Jul 88, 91, 92, 95	Oct 91, 95, 96, 98
		May 81, 82, 83, 84	Jul 97, 98	Oct 99
		May 85, 91, 97	Aug 81, 82, 88, 89	Nov 80, 81, 84, 87
			Aug 93, 94, 98, 99	Nov 88, 89, 90, 91
				Nov 98

Table 4.6: NAO Phases

$$W_n(s) = \sum x_{n'} \Psi^* \left[ \frac{(n' - n)\delta t}{s} \right] \quad (4.17)$$

which by means of the convolution theorem  $F[fg] = F[f] * F[g]$  can be expressed as

$$W_n(s) = \sum \hat{x}_k \hat{\Psi}^*(s\omega_k) e^{i\omega_k n \delta t} \quad (4.18)$$

where the discrete Fourier transform of  $x_n$  is  $\hat{x}_k$  such that

$$\hat{x}_k = \frac{1}{N} \sum x_n e^{-2\pi i k n / N} \quad (4.19)$$

with the angular frequency  $\omega$  defined as

$$\omega_k = \begin{cases} \frac{2\pi k}{N\delta t} & \text{if } k < \frac{N}{2} \\ \frac{-2\pi k}{N\delta t} & \text{if } k > \frac{N}{2} \end{cases} \quad (4.20)$$

The global wavelet spectrum was computed as

$$\overline{W^2}(s) = \frac{1}{N} \sum |W_n(s)|^2 \quad (4.21)$$

Phases	Winter DJF	Spring MAM	Summer JJA	Autumn SON
Positive	Dec 83, 86	Mar 83, 84, 86, 87	Jun 81, 83, 93, 97	Sep 87, 93, 97
	Jan 84, 87	Mar 98	Jul 83, 87, 92, 93	Oct 97
	Feb 81, 86, 87, 98	Apr 80, 81, 83, 84	Jul 95, 97	Nov 86
		Apr 86, 87, 96, 98	Aug 83, 87, 93, 97	
		May 81, 83, 87, 92		
	May 93, 95, 96, 97			
Negative	Dec 90, 94, 99 Jan 91	-	-	Nov 90, 94
Neutral	Dec 80, 82, 85, 88	Mar 82, 99	Jun 80, 84, 85, 89	Sep 80, 81, 85, 86
	Dec 89, 91, 92, 95	Apr 82, 85, 89, 90	Jun 90, 94, 98	Sep 88, 89, 90, 96
	Dec 96, 98	Apr 99	Jul 80, 84, 90, 91	Oct 81, 82, 85, 88
	Jan 80, 82, 90, 92	May 85, 90	Jul 94, 98	Oct 89, 91, 95, 96
	Jan 93, 97, 99		Aug 80, 81, 82, 84	Nov 80, 82, 88, 89
	Feb 82, 92, 93, 97		Aug 86, 88, 89, 90	Nov 91, 95, 96, 98
			Aug 91, 95, 96, 98	
		Aug 98		

Table 4.7: PDO Phases

and the scale averaged wavelet power used to analyse the fluctuations within a range of scales was computed as

$$\overline{W_n^2}(s) = \frac{\delta_j \delta_t}{C_\delta} \sum \left| \frac{W_n(s_j)}{s_j} \right|^2 \quad (4.22)$$

Due to its characteristics, for this study, the selected mother wavelet was Morlet which is defined as:

$$\Psi_0(\eta) = \pi^{1/4} e^{i\omega_0 \eta} e^{-\eta^2/2} \quad (4.23)$$



<b>Phases</b>	<b>Winter DJF</b>	<b>Spring MAM</b>	<b>Summer JJA</b>	<b>Autumn SON</b>
Positive	Dec 97	Mar 83, 87, 98	Jun 83, 87, 97, 98	Sep 87, 97, 98
	Jan 83, 98	Apr 83, 87, 92, 93	Jul 83, 87, 95, 97	Oct 87, 90, 97, 98
	Feb 83, 98	Apr 98	Jul 98	Nov 87, 97
		May 83, 87, 92, 93	Aug 87, 95, 97, 98	
		May 97, 98	Aug 99	
Negative	-	Apr 85, 89	Jun 84	Sep 84, 85
		May 85	Jul 84	Oct 84, 85
			Aug 84	Nov 84, 91
Neutral	Dec 80, 81, 83, 84	Mar 80, 81, 82, 84	Jun 81, 82, 88, 90	Sep 80, 81, 83, 86
	Dec 85, 86, 88, 89	Mar 86, 88, 90, 91	Jun 92, 93, 94, 96	Sep 91, 92, 93, 94
	Dec 90, 91, 92, 93	Mar 92, 93, 94, 95	Jun 99	Sep 96
	Dec 94, 95, 96, 98	Mar 96, 97, 99	Jul 80, 81, 82, 88	Oct 80, 81, 83, 89
	Dec 99	Apr 80, 82, 84, 88	Jul 90, 91, 92, 93	Oct 92, 93, 94, 96
	Jan 80, 81, 82, 84	Apr 90, 94, 95, 96	Jul 94, 99	Oct 99
	Jan 85, 86, 87, 88	Apr 97, 99	Aug 80, 81, 88, 89	Nov 80, 81, 83, 89
	Jan 89, 90, 91, 92	May 81, 82, 84, 88	Aug 90, 91, 92, 93	Nov 90, 92, 93, 94
	Jan 93, 94, 95, 96	May 90, 91, 94, 95	Aug 94	Nov 95, 99
	Jan 97, 99	May 96, 99		
	Feb 80, 81, 82, 84			
	Feb 85, 86, 87, 88			
	Feb 89, 90, 91, 92			
	Feb 93, 94, 95, 96			
	Feb 97, 99			

Table 4.8: WHWP Phases



# 5

## Lagrangian identification of sources of moisture for continental Central America

In chapter 3 the problem of the availability of moisture in the IAS was introduced. From the studies that have analysed this problem, few had as main objective the study of moisture availability and transport to Central America. This is one of the issues that is aimed to be accomplished with this work. In the present chapter, the identification of the sources that provide moisture for precipitation over continental Central America is carried out following a Lagrangian approach. It uses a backward trajectories dataset generated with FLEXPART (as indicated in chapter 4). The mean state of the main sources of moisture is presented for the twenty years analysis period and the seasonality of the sources is explained. The variability of the sources of moisture and their response to the effect of the main climate modes that affect the region are studied using composites. Is the aim of this chapter to provide the most complete details on the horizontal structure of the sources of moisture for Central America.

### **5.1 Identification of moisture sources**

It has been mentioned in chapter 1 that the use of vertically integrated divergence of moisture flux provides information on the regions that may act as moisture suppliers.

From figure 1.5 it can be noticed the presence of a strong divergence region in the vicinity of the tropical Atlantic, the IAS and the ETPac. From figure 1.6, the role of the IAS as a moisture supplier for Central America, the Gulf of Mexico and northern South America can be observed. However, since Central America is a tiny portion of land, a zoom view in the vicinity of the region may be useful. The seasonal averages of vertically integrated divergence of moisture flux and the vertically integrated water vapour flux are depicted in figure 5.1. A strong convergence region over the equator shows the presence of the ITCZ. Larger positive divergence values are noticed in front of South American west coast and the IAS region, similar to the global pattern of figure 1.5. The fields in figure 5.1 show a marked seasonality. Obtaining an estimate of how much of that moisture is actually being transported to Central America is not immediate from this plots (though is a good starting point of the origin of air parcels that contribute to precipitation).

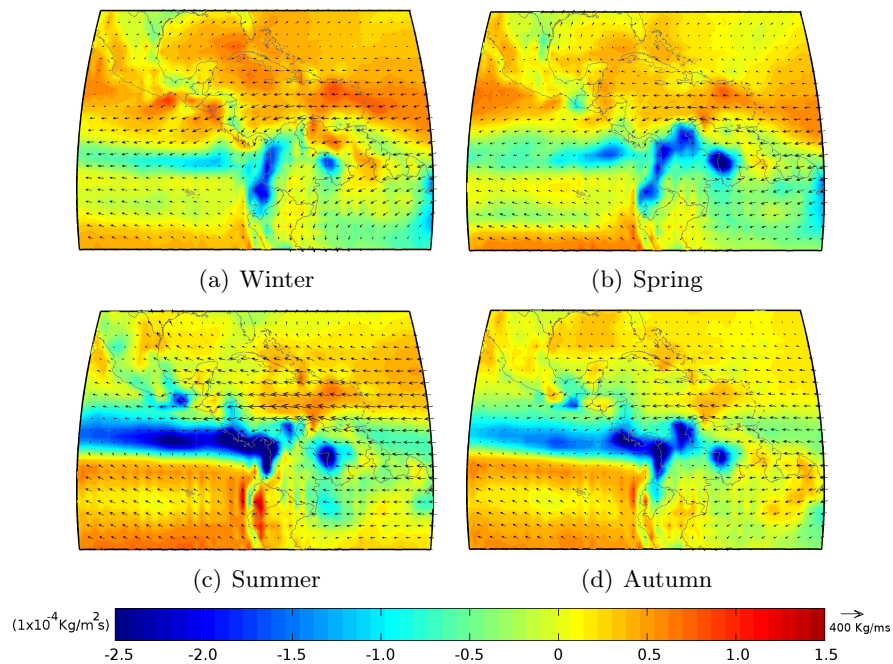


Figure 5.1: Seasonal mean vertically integrated divergence of moisture flux (VIDMF) field (shaded contours) and vertically integrated water vapour flux vector. Contour shades from  $-2.5 \times 10^{-4}$  to  $1.5 \times 10^{-4}$  in  $\text{Kg/ms}$ . Vector reference is  $400 \text{ Kg/ms}$ .

Using the dataset of backward trajectories generated with FLEXPART and ERA-40

data, the method developed by Stohl & James (2004) is used to identify the sources of moisture for Central America. In the exploratory analysis presented in Durán-Quesada et al. (2010) the analysis region was defined as a box centred in Central America and it contained important part of the ocean. Therefore here the analysis domain was restricted to the continental region so that it was defined as an irregular polygon following the coast instead of a box.

### The mean climatology and seasonal cycle

Tracking the air particles that arrive to continental Central America and computing their changes of moisture backward in time,  $E - P$  can be estimated from equation 4.2. The residence time of water vapour in the atmosphere is of the order of ten days (Numaguti, 1999) as well as the moisture-convection feedback time scale in the tropics (Grabowski & Moncrieff, 2004). Integrates of  $(E - P)$  were computed for those ten days and it was found that for Central America, they tend to converge at 6 days so for present analysis 6 days integrates of  $(E - P)$  were used.

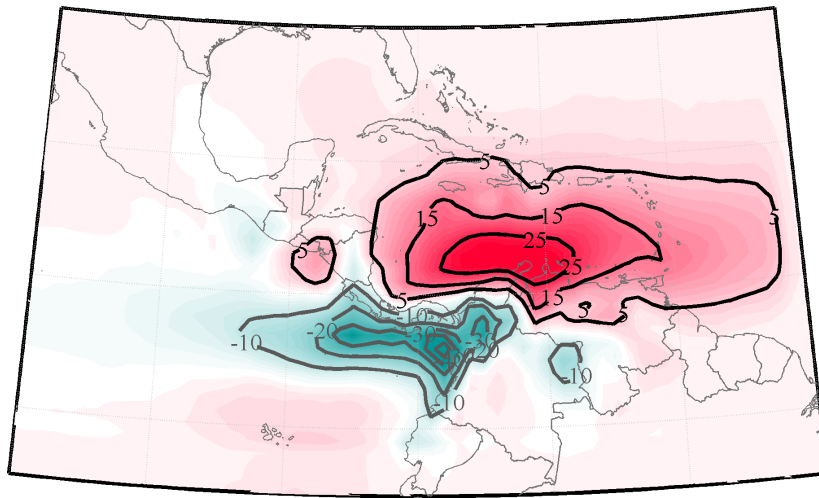


Figure 5.2: Long term mean of the six backward days integrated conditional net fresh water flux  $(E - P)^{-6}$  field in mm/day. Positive contours (in red) every 10mm/day starting in 5mm/day and negative contours every 10mm/day starting in -10mm/day.

Dominance of positive  $(E - P)^{-6}$  values is useful to determine evaporative sources of moisture associated with precipitation over a receptor region. This means that positive

values of the (E-P) field computed for the trajectories backward from a receptor region provide the map of the source of moisture for that region. This is the way the source-receptor relationship can be established. The excess of evaporation observed over the Caribbean Sea is evident from figure 5.2, while a region associated with large evaporation is observed over the ETPac. Both sources of moisture are in agreement with the results of DQ2010. The climatological mean of  $(E - P)^{-6}$  shown in figure 5.2 provides a good picture of the sources of interest but may be neglecting important aspects linked to the seasonality of the sources. The seasonal overview of the of  $(E - P)^{-6}$  field is provided in figure 5.3, which highlights the role of the Caribbean Sea (CS) as the major source of moisture for the region as in figure 5.2. Both intensity and horizontal extent of the CS presents a marked seasonal pattern. So does the source of moisture identified in the ETPac (ETPS), which is characterised for being active only during summer and autumn. Here again, in good agreement with the work by Lachniet et al. (2007). The importance of recycling over northern South America is now noticed from patterns on figure 5.3 (particularly Venezuela Plains and the Magdalena River basin <sup>1</sup>). This region being a source of moisture for Central America was not a direct result of the study of ? and an important finding of the present work.

It can be followed that the CS is a permanent source of moisture for the region while the ETPS is active only during summer and autumn. Note that during winter and spring the CS source is located in the proximity of the Central American coast and retires to the east for the rest of the year with associated intensity variations. The maximum intensity is found (in average) at the end of spring. This is also the period when the core of the contributions has a zonally elongated structure that extends along the Caribbean Sea. As the summer approaches, the core of the CS retires eastward. A decrease in the magnitude of the CS occurs in association with the intensification of the easterly winds. This reflects that stronger easterlies are able to transport moisture from the Caribbean longer distances. Therefore, the Caribbean moisture is able to reach the Pacific whereas contributions to continental Central America decrease. As an implication, the easterly winds are able to modulate precipitation over Central America by modulating the availability of moisture. This supports the proposal of the MSD being a result of the summer intensification of the easterlies as pointed out by ?.

---

<sup>1</sup>one of the rainiest locations on Earth, as indicated in Poveda & Mesa (2000)

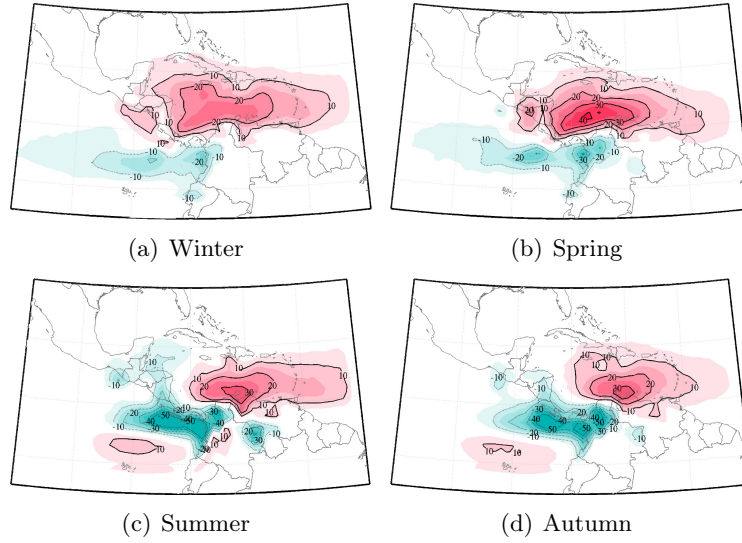


Figure 5.3: Long term seasonal means of the the conditional  $(E - P)^{-6}$  field in mm/day. Positive(red) and negative(green) contours indicated every 10mm/day starting in 10mm/day and  $-10\text{mm/day}$  respectively.

The ETPS starts a slight development by the end of spring and reaches a noticeable intensity by summer that lasts until August. The presence of a source of moisture in the ETPac region results from the existence of a region of strong evaporation (as noticed from figure 1.3 chapter 1). In addition, the southwesterly wind flow intensifies approximately in the same period, allowing moisture to reach the southern part of Central America. The efficiency of the ETPS is strongly constrained to both the northwesterly wind flow and the movement of the ITCZ. The inactivity of the ETPS during winter and spring source may be associated with the southernmost position of the ITCZ. The rate of moisture loss is by far larger than the rate of evaporation, causing that evaporated moisture precipitates over the ocean in the way to Central America, where air arrives drier. Therefore is not able to provide large contributions to precipitation over Central America. On the contrary, as the ITCZ moves northward moisture from the ETPS is allowed to go north and eventually reach Central America until the ITCZ moves south. The ITCZ represents a blocking mechanism for the influence of the ETPac moisture onto Central America.

An oceanic source even less noted in the mean patterns is the Gulf of Mexico (GoM). The monthly means of  $(E - P)^{-6}$  show that during the end of autumn and winter, the

CS extends to the entrance of the GoM. These small influences may be neglected, but in the mean the sum of the contributions from the source of the Gulf of Mexico (GoMS) may account (particularly for northern Central America). Moreover, the importance of the Gulf of Mexico may be magnified by the regional wind conditions, as during winter and early spring, when there is an important wind component pointed southerly to Central America over the Caribbean.

Continental sources of moisture are also found to be important. Recycling of moisture over Central America is expected to be of importance as a result of a) known precipitation cycle and b) vegetal coverage. Central America is a source of moisture (hereafter CAS) for itself mainly during winter and spring, as followed from the seasonal patterns shown in figures 5.3.a and 5.3.b, that is when evaporation exceeds precipitation over the region. Influence from northern South America is identified with particular intensity over the Magdalena river basin and the Venezuela plains region. This northern South America source (NSAS) is of importance during summer and early autumn. However, the seasonal patterns do not provide a proper image of what is actually happening and a look to the monthly means is necessary. Influence from the NSAS<sup>6</sup> is of significance from July to October with the Magdalena river basin exhibiting a maxima of its intensity during September. This excess of evaporation over northern South America is in good agreement with the annual cycle of precipitation in the region featured by a low rainy season between June and September (Restrepo et al., 2006).

It is important to take into account that the horizontal structure of the evaporative sources of moisture provide some information on the conditions of transport and the processes that the air parcels may experience along their trajectories. Figure 5.4 shows the  $(E - P)^{-n}$  for the first, second, fourth and seventh backward days. It can be noticed how the major  $(E - P)^{-n}$  positive values occur to the first backward day ( $n = 1$ ), which implies a strong local contrast between divergence and convergence prior to the arrival of the air parcels. Moreover, the source is much more confined previous to the major moisture loss over the receptor region. The pattern suggests that evaporation is strongly increased over central and western Caribbean. Even when air parcels acquire moisture from the eastern Caribbean, the most relevant uptakes occur in the first four backward days. In the case of the ETPS, the result is different, since the larger intensity occurs

---

<sup>6</sup>see monthly  $(E - P)^{-6}$  fields in appendix B



for the second and third days prior to the arrival while few or no source is noticed for the day before the arrival. Seven and/or eight days before the air arrives to Central America, the air parcels do not contribute significantly to precipitation since the major moisture changes occur over the western Caribbean. This as a result of the regional structures involved in the process of evaporation, SST distribution and zonal winds.

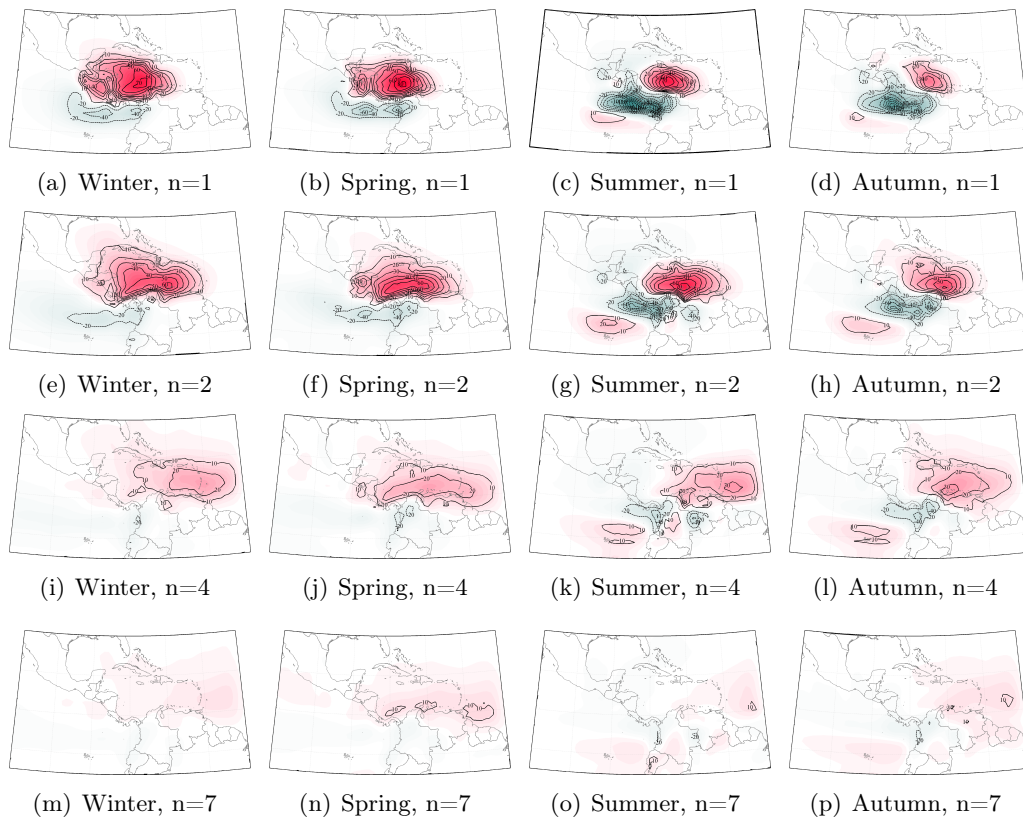


Figure 5.4: Long term seasonal means of the  $(E - P)^{-n}$  field in mm/day. Positive (red) and negative (green) contours indicated every 10mm/day starting in 10mm/day and -10mm/day respectively.

## 5.2 Variability of the sources of moisture

Part of the motivation of the present study was to present an analysis of the interannual variability. That is why after presenting the identification of the main sources of moisture for Central America, the influence of the main variability modes is considered. An

overview of the sensitivity of the field  $(E-P)^{-6}$  to the main variability mods that affect the region is provided by the spatial pattern of the EOFs depicted in figure 5.5. Figure 5.5.a suggests the high sensitivity of the two remote oceanic sources to variability.

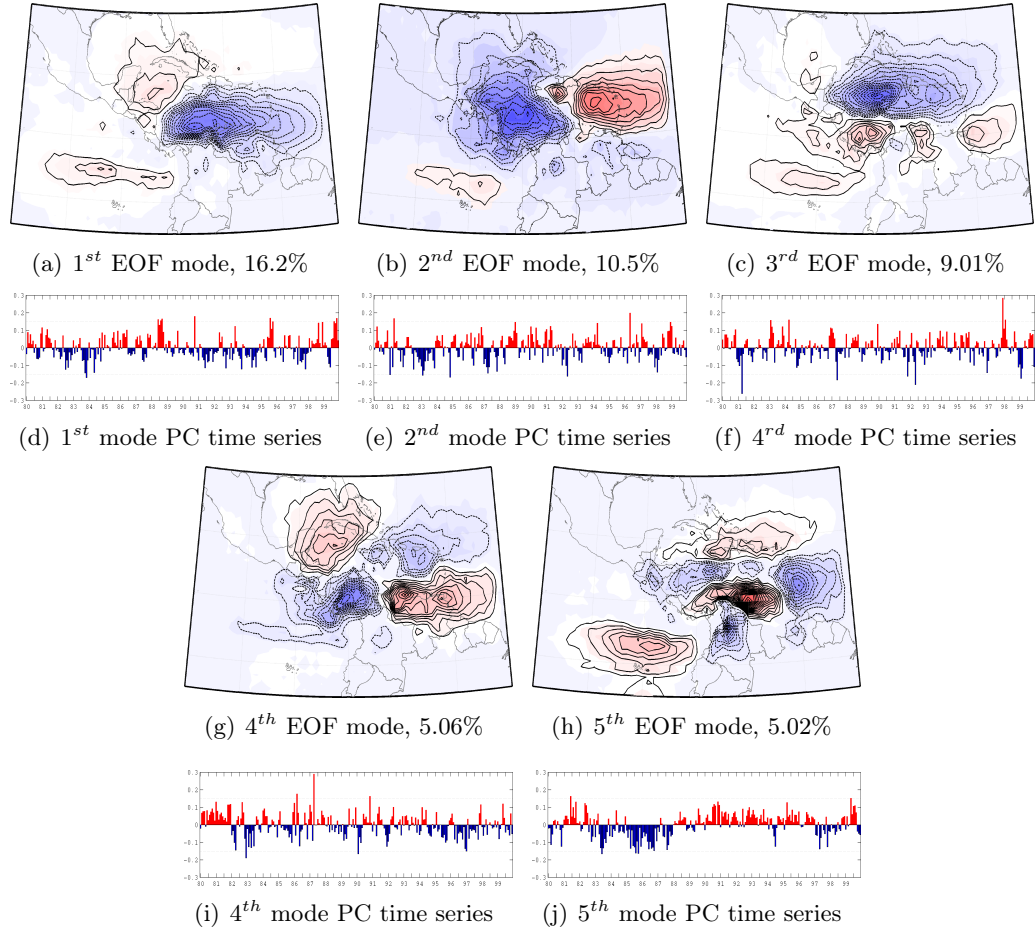


Figure 5.5: First 5 modes of the non rotated EOF spatial pattern for the of conditional  $(E-P)^{-6}$  field computed from the backward trajectories from continental Central America with their correspondent principal component time series and explained variance. First EOF (a) shows the largest variability to be related with the easterly wind flow and evaporation over the ETPS. Second EOF (b) suggests variability of intensity of the CS, third EOF (c) shows a relationship with the fluctuation of the zonal wind, suggesting variability associated to the CLLJ The fifth EOF ( ) shows variability of the NSAS source, with a different behaviour to be remarked between the Venezuela plains and the Magdalena river basin.

First EOF explains 16.2% of the variability, the negative patch that covers the entire Caribbean contrasts with the positive patches in the northernmost Caribbean

region that extends toward the GoM and the region which coincides with the maximum of evaporation that feeds the ETPS. The negative structure shows larger variability associated with the periods of 83-84 and 97-98 while for the positive 88-89, 95-96 and 99 (see the PC series). The negative values of the first PC associated with periods in which the first PC of the zonal wind over the IAS domain presents the same tendency to negative values. The second mode which accounts for a 10.5% of the variability is related with the horizontal extent of the CS. The opposite pattern between the inner and outer Caribbean indicates that when the outer Caribbean has a larger contribution that from the inner Caribbean is reduced and viceversa. The pattern described by the third mode (9% of the variability) is more related with the variability of the meridional position of the source. As the first mode may be associated with the mean easterly flow, the third mode seems to be more related with the fluctuations of the zonal wind. This mode can be associated with the CLLJ as it seems to modulate the contributions from the Caribbean, ETPS, local recycling and transport from the Venezuelan plains. Important peaks on the PC are found at the end of spring for 81, 87, 92 and 98. This suggests a marked sensitivity of this mode to ENSO. The fourth and fifth EOFs account approximately a 5% each, being particularly interesting the pattern of the fifth mode. This describes the variability of the southernmost ETPS as well as the contrast between the components of the NSAS with the PC showing a low frequency variability which seems to range from five to ten years. The latter remarks the importance low frequency variability modes as the PDO may have.

To obtain a more complete picture of the role of the variability modes, composites for positive and negative phases of ENSO, NAO, MJO and PDO were computed for positive  $(E - P)^{-6}$  values that are associated with evaporative sources. Differences between the composites of each phase and neutral conditions were computed in order to provide a direct comparison of the deviations from the neutral conditions when each phase is active. The discussion of the results will be presented individually for each variability mode<sup>2</sup>.

---

<sup>2</sup>the complete monthly composites anomalies are shown in appendix C

## ENSO

In general terms the warm and cold phases of ENSO have an opposite effect on the sources of moisture for Central America. For warm ENSO, the CS is strongly intensified and its structure is confined to the southwestern portion of the Caribbean with an intensified band over northern Venezuela. In January, a westward displacement of the CS starts (as shown by the increase in the magnitude of the CS over the western Caribbean and Central America) while the intensity of the CS decreases significantly over the eastern Caribbean. This displacement peaks in February, when the source region is located crossing Central America and reaching the Pacific side. At this moment the CS has been strongly decreased over the Greater Antilles (figure 5.6.a). The pattern is similar for the following months with decreasing anomalies. During July, the CS is centred over the Caribbean Sea with an intensified branch over Venezuela (figure 5.6.b). Note that for this month, the conditions of the NSAS indicate a decrease over the Magdalena river basin in contrast with the intensification of NSAS. During August, the intensification of the CS drops at the same time that the ETPS starts a significant reduction of intensity until November. The end of autumn is featured by a pattern, that besides the reduction of the ETPS, shows the intensification of the CS with an extension at the east of the Lesser Antilles. Being the latter linked to the decrease of the northern part of the CS with respect to its neutral conditions (figures 5.6.c and 5.6.d).

In the case of the cold phase of ENSO, the eastward displacement of the CS starts during December with an intensified core at the east of the Greater Antilles (figure 5.7.a). In January, the December core is displaced to the south while the CS over the Central Caribbean decreases strongly. The structure of the CS is modified, its intensity increases to the west (centred over the southern Central American Caribbean region) and reduces over the Antilles (figure 5.7.b). The peak of this intensification is reached in May, followed by a drastic reversal of the pattern in June. A strong intensification of an evaporative source west off Costa Rica is accompanied by a marked decrease of the potential source directly over the Caribbean Sea and NSAS (figure 5.7.c). The anomalies that determine these patterns decrease slightly to be reinforced at the beginning of autumn. This occurs when the reductions of the CS reach the region of the Gulf of Mexico. In this period, increases of the ETPS are elongated to the west (figure

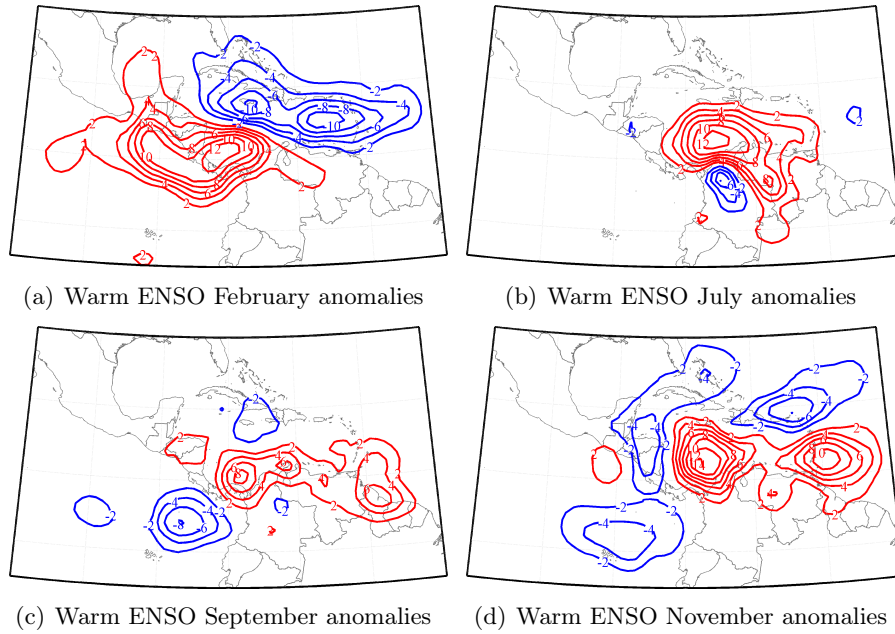


Figure 5.6: Differences between the  $(E - P)^{-6}$  field for warm ENSO and neutral conditions composites. Contours every 2 mm/day, red for positive anomalies and blue for negative.

5.7.d). At the end of autumn, the intensification of the CS over the central Caribbean is remarked.

The  $(E - P)^{-6}$  field and the zonal wind speed at 850mb were regressed onto the Nino 3.4 index. From the regression coefficients shown in figure 5.8, it can be followed that during winter (5.8.a) the positive coefficients are centred in the southernmost portion of Central America with larger values in the Panama Pacific coast. As spring approaches (5.8.b) those positive values extend all over the Central American Pacific coast. For summer and autumn, those positive values dislocate to the Caribbean (5.8.c, 5.8.d) with an important component over the Venezuela plains (5.8.c) (which is maximum during summer). Negative regression coefficients can be noticed over the region occupied by the ITCZ and the Lesser Antilles during winter (5.8.a) and only over the ETPac ITCZ region during spring (5.8.b). During summer, strong negative regression coefficients over the ETPac region contrast with the positive pattern observed over the Caribbean (5.8.c). Moreover, there is a difference in the evapotranspiration pattern over continental Central America, as suggested by the positive (negative) values

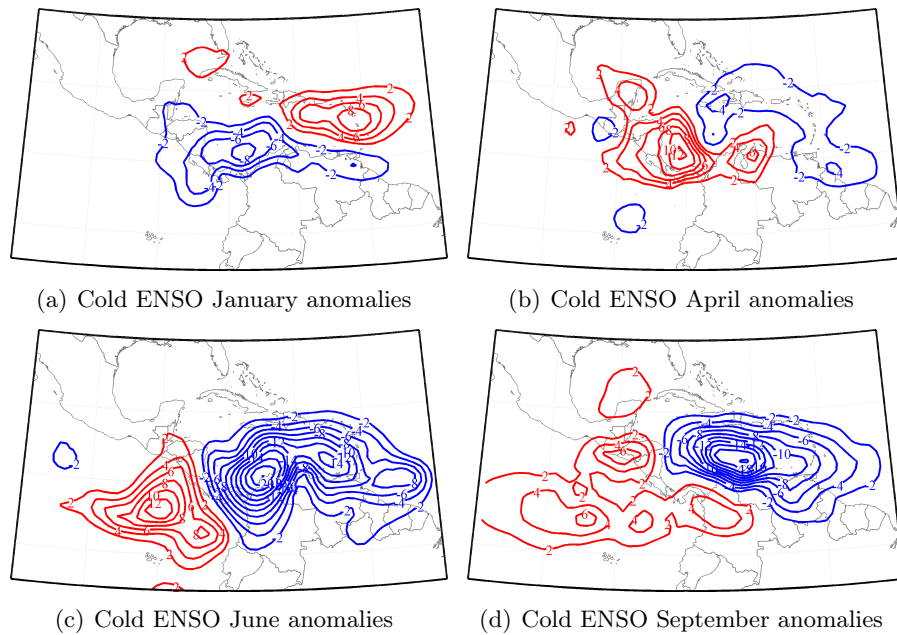


Figure 5.7: Differences between the  $(E - P)^{-6}$  field for cold ENSO and neutral conditions composites. Contours every 2 mm/day, red for positive anomalies and blue for negative..

for southern (northern) Central America. The regression of the zonal component of the wind shows an important shift between the Caribbean and the Pacific. The regression over the Caribbean exhibits negative (positive) regression coefficients during summer and autumn (winter and spring). Meanwhile, over the ETPac positive values are observed all year round. Notice that as more intense are the easterlies more defined becomes the structure of the negative regression of the zonal wind (and more extended to the ETPac). However, during winter (when the CLLJ has the secondary maximum), the structure of the regression coefficients, even when extended through the ETPac, is positive under ENSO (5.8.a).

The contrast between the regression coefficients for the main oceanic sources of moisture highlights the opposite response the sources have to ENSO. This is of great importance as it is related with the variability of precipitation related to the forcing of this mode as will be discussed in the following chapter.

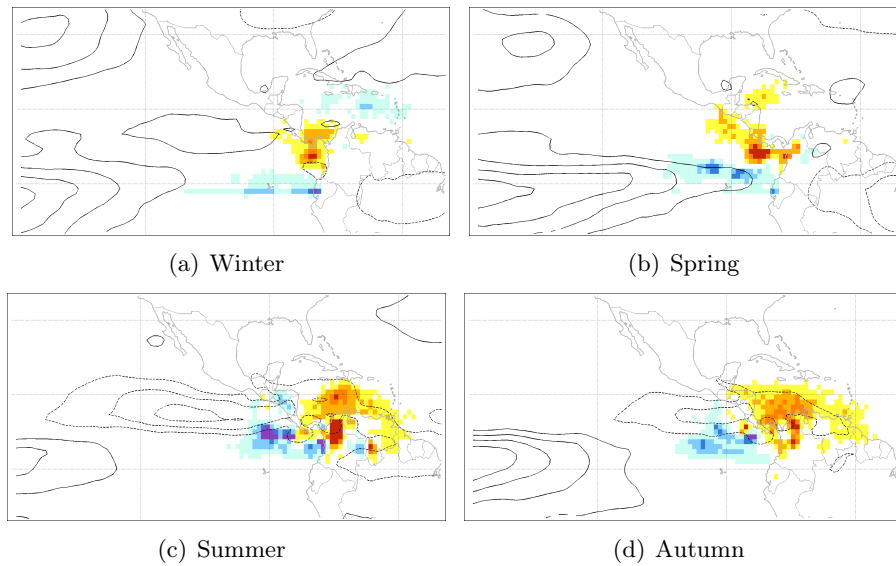


Figure 5.8: Regression coefficients maps for conditional  $(E - P)^{-6}$  and zonal component of the wind at 850 hPa regressions onto the Nino34 index.

## NAO

The influence of the NAO starts to be of importance in spring, with the reduction of the magnitude of the CS (figure 5.9.a) during the positive phase. The intensification of evaporation over the northernmost Caribbean is observed during April, when the ETPS is reduced (figure 5.9.b). A pattern of strong intensification of the source over the northern Caribbean and the reduction of the ETPS feature the end of spring. In early summer, evaporation over continental Central America has decreased in comparison to the neutral years and the CS exhibits a different pattern. In June, the region of major evaporation is retired to the east of the Lesser Antilles (figure 5.9.c). During July, the excess of evaporation over the central Caribbean Sea is intensified for NSAS while decreased in the Pacific coast of northern South America. In August the intensity of NSAS is significantly enhanced. The pattern for September is featured by a well defined intensification of the CS along the horizontal extension of the Caribbean Sea. A band of negative anomalies over continental Central America and the ETPac shows a marked decrease of evaporation that implies a reduction of the CAS and ETPS (figure 5.9.d).

Negative NAO presents the opposite pattern for March compared to the positive

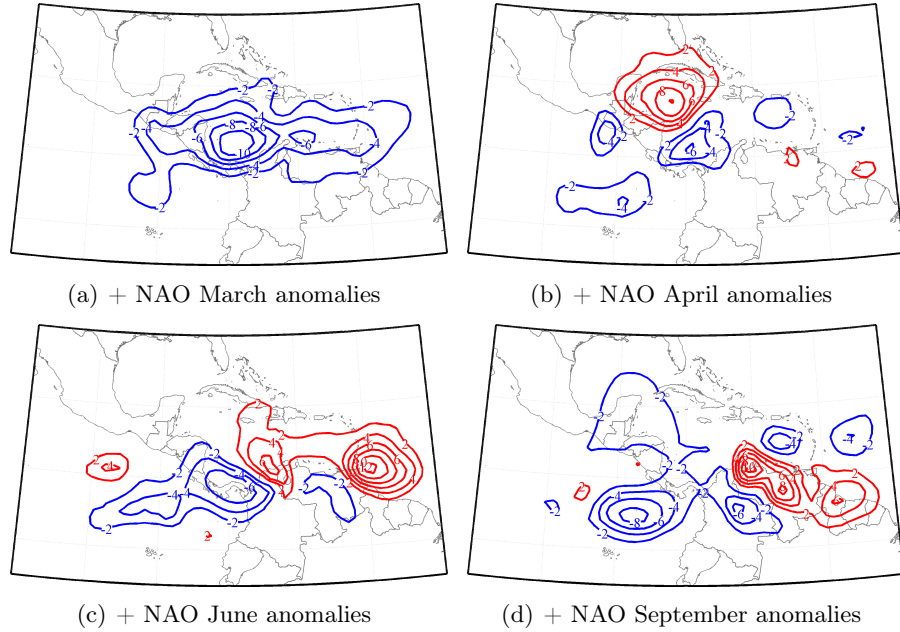


Figure 5.9: Differences between the  $(E - P)^{-6}$  field for positive NAO and neutral conditions composites. Contours every 2 mm/day, red for positive anomalies and blue for negative.

phase. The CS is intensified over the central Caribbean while reduced over the easternmost part (figure 5.10.a). During April, the position of the CS is limited to the westernmost portion of the Caribbean and has a latitudinal extension that reaches the Gulf of Mexico. The CAS is also intensified while the pattern shows a decrease of the evaporation from the middle to the east Caribbean as well as for the ETPS (figure 5.10.b). In July, the evaporation over the westernmost Caribbean and Venezuela decreases. The ETPS is strongly reduced at this moment. Small intensifications of evaporation over different portions of the Caribbean take place until November. When the evaporative source extends from northern Central America to the Greater Antilles with a strong intensification that peaks in front of Honduras Caribbean coast. During the same month, the NSAS as well as evaporation over the Lesser Antilles and a latitudinal band in the Pacific that extends from 13 N to 3S is decreased (figure 5.10.d).

The regression of the  $(E - P)^{-6}$  and U wind over the NAO index (5.11) shows the effect this mode has on the sources of moisture during spring (therefore on pre-



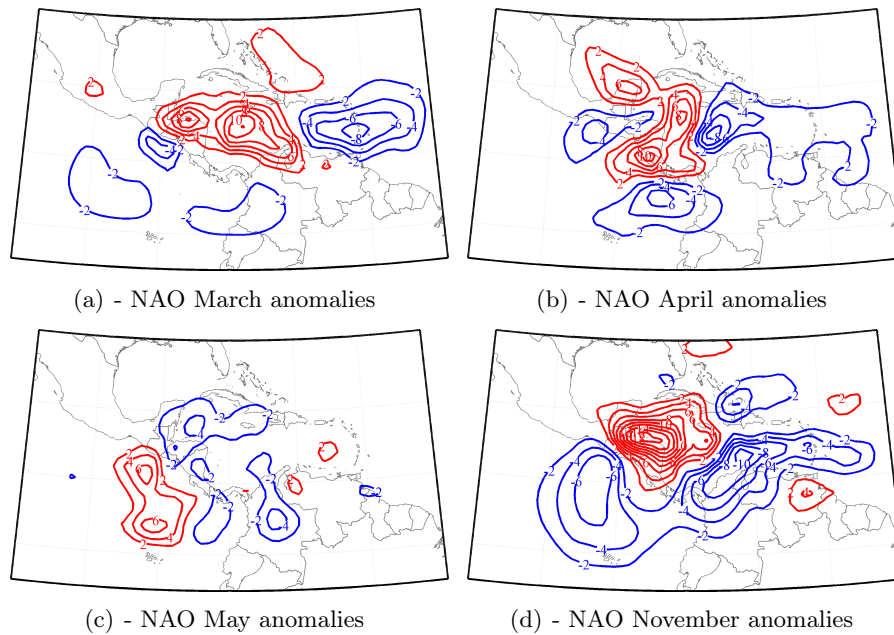


Figure 5.10: Differences between the  $(E - P)^{-6}$  field for negative NAO and neutral conditions composites. Contours every 2 mm/day, red for positive anomalies and blue for negative.

precipitation). As the NAO signal is more intense during winter, its effect becomes more noticeable in spring where precipitation is more intense (compared to the minimum of precipitation during winter). Positive regression coefficients can be observed in the northern Caribbean and southern Central American Pacific coast. Marked negative values can be observed over the region featured by the pass of the ITCZ over the ETPac and the Tehuantepec region, the topographic gap through which easterly winds pass to the ETPac. In spring the fingerprint of the NAO is very important for the northern Caribbean, its effect shows a tendency to enhance the variations in evapotranspiration over Central America. Therefore, this mode may be related with important variations in the continental precipitation patterns.

## PDO

The influence of the PDO is more complex to describe in terms of the observed anomalies patterns. For the positive phase, the decrease of the intensity of the CS occurs for December and January (figure 5.12.a). A short intensification of evaporation over

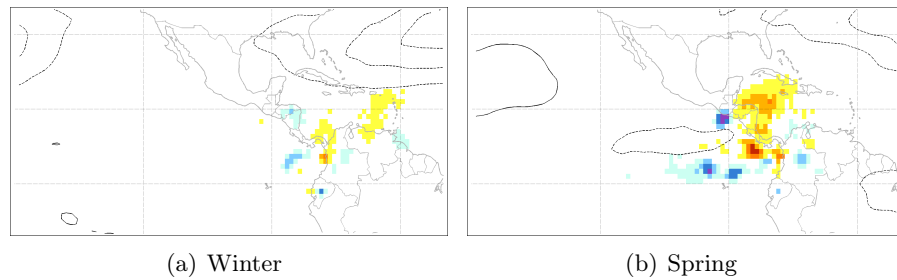


Figure 5.11: Regression coefficients maps for conditional  $(E - P)^{-6}$  and zonal component of the wind at 850 hPa regressed onto the NAO index.

continental Central America during February is accompanied by the decrease of evaporation over the Lesser Antilles (figure 5.12.b). The further decrease of evaporation over the complete Caribbean basin during March is followed by similar conditions in the NSAS and a reduction of the ETPS during April. In May, the ETPS presents a small intensification as well as a region of the Caribbean enclosed between northern Central America and Cuba. Evaporation increases over the ETPac, southern Central America and the border between Colombia and Venezuela during June. Then, the importance of these regions as sources of moisture increases too. Meanwhile, a small decrease of the CS is noticed (figure 5.12.c). During August the evaporative source over central Caribbean increases altogether with a strong intensification of evaporation over Colombia. Small positive anomalies over the Caribbean and ETPac are followed by reductions of evaporation between Nicaraguan east coast and the Greater Antilles for the remaining months. This occurs until November, when evaporation is enhanced over Central America and to the east of the Lesser Antilles while reduced over the Caribbean and the ETPac (figure 5.12.d).

For negative PDO, the evaporative source is intensified over the Lesser Antilles and decreased from the middle Caribbean to the east coast of Central America, with a reduction over the Gulf of Mexico during January (figure 5.13.a). Small decreases of evaporation occur over the Caribbean and west coast of southern Central America for February and March. In April the evaporative source over the ETPac decreases jointly with evaporation over Central America and the transect between northern Central America

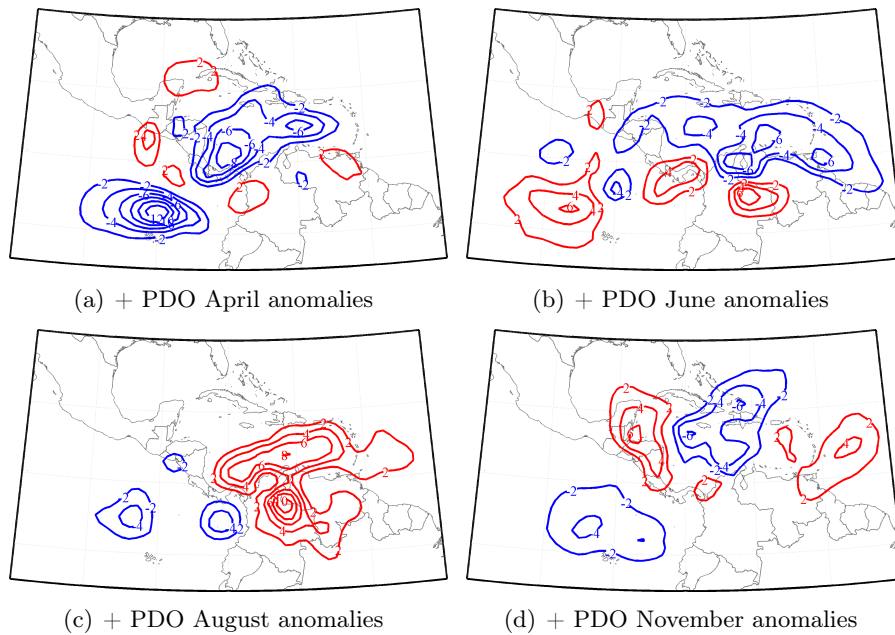


Figure 5.12: Differences between the  $(E - P)^{-6}$  field for positive PDO and neutral conditions composites. Contours every 2 mm/day, red for positive anomalies and blue for negative.

and Cuba. This at the same time that increases over easternmost Caribbean. In May, the reduction of evaporation over southern Central American west coast decreases its intensity and a small increase of the ETPS takes place (figure 5.13.b). The latter, accompanied by the intensification of evaporation over a zonal band extended over southern Caribbean and northern South America. This zonal band of increases of the evaporative source moves northwestern while a reduction of evaporation takes place over the ET-Pac and Colombia (figure 5.13.c). The following months are featured by the reduction of NSAS and evaporation over southern Central America as well as the intensification of CS and ETPS. During September evaporation over Venezuela exhibits a decrease of intensity while an increase is noticed over northern Central America, Panama and the ETPac. For October the increase of evaporation over the ETPac and southern Panama east coast persists while the intensity of evaporative sources decreases over central Caribbean. In November, the evaporative source present a generalised decrease over central and south Caribbean while is intensified over the northern Caribbean, the Gulf of Mexico and the ETPac (figure 5.13.d).

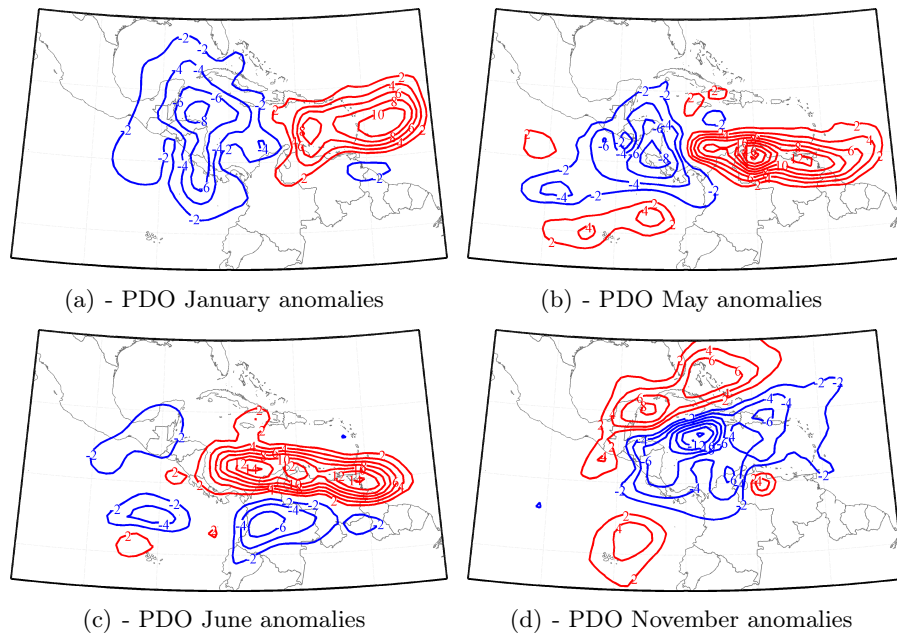


Figure 5.13: Differences between the  $(E - P)^{-6}$  field for negative PDO and neutral conditions composites. Contours every 2 mm/day, red for positive anomalies and blue for negative.

The regression maps (5.14) show positive coefficients during winter all over Central America during winter and negatives in the outer Caribbean (5.14.a). In spring, negative regression coefficients over Panama and the Venezuela Plains can be noticed. The regression map for spring is also featured by positive values over Costa Rica, Nicaragua, northern Caribbean and Costa Rican Pacific coast (5.14.b). The contrast between maximum positive regression values over NSAS and Costa Rica and the negative pattern observed over Central America can be noticed during summer (5.14.c). In autumn, the contrast more noticeable, intense positive regression coefficients for the Caribbean and NSAS while negative for the ETPac region (5.14.d). Positive coefficients for the regression of the zonal component of wind onto the PDO index is observed extending from the TNA to the Gulf of Mexico during winter (5.14.a) and over the Caribbean during spring (5.14.b). Negative coefficients for the zonal wind regression extends from the Caribbean through the ETPac in autumn (5.14.d). It is important to remark that the regression maps show the importance the PDO has particularly for NSAS. The signal of the PDO is noticed to have a remarkable effect on the distribution and intensity of the

sources of moisture mainly during summer and autumn. The strong relation between the PDO and the variations of local recycling implies quite a large response of local precipitation to this mode. Moreover, the impact for the CS is observed during autumn with a very important signal over NSAS. The latter result will be more exploited in the following chapter where the contributions to precipitation are analysed.

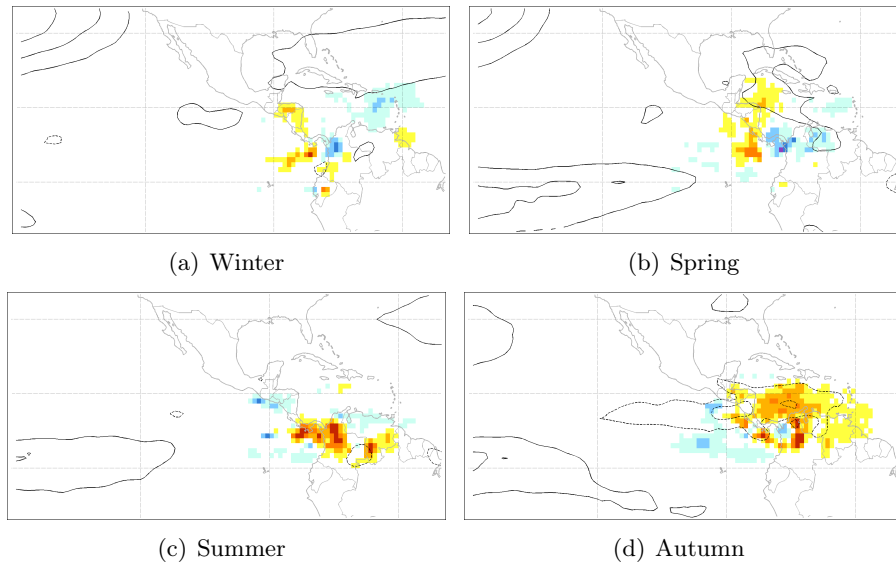


Figure 5.14: Regression coefficients maps for the conditional positive  $(E - P)^{-6}$  field and the zonal component of the wind at 850 hPa regressed onto the PDO index.

## MJO

For the defined positive MJO phase, a generalised decrease of evaporation over the Caribbean takes place during winter. Increases to the east of the Lesser Antilles are more intense in February (figure 5.15.a). The decrease of evaporation is strong over Central America during March. From April to May a new intensification of the evaporative sources CAS and CS while the ETPS shows significant reductions of intensity compared to the neutral years (figure 5.15.c). In June a positive-negative pattern shows evaporation to be increased over the tropical Atlantic coast of northern South America and Colombia while decreased over the Venezuela plains (figure 5.15.e). A reduction of evaporation over the ETPS and CAS west coast is also present during June. A moderate decrease of evaporation over the Caribbean and northern Colombia occurs for July

(figure 5.15.g). This with an intensification of evaporation in the Colombia-Venezuela border in August. Variations for the remainder months are very small. A marked intensification of the evaporative source over the north-westernmost Caribbean is noticed accompanied by a decrease of NSAS, the easternmost CS and the ETPS (figure 5.15.i).

In November, for the negative phase of the MJO, the confinement of the CS and the presence of an intensified GoMS with decreases of evaporation on the borders are noticeable for December. A pattern of small negative(positive) anomalies over the Caribbean (CAS and ETPS) is observed from January to March (figure 5.15.b). The decrease of the easternmost ETPS during April is compensated by the increase of CAS, northern CS and GoMS. For May, an the western ETPS is intensified and decreased to the east. A zonal band of intensified evaporative source is visible along the southern Caribbean with a band of decreased intensity of evaporation just below in June (figure 5.15.f). During July, the band of negative anomalies is vanished and the positive band is transformed into a well defined region of intensified CS and NSAS (figure 5.15.h). Small deviations from the neutral conditions for Autumn are followed by intensified (decreased) evaporation over the Lesser (Greater) Antilles, central-southern Caribbean and ETPac (figure 5.15.j).

The influence of the MJO is relatively small during winter as it increases after spring. The  $(E - P)^{-6}$  and zonal wind fields were regressed onto the MJO index defined in chapter 4. From the regression maps shown in figure 5.16 the positive regression coefficients are noticed to be important over the southern ETPac during spring (5.16.a) with a dislocation to the north and maximum of positive values during summer (5.16.b). Note the positive values over the Venezuela plains and northern Central America. Negative values are observed over the Pacific coast of Central America during spring (5.16.a) and over the Caribbean during summer (5.16.b) in contrast with the positive observed over the ETPac for the same season. Negative regression coefficients are also well defined over the Caribbean during autumn with the largest negative values over the Caribbean coast of Panama and northernmost part of NSAS (5.16.c) in contrast with the positive values extending from the Costa Rican Pacific coast to the west.

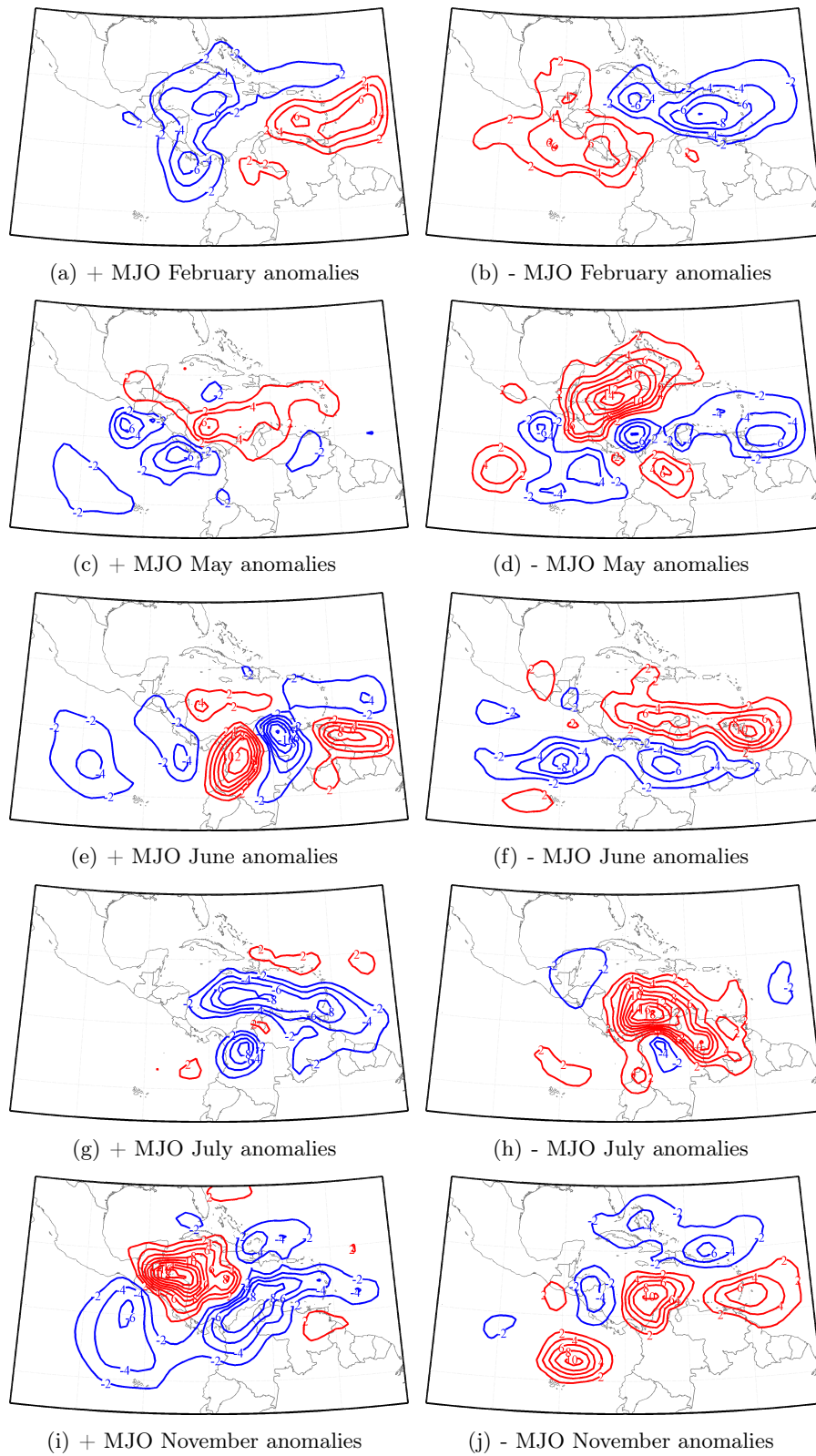


Figure 5.15: Differences between the  $(E - P)^{-6}$  field for positive MJO and neutral conditions composites (a,c,e,g,i). Contours every 2 mm/day, red for positive anomalies and blue for negative and differences between the  $(E - P)^{-6}$  field for warm ENSO and neutral conditions composites. Contours every 2 mm/day, red for positive anomalies and blue for negative MJO (b,d,f,h,j). Positive MJO composites at the left and negative to the right hand side.

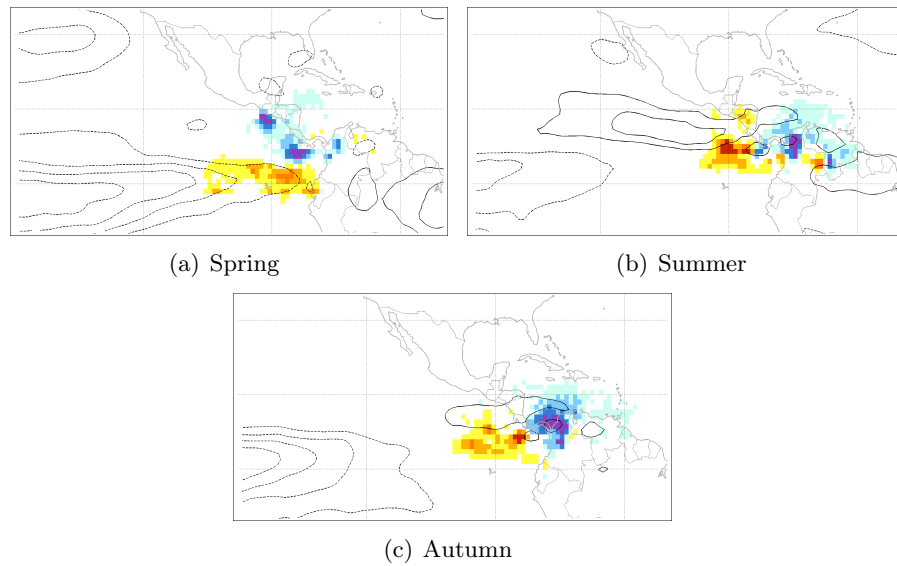


Figure 5.16: Regression coefficients maps for conditional positive  $(E - P)^{-6}$  and zonal component of the wind at 850 hPa regressed onto the MJO index.

### 5.3 Chapter highlights

In the present chapter, the sources of moisture for precipitation over Central America were identified using the Lagrangian methodology described in chapter 4. In good agreement with previous studies, the Caribbean Sea was determined to be the main source of moisture for Central America. Further evidence of the importance of a source over the ETPac region, as provided as in DQ2010 and in agreement with findings using isotopes (Lachniet et al., 2007) but now for a longer time span. The role of northern South America for providing moisture to Central America was determined to be of importance, as well as recycling over Central America. More detailed information on the regional hydrological cycle in comparison to previous studies was provided. The identification of a remote continental source of moisture over Northern South America that has not been documented up to now is of importance for further analysis of the water cycle in tropical America (Durán-Quesada et al., 2012). The identified sources were found to have a well marked seasonal cycle, where month to month variations are of importance for analysing features that are lost in the averaging, as is the case of the Gulf of Mexico acting as a moisture sources. Up to almost a 70% of the variability of



the sources of moisture is explained by the first 5 EOFs modes which suggests that the CS undergoes the most significant variability, both in intensity as in movement of the location of the main source region in the inner/outer Caribbean. An interesting pattern of variability of the NSAS suggests that this source has two components which are modulated in the Venezuelan by low level winds over the plains and by the convergence over the Colombian counterpart. The response to the reviewed variability modes was found to be basically the modulation of intensity but more importantly for the CS the horizontal structure of the source. The low frequency variability of the fifth EOF associated to the ETPS and NSAS is quite interesting and it would be a ideal to study the remote continental source in detail for longer time periods since for this purpose the 20 years series may be too short.



# 6

## Relative contributions to precipitation

The identification of the sources of moisture provided in the previous chapter allowed the determination of the regions that play a role as sources of moisture for Central America. The pattern of the annual cycle describes the variations of the evaporative sources of moisture as a result of the seasonal mean conditions. Response to variability modes was also questioned. This is a good approximation to assess the origin of moisture that arrives to a determined region. The Lagrangian trajectories allow a more specific analysis of the relationship between the moisture available from any source and precipitation. The Lagrangian diagnostics enable the gathering of information of several features of an air mass along its trajectory, for instance of ongoing processes. Here we aim to provide a quantitative estimation of the contribution from the sources to precipitation falling over Central America. Present chapter provides a description of the seasonal mean  $(E - P)^6$  fields from forward tracking for the identified sources of moisture. An evaluation of the estimates of contributions to precipitation is performed considering the estimates for Costa Rica and Panama using precipitation observations. The contributions to precipitation over Central America are analysed. Finally, variability of the contributions is analysed along section and the response of the contributions to the influence of the main variability modes is explained.

## 6.1 Estimation of moisture lost over Central America

From the identification of sources of moisture, five main source regions were found to provide moisture that precipitates over continental Central America. The Caribbean Sea (CS), the Gulf of Mexico (GoMS), Eastern Tropical Pacific (ETPS), Northern South America (NSAS) and local recycling over Central America (CAS), see figure 6.1. Note from figure 6.1 that the region assigned to the ETPS does not exactly match the extension of the evaporative source observed in figures 5.2 and 5.3. However, this selection for the ETPS was made in order to consider not only the climatological mean horizontal extension of the source but to account for the monthly variations of this source as well as its internannual variability, as detailed in section 5.2 chapter 5. The selection made for the ETPS allows the consideration of all possible meridional displacements of the source that may be lost in the averaging of the fields.

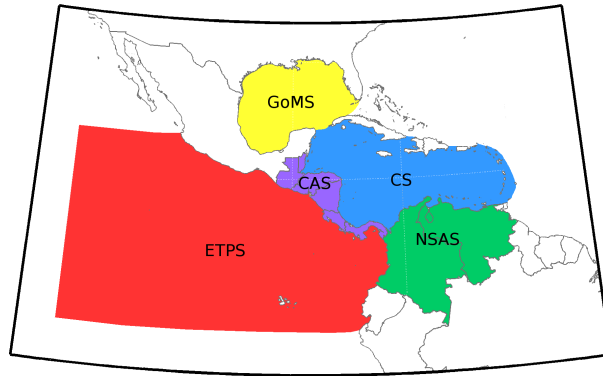


Figure 6.1: Representation of the sources of moisture for continental Central America identified in the previous chapter. Note that the area comprised by the ETPS is more extended in comparison with the regions where the positive values of the conditional  $(E-P)$ -6 field were found, this in order to account for the meridional movements of the source of moisture over this location which varies month to month.

When the air particles are allowed to move forward in time from a source region, the  $(E-P)$  estimation provides further information on the destination where moisture is lost. Therefore those regions for which  $(E - P) < 0$  can be associated to regions where moisture from the sources is lost as precipitation. Integrated  $(E - P)^6$  were computed from the sources, note that as we are interested only in precipitation associated term, only negative values are shown (the sign was inverted to represent precipitation as a

positive term). From the seasonal means of the  $(E - P)^6$  field for the Caribbean Sea it can be noticed that most of its moisture precipitates out of it. During winter, the major contributions from the Caribbean Sea are to precipitation over the Gulf of Mexico and the ETPac region, under the precipitation regime of the ITCZ (figure 6.2.a). The importance of the Caribbean Sea during spring presents a pattern in which larger precipitation originated from Caribbean air masses penetrates inland, the contributions do not go further 100W (figure 6.2.b). This increases precipitation over continental Central America and western Colombia, in agreement with the observed peak of precipitation over Central America. In the same figure, enhancement of precipitation due to Caribbean moisture can be noticed over northern Central America (mainly Guatemala). The intensification of precipitation associated to moisture from the Caribbean is larger in summer. It increases over eastern Mexico and southern Central America and larger  $(E - P)^6$  values are found west of Costa Rica and southwesternmost Mexico (figure 6.2.c). With the correspondent decrease of precipitation associated to the contributions from the CS over northern Central America and western Mexico. This pattern is similar to that of zonal winds, with the locations in which  $(E - P)^6$  is larger being almost the same that the regions where the westward wind flow is enhanced by the presence of topographic gaps. This is, the 'Tehuantepec' (southwesternmost Mexico) and 'Papagayo' (Costa Rica) gulfs. During this period, contributions from the CS to precipitation over the Pacific side of the topographic gaps is larger than 35 mm/day while contributions to precipitation over the Caribbean Sea roughly reach the 5 mm/day at the westernmost side. This in good agreement with the suppression of precipitation over the Caribbean Isles during summer, as known from previous works (see e.g. Magana et al., 1999). Contributions to precipitation over Central America are limited to the south, however it can be observed how the major part of moisture is lost over the ETPac. In autumn, the intensity of the negative values of  $(E - P)^6$  has decreased in the north, but strongly intensified over southernmost Central America (figure 6.2.d). The export of moisture from the Caribbean Sea that precipitates over Central America explains a good part of the differences observed in the precipitation regime of Central America. Up to 40 mm/day are lost over southern Central America while a maximum of 15 mm/day are lost over the northern part of Central America, in agreement with a drier northern Central America compared to the south.

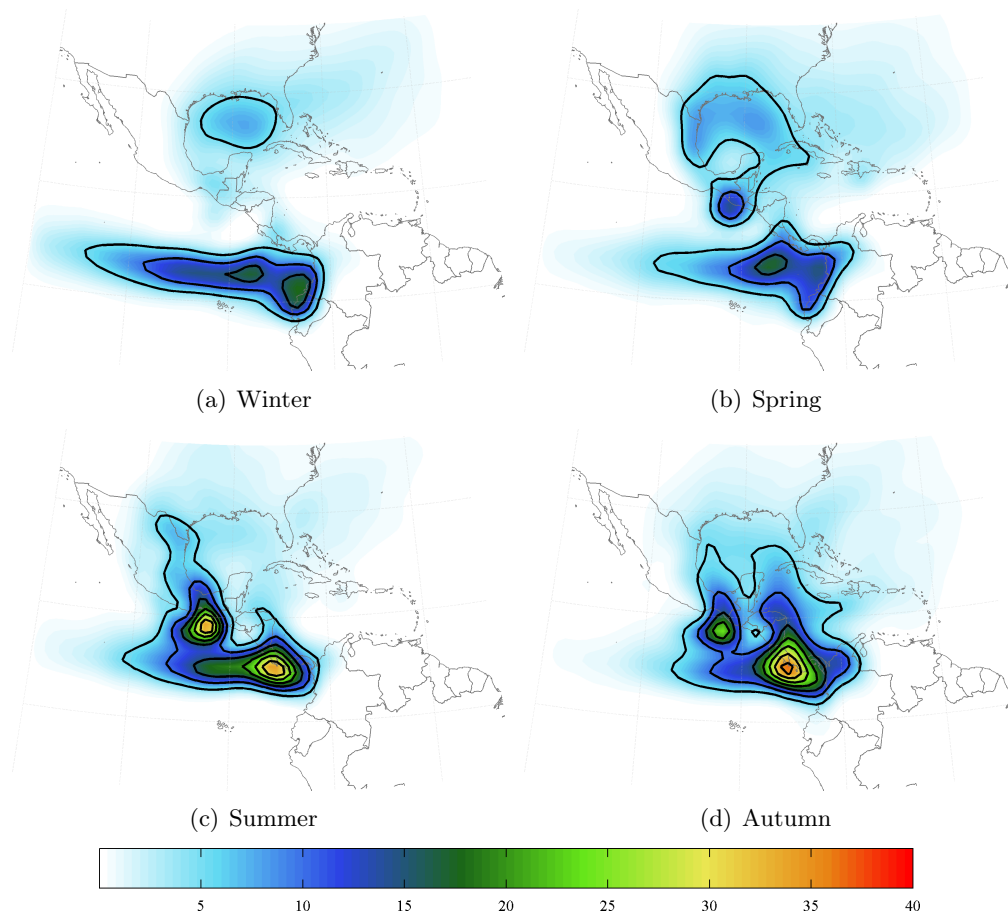


Figure 6.2: Average six days integrates of the conditional  $(E - P)$  field computed forward from the Caribbean Sea for a) Winter, b) Spring, c) Summer and d) Autumn. Larger positive values in yellow and orange show the regions where precipitation associated with moisture from the CS is larger. Values in mm/day and contours every 5 mm/day starting at 5 mm/day.

As for the Caribbean Sea, the  $(E - P)^6$  fields were computed for the other component of the IAS, the Gulf of Mexico. Most of the moisture from this source is lost over the Great Plains and northeastern Mexico. The pattern observed for autumn, winter and spring is quite similar, with larger  $(E - P)^6$  values (up to 15 mm/day) for spring. It is important to notice that during autumn, some moisture is lost over southern Mexico, crossing along Tehuantepec and reaching the Pacific side (figure 6.3.a). Moisture from this source lost over Central America is basically limited to the north. In summer the negative values of the  $(E - P)^6$  field present an extended horizontal structure with a strong presence over Mexico in comparison to the other seasons (figure 6.3.b). These

contributions from moisture of the Gulf of Mexico that precipitates over Mexico is important since moisture lost over this region account later to feed the NAM that is active during this period<sup>6</sup>.

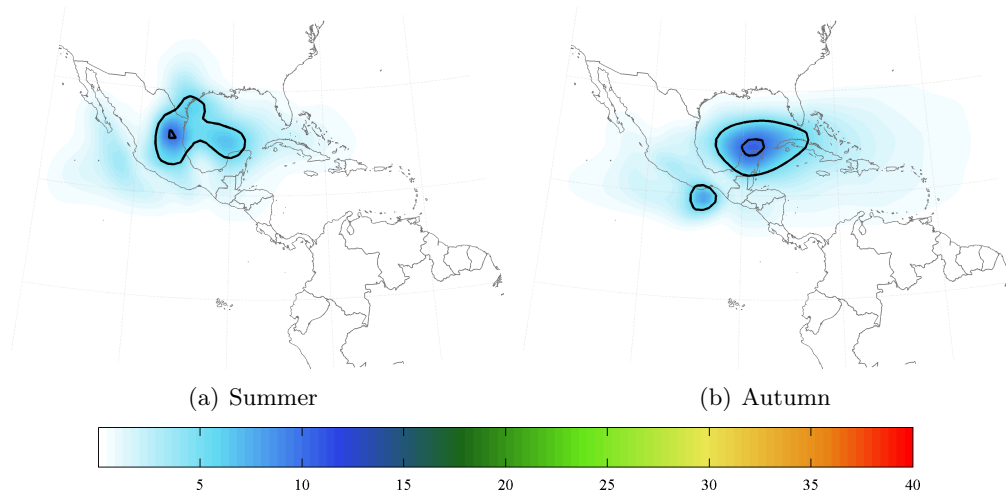


Figure 6.3: Average six days integrals of the conditional  $(E - P)$  field computed forward from the Gulf of Mexico for a) Summer and b) Autumn. Larger positive values are smaller than those found for the CS, most of the moisture from the Gulf of Mexico contributes to precipitation over the same Gulf, however during Summer an important component of precipitation associated with moisture inflow from this source can be noticed to be maxima over eastern Mexico, which is of importance and may enhance the transport of moisture during the active period of the NAMS. Values in mm/day and contours every 5 mm/day starting at 5 mm/day.

Analog to the CS and GoM, seasonal  $(E - P)$ <sup>6</sup> field for ETPS is shown in figure 6.4. There is no moisture from the ETPS being lost in average over Central America during winter, moisture is mainly lost along a narrow band of the ITCZ west of 120W. In spring the pattern is similar to that of winter, with larger moisture losses near the coastal region and over north-easternmost Central America (Guatemala) (figure 6.4.a). During summer a strong increase in the losses of moisture in front of Central America west coast is maximum near 95W. Moisture from the ETPS is lost in considerably important amounts over southern and northernmost Central America while few or no moisture is lost over Honduras and Nicaragua. A similar pattern but much more intensified in the magnitude of the moisture losses is observed for autumn and with more influence over Nicaragua than in the previous months (figure 6.4.b).

In the case of the results for the  $(E - P)$ <sup>6</sup> fields for the continental regions, results

<sup>6</sup>see further details for the sources of moisture for the NAM in Appendix D

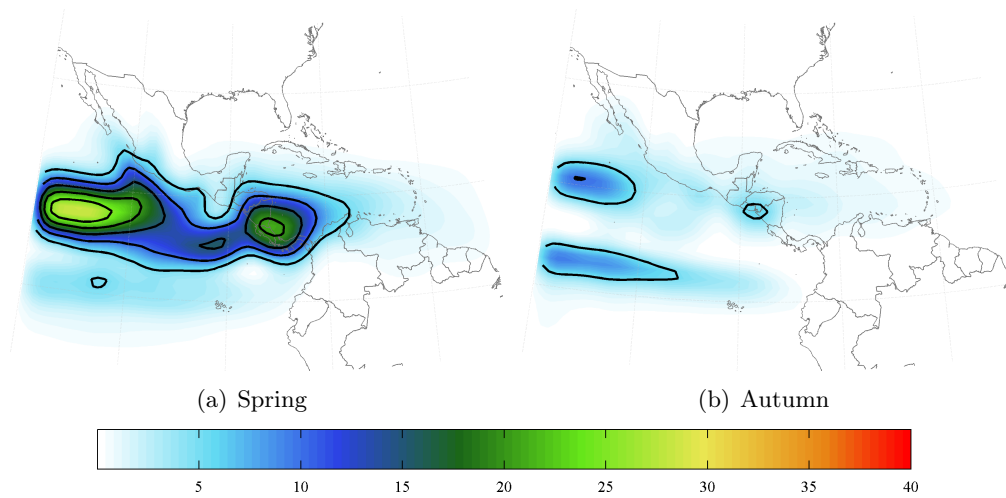


Figure 6.4: Average six days integrals of the conditional ( $E - P$ ) field computed forward from the ETPac region for a) Spring and b) SUMmer . Values in mm/day and contours every 5 mm/day starting at 5 mm/day. Precipitation associated with moisture transported from the ETPS is considerably reduced during Autumn (b) in the vicinity of Central America. However, during Spring (a) strong precipitation due to the presence of the ITCZ is noticed with a significant core of precipitation over Central America. During Autumn, this core is small and constrained to the Pacific coast of northern Central America.

for CAS suggests that precipitation is reduced during winter. Few moisture is available due to recycling because of a minimum of precipitation. In spring, moisture from CAS is lost over the Pacific and in major amounts over the west coasts of Guatemala and El Salvador. A similar pattern is found for summer, with the difference that the amounts of precipitation lost over these regions is significantly larger and some moisture is also lost over southernmost Central America (figure 6.5.a)<sup>1</sup>. Contributions are reduced during autumn. Moisture from NSAS is significantly larger than from local recycling. However, large amounts of moisture from NSAS are lost over the Magdalena and Orinoco river basins. These two basins are the main sink of moisture from the north of South America and only the remaining of moisture is able to be transported and precipitate over Central America. The pattern of  $(E - P)$ <sup>6</sup> field for NSAS shows the smallest contributions to precipitation over Central America during winter and the largest during summer (6.5.b) and autumn. Note however, that during summer most of the moisture (up to 30 mm/day) from NSAS is lost over the northernmost part of Colombia and souther Panama.

<sup>1</sup>remember the heterogeneous precipitation pattern over Central America that allows the MSD to co-exist with intense precipitation in southernmost CA



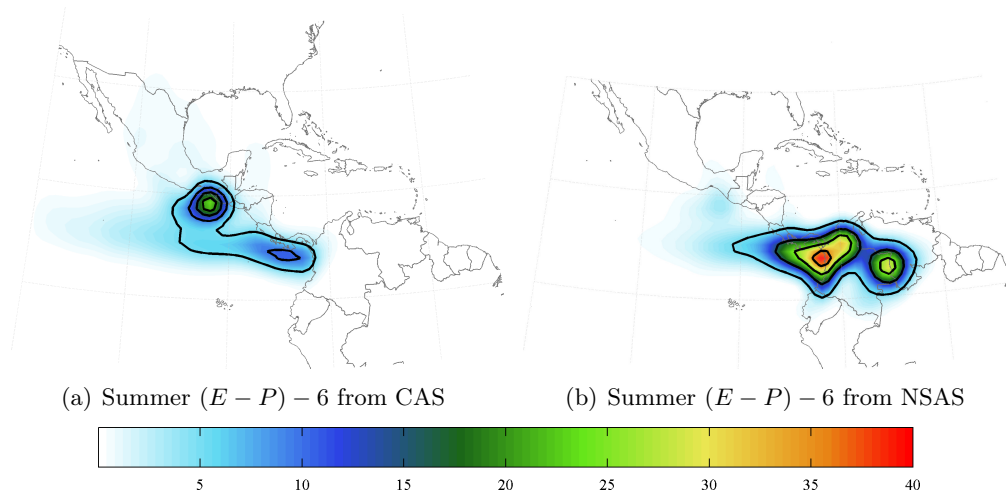


Figure 6.5: Average six days integrates of the conditional ( $E - P$ ) field computed forward for Summer from a) continental Central America and b) Northern of South America. Values in mm/day and contours every 5 mm/day starting at 5 mm/day. Moisture from CAS contributes to regional precipitation due to recycling with the largest contributions over southern Central America and the Pacific coast of Northern Central America and Mexico. Moisture from NSAS is very large during Summer with the largest contributions over the Venezuelan Plains and Northern Colombia as recycling of moisture and with an important contribution over Southernmost Central America.

## 6.2 Relative contributions to precipitation from the sources of moisture

By studying the changes of moisture of the air particles from the source to the receptor region, an estimation of the contribution from the source to precipitation over the target region can be obtained, following the reasoning of Wernli (1997) and Stohl & James (2004), despite the disadvantages of this approximation (see Sodemann et al., 2008). The mean annual cycle of the contributions is plotted in figure 6.6.a as well as their sum and as a reference quantity, the mean precipitation from CMAP. It must be noted that even when the sum of the contributions follow the pattern of CMAP precipitation, interpretation must be cautious. From figure 6.6.a, differences among the sources contributions remark the fact that the importance of each source to precipitation depends on its activity. Contributions from the CS are the largest, contributions from the ETPS are quite uniform after april with a small maximum in summer. Recycling has a large contribution, following the pattern of precipitation while the contributions from NSAS exhibit a single peak during summer. This implies that this remote source is of a great

importance to conserve the bimodal pattern of precipitation over Central America and that on its absence, precipitation may be reduced unless the other sources experience an intensification. The percentage distribution of the contributions is summarised in figure 6.6.b, from which the relevance of the sources can be noticed. This percentage of total relative contributions attributed to each source shows clearly the dominance of moisture coming from the IAS (GoM + Caribbean) all year round. The importance of the ETPS is constrained to summer and winter. While the pattern of the contributions from NSAS represents quite well the pattern of precipitation over northern SA. The increase of the contributions to precipitation during summer are a result of the reduction of precipitation over northern South America. Therefore evaporation and associated availability of moisture transported by local winds increases too.

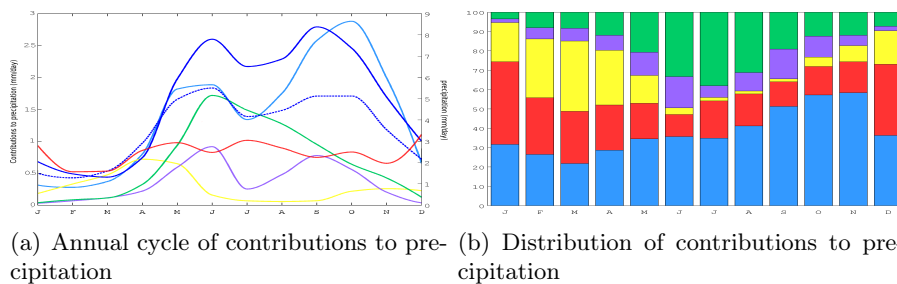


Figure 6.6: a) Mean annual cycle of CMAP precipitation averaged over Central America (dark blue) and sum of the contributions from the individual sources (light blue) (right axis) and relative contributions of the sources of moisture to precipitation (in mm/day) from each source of moisture following the color code of figure 6.1 b) Distribution of the composition of the total estimated of contributions to precipitation from the identified sources of moisture. Note the bimodal distribution of the sum of the relative contributions to precipitation in good agreement with the annual cycle of precipitation from CMAP. The distribution of the contributions to precipitation show the dominance of the oceanic sources of moisture with an important component of the contribution of the NSAS that is developed during Summer.

The increase in the contributions from the CS source during autumn is in good agreement with the rainiest season in the Caribbean side of Central America (Magaña et al., 1999). Moreover, the result reflects the importance of cyclonic system developed in the tropical Atlantic and Caribbean for regional precipitation during this part of the year. Relative contributions from NSAS can account as a secondary source of moisture during summer due to its intensity, result that until now has not been addressed.

### 6.3 Evaluation of the response of the contributions from the moisture sources using observational data

Due the features of the analysis region, is not straightforward and results must be interpreted with caution. As indicated in chapter 4, the availability of long term observations is not the best which result in the fact that evaluation of methods as the one herein used is not easy. First of all, the heterogeneity of precipitation patterns over Central America suggests that any evaluation or validation of estimates of precipitation must consider this distribution. For that reason, for evaluating the estimations of precipitation for subregions of the analysis domain are presented in order to a) deal with the heterogeneous distribution of precipitation and b) to avoid comparing results with averaged observations over regions from which there is no information (Guatemala, Honduras and Nicaragua). Estimates of 'relative' contributions to precipitation over Belize, El Salvador and the region formed by Costa Rica and Panama are computed for each source. The individual contributions were added to obtain a total of relative contributions to precipitation for each subregion. Figure number show the correlation between the estimated contributions to precipitation and observed precipitation for a) Belize, b) Honduras and c) Costa Rica and Panama.

Estimated precipitation from the Lagrangian approach is biased compared to observations in the indicated regions by 23-46% which may be considered to be a high bias. However it is important to remember the condition of the observations data and to notice that the larger bias is that for the location with less number of stations to the north. In addition, a comparison made between estimates from the approach of precipitation over Central America and precipitation from CMAP results in a bias of 29% which could be considered as a reasonably good agreement between estimated and observed precipitation taking into account the difficulties of estimating with more accuracy precipitation in this particular tropical location. Anyway, in order to be more correct in terms of the discussions, we will not refer the estimates as of precipitation but as to relative contributions to precipitation since we are aware that the approximation does not consider further processes that may be of importance for precipitation as microphysical processes.

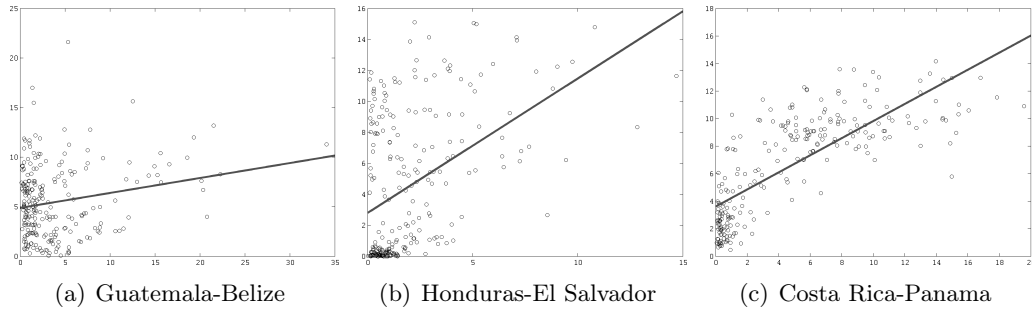


Figure 6.7: Correlations between observed precipitation estimated as the average of the selected rain gauges for different locations of Central America and the relative contributions to precipitation estimated from the identified sources of moisture for a) Belize, b) El Salvador and c) Costa Rica and Panama. The corresponding linear fits are shown by the lines, the largest  $r$  value is found for the region of CRP, notice this result is biased by the amount of rain gauges as their distribution over northern Central America is poorly homogeneous.

## 6.4 Long term time series of contributions to precipitation and associated variability

Once the mean annual cycle was determined, the variations that occur on time are of importance. Figure 6.8 shows the time series for monthly mean of a) CMAP precipitation and contributions from the b) CS, c) ETPS, d) GoM, e) CAS and f) NSAS. The CS was found to be the most important of the sources in terms of contribution to precipitation. By comparing a and b, one can find how some of the peaks of variations correspond for both time series (end of 1988 and 1998). However there are some cases in which variations do not present any immediate correspondence (1982, 1997). Conversely, correspondence is found between precipitation and contributions from other sources. Strong variations for the twenty years time series is found for determined years (1987-1988, 1995, 1997-1999) that are identified as strong ENSO events.

### The mean picture of the variability

The EOF patterns presented in previous chapter a strong relation between the zonal wind and the structure of the CS was appreciated. Variations in the spatial patterns of the evaporative sources over northern South America and the ETPac region were observed to be important. From the variations of the evaporative sources of moisture, variations in the contributions from those sources to precipitation is expected. In the

6.4 Long term time series of contributions to precipitation and associated variability 409

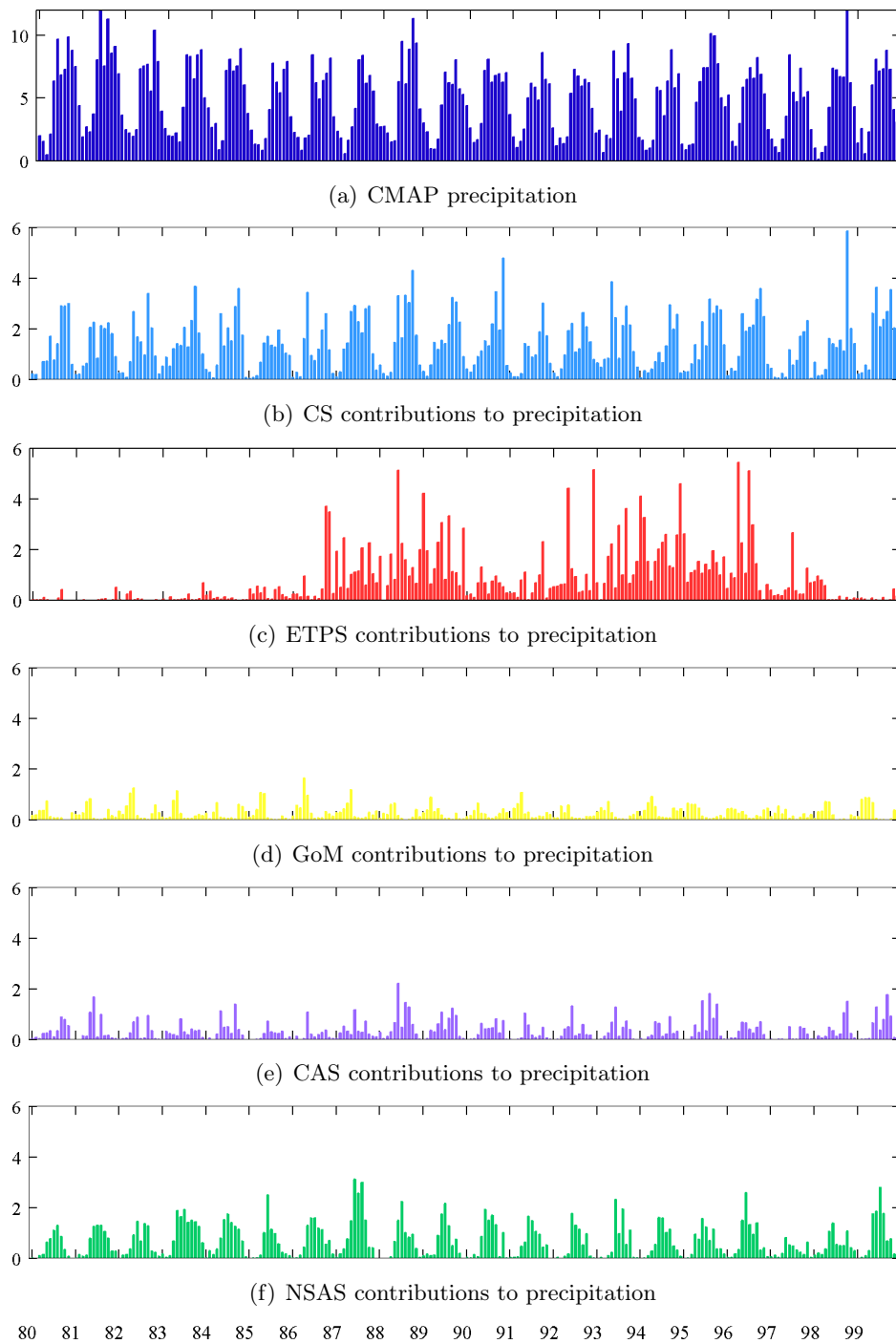


Figure 6.8: a) Time series of monthly CMAP precipitation averaged over Central America for the 1980-1999 period, estimates of relative contributions to precipitation over Central America from a) CS, b) ETPS, c) GoMS, d) CAS and d) NSAS as estimated from the Lagrangian approach, units in mm/day

previous section, a shallow evaluation of the relative contributions to precipitation estimated in contrast with observed data was presented. In order to find the temporal band of larger variations of the contributions to precipitation from the sources, wavelet analysis is applied for the time series once the annual cycle was removed. Wavelet analysis was used on the basis that it enables the reconstruction of the time evolution of the main oscillating components of the time series. Modulus of the wavelet transform are shown in figures 6.9 (a,d,g,j,m). The average wavelet power spectrum for the contributions from the individual sources, similar to the Fourier spectrum, is shown in figures 6.9 (b,e,h,k,n). From the wavelet power spectrum, large variability is found for all the sources except for the GoMS, whose results are out of the statistical significance. The average wavelet power spectrum (significance marked by the dashed line) shows that for contributions from the CS the dominance of variability is on the two years band and that important shifts occur for the one and four years band too. In the case of the ETPS, the dominant period is the 4-8 years band and significant shifts are noticed for the 2-4 and 8-16 years bands. The same pattern of periodicity of variability for the contributions from the CS is found for the contributions from CAS. For NSAS, dominant periods of variability are found for the 2 and 8 years band with further important shifts for 6 and 1.5 years. It is also important to note the irregular pattern of the ETPS, which presents a marked minimum 1980 and 1986 and reduces again 1991 and 1998.

6.4 Long term time series of contributions to precipitation and associated variability 11

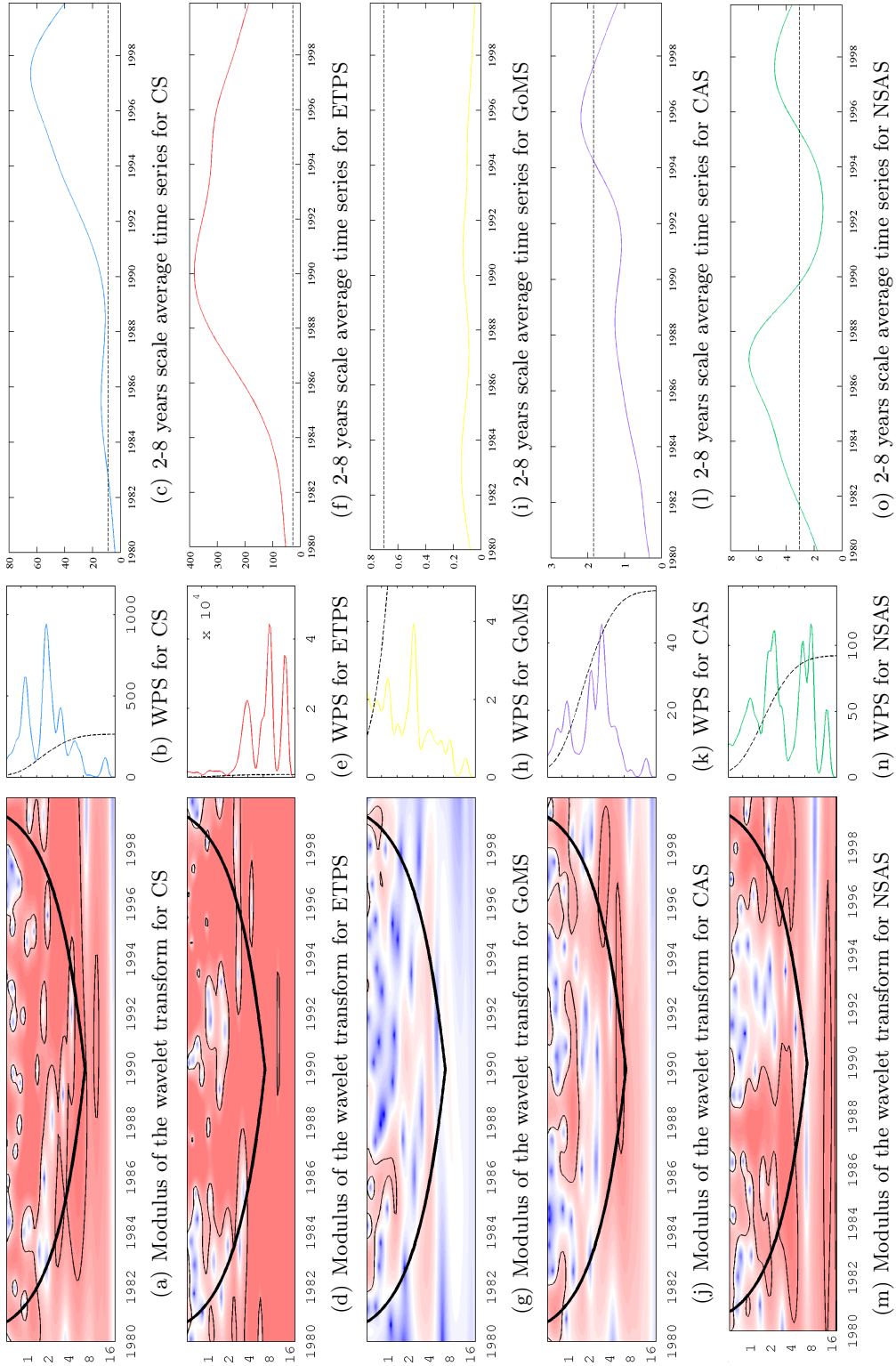


Figure 6.9: Modulus of the wavelet power spectrum for the time series the relative contributions to precipitation over Central America from a) CS, d) ETPS, g) GoMS, j) CAS and m) NSAS, the cone of influence is marked by a thick black line and the contours significant at 95% percent are enclosed by a black contour is indicated for the modulus of the wavelet transform. Average wavelet power spectrum for the same time series: b) CS, e) ETPS, h) GoMS, k) CAS and n) NSAS. Two- eight years average time series (variance) for the same time series: c) CS, f) ETPS, i) GoMS, l) CAS and o) NSAS, 95% significance level is indicated with black dotted line for the average wavelet power spectrum and 2-8 years scale average time series.

In general, the 2-8 years band was found to be the one in which the largest variations occurred, so the 2-8 years scale average time series (variance) were computed. Results from figures 6.8 (c,f,i,l,o) indicate the years at which variance of the anomalies of the contributions to precipitation peak. The CS exhibits a large peak centred in 1990 and 1996. Variance is below the significance level for the GoM and a peak centred in 1996 is noticed for the contributions from CAS. The contributions from northern South America peak with larger intensity centred in 1987 and a secondary maximum by 1997. These results remark the result obtained for the spatial structure of the sources shown in previous chapter, which presented an important variability mainly associated to ENSO. It is also important to notice the suggestion of a low frequency band of variability for the contributions from ETPS and NSAS. Even when the time series may be not long enough, the results present what can be considered as evidence of a strong forcing of the PDO in the contributions to precipitation from these two sources.

### **Evolution of the anomalies of the contributions to precipitation**

From the wavelet analysis it can be followed that the major variability is centred in the 2-8 years band, in which ENSO is the leading mode. It is however, not immediate to determine which seasons are more sensitive to interannual variability. The Hovmoller plot for the anomalies of contributions to precipitation for each source (fig 6.10) provides further details of temporal variability. The CS, with larger variability patterns show increases for the first half of the year during 1983, 1990 and 1993 with marked decreases for 1984-1988, 1992 and 1997-2000. Even more interesting is the anomalous increase of the contributions during summer time for 1982 and 1998-2000. Negative anomalies are observed in 1987 for the contributions from the ETPS, and the patterns of strong positive anomalies is similar to that of the CS but much more intense. Contributions experience a marked strengthening in autumn 1986, summer 1989, summer 1993, winter 1995 and spring-summer 1997. Few variations of importance were noticed for the GoMS (not plotted).

In the case of CAS, important increases are remarked for 1987-1989 (the complete year) and summer 1999. In agreement with an increase of precipitation that may enhance the recycling over the region. Notice however, that for the other sources none increase is found for this period. This implies that the increments of contributions to



6.4 Long term time series of contributions to precipitation and associated variability 13

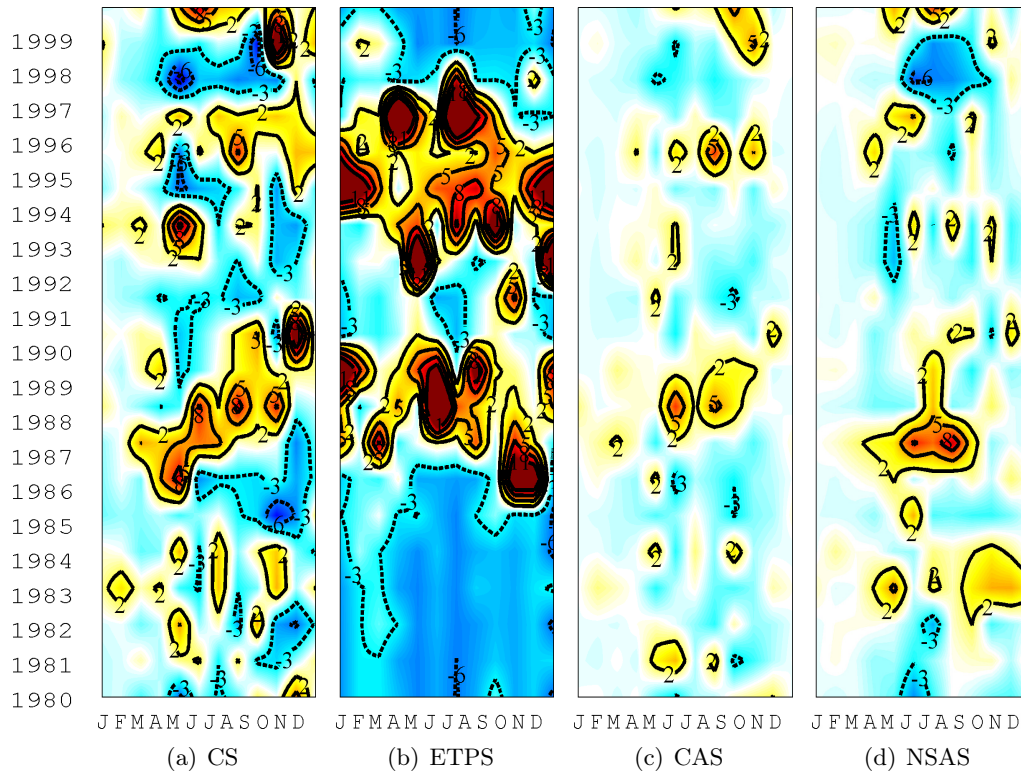


Figure 6.10: Hovmoller plot for the anomalies of the relative contributions to precipitation from the identified sources: a) CS, b) ETPS, c) CAS and d) NSAS. Positive contours every 3 mm/day starting in 2 mm/day and for negative every 3 mm/day starting in 3 mm/day. Values for the contributions from the GoMS are not shown as are considerably small compared to the contributions from the other sources and variability was found to be under the confidence level.

precipitation and precipitation itself were probably, for this period, locally induced. A more complex pattern is described by the anomalies of the contributions from NSAS. An increase in the contributions to precipitation starts in summer 1983 and extends through summer 1984. A similar increase does occur two years with an early intensification at the beginning of summer later but does not penetrate towards the next year. For winter time, the contributions from this source experience a decrease during 1993 and for 1998-1999 a marked intensification occurs for winter while a decrease for summer. Note the intense variability for the contributions from the ETPS, which present a tendency to occur before the onset of a warm El Nino event.

## 6.5 Variations under the influence of main variability modes

The hovmoller plot shown in figure 6.10 evidences the structure of the time variability of the intensity of the contributions to precipitation from the sources of moisture. The patterns described for determined years suggest the influence of determined modes of variability, as described previously for the spatial patterns of the sources of moisture in chapter 5. To evaluate to which extent the variability modes trigger the variability of the contributions to precipitation, the percent composition of the total of contributions was estimated. Monthly composites for each mode are shown for positive, neutral and negative conditions.

At the beginning of winter, warm ENSO is featured by a decrease of contributions from the Caribbean compensated by the increase of contributions from NSAS. As the winter advances, the enhancement of the contributions from the ETPS are associated with the cold ENSO events (6.11.a). Warm ENSO is associated with the decrease in the contributions from the CS, and the intensification of local recycling at the end of winter. During spring, the ETPS shows significant variations, a pattern that is reversed if compared to winter. Cold ENSO triggers a sharp decrease of the ETPS that is compensated by increments in the contributions from the GoMS (6.11.b). In summer, warm (cold) ENSO is related to the increase (decrease) of the intensity of the contributions from the ETPS. The opposite pattern is noticed for the contributions from NSAS (6.11.c).

Under the influence of NAO, the CS experiences decreases for the negative phase during January (6.12.a), April (6.12.e) and July (6.12.h) and increases during March (6.12.d). The magnitude of the contributions from GoMS is reduced for this phase during December (6.12.a). Large variations in the intensity of the contributions from the ETPS are noticed for this mode. A marked increase in the contributions from this source during is linked to the negative phase. The other sources experience small variations, most of them associated to the negative phase.

In the case of the PDO, variations tend to be more noticeable for winter and spring (6.13.e). For November, positive PDO enhances the intensification of the contributions from NSAS with the further reduction of the contributions from local recycling over Central America, then a reduction of CAS (6.13.l). During December, a decrease of the

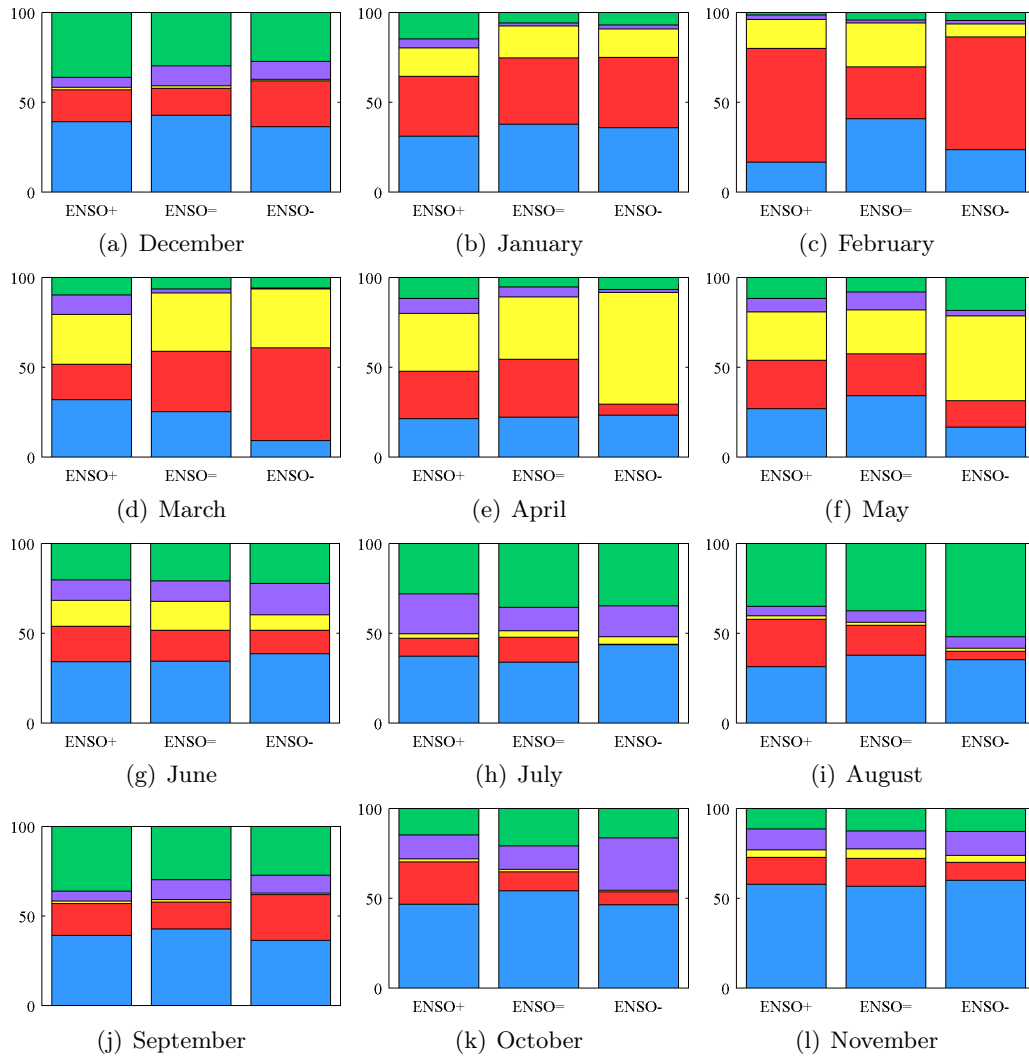


Figure 6.11: Distribution of the monthly mean composites of the relative contributions to precipitation from the sources based on composites for warm, cold and neutral ENSO.

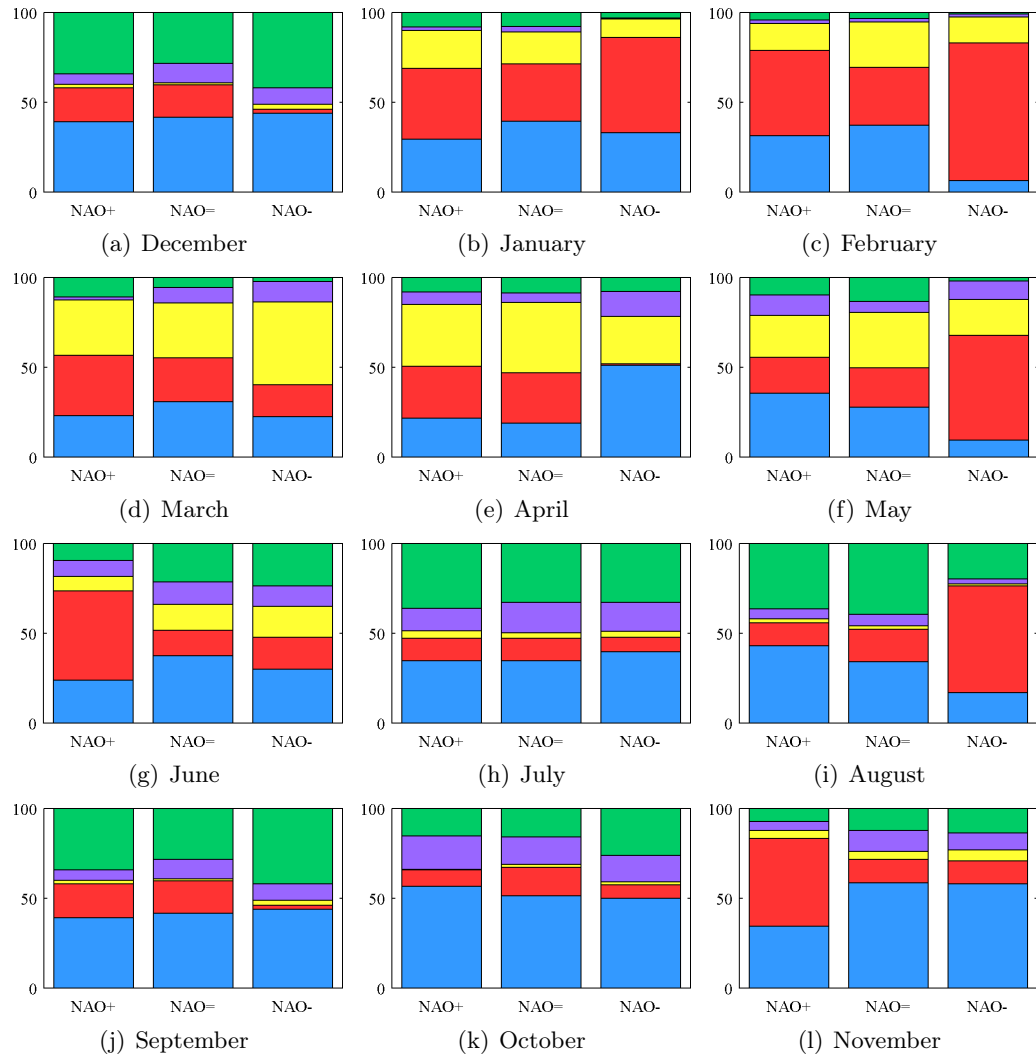


Figure 6.12: Distribution of the monthly mean composites of the relative contributions to precipitation from the sources based on composites for positive, negative and neutral NAO.

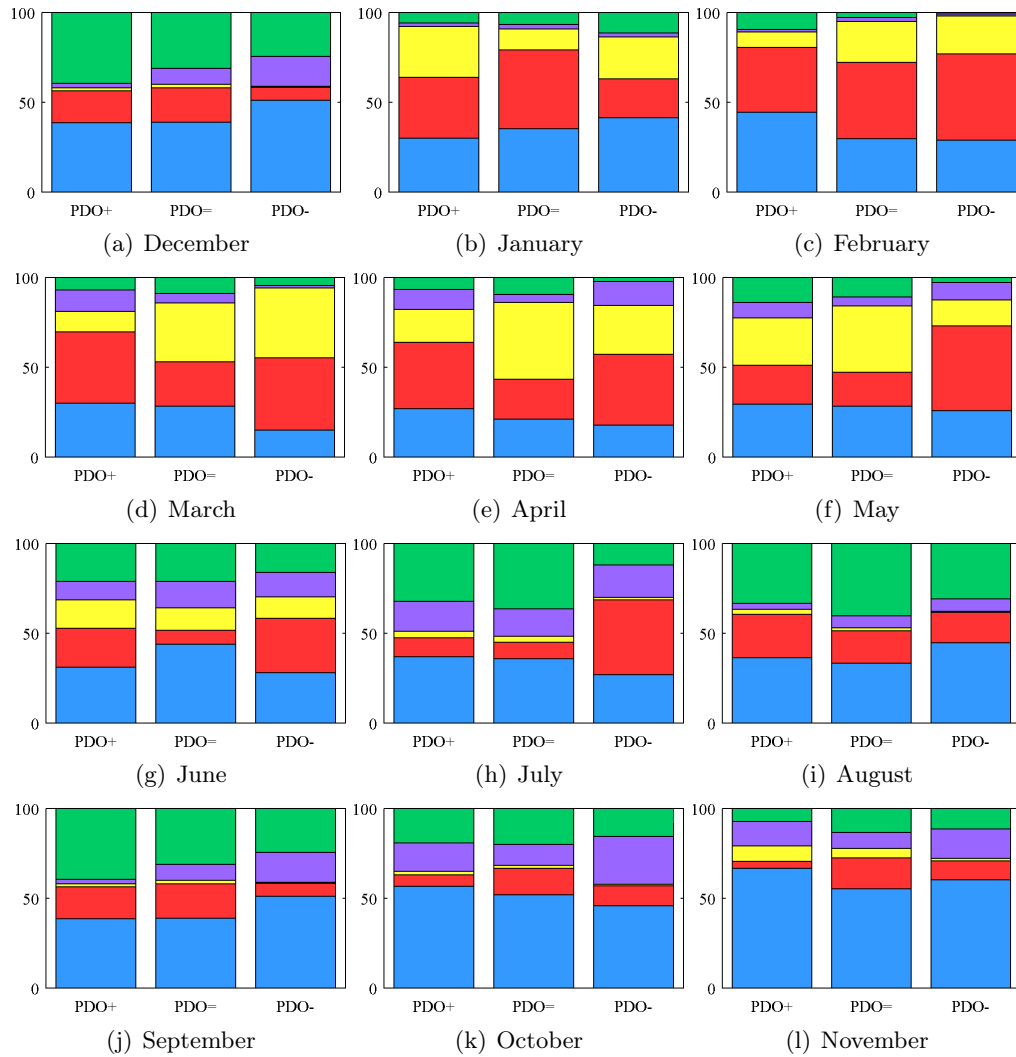


Figure 6.13: Distribution of the monthly mean composites of the relative contributions to precipitation from the sources based on composites for positive, negative and neutral PDO conditions.

contributions from the CS and ETPS is compensated by the increase of the contributions from the GoMS (6.13.a). The contributions from CS (ETPS) increases in positive PDO for late winter (figs 6.13.b and 6.13.c). At the beginning of spring, positive PDO seems to favour the increase of contributions from the Gulf of Mexico (6.13.d). Negative phase favours the strong reduction of the contributions from the GoMS but the intensification of the contributions from the ETPS. Few variations are found for the remaining months and is also important to remark that negative PDO favours a more active ETPS in terms of contributions during June (6.13.g).

Under the influence of the MJO, a similar case as for NAO occurs, with the main variations being more noticeable during winter. In general, MJO negative (positive) phase is related with the decrease (increase) of contributions from the Gulf of Mexico. This decrease is strongly marked during December, in which the contributions from the GoMS almost vanish. The reduction of the contributions from the GoMS are compensated by the intensification of the contributions from the ETPS and CS. At the end of winter, the negative phase of MJO seems to favour the increase of local recycling compared to the neutral conditions and the positive phase, for which recycling is reduced. Notice that the CS is reduced (increased) for positive (negative) MJO. Some less significant variations are found for spring time and the remaining months. Transport from NSAS is enhanced during June by the positive phase while the Gulf of Mexico is in October for the negative phase.

Lagged correlations were computed between the time series of the anomalies of the contributions from each sources and the climate indices correspondent to each variability mode. The summary of the cross-correlated functions between the modes and the anomalies of contributions from the sources is presented in figure 6.15. The lagged correlations with El Nino 3.4 index, show that ENSO lags between 2 and 6 months the contributions from the CS (figure 6.15.a) and between 2 and 4 months those from the ETPS (figure 6.15.b). At the same time that lags between 2 and 7 months the relative contributions due to local recycling (figure 6.15.c). No statistically significant results were found for the other sources.

From the composites, the relationship between the variations due to the forcing of NAO was not completely clear, the cross-correlation function clarifies the signal and facilitates the interpretation of the results. The presence of NAO is found to lag 6

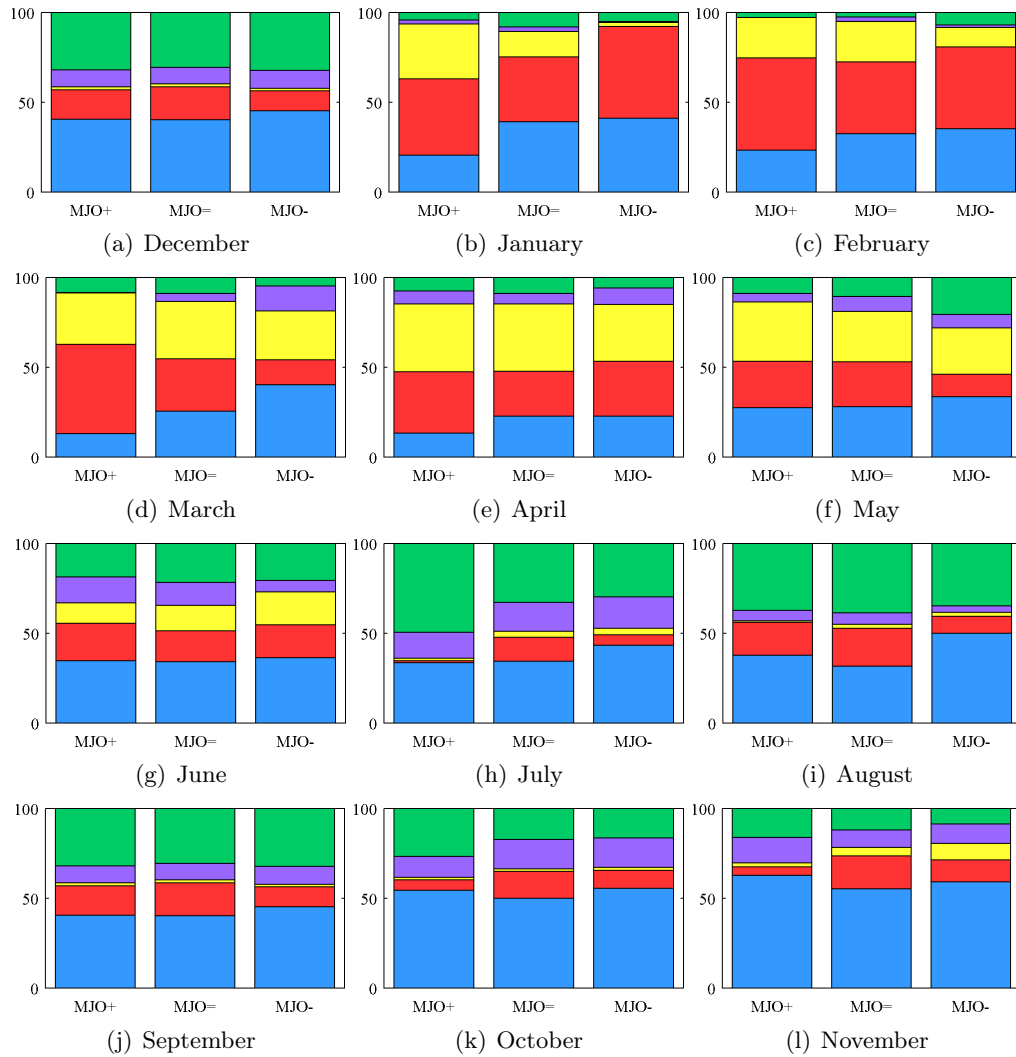


Figure 6.14: Distribution of the monthly mean composites of the relative contributions to precipitation from the sources based on composites for positive, negative and neutral MJO.

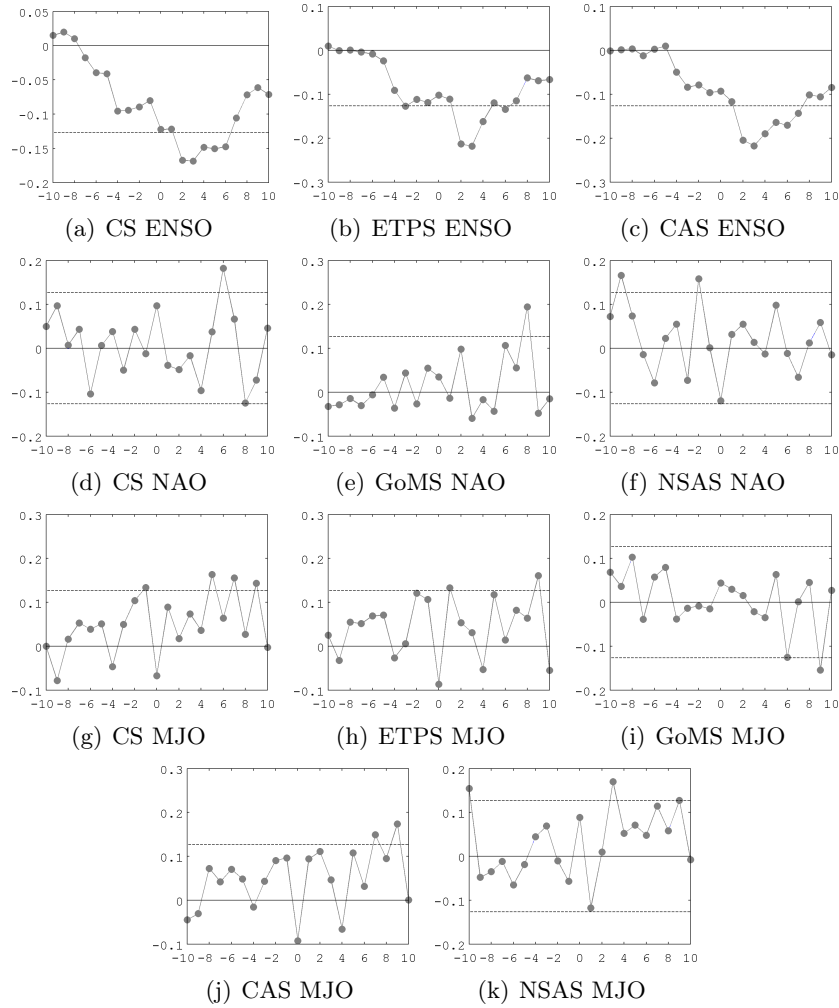


Figure 6.15: Lagged cross-correlation functions computed between the contributions from the sources and the indices for ENSO: a), b) and c) NAO: d), e) and f) and MJO: g) to k) . The 95% significance level is indicated by the dotted line.

months the contributions from the CS and 8 those from the GoMS (figures 6.15.d and e). No significant relation is found for the ETPS and local recycling. A lead relation was found for the NSAS at -1 and -8 (figure 6.15.f). Results for the PDO are below the significance level (unfortunately the time series is not long enough to capture complete PDO cycles). The influence of the MJO is significant for the five sources. It is found to lag the contributions from the CS between 6 and 9 months (figure 6.15.g), 9 months the contributions from ETPS (figure 6.15.h) and lead 9 months those from the GoM. Lags



of 7 and 9 months are found for the contributions from the CAS (figure 6.15.j). A faster response of the NSAS source to the MJO is found by a lag of 3 months (figure 6.15.k). This results are of importance since will be considered to analyse the conditions under which moisture is transported from the sources to continental Central America where it precipitates.

### **ENSO and contributions to southern CA**

The ENSO mode has been shown to modulate the regional distribution of precipitation (Vázquez et al., 2003). The ENSO cycle of 1997-1999 is of particular interest because of its strong warm phase during 1997. Some authors have analysed the effect of the El Niño of 1997 on tropical ecosystems and its wider biological impact (Fiedler, 2002). Moreover, the 1997 warm phase of the ENSO was seen to affect the production and supply of electricity in SCA. In Costa Rica (where most of the power is generated in hydro-electric power stations), the generation of electricity was affected by the reduction in pluvial discharge as a result of the effect of the ENSO on local precipitation (Amador et al., 2003). The timeseries for observed precipitation and relative contributions from the sources to precipitation over CRP are shown in figure 6.16 with black and gray lines respectively. The order of magnitude for both series is the same and the pattern followed for the two variables is in good agreement, which indicates that the estimated moisture losses from the sources over CRP shows a relatively good correlation with observed precipitation ( $R^2 = 0.52$ ). This result is encouraging since it provides an evaluation of the skills of the applied methodology for analysing moisture transport at a very regional scale in complex areas.

Anomalies of averaged precipitation and the sum of the contributions to precipitation over CRP are shown in figure 6.16 (a and b) with black and gray lines respectively under the same values range of the left axis. The Nino 3.4 index is also plotted, warm and cold ENSO events are shown in light red and blue respectively (right axis). The pattern of the relative contributions to precipitation follows a relationship of negative anomalies (reduction in the contributions) for the warm ENSO events and the opposite pattern for cold ENSO (increases). This except for the 1997 event, for which positive anomalies are found. The peak of excess of precipitation during the 1985-1986 cold event is delayed approximately six months with respect to the peak of the positive

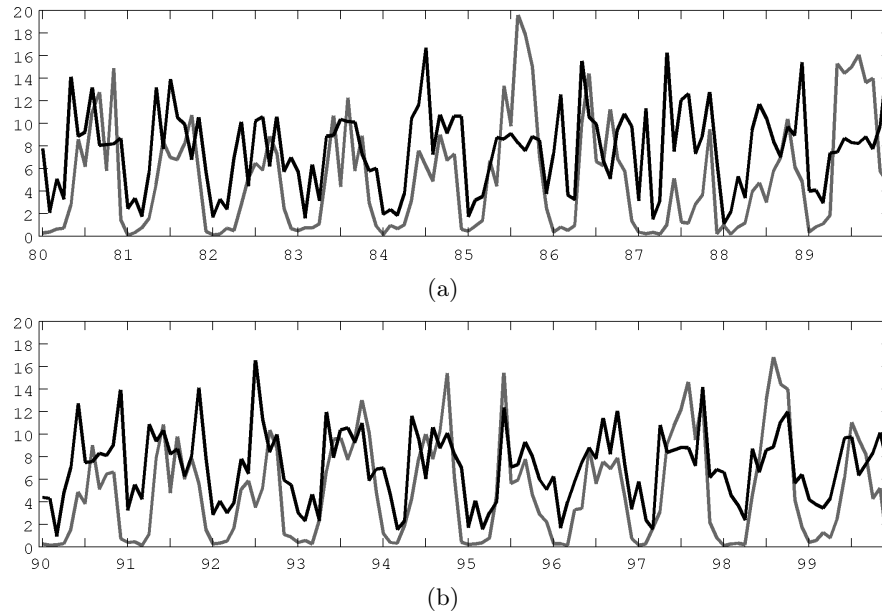


Figure 6.16: Time series for averaged observed precipitation over Costa Rica and Panama (black line) and the sum of the estimates of relative contributions to precipitation from the identified sources (gray line) for the analysis period.

anomalies of the contributions. This suggests a lagged relationship between the contribution from the sources and precipitation. The cross correlation function (see figure 6.17) shows a peak at the zero-th lag, indicating the immediate response of precipitation to the contributions from the sources. Another significant peak of correlation for the 7 months lag shows that the contributions from the sources lag observed precipitation in the order of 7 months. The contributions from the sources are important for on-time precipitation events but also for the posterior events. The latter may be a result of the role that moisture transported from the sources play for regional water storage.

The anomalies of the contributions to precipitation over CRP from the individual sources for the 82-83 warm ENSO event is provided in figure 6.18.a (left axis for the scale of the anomalies of the contributions and right axis for the scale of the Nino 3.4 index shown by the black line). Observed precipitation is reduced during the peaks of the warm event. Variations are small for the contributions from the GoMS and a generalised decrease of the contributions from the rest of the sources is noticed. With those being of the same order for the ETPS, CS and NSAS during the first part of

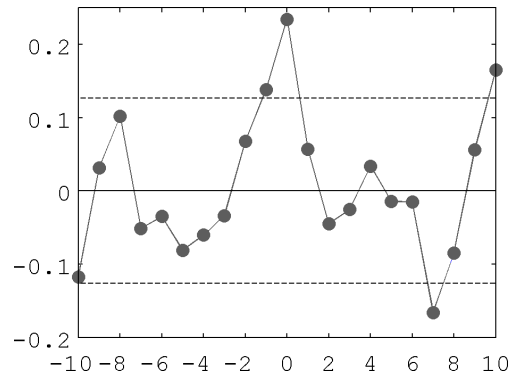


Figure 6.17: Cross-correlation function for the contributions from the sources and observed precipitation.

the event. During the second peak of this warm ENSO event, the CS suffers the larger variations. Meanwhile the reduction of the contributions from the other sources become smaller as the cycle ends. Note that the end of the cycle enhances an intensification of the contributions from NSAS. Moreover, the contributions from ETPS and NSAS increases at the beginning of autumn, before the warm event matures. Results from the cold ENSO event of 1988-1989 (figure 6.18.b) show that a strong increase of the contributions from the sources (except GoMS) is observed to precede the peak in the increase of observed precipitation between 0 and three months. It important to note that the positive anomalies of the ETPS and CAS present a single peak during the start of the cold episode. This occurs while the CS and NSAS presents two peaks, one for each peak of negative ENSO index. It can be followed that the response of the sources depends on the location of the source. During the second peak of the cold ENSO, precipitation is substantially reduced compared to the first peak. It can be argued that the observed decrease of precipitation in autumn for this cold ENSO, result from the general decrease of the contributions from the sources, which corresponds to the increase of evaporation (less moisture available as precipitation) over southern Central America as noticed from figure 5.7.d (previous chapter).

The 1997-1999 period provide us the opportunity of analysing a complete continuous ENSO cycle of particular strong intensity. The results for the former cold ENSO (light blue shaded) shows an increase of precipitation during the peaks of negative ENSO

index<sup>9</sup>. Relative contributions from the sources increases significantly previous to the peak of precipitation at the end of the analysis period. The cold ENSO event has a fast and intense triggering the variations in the contributions from the sources. This lead precipitation over CRP and that the response of the sources obeys to their location (Atlantic or Pacific regime). However, the case of the 1997 warm ENSO does not reflect the mean expected pattern. Even when contributions from the sources are decreased during this phase (as in the 1982-1983 case) increases of observed precipitation occur during the first part of the event. During autumn 1997 the intensification of precipitation coincides with the increase of the contributions from the sources of moisture. This is important in the sense that it is normal to associated a generalised decrease of precipitation to warm ENSO events without a proper consideration of the response to individual events and stages of them. It is important to point out from these results that the Lagrangian approach provides relatively accurate (and very valuable) information on how both moisture transport and precipitation may vary along events associated to ENSO phases. These results also remind us of the importance of considering the analysis of individual subregions when handling with small complex domains as Central America, for which the generalisation of patterns may conduct to erroneous conclusions.

## 6.6 Variability of local recycling of moisture

The importance of the main variability modes in the modulation of precipitation in the IAS region has been widely discussed (see e.g Giannini et al 2001 and more recently Wu and Kirtman, 2011). In the last year an increase in the number of publications on climate modelling of precipitation variability over the region have been published as several groups aim to provide details on the variability of precipitation over Central America (see e.g Rauscher et al., 2011, Diro et al., 2012) as well as studies related to climate change (Karmalkar et al., 2011). The heterogeneity of the distribution of precipitation implies that the different regions of Central America may have a different response to the same variability mode. The response to the forcing from the remote

---

<sup>9</sup>since the period ends in December 1999, the ENSO cycle is not strictly complete, however as the ENSO index becomes more negative after November 1999, a tendency in the pattern of precipitation and contributions from the sources to be increased can be noticed

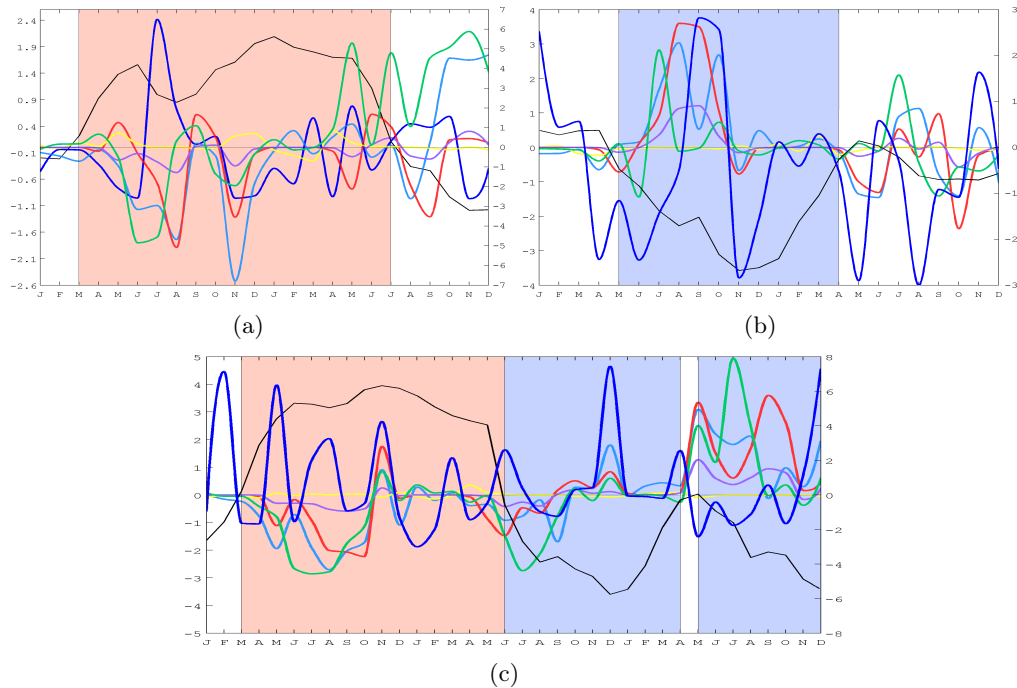


Figure 6.18: Time series for averaged observed precipitation over Costa Rica and Panama (black line) and the contributions to precipitation from each source for a) warm ENSO 82-83, b) cold ENSO 88- 89 and c) ENSO cycle of 1997-1999. Notice the Niño 3.4 index is shaded for reference.

sources will be described in detail along the next chapter as transport may be discussed first. Herein we will focus with more detail on the response of the contributions to precipitation due to the recycling of moisture. As for the rest of this work, Central America can be subdivided in four regions. The southernmost portion in which Costa Rica and Panama share some common climate features (CRP), Nicaragua (Nic) which is a subregion itself as it shares features with southernmost part of Central America but also with the northern regions. Honduras and El Salvador (HS) can be considered as another subregion which shows a differentiated behaviour with the southern region, while Guatemala and Belize (GB) constitute the northernmost portion of Central America, being featured by a contrasting behaviour compared to the south as well as for sharing the climate features of Mexico. As the response to ENSO was considered in the previous section, here we aim to make some remarks on how MJO, NAO and PDO may trigger variability of recycling over the subregions of Central America. Using the climate indices for those signals, the contribution to precipitation due to recycling estimated through

the Lagrangian approach is matched with the climate indices to determine whether a relationship can be found. Dispersion plots are constructed for each month to represent the relationship between the recycling and the intensity and phase of each variability mode. Weighted group means are computed before constructing the best fit and evaluate the linear trend in search for the most direct link between recycling and the variability modes. CRP shows the largest response to MJO for late Spring (fig 6.19.a) and Summer (fig 6.19.c), negative MJO was found to be related with an intensification of the recycling whereas the positive phase of the MJO seems to favour the decrease of recycling. A similar response was found for Nic during Summer and HS for early Autumn, see figures 6.19.f and 6.19.g respectively. The response of GB differs a bit in comparison to other regions, during part of Winter (fig 6.19.h) and Spring (6.19.i) positive (negative) MJO is related with the increase (decrease) of recycling over northernmost Central America. The opposite pattern is observed after Summer (fig 6.19.j), becoming more intense during Autumn (fig 6.19.l) for this region.

As the NAO is active during Winter, its forcing is more important for those months. In the case of CRP, response of local recycling to NAO forcing was found to be more marked for November (fig 6.10.a) with positive (negative) NAO triggering the decrease (increase) of recycling, while Nic and HS do not present a marked response to NAO. On the other hand, recycling over the GB region has a large response to NAO during February (fig 6.20.b) with the same trend as for CRP, decreasing (increasing) recycling for positive (negative) NAO.

Finally, the response of recycling to the PDO was found to be of major importance for the northern portion of Central America. For GB positive PDO seems to be related with an intensification of the recycling while the opposite occurs for negative PDO during April (fig 6.21.a). For both HS and GB, a marked trend for reduced (intensified) recycling is noticed during September (fig 6.21.b for GB and fig 6.21.c for HS) for positive (negative) PDO.

## **6.7 Chapter highlights**

A simple evaluation on the performance of the approximation for estimating precipitation due to the contribution of the sources of moisture was carried out using available

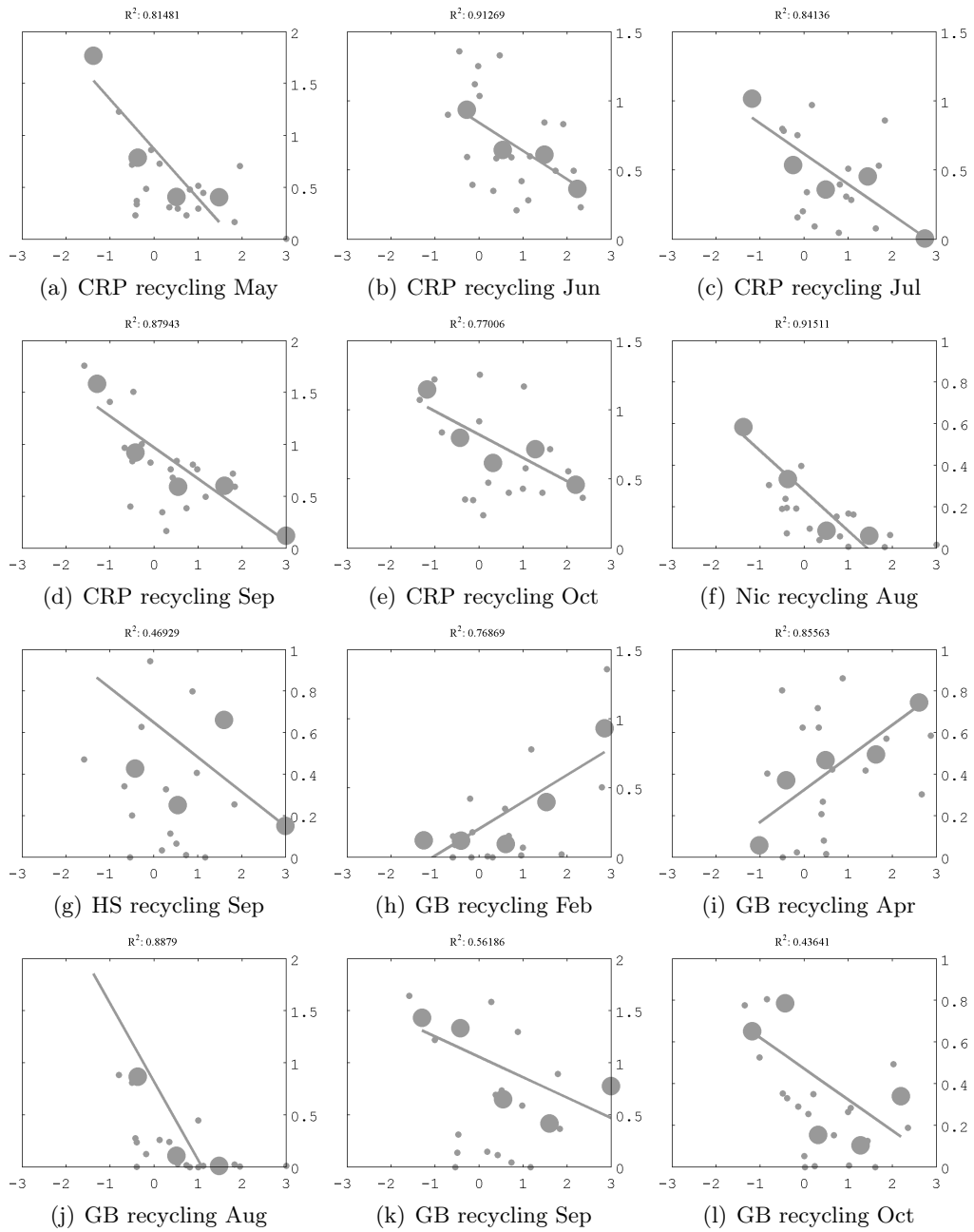


Figure 6.19: Scatter plots of the monthly estimates of recycling computed through the Lagrangian approach as a function of the MJO index. Group means are shown by larger gray filled circles and the gray line shows the best linear fit based on the weighted group means,  $R^2$  is also indicated.

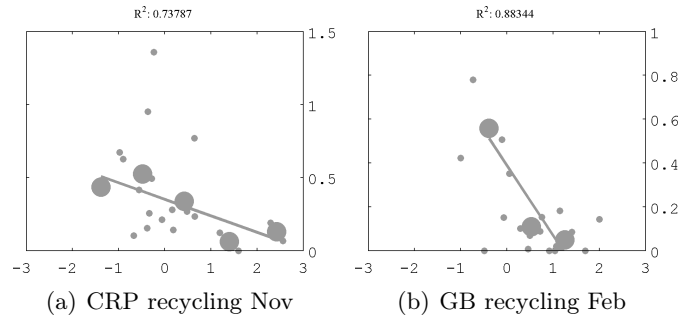


Figure 6.20: Scatter plots of the monthly estimates of recycling computed through the Lagrangian approach as a function of the NAO index. Group means are shown by larger gray filled circles and the gray line shows the best linear fit based on the weighted group means,  $R^2$  is also indicated.

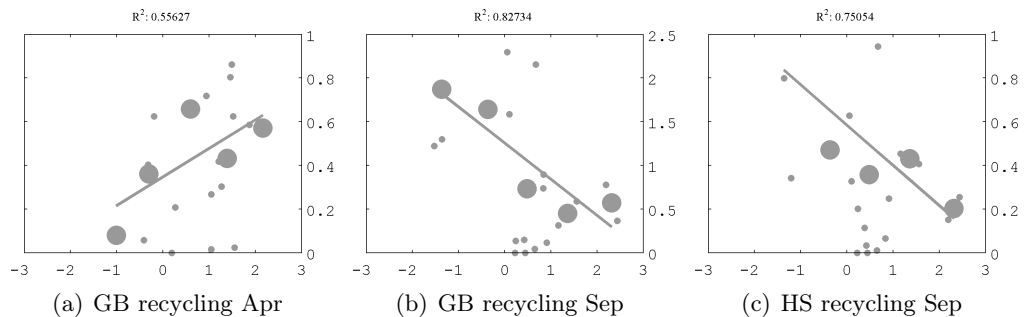


Figure 6.21: Scatter plots of the monthly estimates of recycling computed through the Lagrangian approach as a function of the PDO index. Group means are shown by larger gray filled circles and the gray line shows the best linear fit based on the weighted group means,  $R^2$  is also indicated.

observations of precipitation for Costa Rica and Panama. The results indicate relatively acceptable biases of the estimations of precipitation over the region using the Lagrangian approach. This is in the basis that the estimations of precipitation do not account as total precipitation but for a relative contribution to the total. This result is encouraging and suggests that the Lagrangian methodology applied reproduces not only the seasonal cycle of precipitation but also enables the study of the variability of observed precipitation in terms of the variability of the sources that provide moisture for Central America. The importance of the remote continental sources, in this case NSAS, to maintain the seasonal cycle of precipitation over Central America is quite important as it has not been considered before. The role of the contributions from the ETPS may be more related with precipitation in the Pacific regime. From this anal-



ysis, the variability of precipitation was found to be strongly bounded to the effect of ENSO, despite the influence of other modes is also important. The pattern described by the contributions from the ETPS resembles not only the pattern of the PDO but also that of drier than normal conditions over some locations of Central America (mainly Nicaragua). A more detailed analysis of the variability of this source may provide valuable knowledge in terms of the dynamics of drought associated with the variability of the evaporation, the ITCZ and transport of moisture over the ETPac region. The analysis of local recycling allowed us to show the differences observed for each subregion of Central America, which are in good agreement with the climatological differences observed in precipitation. The local response to the forcing of the main variability modes describes a different response to the modes depending on the location of the subregion. This highlights the importance of considering the subregions for climate analysis in order to provide a more accurate picture of the regional water cycle. Moreover, taking into account Central America as a single region provides good information on local precipitation, moisture transport and recycling, however a more proper analysis requires considering Central America as a complex region in which small regions despite near may present a complete opposite behaviour. The recycling of moisture was found to present a more uniform response to the forcing of the MJO, or at least at the effect it seems to have for Autumn, as the four subregions into which Central America was divided present a decrease (increase) in the recycling of moisture for positive (negative) MJO. Meanwhile for the PDO and NAO modes, the direct relationship between the variability modes and local recycling were found to be small compared to those observed for the estimated recycling for MJO. Here, the most important result is that the variations in the contributions to precipitation over Central America, which also affects the recycling require a better understanding of the transport of moisture, that will be treated in detail in the following chapter.



# 7

## Dynamics of transport

In the previous chapter, a quantitative estimation of the relative contribution to precipitation from the identified sources of moisture was provided. These relative contributions to precipitation are an estimation of how much moisture is transported from the sources to the correspondent target region. One of the advantages of using a Lagrangian formulation, is that for the trajectory followed by a particle from one point to another, the given properties of the particle are known. In the case we are interested in, the position and moisture of the air particles are known at every time step. In the case of backward trajectories, this formulation is important since it enables us to reconstruct the history of air particles before they reach a receptor source with knowledge on the changes that the properties of the air parcel experienced previous to the arrival. In the previous chapters 5 and 6, the results provided information on the final conditions of the air parcels, since the ultimate interest at the moment was precipitation. However, the information of air parcels we can obtain from the Lagrangian trajectories allows a more detailed study on what has happened in-between since the air parcel was at a determined position to the arrival to the receptor region. In order to extend our framework and investigate the process of transport of moisture, the analysis of the trajectories before the arrival to the target region is performed.

## 7.1 Origin of air masses

Air masses arriving to Central America may provide part of the moisture that accounts for precipitation. In the previous chapter, the identification of the main sources of moisture for Central America determined the presence of sources over the Caribbean Sea, The ETPac region, a remote source over northern South America and Central America itself. Once a general idea on where moisture may come from is obtained, a good question may be where does the air that contains (and transports the moisture) come from? In order to answer this question, the trajectories followed by the air parcels arriving to Central America must be reviewed. A way to do so is to follow the air parcels backward in time and evaluate their positions at determined time steps. Since we are interested in a 6 days time scale, air parcels were tracked backwards in time a total of 48 time steps (remember the time step used is three hours) to identify their positions and classify the trajectories according to it. For each of the subregions into which Central America was divided <sup>1</sup>, the air parcels were found to come for three main remote sources (Caribbean, Gulf of Mexico and ETPac) for GB, HS and Nicaragua. For CR-Panama, the northern South America region is added to the list of origin locations mentioned for the rest of subregions. From the total of air parcels arriving to each subregion, the percentage of the particles with origin in each source region was estimated in a seasonal basis to give an idea of the regions from which the air parcels come from. Figure 7.1 shows these estimated percentages, from which can be noticed the large difference between particles from the Caribbean and from the other sources. For the northern most part of Central America (GB and HS), the amount of air parcels from the Caribbean is quite uniform except for summer when an increase of a 20% is observed. At the same time that the amount of air particles from the Gulf of Mexico has decreased almost to zero for that season. These summer variations are a bit larger for GB than for HS. This suggest an increase in the efficiency of moisture transport. During winter, a decrease of the air particles from the ETPS is compensated by the increase of air particles from the GoMS. The case of Nicaragua looks alike northern Central Central America in the mean pattern of the distribution. However, variations as not as large for summer as for them and in change, a decrease in the amount of

---

<sup>1</sup>criteria for dividing the region was based on the heterogeneity of precipitation patterns as indicated in previous chapter

air parcels with origin over the Caribbean responds is fulfilled by the increase of those from the Pacific during Autumn. Southernmost Central America, (CR and Panama), presents a distribution well differentiated from the rest, here air parcels also originate over northern South America. For winter and even spring, the origin of air parcels is distributed between the Caribbean and northern SA and by summer a sharp decrease of Caribbean air parcels is noticed while a strong increment of air parcels originates on northern SA and the ETPS. The amount of air parcels originating at the GoM is very small. For autumn the pattern is also modified, air parcels come from the Caribbean, northern SA and in a major amount from the ETPS.

Year to year variations are a feature of the 'amount of air particles' travelling to the different locations of Central America. Table 7.1 to 7.4 show the percent distribution of air parcels that precipitate over the subregions of Central America according to their origin. for the months of February, May, July and October respectively. It can be noted the precipitation due to transport from remote sources is controlled by those contributions from the ocean, except for CRP which has an important component of moisture being transported from NSAS. The case of CRP and even Nicaragua is interesting since it shows a sharpened seasonality in the transport. Note that for CRP, during July a significant fall in the air particles from the Caribbean Sea occurs, which is compensated by the increase in the transport from NSAS. The latter being possible due to the intensification and configuration of the low level winds over the Caribbean. The easterly flow provides a mechanism through which the moisture from NSAS increases over the coast and enters a convergence region that develops in the Caribbean coast of Central America. For the northern subregions (GB, HS) during July, the influence of air from NSAS also increases. The mechanism is the same as mentioned for CRP, the presence of the maximum of the CLLJ couples with the wind flow from NSAS. It provides the strength to the flow from NSAS to travel longer distances. The curvature of the CLLJ is also fundamental in providing the conditions that favour the effective transport to GB and HS.

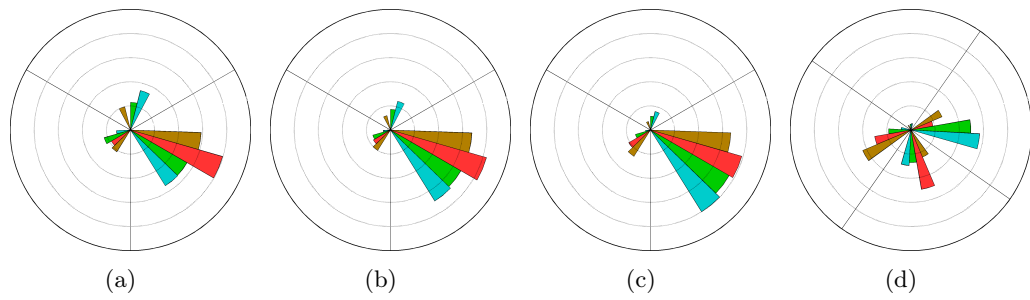


Figure 7.1: vertically integrated divergence of moisture flux (VIDMF) field (shaded contours) and vertically integrated water vapour flux vector.

Year	GB			HS			NIC			CRP						
	CAR	GoM	ETPS	NSAS	CAR	GoM	ETPS	NSAS	CAR	GoM	ETPS	NSAS	CAR	GoM	ETPS	NSAS
1980	30.8	1.4	67.2	0.6	52.1	1.7	45.0	1.1	72.2	0.6	25.4	1.9	62.9	1.6	7.8	27.7
1981	52.3	0.0	47.7	0.0	69.3	0.0	29.3	1.5	69.8	1.0	15.9	13.3	37.4	2.6	1.5	58.5
1982	63.3	0.0	36.7	0.0	81.8	0.0	17.9	0.2	84.5	0.2	9.0	6.3	40.5	20.5	1.9	37.1
1983	8.7	10.2	80.5	0.7	32.6	5.3	61.0	1.1	52.4	4.8	33.3	9.5	31.9	8.0	7.0	53.0
1984	48.6	0.0	51.2	0.2	70.0	0.0	22.8	7.2	70.8	0.5	9.9	18.8	28.6	5.3	1.2	64.8
1985	62.0	0.0	35.1	2.9	75.5	0.0	19.2	5.2	73.2	0.0	14.0	12.8	28.7	0.0	0.2	71.1
1986	38.2	0.0	61.8	0.1	59.9	0.2	31.5	8.4	64.9	1.0	21.6	12.4	54.8	3.7	9.8	31.6
1987	39.8	0.4	57.3	2.4	47.2	2.3	36.7	13.8	40.1	3.2	23.2	33.4	16.4	1.9	8.7	73.0
1988	43.2	0.0	55.7	1.1	70.4	0.0	26.8	2.8	78.6	0.0	11.3	10.1	46.8	1.8	1.5	49.9
1989	64.7	0.0	34.8	0.5	76.5	0.4	22.3	0.8	75.3	1.2	18.8	4.7	48.8	5.2	10.2	35.8
1990	47.4	1.4	50.5	0.6	69.7	1.5	26.9	1.9	74.5	6.7	10.1	8.7	56.3	13.0	2.7	28.0
1991	51.9	0.0	47.8	0.4	65.6	0.0	32.2	2.2	68.7	0.0	20.3	11.1	43.8	0.2	6.4	49.6
1992	26.1	2.4	70.4	1.1	43.9	0.0	54.4	1.7	62.7	0.8	27.6	8.8	41.9	2.7	5.5	49.9
1993	18.2	0.0	81.4	0.4	39.7	0.0	60.1	0.3	65.4	1.3	30.3	3.0	63.0	3.7	2.6	30.6
1994	67.6	0.0	32.4	0.0	89.2	0.0	10.8	0.0	92.3	1.4	1.8	4.5	36.1	19.2	4.0	40.7
1995	32.7	0.0	66.7	0.6	51.8	0.1	46.0	2.1	66.1	0.0	28.8	5.1	47.1	4.2	8.1	40.6
1996	26.9	0.0	73.1	0.0	50.6	0.1	48.3	1.0	68.6	0.3	25.0	6.1	53.7	1.7	5.9	38.8
1997	68.9	0.0	28.9	2.2	80.4	0.0	10.5	9.1	66.8	0.3	2.8	30.1	28.9	3.8	0.7	66.6
1998	9.7	5.1	83.1	2.0	27.0	1.8	63.4	7.8	33.9	10.4	40.2	15.5	13.7	13.2	16.9	56.3
1999	33.7	0.0	66.0	0.3	52.3	0.0	47.7	0.0	71.4	1.3	25.	1.7	56.6	10.0	5.1	28.3
<b>Avg</b>	<b>41.7</b>	<b>1.0</b>	<b>56.4</b>	<b>0.8</b>	<b>60.3</b>	<b>0.7</b>	<b>35.6</b>	<b>3.4</b>	<b>67.6</b>	<b>1.8</b>	<b>19.7</b>	<b>10.9</b>	<b>41.9</b>	<b>6.1</b>	<b>5.4</b>	<b>46.6</b>

Table 7.1: February Month

Year	GB			HS			NIC			CRP						
	CAR	GoM	ETPS	NSAS	CAR	GoM	ETPS	NSAS	CAR	GoM	ETPS	NSAS				
1980	36.6	1.7	58.5	3.1	46.6	2.0	31.9	19.5	37.1	4.0	12.5	46.4	6.6	14.6	1.7	77.1
1981	34.5	3.8	61.6	0.1	47.5	12.4	34.3	5.9	36.4	26.3	22.3	15.0	6.3	43.6	7.3	42.7
1982	30.1	4.7	63.4	1.8	38.5	11.2	46.2	4.1	34.0	25.2	34.4	6.3	12.5	43.6	12.9	31.0
1983	63.4	3.3	33.0	0.2	77.3	0.5	7.3	14.9	65.0	2.0	1.7	31.4	14.5	16.6	1.2	67.7
1984	40.8	12.0	41.1	6.0	50.7	7.8	12.4	29.2	36.9	5.2	2.6	55.4	15.3	22.3	3.7	58.7
1985	47.6	0.4	51.8	0.2	65.4	0.0	24.9	9.7	54.3	0.9	12.4	32.4	16.8	17.9	5.8	59.4
1986	32.8	1.2	62.2	3.8	37.4	4.8	44.7	13.1	33.9	16.4	30.6	19.1	15.1	38.5	10.0	36.3
1987	44.7	2.3	53.0	0.0	68.7	0.4	26.9	3.9	61.1	9.1	11.5	18.3	26.5	17.4	4.1	52.0
1988	23.4	5.8	69.7	1.1	34.0	9.8	49.3	6.9	40.1	17.3	29.3	13.3	12.9	31.5	8.3	47.3
1989	41.5	2.5	48.1	7.8	53.5	2.6	27.7	16.2	54.0	7.6	11.8	26.6	16.1	26.2	2.6	55.1
1990	40.0	4.4	51.6	4.0	39.7	15.5	27.6	17.2	28.1	27.3	16.5	28.1	10.9	27.3	5.3	56.5
1991	42.0	7.3	48.0	2.8	41.8	17.9	28.7	11.6	26.2	33.7	17.9	22.2	7.2	40.9	2.6	49.3
1992	30.4	0.1	69.5	0.0	49.2	0.0	50.0	0.8	62.2	1.0	30.5	6.4	38.2	9.7	5.4	46.7
1993	28.5	6.5	65.0	0.0	43.0	12.9	41.8	2.3	38.2	31.4	25.9	4.5	16.8	42.7	10.0	30.5
1994	44.1	1.0	50.7	4.2	54.5	0.1	30.3	15.2	37.2	4.6	17.4	40.8	6.0	28.9	5.7	59.5
1995	39.5	4.7	53.3	2.6	45.6	11.2	23.1	20.1	24.2	17.2	12.3	46.3	6.2	33.0	4.3	56.4
1996	31.0	9.0	53.9	6.1	37.5	15.4	26.4	20.8	26.9	22.2	11.1	39.7	5.7	40.2	4.5	49.6
1997	67.4	0.0	29.5	3.2	77.7	0.0	8.8	13.5	46.4	1.9	0.6	51.0	6.6	0.1	0.0	93.3
1998	35.9	0.0	62.3	1.8	48.8	0.1	36.1	14.1	53.5	2.2	21.7	22.6	21.4	20.6	5.8	52.2
1999	51.2	0.0	45.5	2.4	58.8	0.0	24.8	16.4	38.5	7.2	14.0	40.3	8.0	34.6	6.3	51.1
<b>Ave</b>	<b>40.3</b>	<b>3.5</b>	<b>53.6</b>	<b>2.6</b>	<b>50.8</b>	<b>6.3</b>	<b>30.1</b>	<b>12.8</b>	<b>41.7</b>	<b>13.1</b>	<b>16.9</b>	<b>28.3</b>	<b>13.5</b>	<b>27.5</b>	<b>5.4</b>	<b>53.6</b>

Table 7.2: May Month



Year	GB			HS			NIC			CRP						
	CAR	GoM	ETPS	NSAS	CAR	GoM	ETPS	NSAS	CAR	GoM	ETPS	NSAS	CAR	GoM	ETPS	NSAS
1980	72.4	1.0	8.7	17.9	55.2	0.0	1.7	43.1	22.0	1.1	0.1	76.8	3.1	12.8	0.6	83.5
1981	71.5	0.5	7.1	20.9	55.8	0.4	0.2	43.6	29.2	1.0	0.5	69.4	7.0	22.2	1.8	68.9
1982	71.6	0.1	0.1	28.2	50.0	0.9	0.0	49.1	14.1	1.5	0.0	84.4	2.4	10.8	0.1	86.6
1983	64.2	0.2	0.8	34.8	34.8	0.0	0.1	65.1	10.2	1.5	0.0	88.3	3.1	19.9	1.2	75.8
1984	61.0	7.2	11.8	20.0	46.3	6.2	1.2	46.3	19.0	6.1	0.5	74.4	5.5	27.1	0.9	66.5
1985	66.5	0.8	5.1	27.5	50.2	1.9	0.3	47.6	26.2	2.4	0.2	71.2	8.1	20.0	0.9	70.9
1986	63.7	0.3	0.2	35.9	44.9	1.4	0.0	53.7	13.2	5.1	1.1	80.6	2.1	16.4	0.8	80.7
1987	58.2	2.7	2.3	36.8	41.0	3.9	1.5	53.5	12.9	7.9	2.1	77.0	2.9	32.1	1.9	63.1
1988	64.0	3.6	12.9	19.5	52.4	5.5	4.6	37.4	27.4	7.5	2.3	62.9	4.3	31.7	3.3	60.8
1989	61.9	11.6	10.7	15.8	49.3	12.6	3.0	35.1	20.2	11.6	2.9	65.2	3.8	26.0	1.3	68.8
1990	70.4	0.8	5.9	22.9	59.8	0.5	0.1	39.6	35.5	1.7	0.3	62.5	7.2	18.5	0.7	73.6
1991	59.4	8.8	18.8	12.9	57.7	4.1	3.8	34.4	30.7	2.9	0.9	65.5	3.9	23.5	1.6	71.0
1992	67.0	1.4	17.	29.9	48.6	0.6	0.0	50.8	16.0	1.6	0.0	82.4	2.3	18.1	0.6	79.0
1993	63.6	8.0	2.9	25.6	51.7	6.0	1.1	41.2	31.3	3.7	0.1	64.9	5.6	17.1	0.5	76.9
1994	72.1	0.0	8.9	18.9	57.5	0.0	1.7	40.7	19.9	0.7	0.1	79.3	3.2	16.5	0.8	79.5
1995	71.8	2.2	2.3	23.7	55.7	2.2	1.1	41.0	27.2	5.4	1.0	66.4	6.9	34.8	3.4	55.0
1996	47.5	10.7	25.2	16.6	37.7	15.5	14.7	32.1	20.8	21.4	12.2	45.6	7.2	32.4	5.0	55.5
1997	68.8	0.3	1.6	29.2	50.9	0.3	0.7	48.2	14.7	1.3	0.3	83.8	1.4	5.7	0.0	92.9
1998	63.9	6.4	7.5	22.2	58.2	5.8	1.4	34.6	32.9	8.4	0.2	58.6	7.1	11.2	0.4	81.3
1999	54.0	11.3	20.4	14.3	52.0	10.3	10.0	27.7	35.7	8.2	4.9	51.2	5.9	25.8	3.8	64.4
<b>Avg</b>	<b>64.7</b>	<b>3.9</b>	<b>7.7</b>	<b>23.7</b>	<b>50.5</b>	<b>3.9</b>	<b>2.4</b>	<b>43.2</b>	<b>23.0</b>	<b>5.1</b>	<b>1.5</b>	<b>70.5</b>	<b>4.7</b>	<b>21.1</b>	<b>1.5</b>	<b>72.7</b>

Table 7.3: July Month

Year	GB			HS			NIC			CRP						
	CAR	GoM	ETPS	NSAS	CAR	GoM	ETPS	NSAS	CAR	GoM	ETPS	NSAS				
1980	52.1	2.4	39.2	6.2	55.4	10.5	20.6	13.5	25.8	29.3	16.2	28.8	4.1	44.5	4.7	46.7
1981	64.3	2.8	22.5	10.5	62.6	2.9	8.1	26.4	48.2	8.7	2.8	40.2	15.2	40.9	2.5	41.5
1982	36.5	1.6	55.6	6.3	44.1	8.5	33.0	14.3	34.2	17.3	18.4	30.0	15.9	38.7	5.3	40.1
1983	58.2	4.0	28.3	9.5	60.0	2.5	13.3	24.2	31.7	6.7	5.3	56.3	7.8	41.9	5.8	44.5
1984	80.9	0.0	17.6	1.4	88.0	0.0	1.7	10.3	63.2	1.2	1.7	33.9	19.3	37.3	3.0	40.4
1985	46.2	3.0	44.9	6.0	45.4	4.9	31.1	18.7	31.6	11.3	22.9	34.2	12.7	32.6	5.6	49.2
1986	48.6	0.2	40.6	10.5	56.4	2.2	16.6	24.8	42.0	8.8	8.5	40.7	16.7	38.1	5.8	39.4
1987	21.1	2.6	76.3	0.0	52.2	1.9	44.7	1.1	53.0	7.8	33.0	6.2	23.6	44.6	13.7	18.1
1988	50.3	12.8	34.1	2.8	75.7	9.0	8.8	6.4	64.9	13.2	2.4	19.6	22.9	46.9	6.5	23.6
1989	33.1	8.7	52.6	5.6	44.5	11.6	24.8	19.1	48.6	12.1	9.2	30.2	15.9	35.5	2.6	46.0
1990	24.1	11.1	64.6	0.2	39.9	6.1	50.1	3.8	32.0	22.8	37.0	8.3	10.6	54.2	16.2	19.0
1991	54.8	1.6	37.1	6.6	53.2	0.2	26.8	19.8	39.5	9.6	18.2	32.7	9.9	43.3	6.6	40.2
1992	44.8	6.0	42.5	6.7	54.9	5.1	21.3	18.7	44.3	8.6	6.6	40.5	11.5	32.6	3.9	52.1
1993	47.6	4.3	37.1	11.0	52.7	3.9	7.9	35.5	38.7	7.3	1.5	52.5	10.0	37.1	2.7	50.2
1994	32.5	8.4	52.4	6.7	40.0	12.0	29.1	18.9	37.3	18.3	13.6	30.8	10.2	48.1	6.0	35.7
1995	19.9	9.8	70.1	0.3	24.6	10.1	59.2	6.1	17.0	26.9	43.3	12.7	3.8	59.8	14.4	22.0
1996	28.3	5.4	62.9	3.5	41.4	5.4	37.5	15.6	27.4	28.1	25.1	19.4	8.3	45.9	8.3	37.5
1997	30.7	12.1	53.6	3.5	33.8	12.6	41.3	12.3	31.7	15.4	34.9	17.9	11.1	29.6	19.4	39.9
1998	43.6	14.2	29.1	13.0	40.9	15.0	21.1	23.0	27.6	23.3	20.6	28.5	6.4	43.2	10.6	39.9
1999	27.3	4.6	62.1	5.9	20.6	9.5	49.5	20.5	12.1	28.6	34.0	25.3	4.9	59.3	15.6	20.2
<b>Ave</b>	<b>42.2</b>	<b>5.8</b>	<b>46.2</b>	<b>5.8</b>	<b>49.3</b>	<b>6.7</b>	<b>27.3</b>	<b>16.7</b>	<b>37.5</b>	<b>15.3</b>	<b>17.8</b>	<b>29.4</b>	<b>12.0</b>	<b>42.7</b>	<b>8.0</b>	<b>37.3</b>

Table 7.4: October Month

## 7.2 The structure of transport

In chapter 5, the main sources of the moisture that contributes to precipitation over Central America were identified. To establish how do the transport process occur it is necessary to know how is air moving. With such a large amount of air parcels, to obtain a mean picture a clustering technique was used to reduce a large set of backward trajectories into a smaller set of trajectories. A first separation of the trajectories aimed to retain those that contributed for precipitation. As we are interested in the air particles that account for precipitation in the subregions, we are mainly concerned on those particles that always circulated along their trajectories below the tropopause level. Those particles which at any moment crossed upper the tropopause were neglected, then those that were found to contribute to precipitation in the determined regions were retained for analysis. Note that the height of the tropopause was considered as given by the ERA-40 Reanalysis data. For each of the subregions in which Central America was divided, air particles arriving to them were identified in order to obtain the climatological mean air streams in a monthly basis. The general picture of these air streams looks quite alike for the different regions, despite the differences related mainly due to the position of the target region. The mean air streams for May are shown in figure 7.2 for each region to highlight this condition. As can be followed from this figure, air moves to the different locations of Central America mainly from the following regions: a) CS b) ETPS, c) GoMS and d) NSAS for southernmost Central America (7.2.d). Air moves from the Caribbean permanently while the movement of air from the Gulf of Mexico and ETPac is seasonally constrained. For GB, HS and Nicaragua air moves from the Gulf of Mexico (ETPac) between October and May (May and November). While in the case of Costa Rica and Panama, less air moves from the Gulf of Mexico between October.

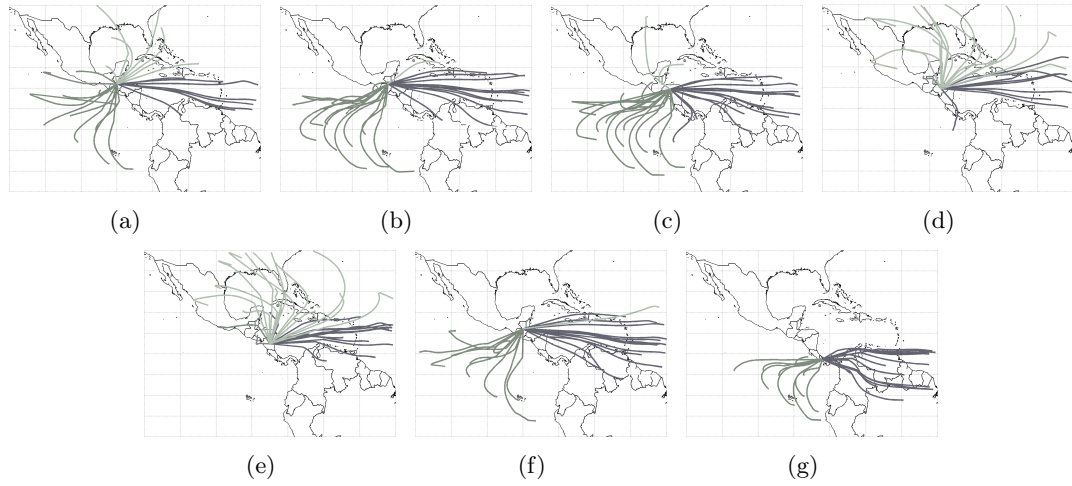
**The horizontal structure of the mean airflow**

Figure 7.2: Mean climatological air streams for the trajectories losing moisture over different locations of Central America.

### 7.3 The content of air moisture along the trajectories

Moisture content of an air parcel varies along its trajectory depending on different conditions (vertical movements, evaporation, precipitation). This way, an air parcel can be dry at one point of the trajectory and later on the moisture content can be increased (known as uptake) or the inverse process can occur. These points for which the major moisture uptakes take place are of importance since they give a more accurate idea on the location of a punctual source of moisture associated to the trajectory of individual air parcels. To ensure this, it is first important to identify the variations of moisture that air parcels undergo along their trajectories. This to determine the regions over which the moisture of the air parcels is increased. In the computation of the mean air streams using the clustering algorithm, the specific humidity was averaged at each time step for all the particles belonging to the same cluster. This allowed us to obtain an estimate on the mean moisture content of the air streams along the trajectories (backward in time). Figures 7.3 to 7.6 present the results of the climatological mean air streams and their associated moisture content for GB, HS, Nicaragua and Costa Rica and Panama respectively.

The four regions have in common the low moisture content of the air flowing from GoMS. This result is reflected in the small contributions to precipitation from this region, as shown in chapter 6 (see figure 6.2.d). Also, for the four regions, the major moisture content of the particles' trajectories is located over the oceanic regions (CS and ETPS). Moreover, it can be noticed that the largest values of mean specific humidity are those from the trajectories circulating over the ETPac. A question here might be why the contributions to Central America from the ETPS are then so low? By examining the temporal evolution of the moisture content of the trajectories it can be observed how the major changes in specific humidity occur over the ocean before the trajectories reach the target region. This implies that even when the largest moisture uptakes occur for the ETPS, they contribute to precipitation over the ocean rather than continental Central America, which then receives smaller contributions.

From figure 7.3 and 7.4, regarding air parcels travelling from the Caribbean can be noted that for winter and early spring, the moisture content is too low and as a result contributions to precipitation small. For the remainder of spring, and early summer,

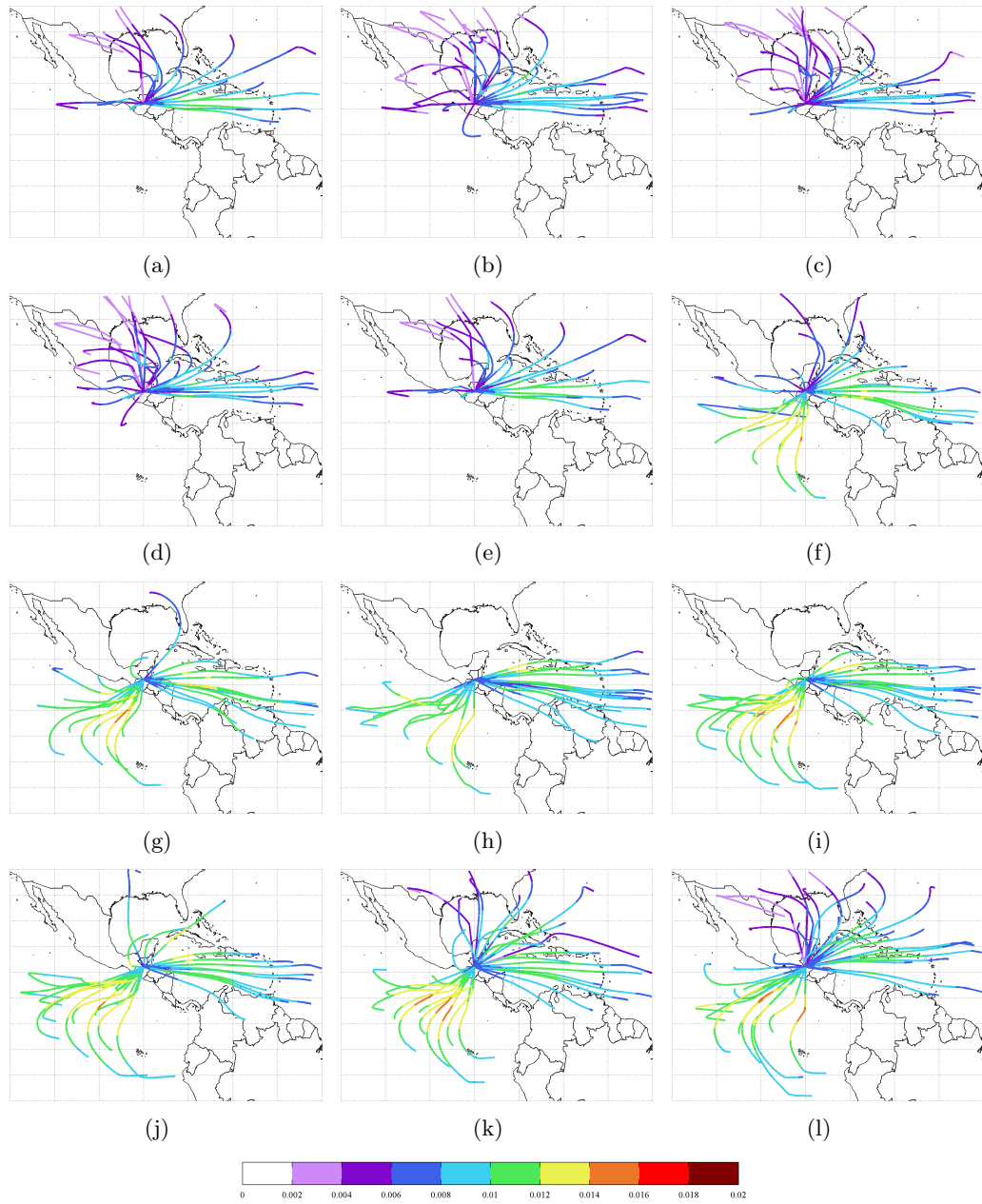


Figure 7.3: Mean climatological air streams for the trajectories losing moisture over GB and associated moisture content.

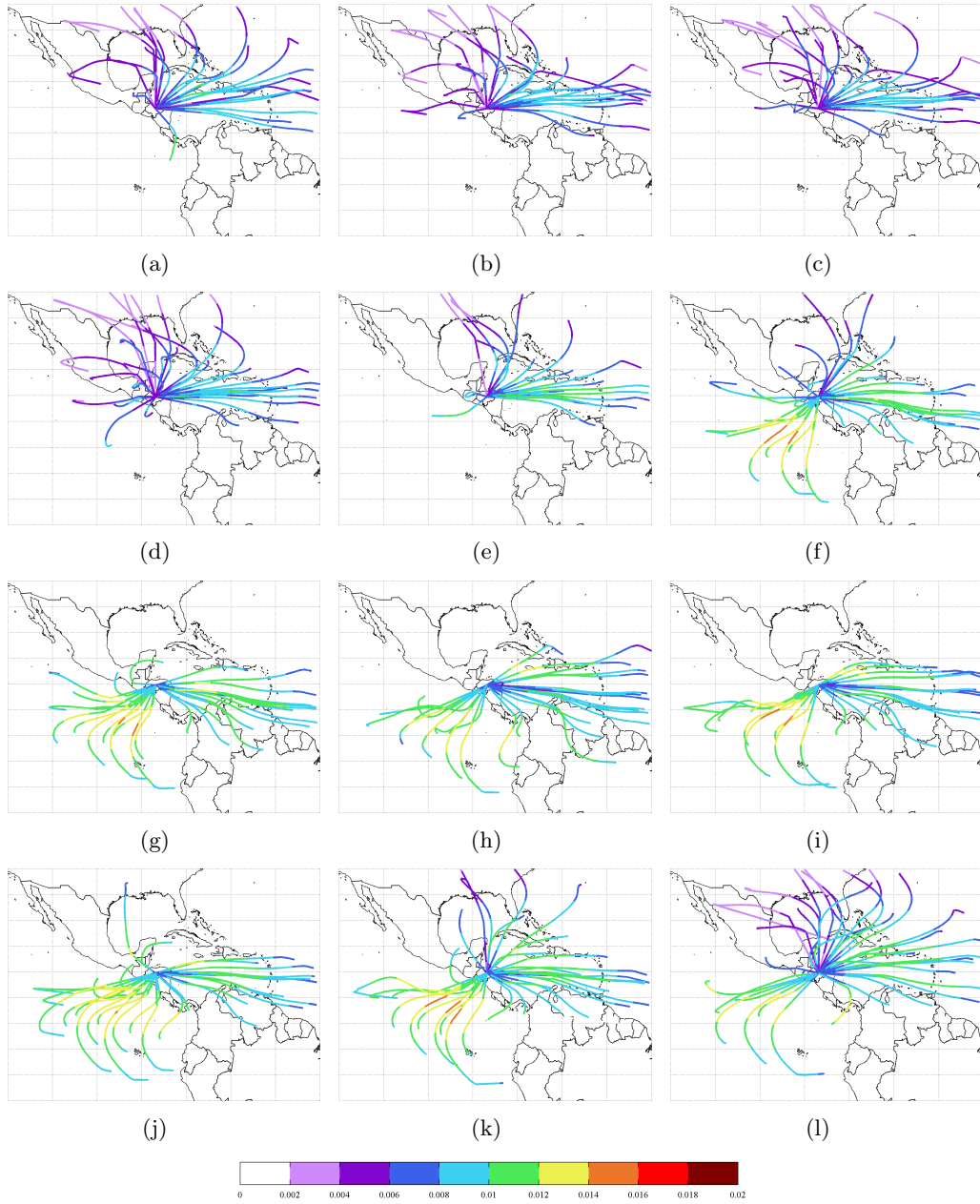


Figure 7.4: Mean climatological air streams for the trajectories losing moisture over HS and associated moisture content.

particles are moister and the specific humidity at the arrival point quite small, which implies larger contributions to precipitation. Notice that between June and August the differences in the moisture content is reduced compared to the previous months. This implies that less moisture is being left over the target at the arrival so contributions to precipitation are reduced. Moreover, the moisture content of the trajectories itself is in average lower compared to other periods, which implies drier trajectories during summer leaving even less moisture over Guatemala, Belize, Honduras and Salvador. During Autumn, differences become larger and also the moisture content of the trajectories, so contributions to precipitation rise. This reduction in the moisture content of air parcels reaching GB, HS from the Caribbean causes a decrease in the contributions to precipitation, in good agreement with the presence of the MSD.

The situation of the air parcels from the ETPac region is a little different since even when the differences are similar to those from the Pacific, the moisture content of the air parcels is larger. So that over the northernmost portion of Central America, the moisture transported from the Pacific is key for determining the summer precipitation. The case of the trajectories arriving to Nicaragua (figure 7.5) is similar, but with the difference that moisture lost over the continental region becomes larger in October and not September as for the northern regions. This suggests that the dry season present during summer may be more extended in Nicaragua than in the northern neighbor region. In the case of southernmost Central America (fig 7.6) the arrival from particles from the ETPS occurs all year round except for March. A strong increase on the amount of particles occurs after the end of spring. During winter, the content of moisture of the air parcels increases modestly over the Caribbean. During summer, trajectories from the central Caribbean are significantly reduced and air masses coming from the east have an increase of its moisture content over the northernmost region of Venezuela. This intensification of the moisture content is sustained over the Caribbean until it reaches the continental region of Costa Rica and Panama, where the strong decrease in the moisture content indicates precipitation have occurred. This pattern is also present during autumn, but air parcels from the east travel a little bit northern, so the uptake locations resides in the Caribbean Sea rather than NSAS.

The location of the main uptake regions can be also identified as shown by the variations in the moisture content. Two locations are featured by the enhancement of



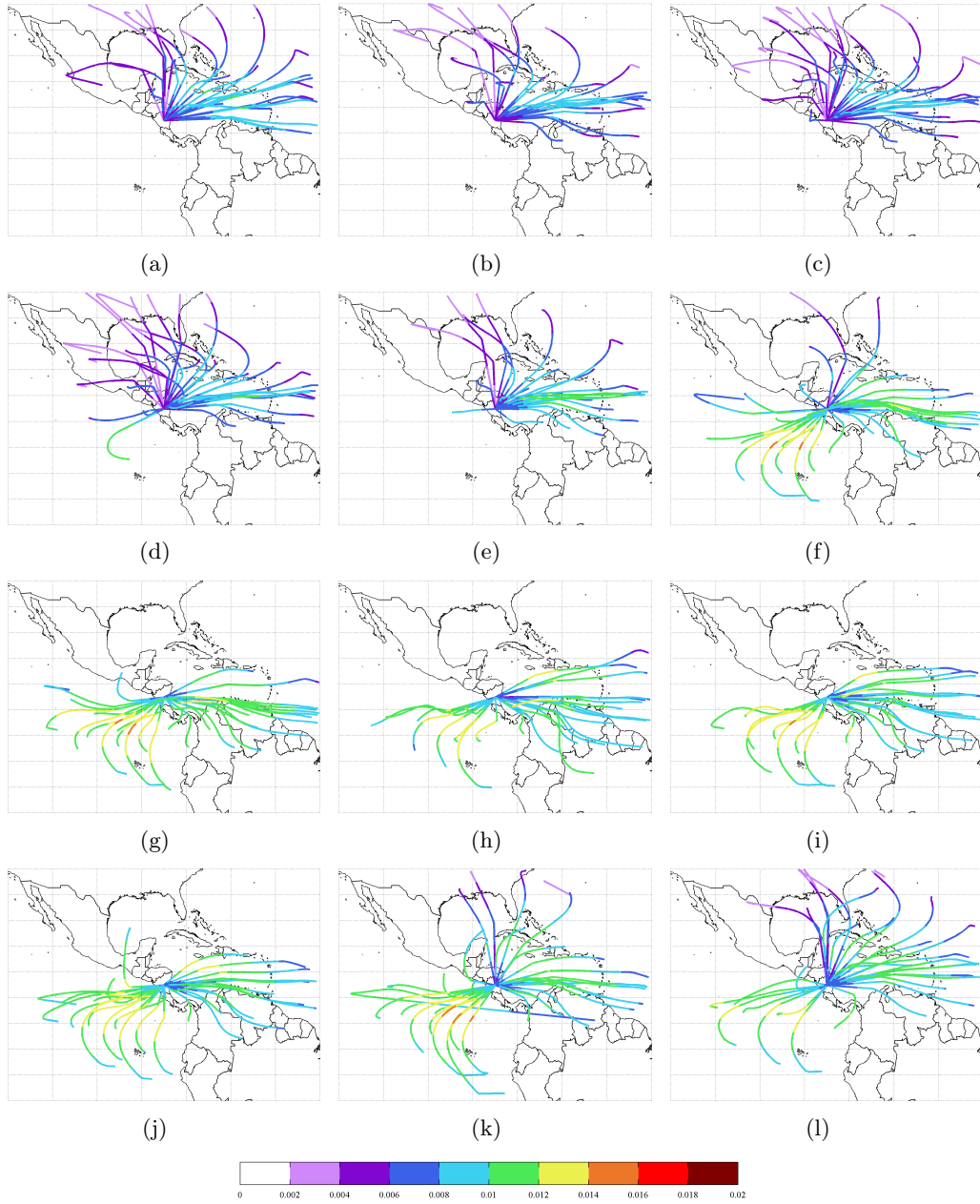


Figure 7.5: Mean climatological air streams for the trajectories losing moisture over Nic and associated moisture content.

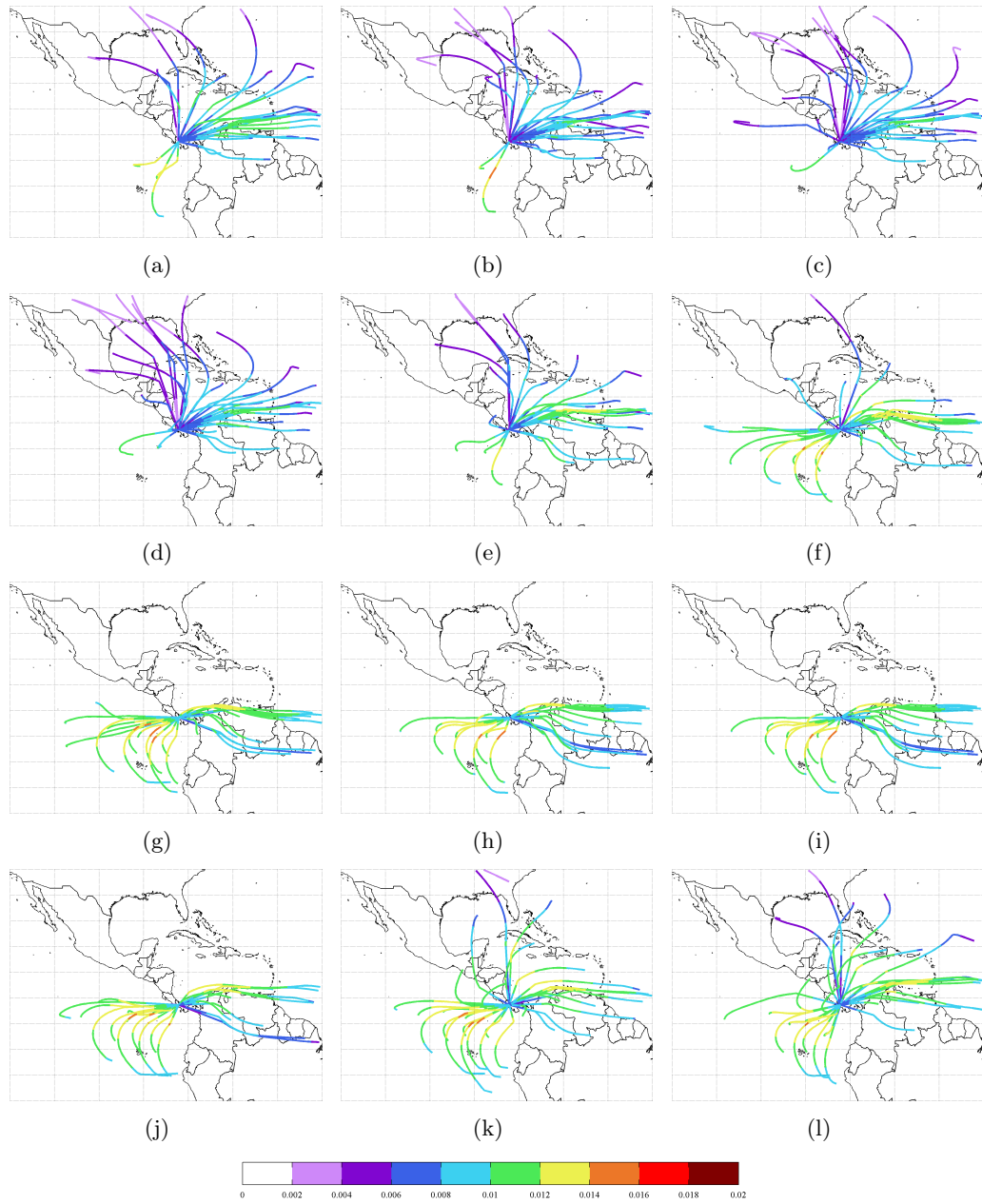


Figure 7.6: Mean climatological air streams for the trajectories losing moisture over CRP and associated moisture content.

the increase of the mean moisture content of air particles, the region over the ETPac and the Caribbean Sea. For the different arrival locations defined, it can be observed the fact that despite the origin of the air parcels, those are relatively dry and moisture increases undergo for very specific locations. Uptake over the ETPac is well constrained to the region of intense evaporation (see figure 1.3, chapter 1) which implies that evaporation is the process that triggers the moisture history of the air parcels under the Pacific regime. As is normal, few or no intense uptake occurs when the ITCZ is located over this region as is known to happen during (mid-end) winter and part of spring. Periods that correspond to the poor activity of the ETPS and moreover, with the decrease in the contributions to precipitation, in agreement with results shown in chapter 6.

### **Vertical structure of the air streams**

The climatological averaged air streams described in previous section show in details the mean path followed by the air parcels between the sources to the arrival locations, this is, the mean horizontal picture of transport, and the regions of major uptake. The air flow from the Gulf of Mexico was mentioned to be particularly dry, and it was speculated to be related with the height of the flow. Note that it can be said that as lower the level of the air parcels larger is the content of moisture. However, it is also important to know with accuracy the vertical structure of air, since it provides information on mixing processes and vertical variations associated with determined systems.<sup>11</sup> As for the horizontal structure, the climatological averages of the vertical structure of the air streams are presented for the defined subregions. Figure 7.7 to 7.9 show the average vertical structure of the climatological clusters for each subregion of Central America coming from each source region. After the classification of the tropopause air particles was done, it was found that more than 87% of the air particles that contributed to precipitation circulated below approximately 4Km height. Moreover, most of the retained air particles that has the largest moisture content circulated below 3Km, for such reason results presented in the following plots use this height limit in order to present with more detail the vertical structure of the average clusters.

---

<sup>11</sup>this is of great importance for case analysis because the vertical structure provides information on several atmospheric processes.

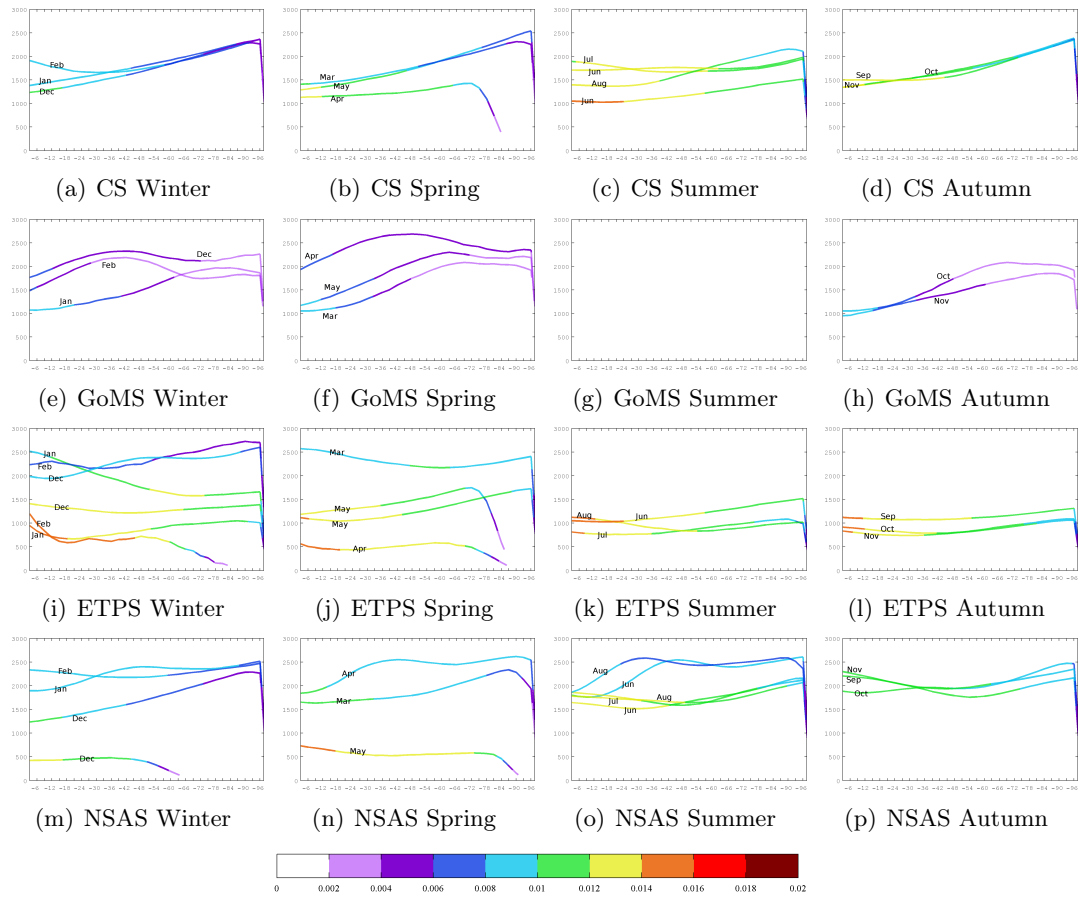


Figure 7.7: Mean climatological air streams for the trajectories losing moisture over CRP and associated moisture content.

For southermost Central America, named the CRP region, the larger contributions are noticed to come from CS, ETPS and NSAS as shown in previous chapters. The vertical structure of the transport show a good coherence with the wind flow, which is well known to be low level in average. For the air travelling from the CS, a significant increase in the moisture uptake is found during summer (fig 7.6.h). This uptake takes place up to 3 days before the arrival of the air masses into CRP when precipitation occurs. It can be noticed how during late spring (fig 7.6.e) and early Summer (fig 7.6.f), a strong increase in the moisture content of the air particles occurs (Jun, fig 7.7.g). Moist air that contributes to precipitation over CRP from the CS is in average below the 2Km and its height decreases importantly as moisture increases (as a result

of the weight increase). During Summer and early Autumn, the moisture uptake occurs over the inner Caribbean, where the easterly flow is known to peak (as noticed from the horizontal structure in previous section). Air travelling from the GoMS is very dry in comparison and presents a very variable vertical structure, with a reduced amount of air particles that contribute to precipitation during summer, as the wind flow from the Caribbean moves northward due to the increased intensity of the CLLJ. The case of the transport of air particles from the ETPS is particularly interesting as two well differenced air flows can be noticed. During winter (fig 7.6.a) and spring (fig 7.6.k) the presence of a very moist and very low level flow is remarkable at the same time that a drier air flow layer is noticed at higher altitudes. The latter flow is associated with the westerly winds regime whereas the lower level moist flow is found to be related with the more near surface air flow from the southwest. As Summer approaches, the upper dry flow vanishes (fig 7.6.g), during Autumn, the vertical structure of the air flow from the ETPS is basically the same as for Summer. Note that the largest uptake of moisture occurs for the low level air flow as it is directly related with the region where evaporation is larger. Moreover, the uptake linked to precipitation is remarkably stronger during February and it is maintained during a larger time period. This suggests that the southwesterly flow plays a primary role for triggering evaporation from the ocean surface and that moisture increase that results from it contributes directly to precipitation over CRP. On the other hand, moisture transport from the NSAS is not as lower level as that coming from the oceanic regions. Air from this source is as that from the GoMS very dry, except after May (fig 7.6.f) when moisture uptake increases. This marks the start of the contributions from this source that was found to be active during the Summer period. As Summer ends, the airflow from this source returns to its dry conditions.

For Nicaragua, the vertical structure of the air flow from the CS looks alike for CRP but with uptake being less intense and occurring in the first 24 hours before the arrival (figures fig 7.8.a to fig 7.8.d). Air from the GoMS is featured to be even drier than for CRP and also by flowing at higher altitudes as it travels upper the 3 Km (fig 7.8.e to fig 7.8.h). Meanwhile air from the ETPS shows no airflow below the 3Km height in average as air that contributes to precipitation during this period is upper level and even drier. During May, the flow separation in the vertical also occurs as found for CRP,

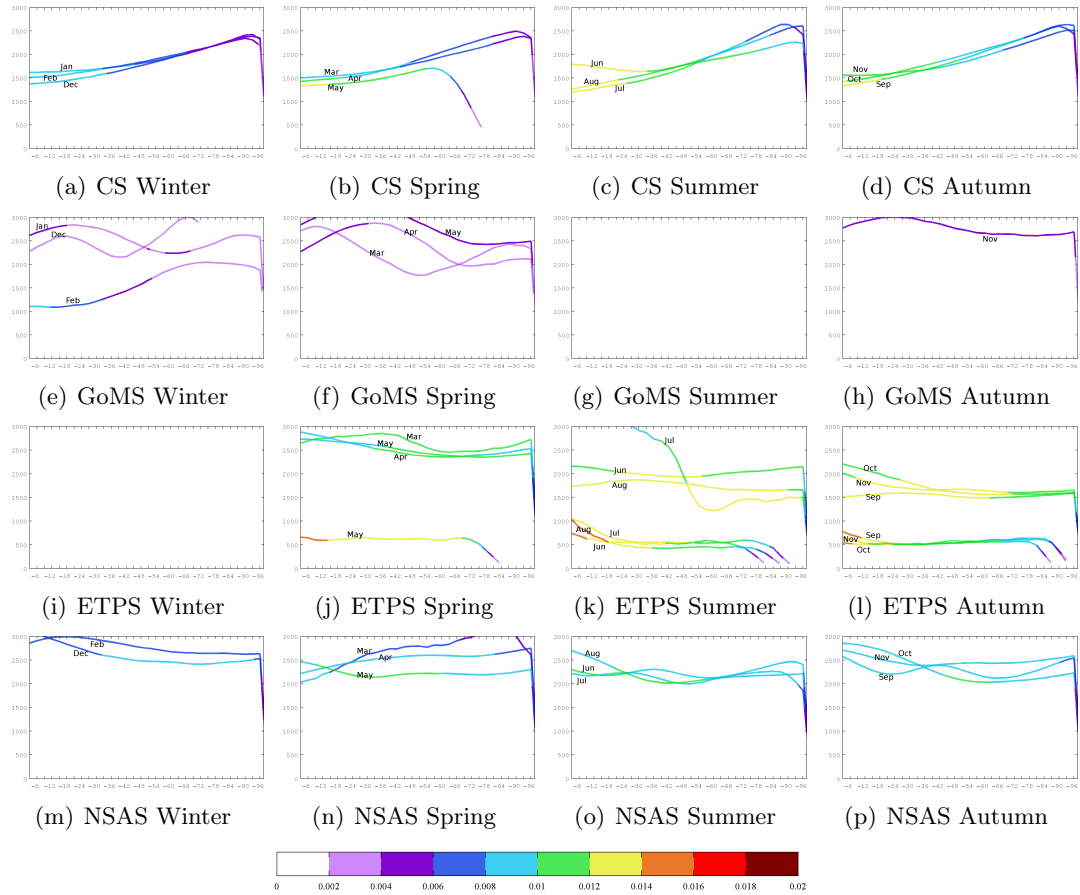


Figure 7.8: Mean climatological air streams for the trajectories losing moisture over Nic and associated moisture content.

with the separation being even more marked for the air travelling to Nic (fig 7.8.j). This air flow separation, different from what happened for CRP, is found to remain for the rest of the year with a peak of uptake during summer (fig 7.8.k). It is also worth to notice that the moisture content of the air particles travelling at 'upper' levels from the west have an important moisture content as moisture uptake is intense even 96 hours prior to the moment in which precipitation occurs. The fact that the moist content of the air is conserved for longer time periods implies that less rainout occurs along the trajectory of the air parcels. In the case of the lower level flow, the moisture gains are constrained to the day previous to the arrival, except for May as for CRP. Air flow from NSAS is in average found to circulate at upper levels, it is very dry and no significant

moisture uptake is found in average as for CRP. This result suggests that the transport of moist air from NSAS to the North is very well constrained by precipitation (and the mountain range) over CRP. Therefore, a decreasing influence of the transport from NSAS is expected as we move North, and as it was shown in previous chapter.

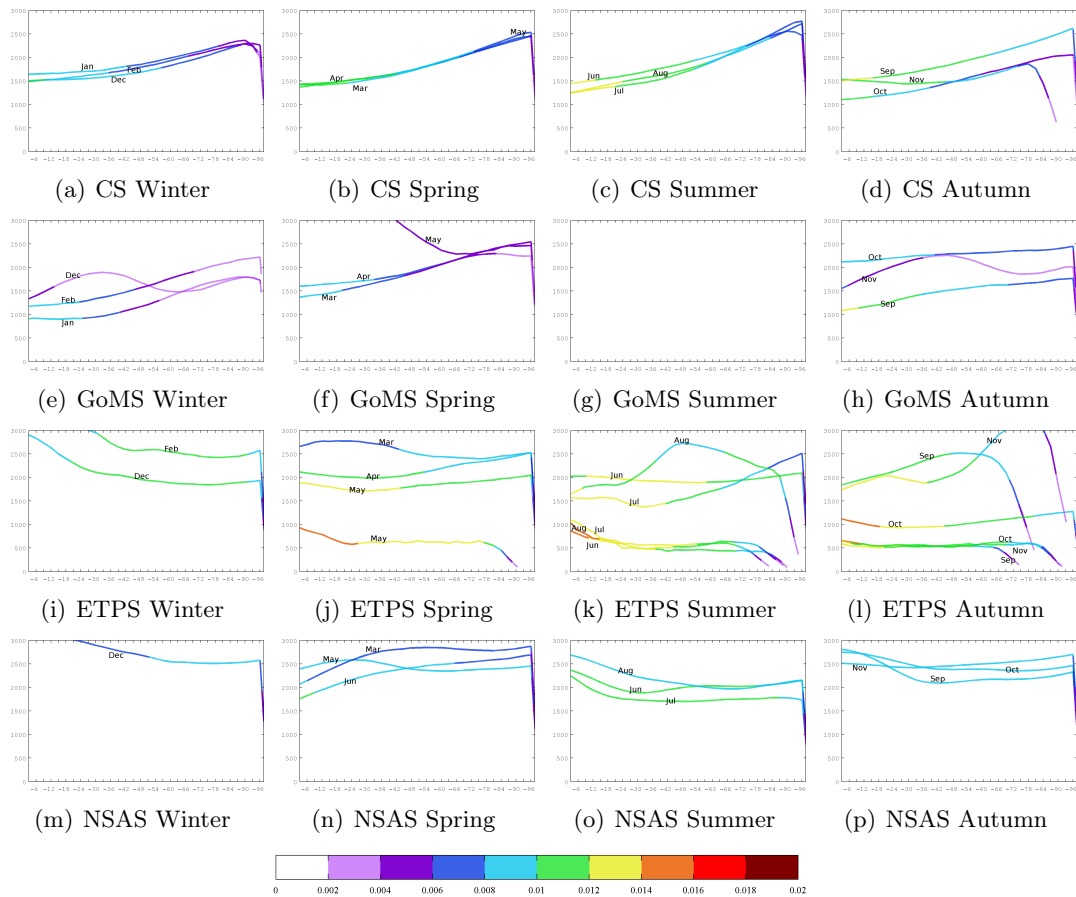


Figure 7.9: Mean climatological air streams for the trajectories losing moisture over HS and associated moisture content.

Similar to what was found for CRP and Nic, moist air transport from the CS to HS shows a coherent structure with increasing moisture uptake during winter (fig 7.9.a to fig 7.9.10) with the flow level below the 1.5 Km. Transport from the GoMS is drier and it was found to circulate at lower levels, particularly in September (fig 7.9.g), when it is found to flow below one kilometer height with the largest moisture uptake in the first 24 hours prior to precipitation. The flow separation for the air flow travelling from

the ETPS is also noticed, during winter the solely presence of the upper level flow is noticed (fig 7.9.i) which is also found to be higher in altitude compared for the same period for Nic. The development of the moist inflow from the lower levels is noticed with intense moisture uptake for May as for the other two subregions analysed (fig 7.9.j). It is important to remark that for Summer (fig 7.9.k) and Autumn (fig 7.9.l) the height of the upper level flow has decreased compared to the other subregions. Moreover, a significant increase in the moisture uptake is noticed, being very important during the previous 48 hours before the arrival of the air parcels to the target location for both upper and low level air flow. Air travelling from NSAS (fig 7.9.m to fig 7.9.p) is found to circulate at higher levels. Moist air transport from the sources of moisture for GB presents a vertical structure very similar to that described for HS, with the upper level air flow having the largest moisture uptake during spring (fig 7.9.j) and summer (fig 7.9.k) going back up to 4 days before the arrival of the air particles to the target.

## 7.4 Dynamics of transport

A strong relationship between the wind fields and sources of moisture (and associated contributions to precipitation) is determined. Looking to the horizontal structure of the mean airflow, it is quite consistent with the low level wind vector. So the link between wind and precipitation is not surprising since this relationship is known for several regions worldwide. The Lagrangian approach provides an integral overview of the regional water cycle, evaporation from the oceans and consequent moisture uptake along the transport of air masses from the oceanic sources to the continental region. Figure 7.10 shows the seasonally averaged low level wind field.

From the seasonal patterns of the wind vector, it can be followed that the low level winds play a major role in the transport of moisture. In the case of the transport of moisture from the Caribbean Sea and NSAS, the strong easterly flow is fundamental (as pointed out Durán-Quesada et al., 2010). During winter, the easterly winds are curved south-westward so that wind is able to carry moisture into southernmost Central America. Note that the conditions of the wind flow imply a reduction of the intensity of the wind between northern Caribbean and the Gulf of Mexico. Moisture from upper levels is able to go downward. The gradient between the ocean and land is reduced and air is able to penetrate into the continent where it can contribute to leave moisture



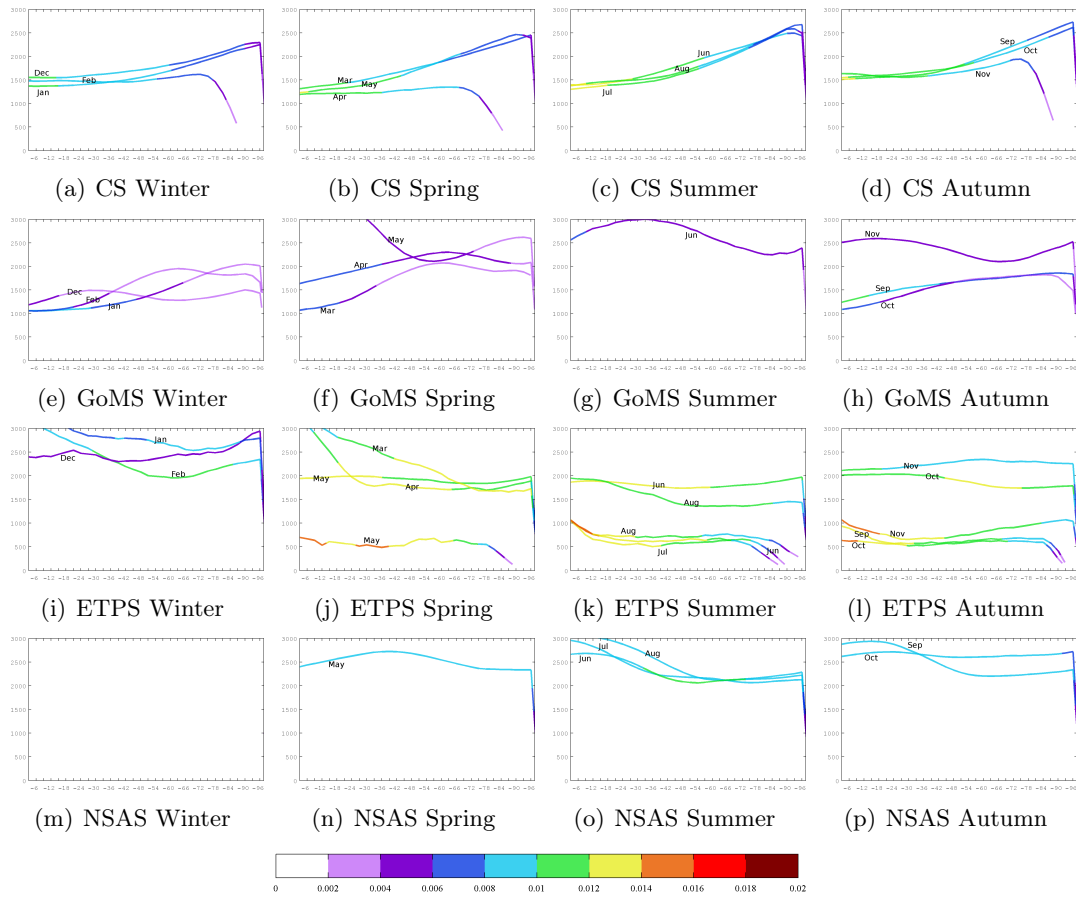


Figure 7.10: Mean climatological air streams for the trajectories losing moisture over GB and associated moisture content.

over the northernmost portion of Central America. This explains the increase of the contributions from the Gulf of Mexico that are of importance during winter and early spring. The secondary peak of the low level jet also explains why even when moisture is being transported to Central America, the peak of precipitation does not occur for winter. Note from figure 7.10.1, that during late winter the contributions from the Caribbean are reduced and they start to grow again after April. As the CLLJ secondary peak intensifies, more moisture is transported toward Central America. However, due to the width of Central America and moreover to the presence of topographic passes, this intensified wind is funneled through the topography gaps and penetrates far into the Pacific.

As the CLLJ starts to decrease in intensity, the moisture transported from the east is not able to cross to the Pacific (note that the wind flow over the topographic gaps of Tehuantepec and Papagayo decreased considerably). Moisture is available to precipitate over Central America if the instability conditions are favourable. This marks the spring peak of precipitation over Central America. On the other side, over the ETPac, during winter and spring, even when the ITCZ is not as strong the wind flow is southwestward and moreover, the intensity of the easterly flow of the CLLJ, Papagayo gap, reduces it even more. This result in few chances for moisture from the Pacific to reach Central America, making that the amount of moisture transported be almost zero. Again in spring, when the easterlies are reduced, the flow from the NSAS coast can follow some parts of Central America, where it can contribute to local precipitation.

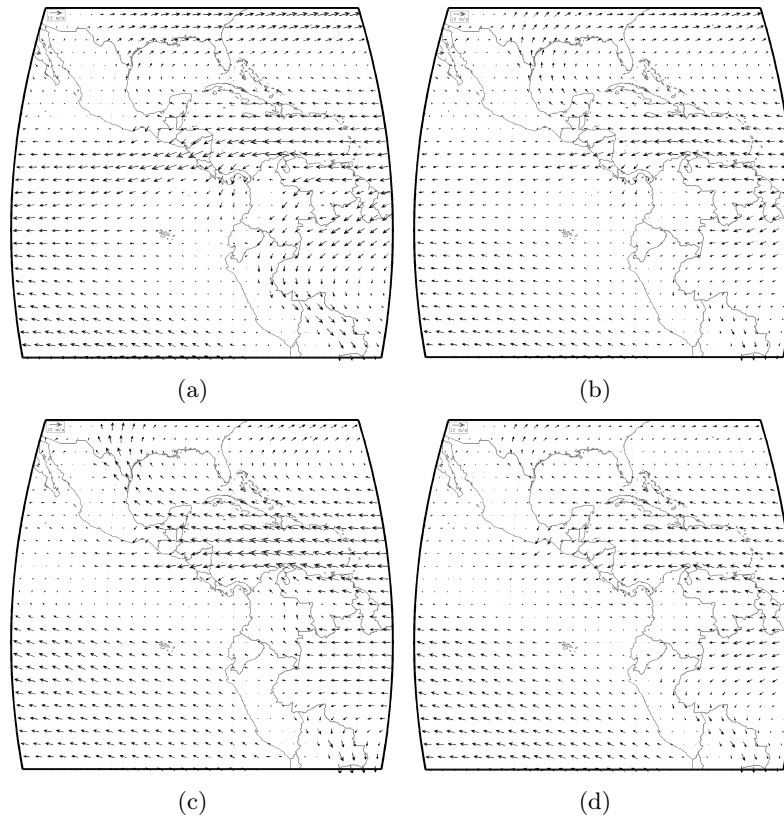


Figure 7.11: Climatological seasonal wind at 850hPa for the 1980-1999 period from ERA-40 Reanalysis .

During summer, two key features of the regional climate are present, the MSD and

the CLLJ. The main peak of the CLLJ differs from the secondary in the intensity but more importantly in the orientation of the flow. During summer, the CLLJ develops a northward branch, moisture from the Caribbean Sea is then transported in the direction of the wind flow which by this time does not point to southern Central America. Instead it point zonally through northern Central America and follows the coastline toward the Gulf of Mexico. The direct result is the inhibition of wind flow from the Gulf of Mexico to travel to northern Central America by the same mechanism that inhibited wind from the Pacific to travel towards Central America. The reduction of wind flow to southern Central America results in a decrease of transport of moisture to this region. The magnitude of the wind that is almost completely zonal toward northern Central America and has a similar effect to that of the topographic gaps. Then moisture transported in this direction and reaches the Pacific instead of accounting for precipitation over northern Central America. The strengthening of the Tehuantepecers and the Papagayos induces the moist easterly flow to go west into the Pacific (see figure 7.11.c). The moisture from the Caribbean being transported to the Gulf of Mexico, the Great Plains and the Pacific reduces the availability of moisture to precipitate over Central America. This causes a generalised decrease of precipitation over Central America during summer. The wind conditions favour the transport of moisture from NSA to southern Central America. Note that even when the wind flow does not point to this region, as a result of the flow direction, the transport from NSA to central America is favoured. This explains the strong reduction of contributions from the Gulf of Mexico, the decrease of those from the Caribbean and the intensification of contributions from NSA. In the case of the ETPac, southwestward flow is less zonally west and the gradient allows the wind low near the coast to become more meridional and point north, turning a bit south-eastward and favouring the transport from the ETPac. In addition, evaporation increases over this region during summer, increasing the availability of moisture to be transported from this region. During this period, the ITCZ is at the northernmost position so moisture from the ETPac does not have to overpass this obstacle and is free on its way to Central America. As the CLLJ decreases considerably during autumn, wind transports moisture more efficiently to Central America, the wind flow does not favour more the transport of moisture from the NSA and the Gulf of Mexico. As a result, contributions from the Caribbean Sea increases while those from NSA and the

Gulf of Mexico are reduced. Contributions from the ETPac are maintained until the ITCZ moves southward and inhibit the passage of moist air to Central America by inducing it to precipitate over the ocean before reaching the continental region.

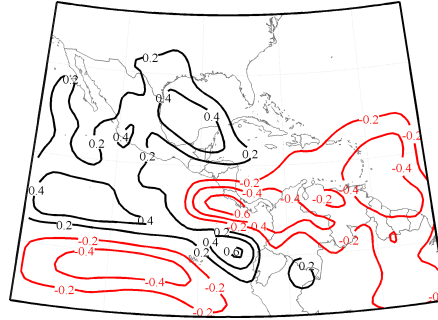


Figure 7.12: Significant correlation pattern between the intensity of the  $(E - P) - 6$  field for Central America and the surface wind field .

The importance of low level winds is not only associated to the transport of moisture but also with the increase of evaporation and the correspondent intensification of the evaporative sources of moisture over the ocean, as described by equation 1.2. This influence of the wind field is summarised in the spatial correlation pattern shown in figure 7.9. The negative correlation between the intensity of the surface winds over the Caribbean Sea (and parts of Central America) are related with the fact that as the easterlies become stronger, the moisture available in these regions is transported westward. Which implies a reduction in the contributions to precipitation, therefore a decrease in the intensity and horizontal extension of the region as a source of moisture for Central America. Positive correlations over the norther ETPac are associated to the transport of moisture due to low level winds, as the westerlies are increased (decreased) moisture is (not ) transported from this region to Central America. Finally, the negative correlations in ETPac region are related to the intensification of the moisture sources due to the intensification of evaporation. The increase of the easterly flow over this region is associated to the intensification of evaporation over this region so that as more negative (the convention for the zonal wind was used as positive to the east) is the wind, larger is the evaporation (equation 1.2) and for instance more moisture is available to the transported to neighbor regions.

### A conceptual model for the modulation of moisture transport

The information provided by the trajectories is very valuable in the sense it allows the identification of transport structures and by tracking the moisture content the regions where moisture of air is increased can be assessed. With this framework, we are now able to discuss how the process of the transport of moisture takes place.

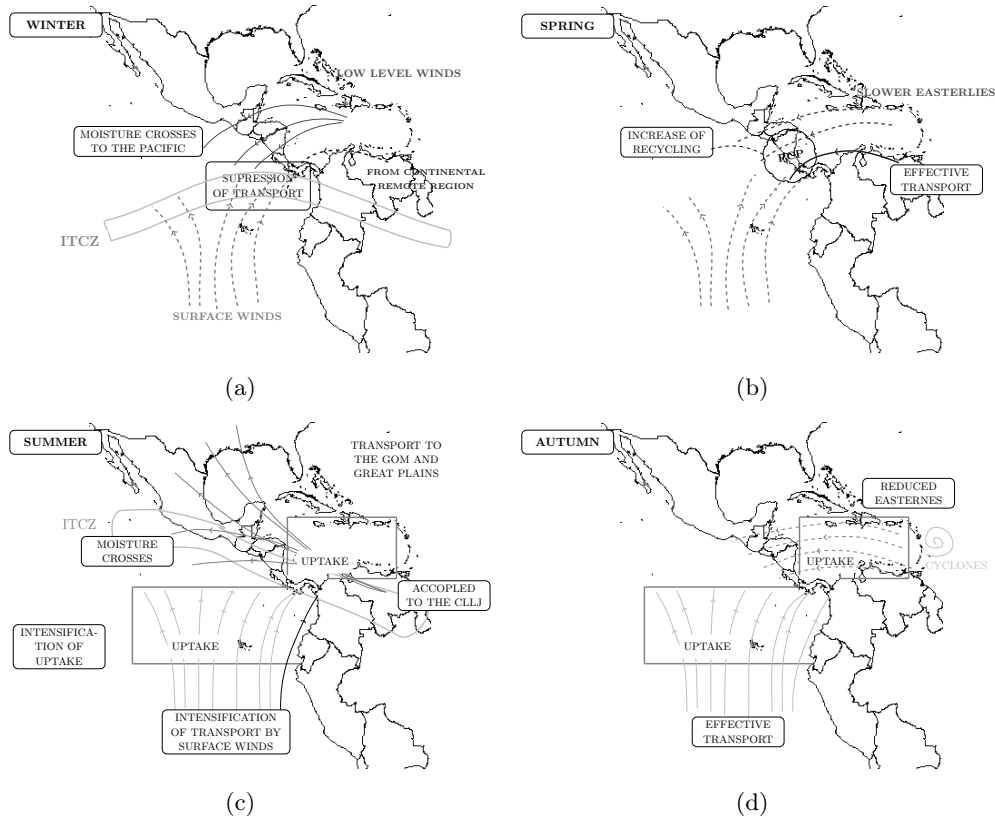


Figure 7.13: Significant correlation pattern between the intensity of the  $(E - P) - 6$  field for Central America and the surface wind field .

The structure of the trajectories revealed that low level winds are the main moisture conveyors for the moisture that reaches Central America. In addition, the evaluation of the moisture content along the trajectories show that moisture uptake is important in the regions where winds are strong (in agreement with the dynamics behind evaporation) but also that moisture is lost under the ITCZ (as is a natural result). Following diagram number , it can be noticed that the transport of moisture from the Caribbean (associated

to the CS) is mainly driven by the component of the easterlies, featured during winter for the secondary maximum of the CLLJ which in this period is turned south-west. As the intensity of the wind is strong, part of the moisture is able to reach to the Pacific following the structure of the airflow. The southeasterly flow over the ETPac has a modest intensity that is even more decreased by the presence of the easterlies. The interaction between this two fluxes results in the inhibition of moisture from the ETPS to reach Central America. Moreover this region where the wind converges is under the ITCZ, which at this moment is at its southernmost position. Moisture being transported from the ETPS has then two barriers, the easterly flow and the ITCZ. Most of the moisture transported from NSAS precipitates in the way to Central America and when the air reaches the contribution is small since air is drier as has left moisture over the ocean. During spring, the reduction of the easterlies is responsible of the moist air from the CS to circulate over Central America and not being able to go further, the ITCZ is moving northward and the CLLJ is not a barrier anymore for the low level flow from the south. The intensity of the easterly flow is such that moisture from NSAS is also transported and Central America becomes the region over which moisture flux from several directions converge, increases the probability of precipitation and with it the recycling of moisture which is also an additional source of moisture. This situation suggests the increase of precipitation during spring as is observed to happen.

During winter, the results from chapter 5 indicated that the intensity of the CS is decreased while the ETPS is increased significantly compared to the previous months. The trajectories show an important increased in the uptake of moisture over the ETPS which results in moister low level winds, uptake of moisture also increases over the Caribbean despite the reduction observed for CS. The picture now is different, during summer the ITCZ is at its northernmost position (reduced or no influence over the ETPS), the CLLJ is at its maximum intensity (uptake increases as a result of drag) and the northward branch of the CLLJ is developed. As the winds turn north, moisture from the Caribbean moves with the wind away from southern Central America, reducing the contributions. Moreover, the air flow from NSAS is coupled with the CLLJ and transport to Central America is reduced from this source. The results suggests the decrease of moisture transport from the Caribbean and for instance of the contributions to precipitation. Since the winds are turned in the opposite direction, the interaction between

the easterly flow and the southwesterly flow does not occur and the intensified wind from the Pacific is able to transport the moist air (notice uptake has increased) to Central America. The structure of the CLLJ during summer indicated that over southern Central American Caribbean coast a region of low level convergence is developed. This convergence pattern and the effective transport from the ETPS explains why southern Central America is less affected by the MSD. Precipitation during summer is basically constrained to the small contributions from the CS and the larger contributions from the ETPS, so that the ETPS leads summer precipitation during summer. In autumn, the easterly flow is a minimum, moisture transport from the ETPS account for big part of precipitation since winds are still strong. During this period the cyclone genetic activity has increased and those systems become to control large part of the observed precipitation. Transport from the inner Caribbean is suppressed but increased from the outer Caribbean, as this moisture is transported quickly by the cyclonic systems.

## 7.5 Chapter highlights

The 'origin' of the air masses that provide moisture for Central America was determined, with most of the flow coming from the Caribbean Sea. The application of the clustering algorithm described in chapter 4 enabled us to reduced a huge amount of data into reduced sets of clusters containing the mean information of the trajectory followed by the air particles. The structure of the transport was analysed in a climatological basis by means of the clusters of trajectories followed by the air parcels. This structured revealed a dominant component of the low levels winds as moisture conveyors. The efficiency of transport was determined to be associated with the intensity of the winds but also with the increases of moisture along the trajectories via uptake. The complex process of moisture transport and interaction among the components of regional climate was simplified to be presented in a simple conceptual model that contains the most relevant details on the transport of moisture. In addition, the response of the contributions to precipitation to the modes of variability was analysed taking also into account the effect of the variations in the amount of air transported from the evaporative sources as well to the effect of a key moisture modulator structure, the CLLJ. The results suggest that in some cases the variations of the relative contributions to precipitation are strongly related with the variability of the amount of air transported whereas in some other cases

the variability in the content of moisture is more important. The interpretation of the interannual variability of the precipitation associated with the transport of moisture is quite complex as the same mechanism may be able to modulate both the transport and the moisture content of air particles. As feedback between the mechanisms becomes more active, the more complex is the system. Despite the high non linearity, some directly linear relationships were found to be useful in the simplification of the problem. The latter may allow us to focus on determined processes that lead to the variability of the regional water cycle. This is of particular importance and it can be used to identify determined structures that need the major improvement in climate modelling to obtain a better representation of the precipitation in the IAS region. Furthermore, these results encourage the use of the applied methodology for other complex regions within the tropics such as the convergence zones and the monsoon-like circulations. In the particular case of Central America, the mechanisms described enable us to pinpoint the key elements that need further study. The CLLJ has become an important element of study in the region, but the results suggest that there is a lot more of interactions with this structure that affect the region in several ways. Following chapter will be focused on providing more detail on the role this structure plays to modulate regional precipitation patterns.



# 8

## Role of the CLLJ in the modulation of the transport of moisture

At the end of chapter two, among the main features of the climate in the IAS region, the CLLJ was introduced. Later, in chapter seven, the importance of low level winds for the regional transport of moisture was highlighted based on the average pattern of the trajectories followed by air parcels that precipitate over different regions of Central America. The presence of the CLLJ was used to explain the predominant features of the spatial distribution of the Caribbean Sea evaporative source of moisture. Moreover, it was indicated the simple process through which precipitation is inhibited in the presence of the CLLJ maximum winds as well as how this structure inhibit the transport of moisture from other sources (in agreement with results from previous studies). Herein we are interested in a more detailed Lagrangian overview of the transport of moisture. Despite the importance of the five sources, we are particularly interested in the transport of moisture from the Caribbean Sea and the role of the CLLJ on its modulation.

## 8.1 The climatological structure of the transport of moisture from the Caribbean

From the vertical structure of the transport of moisture from the 'Atlantic regime', the presence of well defined low level air streams was identified. It was noticed how the influence of these air streams became more important in terms of amount of air particles and moisture as northern the receptor (sink) region was located. The latter is basically a result of the presence of the CLLJ which is responsible for the modulation of the transport of moisture over the Caribbean. A first point to asses is how do the air streams related to precipitation over Central America react to the presence of the CLLJ. Figure 8.1 presents the monthly mean clusters of air streams associated to precipitation over each subregion of Central America with the contours of mean zonal wind at 850hPa. The vertical structure of the clusters (air streams) is shown for the first 96 hours previous to the arrival of the air to the target (where it precipitates). This corresponds to the time in which the air particles undergo the larger moisture changes. During winter the flow is relatively dry and the distribution of the amount of air particles that accounts for precipitation over Central America is quite uniform. During spring, moisture increases along the trajectory of the air over the easternmost Caribbean and the intensification of the moisture uptake is noticed. The moisture uptake increases so that in May reaches a maxima approximately over 75W, which is actually the location of the CLLJ core (in good agreement with the forcing of the winds on oceanic evaporation as indicated in chapter 1). Note that after the February maximum of the CLLJ, winds are decreased at the end of spring a new intensification of the easterlies occurs towards the summer maximum. Moisture uptake is increased by the intensification of the winds and the speed of the wind flow is such that air can travel to the west but not as strong as to force most of the wind to cross to the Pacific. Enhancing the moisture losses over Central America. The wind flow from the east has not yet have a completely develop northward branch. Then, wind still has an important southwestward component that favours precipitation over Central America.

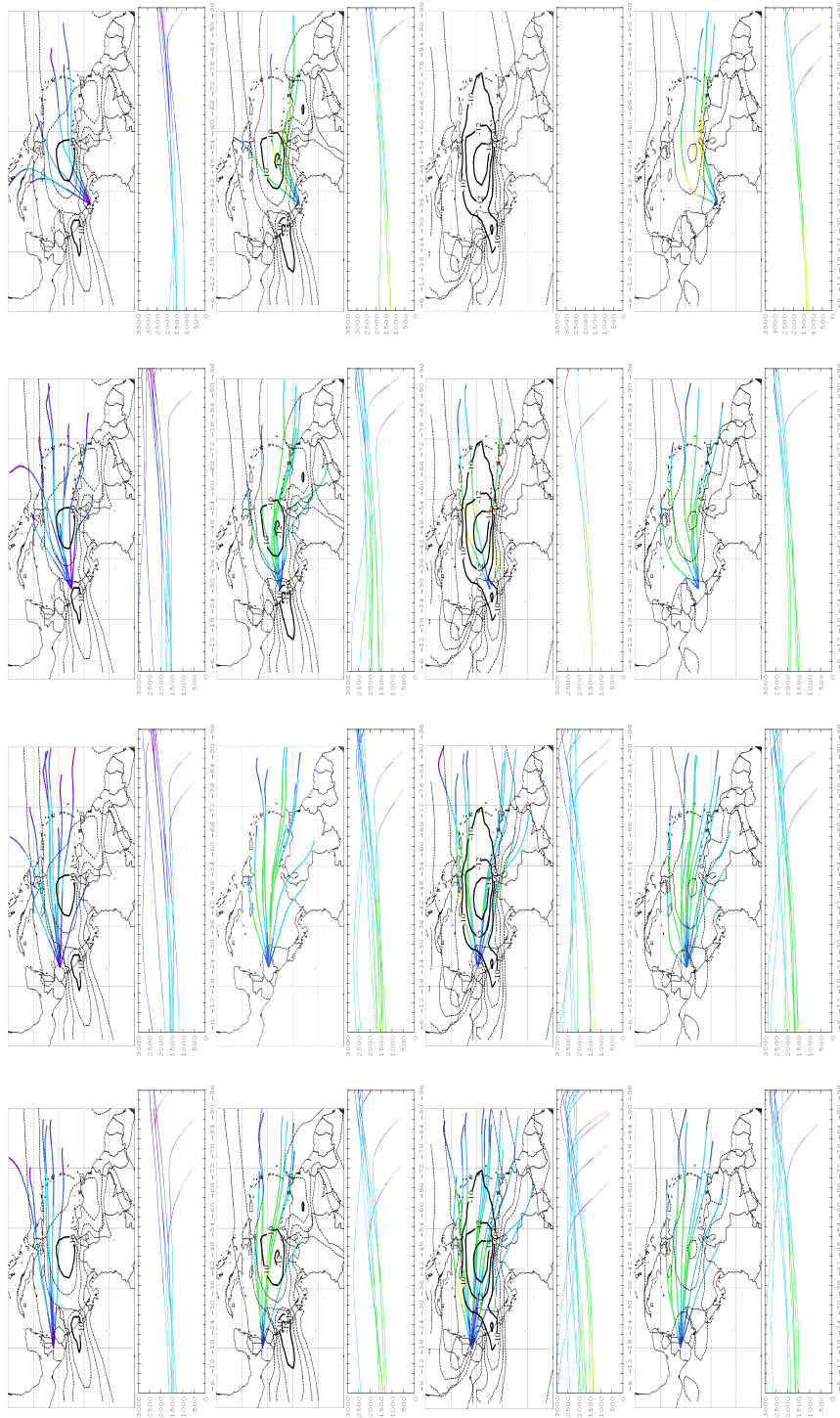


Figure 8.1: Zonal and vertical structure of the moisture transport.

In summer, as the CLLJ intensifies and the northward brach is developed, the distribution of the amount of air particles related to precipitation decreases considerably to the southern target regions compared to the increased observed for those over the northern receptor locations. Moisture uptake maxima is still enclosed by the CLLJ core and is also worth to notice the changes in the vertical structure of the trajectories followed by the precipitating air particles. For spring the moister jet-linked trajectories are below the 1500 m and in summer air has been lifted and is located over this level.

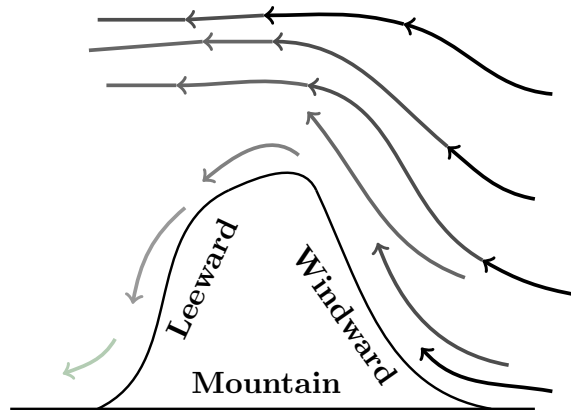


Figure 8.2: Significant correlation pattern between the intensity of the  $(E - P)^{-6}$  field for Central America and the surface wind field.

This is an interesting difference if compared to the flux during the February maxima, the reason for this differences of the vertical structure are a result of the structure of the CLLJ itself. An important detail is that, depending on both wind speed and altitude of the flow, due to the presence of the mountain range in Central America, topographic convection can be forced which implies losses of moisture in the leeward of the mountains (see diagram in figure 8.2). This is associated with the increase in the contributions from the CS. This will correspond to a more intensified magnitude of the  $(E - P)^{-6}$  in the inner Caribbean. This occurs during the February maximum of the CLLJ, with strong very low level winds. On the contrary, during the summer maximum, as was pointed out in previous chapter, the vertical structure of the CLLJ (as followed from the trajectories) indicates the jet to be located at higher altitude. This is that the strong

winds can pass through the Pacific with a minimum interaction with the mountain system so that topographic precipitation is not enhanced as is when the air flow is lower. As indicated in chapter 2 and depicted in figure 2.8.b, during the July maximum the CLLJ penetrates higher in the troposphere. This is important since it may be related to an additional influence of the CLLJ in triggering precipitation. The CLLJ is then related to precipitation not only by transporting moisture between regions but also by forcing variations in the instabilities that lead to the formation of precipitation. Moist air particles that go upper in the atmosphere are strongly related to tropical convection, as upper moist air goes more unstable becomes the layer enhancing convection and the fall of the moisture as precipitation in a sub-saturated environment. This may account for the differences observed in the contributions to precipitation during the two CLLJ maximums, for which even when precipitation is reduced it is still larger for summer compared to winter (as precipitation).

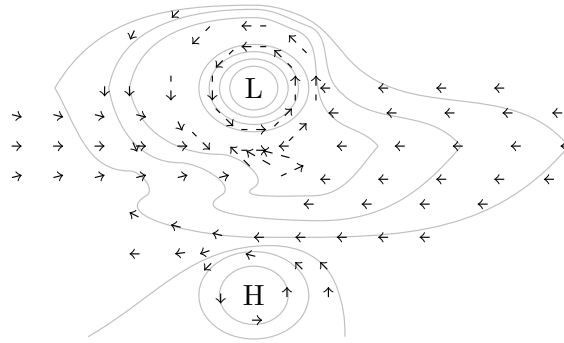


Figure 8.3: Significant correlation pattern between the intensity of the  $(E - P) - 6$  field for Central America and the surface wind field.

During autumn, more air particles are transported to Central America from the Caribbean and moisture uptake occurs over the complete Caribbean Sea. Moreover, the air flows at higher altitudes for the northern Central America regions compared to the southern, for which a very strong flow is observed at lower altitudes in comparison. This wind flow carries important amounts of moisture and it can be observed how the separation of the streams becomes smaller and the moisture larger as southern is located the receptor/sink. This indeed, may not be associated with the CLLJ but attached to the SST gradient between the Caribbean Sea and the ETPac, which exhibits a maximum

during October due to the seasonal cycle of the WHWP as mentioned in chapter 2. The effect of warmer Caribbean SST induces Gill-type heat-induced response (Gill, 1988) (see diagram in figure 8.3), the ETPac westerly winds increases to balance the SST gradient, reducing the intensity of the flow from the Caribbean that enables most of the moisture content carried by the easterlies to precipitate over Central America (see figure 6.2.d chapter 6) (note that low level wind convergence may be enhanced for very strong gradients). This heat-induced response is therefore strongly linked with the sharp decrease of the easterlies that feature the absolute minimum of the CLLJ during October. Note that this thermal driven response of the flow provides a mechanism through which the role of the WHWP can be explained.

## **8.2 A reduced model for the role of the CLLJ as a modulator structure**

A fundamental point here is the position of the analysis region, as the CLLJ develops nearby the equator the geostrophic approximation may not be suitable to describe very local features of climate. From the structure of the CLLJ, it can be followed that a south(equator)-ward component is developed which remarks the importance of considering the problem of the non geostrophic component of the flow. The two components of the non geostrophic wind play a role for determining the locations over which divergence (convergence) is enhanced or not. The basic dynamic assumptions lead to an approximate representation of the patterns of convergence and divergence produced by the variations in the intensity of the wind for low level jets. Those patterns are produced by the cross stream component of the non geostrophic wind as a result of the accelerations (decelerations) of the wind flow at the jet entrance (exit) region (REF). Upper level divergence is enhanced by strong along streams variations in the flow since the along stream component presents an effect on the convergence and divergence patterns due to curvature. The combined effect is the enhancement of the upper level divergence in the right entrance and left regions. This as discussed in Amador (1998) implies a pattern of convergence (divergence) in the rear (front) to the left of the jet axis and the opposite pattern to the right of the jet axis, as summarised in figure 8.4. In the case of the CLLJ this assumptions lead to an explanation of the differences observed in the distribution of precipitation over Central America between the northern

and southern regions. This reasoning as proposed by Amador (1998), following the representation of the cross circulations. The importance of this relies in that it provides a dynamical framework that can be used to explain the role the CLLJ has for transport moisture as potential modulator of precipitation and the activity of the neighbor sources of moisture by these convergence/divergence patterns attached to it.

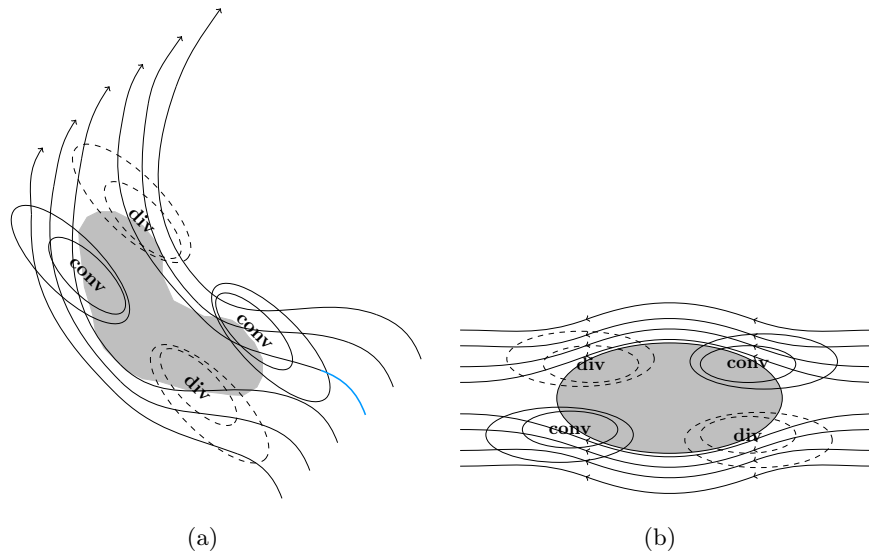


Figure 8.4: Significant correlation pattern between the intensity of the  $(E - P)^{-6}$  field for Central America and the surface wind field .

By analysing the mean wind fields, SST, mean clusters of trajectories and their correspondent moisture changes and vertical velocity (see figure 8.5) a simplistic model to describe the main features of transport of moisture to Central America due to the CLLJ in terms of regional climate features is proposed. The idea of this simplification is to provide a general notion of the most important mechanisms that interact to determine whether the moisture transport via the CLLJ results in increases/decreases of precipitation over the region. For the months in which the CLLJ is more intense different different scenarios can occur: a) winds can be very strong, the structure of the CLLJ is well defined and most of the moisture goes directly to the Pacific side, b) CLLJ intensity is not so strong and moisture can be lost over Central America (similar as occurs when the wind flow interacts with local topography), c) easterlies are very small and moisture is not even able to reach the Caribbean coast of Central America.

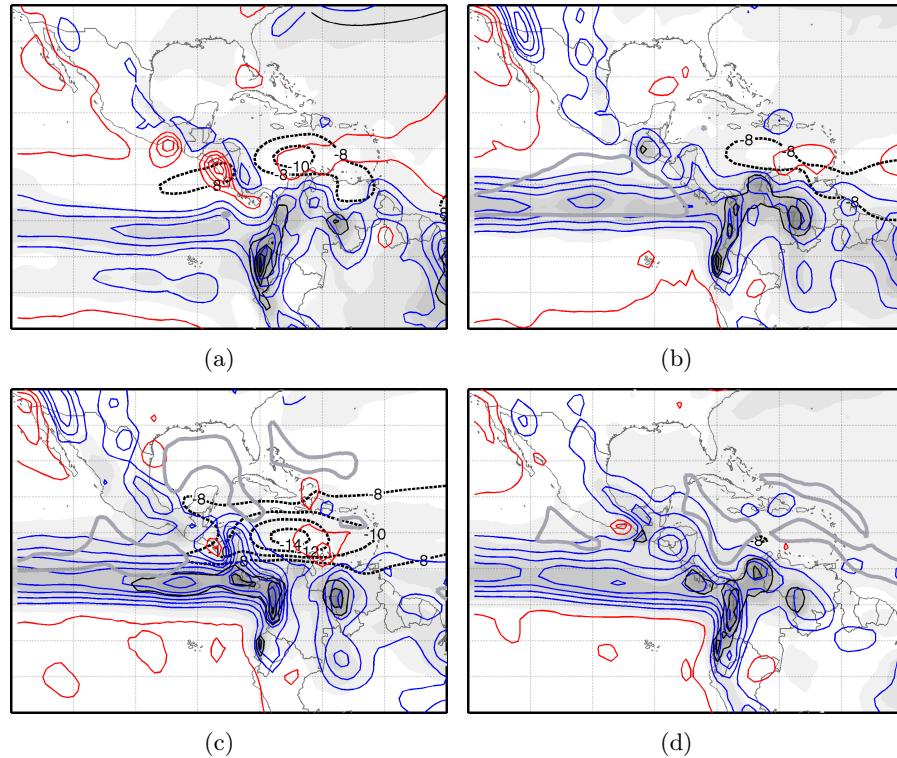


Figure 8.5: Significant correlation pattern between the intensity of the  $(E - P)^{-6}$  field for Central America and the surface wind field.

For the first two cases, an additional mechanism must be taken into account, the SST gradient between the Caribbean and Pacific. And a generalisation can be proposed so that: a) Very strong CLLJ, with winds higher than 15 m/s (despite the direction of the SST gradient between the Caribbean and Pacific) results in most of the moisture being transported directly towards the Caribbean (fig 8.6.a), b) CLLJ is intense and the SST gradient points to the Pacific, this results in an even strengthened CLLJ and most of the moisture passes through the Pacific (fig 8.6.b), c) The CLLJ is strong and the gradient between the two ocean basins is almost zero, some of the moisture transported from the Caribbean Sea can contribute to precipitation (fig 8.6.c), d) CLLJ is intense and Caribbean is warmer than the Pacific, this results in a decrease of the winds that enhance the transport to Central America, where precipitation due to contributions from the CS is increased (fig 8.6.d), e) the easterly flow is not strong and the SST gradient indicates a warmer Pacific, a thermal forcing accelerated the easterly flow moderately and



transport of moisture to Central America from the Caribbean is enhanced (fig 8.6.e), f) As in e but for a bit more intense winds, moisture transport is enhanced and if the conditions for triggering convection are favourable, the contributions to precipitation from the CS are increased (fig 8.6.f), g) the easterly flow is slower and no important gradient between the Caribbean and Pacific SST is observed, this situation implies that no thermal forcing accelerates the winds and moisture transport will depend solely on the wind speed so that its is between 8 and 12 m/s the transport is enhanced (fig 8.6.h), i) wind speed is between 8 and 12 m/s and the SST gradient points towards the Caribbean, a decrease on the easterlies is the responsible for the decrease in the transport of moisture. It is important to point out that whether the intensity of the easterly flow is very strong or not is determined by a threshold wind speed that according to the mean fields for the analysis periods can be set to approximately 12 m/s.

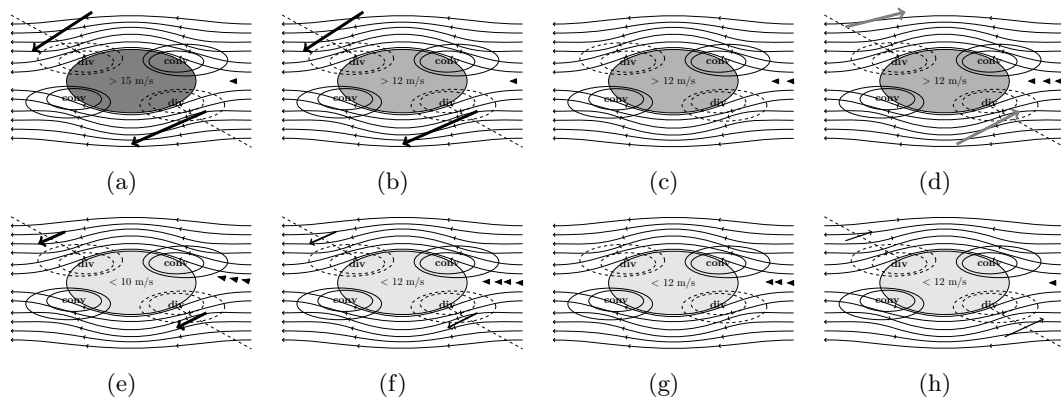


Figure 8.6: Sketch providing a summary of the conditions of the intensity of the CLLJ and the SST gradient between the Caribbean and ETPac that trigger the major changes in the transport of moisture from the Caribbean and associated precipitation.

Note that even when this is not a realistic model of the regional processes and does not account for all the scales of transport, provides a good approximation for evaluating both the mean state of the sources of moisture, transport and associated precipitation. Moreover, it may be useful to determine how changes in the wind and SST conditions can influence the components of the regional cycle.

### 8.3 The CLLJ as moisture transport and precipitation patterns modulator

Once the mean structure of the transport of moisture from the Caribbean Sea (and even the NSAS) was presented and the mean structure of transport due to the CLLJ under the influence of the variability modes introduced, we are interested in analysing further details on the role the CLLJ may play. At the end of previous chapter, a simplified model of the transport of moisture in the region was presented which shows the interaction between some of the regional climate structures. Meanwhile in the present chapter the CLLJ was determined to be associated with the efficiency of the transport and moreover with the spatial structure and the amount of uptake. These results derived from the trajectories suggests that the structure, then the intensity of the CLLJ plays a major role in the transport of moisture. Here we present the analysis of the mean features of the CLLJ contrasted with the results of the sources of moisture in order to identify if there are any reliable variability patterns that may match between the two spatial structures. The analysis of the mean fields for both parameters do not provide us the required information to evaluate the relation from a dynamical point of view, since we are more interesting in advertising how variances between both may be associated we used composites for the positive and negative phase of the studied signals. This to provide a further explanation to the results described at the end of chapter 5 in terms of the dynamics of transport lately discussed. The  $(E - P)^{-6}$  fields, zonal wind speed and vertical velocity at 850hPa were used for this analysis, composites were computed as described in chapter 4. Vertical velocity is used to identify the convergence/divergence patterns associated to the structure of the CLLJ and evaluate how is it associated with the evaporative sources by modification of the divergence/convergence regions.

In the case of ENSO, it can be noticed how a positive phase weakens the February maxima (fig 8.7.a) and the convergence associated to the left of the jet core does not develop. This may result in the absence of precipitation in the Caribbean coast of Central America since divergence is increased. This pattern follows during the rest of winter and part of spring. The latter in good agreement with the known effect of the CLLJ to decrease rainfall maxima of May during positive ENSO (fig 8.7.b). This pattern is reversed and during negative ENSO the convergence occurs as a result of the

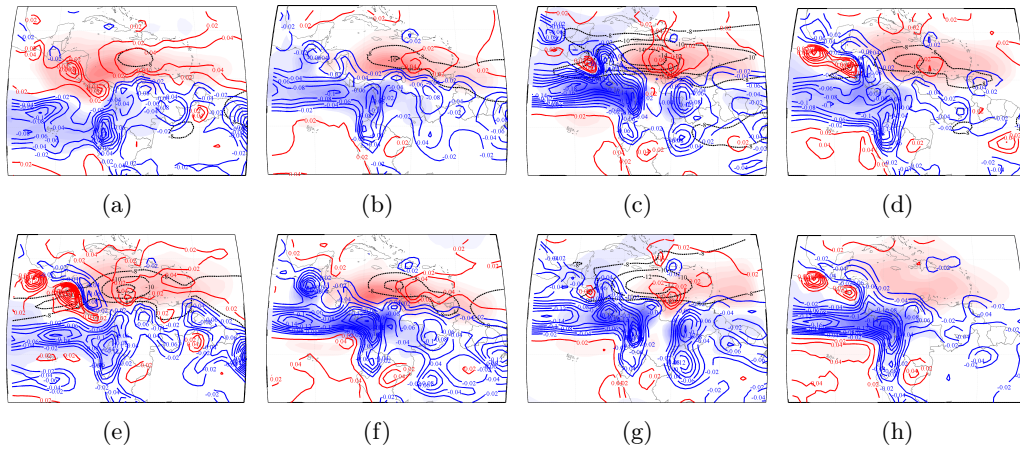


Figure 8.7: Analysis of transport of moisture for ENSO.

intensification of the intensity of the jet (fig 8.7.c). Note that in May the evaporative source in the CS is decreased compared to the negative phase (fig 8.7.f). This results from the decrease of the jet intensity and to the small gradient between the CS and the ETPac. During July (fig 8.7.c) the situation is reversed to that of February, due to the development of the northward branch, the divergence/convergence structures are also curved and during the negative phase the intensification of the jet increases the convergence, probably as a result of the westwards bifurcation.

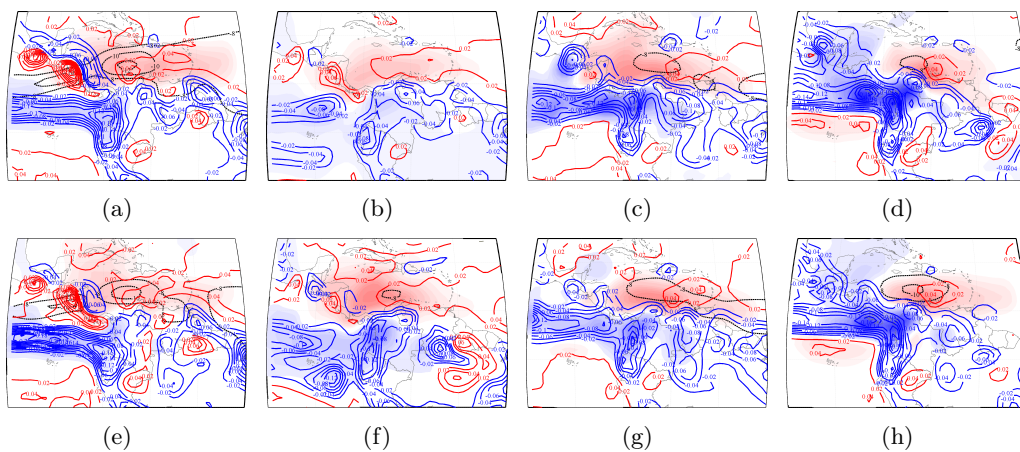


Figure 8.8: Analysis of transport of moisture for NAO.

Under the influence of NAO a weaker CLLJ is observed during February for the negative phase (fig 8.8.a) while a strengthen for the positive phase (fig 8.8.e). As for ENSO, a stronger jet is related with a well defined of the convergence/divergence patterns associated to the presence of the CLLJ. From which the convergence indicates (as is also observed and known from observations) that precipitation increases over this region. The intensification of the easterly flow during spring, linked to the negative phase favours the intensification of the CS.

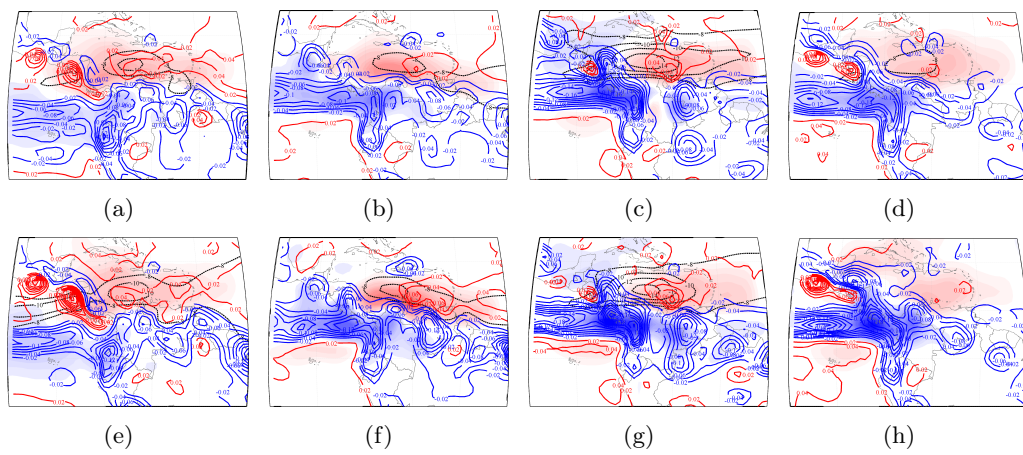


Figure 8.9: Analysis of transport of moisture for PDO.

The case for the PDO shows little evidences of variations, the component of the Caribbean seems to be not very sensitive to this mode as does the SST in the Pacific. However, it can be noticed in figures 8.9 that the positive phase of the PDO is associated with divergence over Central America (particularly over the Pacific coast) and more convergence during the negative phase. This is in agreement with the findings shown in chapter 5, when it was indicated that the contributions from the ETPS experienced a significant decrease during the first part of the 80s, a period by a positive PDO.

During February when the MJO is in a positive phase, the jet is increased and as a result the convergence pattern with a similar pattern for negative phase during July in which the bifurcation of the jet occurs and seems to have an effect joint with the increase of the flux from the ETPac due to the ascent to the GoM. The negative phase is associated with the intensification of the mentioned patterns as the the wind flow that characterises the jet is more confined. This implies that the presence of the CLLJ

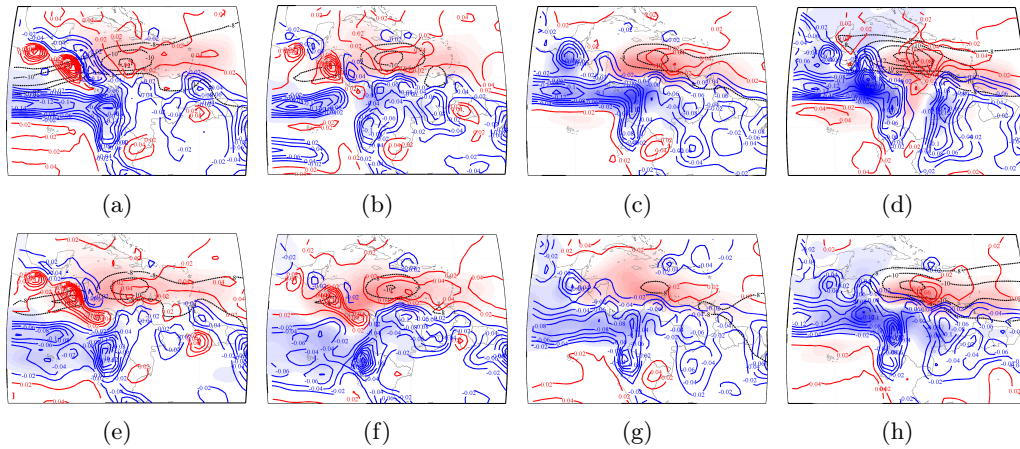


Figure 8.10: Analysis of transport of moisture for MJO.

and convergence associated over the Caribbean coasts of Central America is useful to explain heterogeneity of the regional precipitation patterns.

In general terms it can be said that the strengthen of the CLLJ intensifies the convergence over the eastern Central American coast. This is associated with the increase of precipitation to which moisture transported from the central Caribbean contributes. Note that what defines the convergence/divergence patterns in the Caribbean and Central America is basically the structure of the CLLJ as given by the simple dynamic considerations of the cross circulations (represented in the graphics by the vertical velocity at 850hPa). The superposition of the CLLJ intensity and vertical velocity altogether with the E-P field illustrates quite well how the CLLJ influences the structure and intensity of the evaporative source of moisture in the Caribbean and the relation this has with the cross circulation pattern. As noticed from the cases describes before, there are some cases, especially during spring, when the presence of intensified easterlies do not set the complete background for describing the intensity and extension of the source, as well as the efficiency of transport. It was mentioned that the SST gradient between the Caribbean and the ETPac region was determinant in those cases. Moreover, the gradient is in part a measure of the activity of the WHWP. Based on the results obtained and the discussions, a conceptual model for the distribution of the evaporative source of moisture over the CS as it accounts for precipitation of Central America is proposed.

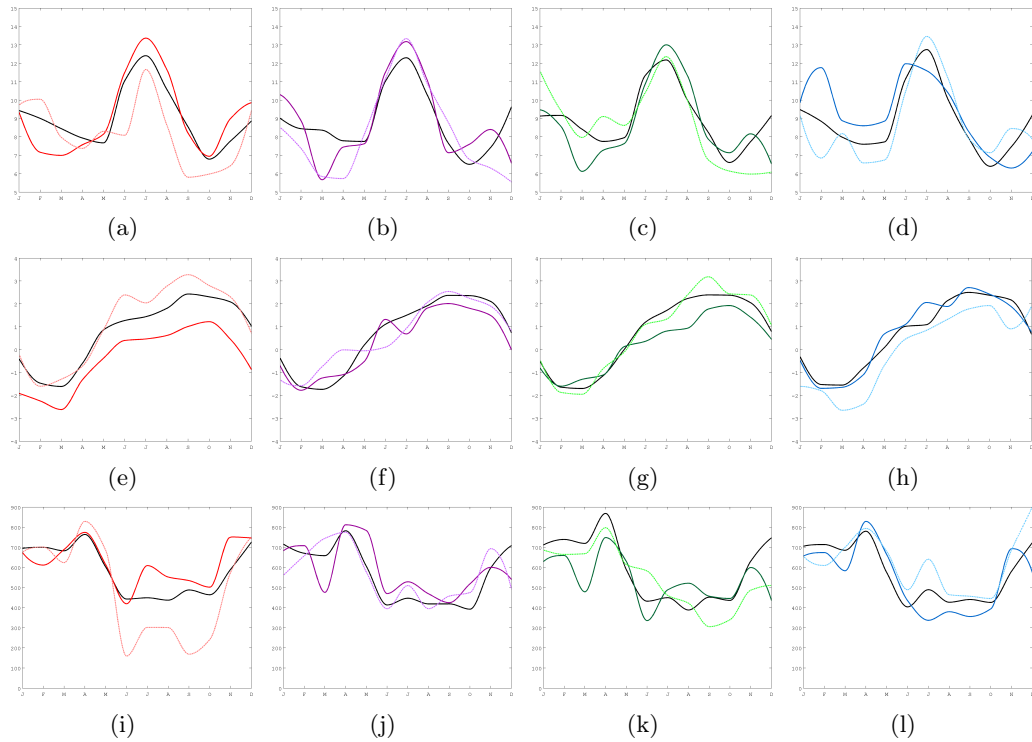


Figure 8.11: Indices for the intensity of the CLLJ, SST gradient and conditional  $(E-P)$ -6 over the Caribbean Sea for the positive and negative phases of ENSO, NAO, PDO and MJO.

A definition of the CLLJ intensity through an index as defined in chapter 4, the SST gradient between the Pacific and the Caribbean Sea and the total integrate of the backward conditional  $(E-P)^{-6}$  for the Caribbean Sea for the neutral years as well as for the positive and negative phases of the variability modes is used to identify the pattern that defines the transport of moisture from the Caribbean Sea and Central America. It has been shown how the major changes occur, as is expected, during the months when precipitation over Central America presents both maximum and minimum values. During the periods in which the CLLJ is a maximum, the transport is directly driven by the jet. Convergence and divergence patterns associated with the jet axis are key to define the horizontal extension of the regions that may contribute as sources and of those in which low level convergence is enhanced and associated to precipitation. Whereas during those periods in which the CLLJ is not the dominant feature variations in the transport of moisture are triggered by the SST gradient between the Caribbean and

the ETPac. As the difference between SST in the Caribbean and the Pacific becomes more positive. The contributions from the CS drops meanwhile the fall of this gradient in favour of a warmer ETPac enhance the increase of the transport. More importantly, a CLLJ intensity of the order of 12 m/s seems to be the threshold to determine when the CLLJ allows moisture to be transported to Central America. For larger values of the CLLJ intensity, moisture from the Caribbean is directly transported to the Pacific side (or northern to the Gulf of Mexico). This reduces the direct transport to Central America. Conversely, under this value the role of the SST gradient becomes important in determining the features of transport.

## 8.4 Modulation of the moisture transport, CLLJ and variability modes

In chapter 5, the effect of ENSO, NAO, PDO and MJO on the spatial distribution and intensity of the sources of moisture was described. In general, the largest variations were observed for the CS which suggests a large variability of this source of moisture. Even when the ETPS also presented important variations, herein we will focus on how do the variability modes affect the transport of moisture from the Caribbean Sea.

First of all, it is important to mention that since we are interested in the complete representation of the response of the backward trajectories, instead of computing composites, the most extreme phase of each considered variability modes were selected. We want to make clear that this is not directly comparable to the anomalies presented in chapter 5, even when the main structures of the changes forced by the modes is. Those months with most extreme values for each correspondent phase were selected for the comparison, this in order to compare a strong negative with a strong positive phase for each mode to show the contrast . Instead of using clustering to reduce the dataset for the cases, we preferred to make a selection of the particles to isolate a particular transport associated structure. The easterly flow was selected as moisture conveyor structure, with special attention to the CLLJ. For this reason, from the total of particles, those that lost moisture over the receptor/sink subregions in which Central America was divided were selected. Those associated to the clusters that circulate from the Caribbean and along the time their trajectories were below 2500m were extracted. After this, another selecting condition was imposed, those particle that have circulated

at any time over the region of influence of the CLLJ were considered as associated to the main easterly flow that features the CLLJ (as indicated in chapter 4). After the selection process, the particles that were at any time associated with the CLLJ when active or with its influence region when inactive were retained for the analysis.

## **ENSO**

We are interested in the months where precipitation becomes more important as well as the transport associated structures. Since larger variations were found to occur for February, May, July and October, the discussion will be focused on these months. In order to consider the variables of geopotential height, SST differences and the intensity of the CLLJ, the indices defined in chapter 4 are summarised in figure 8.11. For the case of ENSO, during the warm phase of February 1983, a reduction of the winds is noticeable that enhances the efficiency in the transport of moisture to Central America. Due to the structure of the February maxima, the major transport occurs towards CRP and decreases as the sink is located north (8.12.c). During the negative phase (1989), the CLLJ is intensified so that less moisture is transported to Central America. The identification of two air streams at different heights implies that stronger winds during this month enhance the downward transport of drier air. The positive phase is associated with an increase in the geopotential gradient while the opposite occurs for the negative phase at the same time that SST is warmer over the ETPac. During May, the results suggest an intensified moisture flow from the Caribbean to CRP for the positive phase of 1992 (fig 8.12.g) for which the uptake region is located over the complete Caribbean basin opposite to the negative phase of 1988 when the amount of transported trajectories is smaller. The pattern is similar to February and the transport decreases northward (figs 8.12.c, 8.12.f). During the strong warm ENSO, July (1997) the CLLJ is significantly intensified by the rise of positive SST anomalies over the ETPac that induce a strengthening of the easterlies, therefore, of the CLLJ. This results in a marked decrease of moisture transport from the Caribbean Sea that is particularly sharpened for Nicaragua (fig 8.12.k). This result is remarkable since this decrease may be related with the presence of drought conditions for this period over Central America as indicated by the mean PDSI, which is higher for Nicaragua (see figure 8.13). During the cold event of 1988, the decrease of the intensity of the CLLJ is associated with the



intensification of the transport. During October, ENSO seems to be an important influence in the variations of precipitation between the different regions of Central America. Warm ENSO favours the transport of moist air to the north while the cold phase does for the south. As the intensity of the CLLJ is more reduced than normal for the cold phase, the transport is enhanced and moreover the uptake of moisture occurs over a more extended area of the Caribbean and beyond the Lesser Antilles, as suggested by the anomalies composites of the E-P field for cold ENSO during summer.

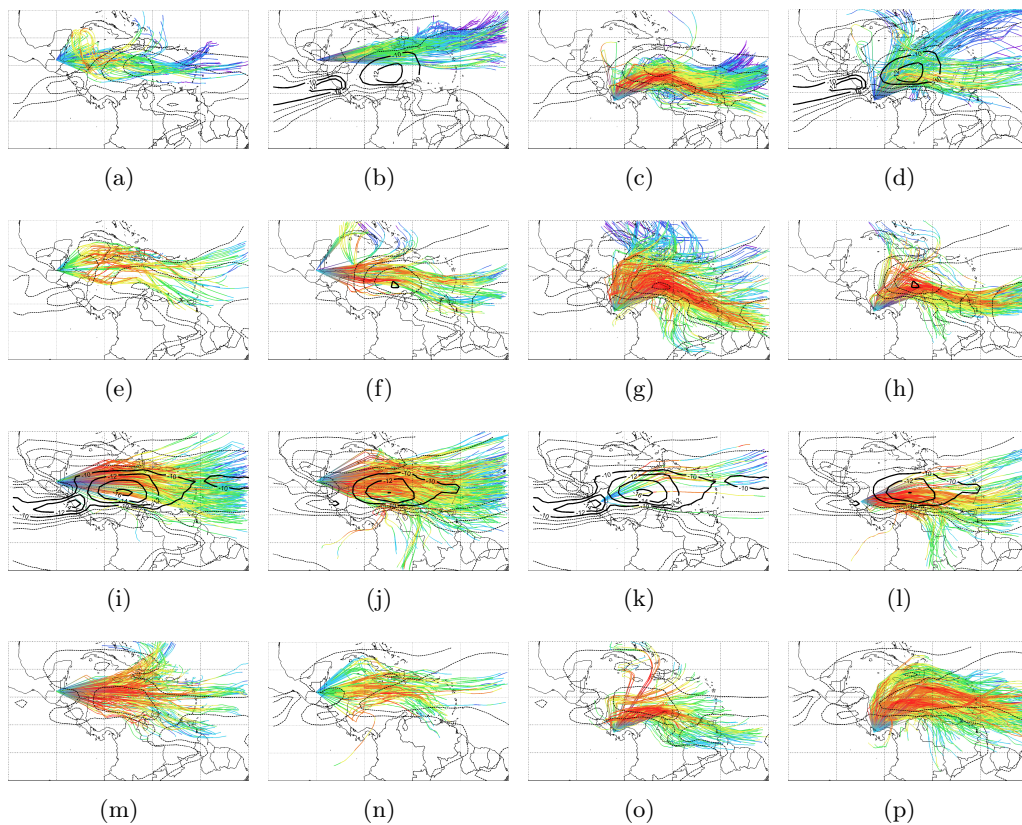


Figure 8.12: Analysis of transport of moisture for extreme ENSO.

The influence of NAO is more related to the structure of the flow rather than the amount of moisture transported for February, even when the air is drier during the negative phase (1986) (fig 8.13.d). An interesting observation is that for the positive phase of 1989, the flow that reaches Nicaragua presents a well separated structure of drier upper level flow and moist low level flow (fig 8.13.c). A strong intensification

of the transport of moisture is noticed with strong uptake over the Caribbean (more intense as southward) and with an increase of the moist flow from NSAS being transported by the easterlies associated with the CLLJ core location (fig 8.13.g, 8.13.h). For the negative phase the decrease of the transport efficiency that lead precipitation over Central America is associated with the intensification of the easterlies. During July, the results suggests that few influence of the NAO is exerted to the wind flow (as expected since the major variations may be associated to winter since is a winter time structure). Transport is slightly larger for the negative phase . In October, a small intensification of the easterly flow is associated with the reduction of the moist flow contributions to precipitation over Central America (fig 8.13.o).

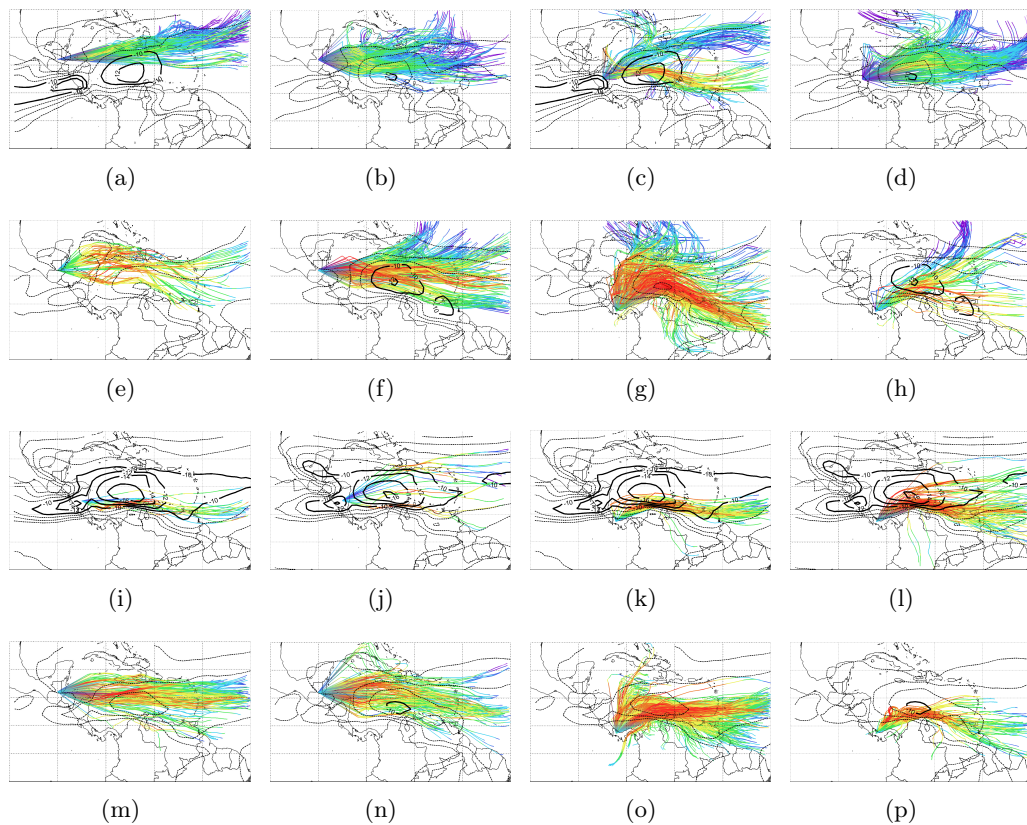


Figure 8.13: Analysis of transport of moisture for extreme NAO.

The influence of the PDO alter both the moisture content transported and the direction from which the flow is travelling. During the positive phase of February 1987,

dry air from the Caribbean and the Gulf of Mexico rise its moisture content in from of Central America coast to precipitate in the following 24 hours over Central America (fig 8.14.a, 8.14.c). Whereas during the negative phase of 1991, the CLLJ was intensified and transport decreased (fig 8.14.b, 8.14.d). During May, for the positive phase of 1996 the transport is increased and the structure of an early CLLJ is noticed. As the intensity increases but is not as large as to force all the air to pass to the Pacific, the transport of large amounts of moisture is very efficient, particularly to CRP (fig 8.14.g ) compared to the situation of the negative phase of 1999. Beyond the earlier development of the CLLJ, a southward branch is well defined and moisture uptake takes place along the southernmost Caribbean (figure). During July, an enhanced CLLJ is noticed for the positive phase (fig 8.14.j). A bit larger transport for the positive phase of 1983 for the northernmost part of Central America and for CRP with less transport for the HS region and particularly reduced transport to Nicaragua, which is actually almost null. This may be associated with the 'bands' that divided Central America into very dry and moister regions. The case of the dramatic reduction of the transport to Nicaragua corresponds again to a severe drought event . It can be concluded in this case, that drought conditions over Nicaragua are strongly forced by the decrease of the transport of moisture from the CS . Finally, during October, the positive phase of 1997 presents stronger transport of Central America (fig 8.14.m) and reduced for CRO (fig 8.14.o) while the negative phase of 1999 presents the opposite pattern and the transport to CRP is stronger compared to the positive phase when is very small (fig 8.14.o, 8.14.p).

The structure of the sources of moisture suggests that for positive (negative) MJO phase, there is a decrease (increase) on the intensity of the inner Caribbean as a source of moisture for Central America, as is observed from the structure of the flow for February. This is associated with the strengthen of the CLLJ during positive MJO (1985) that lead to stronger winds and less contributions to precipitation (fig 8.15.a, 8.15.c). In comparison the CLLJ is decreased during negative MJO of 1980 and moisture transport if intensified towards Central America, with an important southward component that increases the transport to CRP (fig 8.15.d). The positive MJO of May 1990 is associated with an intense earlier development of the CLLJ. The earlier developed northward branch results in the reduction of the transport of moisture to southernmost Central America (fig 8.15.g). Conversely, the transport is greatly intensified during the negative

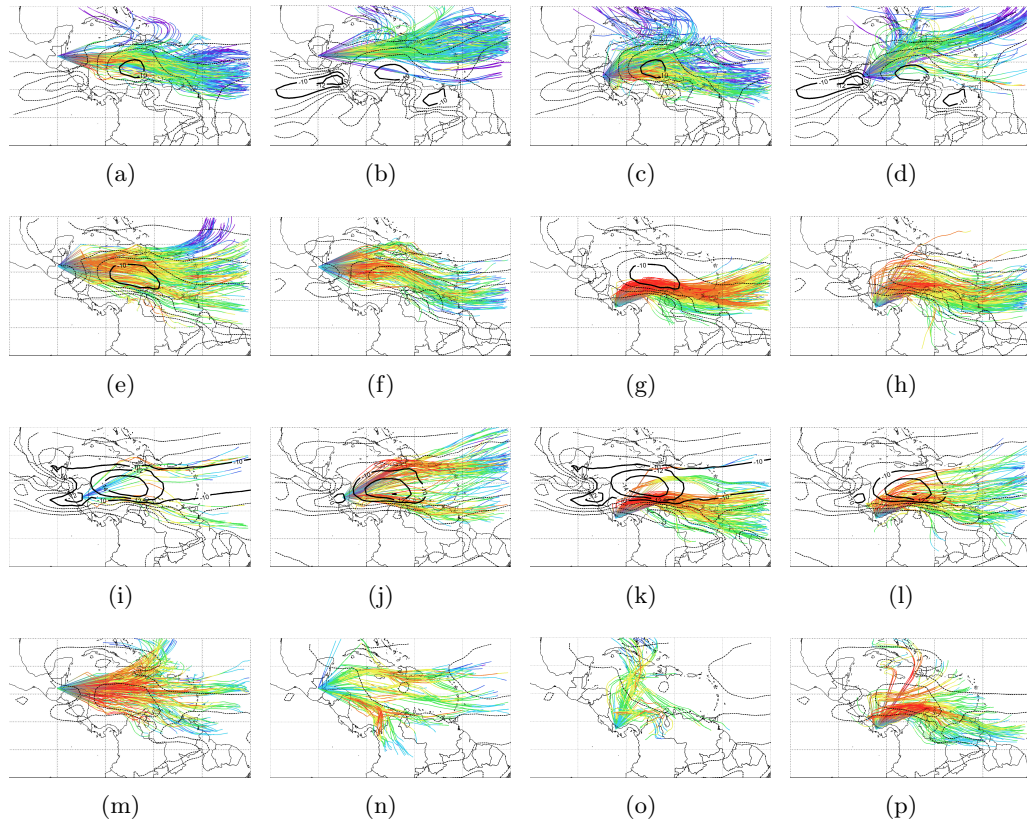


Figure 8.14: Analysis of transport of moisture for extreme PDO.

phase of 1983, for which moist air comes outside the Caribbean (the source is extended to the tropical Atlantic<sup>1</sup>). This phase event was characterised by the presence of an anomalous cold tropical Atlantic. During July, for the negative MJO of 1987, a very strong intensification of the flow undergoes, however, its effect is not the suppression of transport to Central America completely but the funneling of the winds. Note that intense moisture increases are observed below the axis of the jet in agreement with the enhancement of divergence to the left of the axis of the jet in the front. Meanwhile a relatively uniform distribution of the transport is noticed for the 1981 positive phase (figs 8.15.i-l). During October, the positive phase of 1999 is featured by small transport of moisture from the Caribbean Sea by the easterlies with an even more reduced transport

<sup>1</sup>the importance of anomalous SST over the tropical Atlantic has been studied by Kucharsky et al., 2010.

to CRP (fig 8.15.o). This results in a more reduced than normal easterly flow during October. On the other hand, for the negative event of 1997 an increased transport is observed, note that this corresponds to a warm ENSO related event, which implies winds intensification. Since winds during October are very reduced, the intensification due to the warm phase of ENSO may help to favour the transport to Central America. It is also important to note that under the positive phase, the flow from NSAS is able to reach northernmost Central America after gaining moisture over the Caribbean Sea.

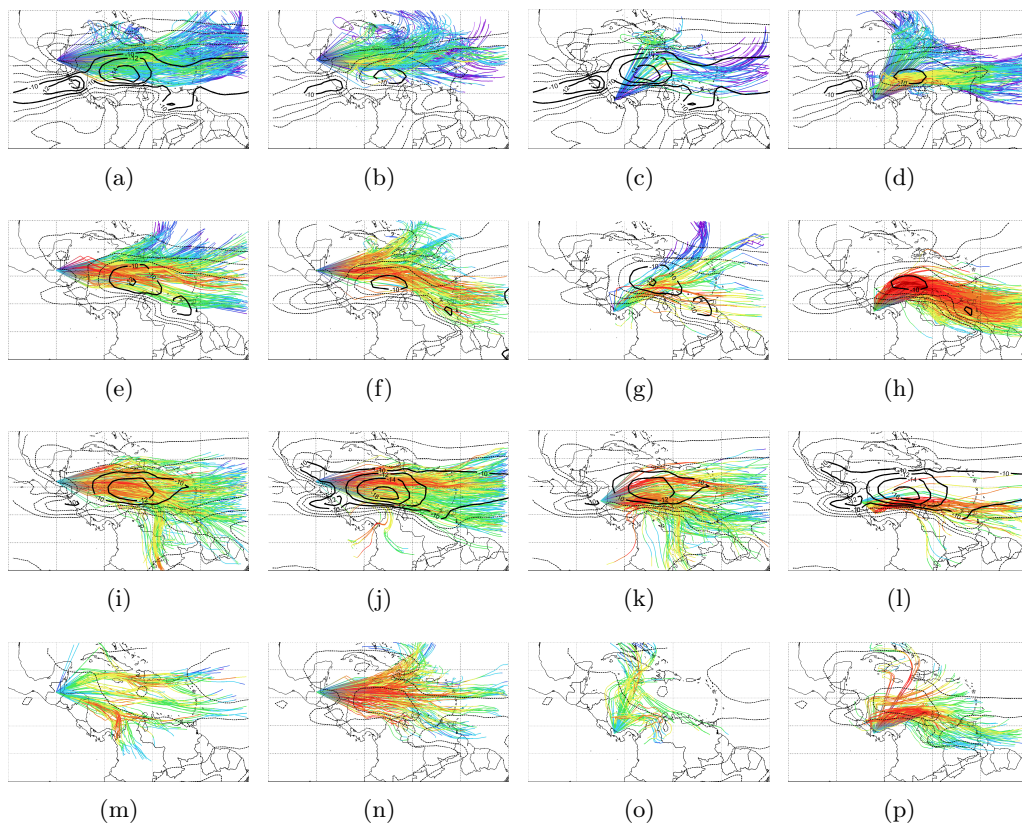


Figure 8.15: Analysis of transport of moisture for extreme MJO.

The results shown in figure number allows to compare directly if the simplified model proposed in previous section is able to reproduce the mean response of the intensity of the moisture source to variations in the intensity of the CLLJ <sup>2</sup> and the SST gradient between the Caribbean and Pacific. It can be followed that in most of the cases, the

<sup>2</sup>Easterlies over the same region of the CLLJ for those months in which the CLLJ is not active.



results provided in figure 8.11 can be predicted by the simplified model. Which suggest that the performance of the model for evaluating mean conditions under determined circumstances is reasonably good. However, there are some cases in which the expected response of the source is found to be delayed compared to the observed. This differences, which are too few, are normally associated to those cases in which the intensity of the CLLJ is stronger than 14 m/s. Here we detect that when the CLLJ is very strong additional interactions need to be considered. Our proposal is that the response may be found in the vertical structure of the CLLJ. Indeed, those cases in which winds are stronger than 14 – 15m/s and the results observed in the average do not agree with those predicted from the model correspond to cases in which the vertical structure is modified. For very strong easterlies (larger than 14–15m/s) in which the flow is confined to the lowest levels (below 1500m) the contributions from the source to precipitation are increased. This because topographic convection (fig 8.2) is enhanced so moisture transported from the Caribbean is more able to precipitate over Central America.

### **Precipitation associated to the transport of moisture, role of the CLLJ and response to variability modes**

The complexity of the interactions that take place in the IAS region are clear at this stage of the work. Despite the non-linearity of the climate system, determining the most direct linear relationship between different parameters may allow the identification of key connections between processes that may help to understand more complex interactions. Along this chapter, the role that the CLLJ plays as a moisture transport modulator structure, as well as its importance by increasing evaporation and convergence in the region have been discussed. To finally try to close the picture of the relationships between evaporative sources of moisture, transport and precipitation at different time scales, we would like to present a final discussion on the response of precipitation associated with the transport of moisture from the remote moisture sources. On the value of the work performed and as an additional contribution, we would like to establish a linkage between precipitation due to transport of moisture and the role of the CLLJ analysed from the perspective of the response of these three components (precipitation, moisture transport and the CLLJ) to the variability modes. Scatter plots were constructed for these three parameters in the same way as indicated in chapter

6, in order to make as clear as possible the picture of how the parameters respond to ENSO, MJO, NAO, PDO and the WHWP. In addition, slices of the zonal component of the wind and relative humidity along the CLLJ core position (75W, 12N) were obtained from the composite averages for positive, neutral and negative phase of each variability mode, in order to also show how the response of the structure of the CLLJ may have an impact on the other parameters.

Under the effect of the ENSO mode, the transport of moisture to CRP from the CS has the largest impact during late Spring, with the amount of air particles increasing as the easterly wind flow intensifies for warm ENSO (fig 8.12.a) corresponding the increase of air transported from the source with the intensification of the contributions to precipitation from this source. In this case, an increase of the contributions to precipitation from CS to CRP results from the increase of air transported. During April, the result found is different, in this case the largest response is noticed for the transport from the GoMS (fig 8.12.b). The easterly flow decreases this month for warm ENSO and increases strongly during the cold phase, when its vertical structure denotes an intensification of the flow at higher altitudes compared to the neutral and warm phases. For the transport from the GoMS, the role of the trade wind is to reduce the flow towards the south, so that the amount of air particles travelling from the GoMS is reduced (increased) for warm (cold) ENSO. However, there is no net increase of associated precipitation to this source as the amount of air transported increases, on the contrary, contributions to precipitation are reduced for warm ENSO. This result implies that the air particles transported during the cold phase are in average drier than for the warm ENSO phase and that convection may not be favoured. For Nicaragua, the decrease of the CLLJ during February for the warm phase of ENSO induces an increase in the transport from GoMS (fig 8.12.c) but with similar results to those found for CRP during April, this is, a reduction of contributions to precipitation associated to GoMS. During May however, as the intensity of the easterlies is intensified during warm ENSO, the transport from the CS associated with precipitation over Nicaragua is reduced but contributions to precipitation from the source increase, as the moisture content is intensified (fig 8.12.d). For the HS region, the reduction of the intensity of the easterly wind during warm ENSO is directly related with the decrease in the transport of air and the consequent reduction of contributions to precipitation from the ETPS

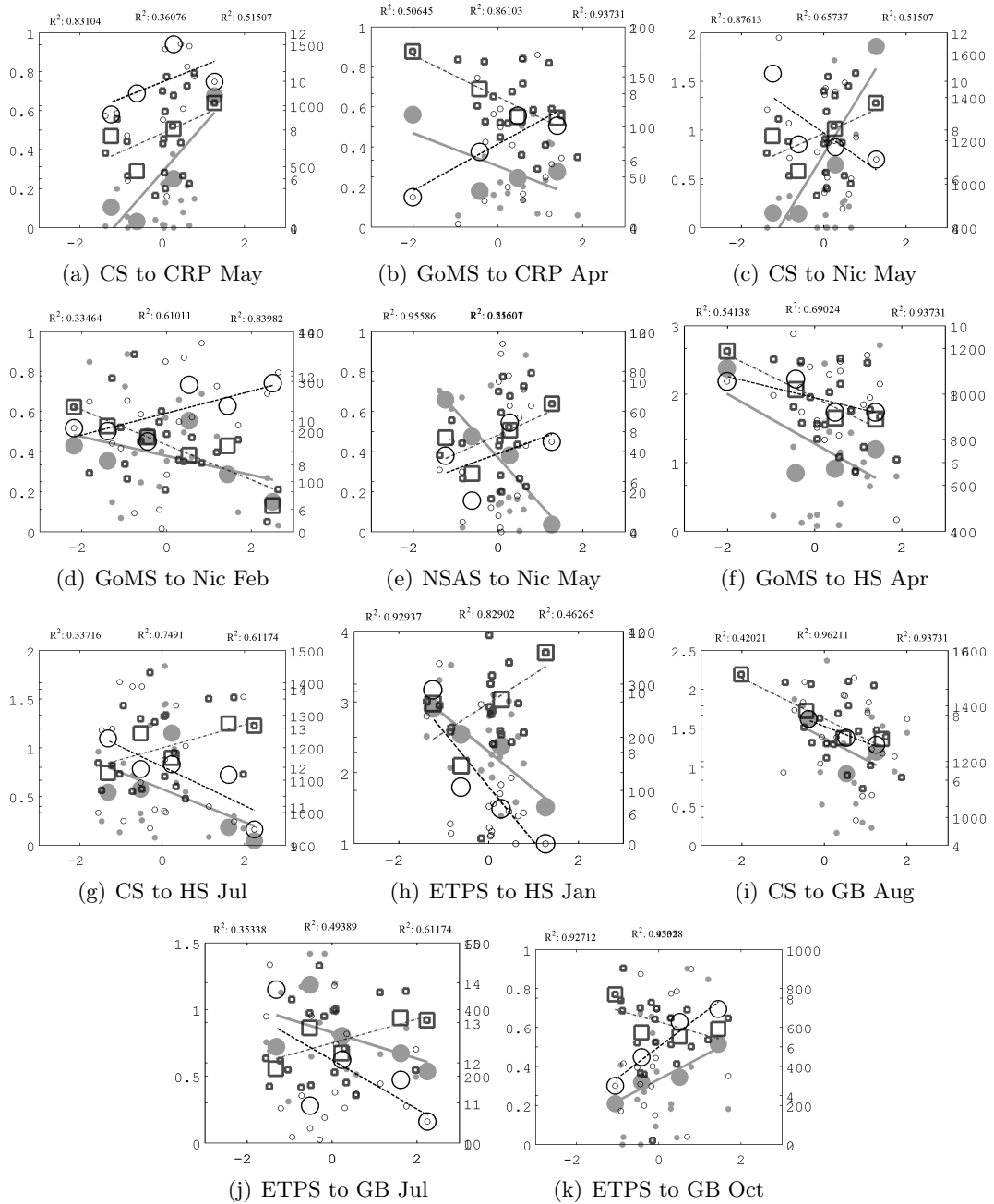


Figure 8.16: Scatter plots for the amount of air particles transported from each remote evaporative source to the target region (open circles), for the relative contributions to precipitation from the source to the target (filled gray circles) and the CLLJ index (open squares) .



during January (fig 8.12.e), indicating that for this source the amount of air particles is associated with precipitation which are increased for cold ENSO, showing how increased easterlies are able to modulate the transport from the ETPS. During April, a direct response to the intensity of the wind is associated with the transport and contributions to precipitation from the CS (fig 8.12.f) as the three decrease (increase) for warm (cold) ENSO. For the same source, the pattern reverse in Summer (fig 8.12.g) when intensified CLLJ during warm ENSO is associated with the reduction of the transport of air that precipitates over CRP and the contributions to precipitation from this source. With the further implication that warm ENSO inhibits the transport from the CS to HS as the more intense winds moves moist air toward the ETPac, as has been previously discussed. Air flow from the ETPS that moves towards GB is also influenced by the easterly flow as the increased CLLJ during summer (fig 8.12.h). The opposite is found for Autumn (fig 8.12.i) with the reduction of the easterly flow during this month is associated with the increase of both transport and associated contributions to precipitation from the ETPS.

For CRP, the main influence of the MJO seems to occur during summer as the airflow from the ETPS is reduced as the CLLJ is intensified during positive MJO (fig 8.15.a), despite the decrease of the transport and increase in the contributions to precipitation are noticed. Meanwhile, transport of air masses from the NSAS is increased with the intensified CLLJ but with a reduction in the contributions to precipitation associated with the source (fig 8.15.b). The CLLJ decrease (increase) found for positive (negative) MJO is found to trigger the intensification of both the transport of air masses from the ETPS and the contributions to precipitation over Nic from this source. For the HS region, significant linear relationship between the CLLJ, transport of moisture and contributions to precipitation was found only during April for the transport from the GoMS. decreased easterly flow associated with the increase of the transport of air masses but with the resulting decrease of contributions to precipitation from the source (fig 8.15.c). The intensification of the CLLJ during August is related with the increase of air particles transported from the CS to GB and also with the increase of the contributions from this source with precipitation over GB during positive MJO (fig 8.15.d). During January, a decrease in the transport from the ETPS (and contributions to precipitation) is found to occur for positive MJO, however no relation is found

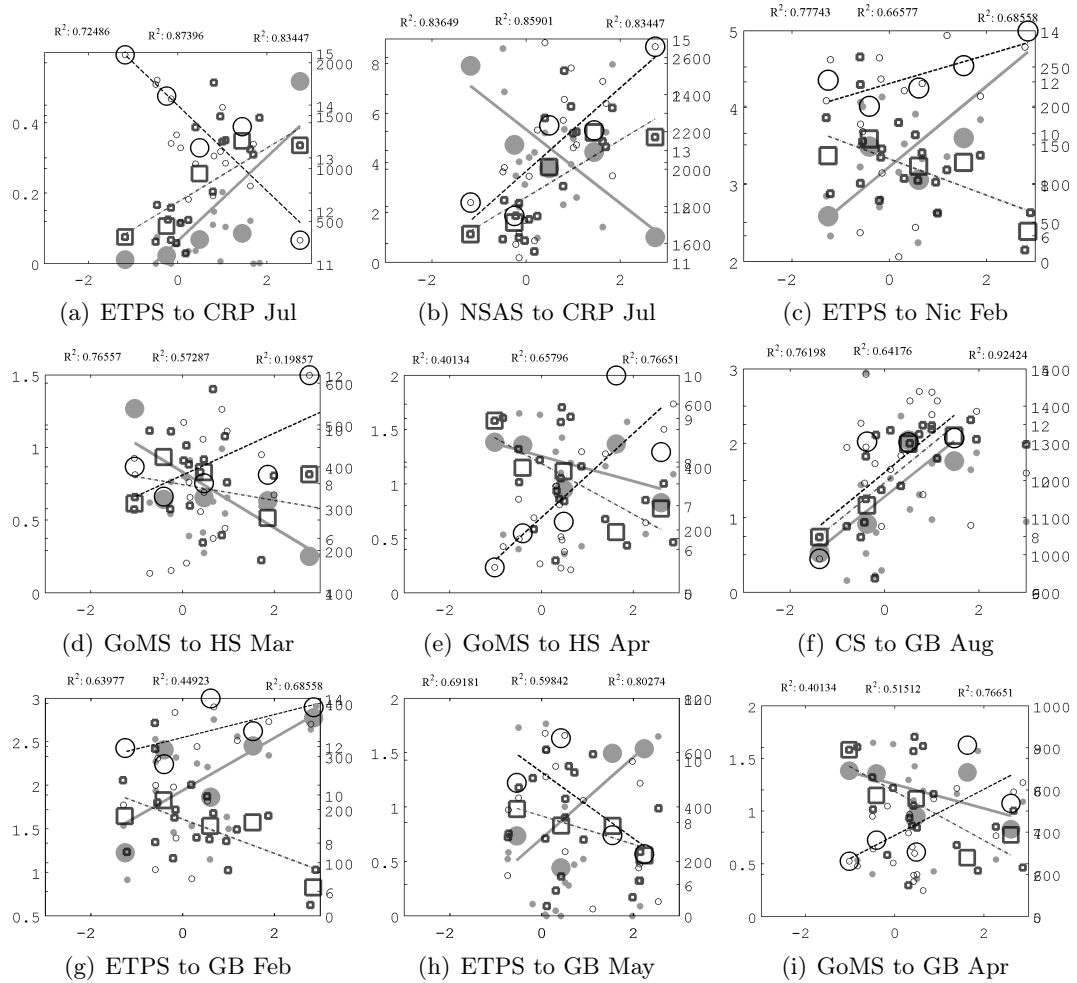


Figure 8.17: Scatter plots for the amount of air particles transported from each remote evaporative source to the target region (open circles), for the relative contributions to precipitation from the source to the target (filled gray circles) and the CLLJ index (open squares) .

with the easterly wind flow. In February, as the CLLJ decreases for the positive MJO phase, transport of air from the ETPS is enhanced, increasing the contributions from this source to precipitation (fig 8.15.e). In Spring, even when the decrease occurs for the transport of air particles occurs for the positive phase, the contributions to precipitation increase (decrease) for positive (negative) MJO. Note that the intensity of the flow is also reduced, opening the question of what may cause the marked increase of contributions to precipitation apart from the more or less obvious increase of the

moisture content of the air travelling from this source.

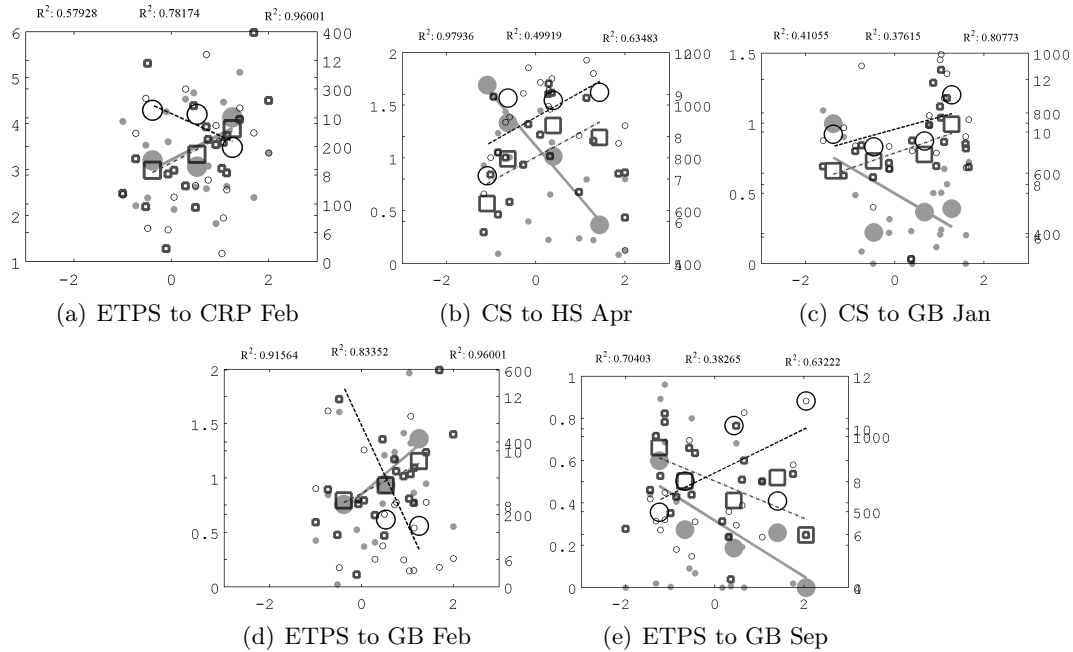


Figure 8.18: Scatter plots for the amount of air particles transported from each remote evaporative source to the target region (open circles), for the relative contributions to precipitation from the source to the target (filled gray circles) and the CLLJ index (open squares) .

The reduction (intensification) of the transport of moist air from the ETPS to CRP during February for the positive (negative) phase of the NAO seems to be related with the increase of the intensity of the CLLJ, however the decrease of the transport do not cause a fall in the contributions from this source to precipitation over CRP but an increase (fig 8.13.a). No significant linear relationship between moisture transport, the CLLJ and contributions from the sources to precipitation is found for the Nic region. The increase of the wind flow is suggested by the results shown in figure (8.13.b) to be related with the intensification of the amount of air particles transported to the HS region from the CS for positive NAO during April. However, no increase in the contributions to precipitation from this source is noticed but the decrease. During January, positive NAO triggers the increase of the intensity of the easterly flow, increasing also the amount of air particles transported from the CS to GB, with an associated reduction in the contributions to precipitation (fig 8.13.c). During February, the increase of the

intensity of the CLLJ results in a reduction of the transport of air particles from the ETPS, conversely to what may be expected, a increase of precipitation associated with the transport from this source is found (fig 8.13.d). For the same source (ETPS), the decrease of the intensity of the easterly flow noticed in September (fig 8.13.e) favours the increase of the amount of air particles transported whereas contributions to precipitation are reduced for positive NAO.

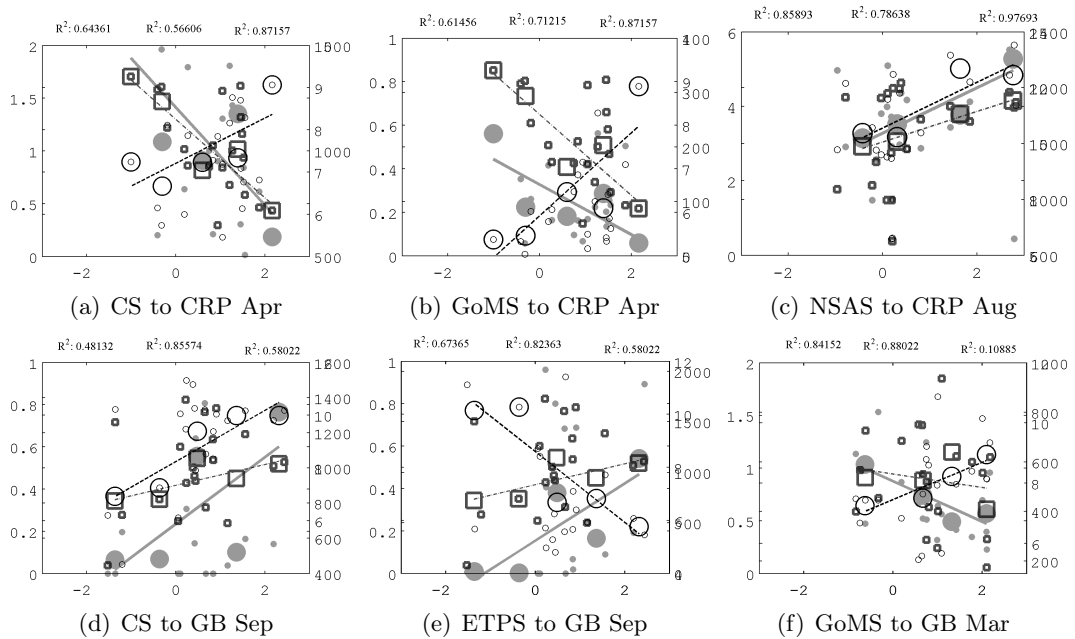


Figure 8.19: Scatter plots for the amount of air particles transported from each remote evaporative source to the target region (open circles), for the relative contributions to precipitation from the source to the target (filled gray circles) and the CLLJ index (open squares) .

The response noticed for the PDO indicates that for CRP the decrease of the easterly flow for positive PDO is related with the increase of the transport of air from CS during April but that a reduction in the contributions to precipitation from this source occurs (fig 8.14.a) and the same result is found for the transport and contributions from the GoMS (fig 8.14.b). During September, an interesting result is found for the transport from the NSAS, it is increased for the positive PDO phase as the easterlies are intensified resulting in the intensification of the contributions from this source to precipitation over CRP (fig 8.14.c). For the same month, a similar result is found for the transport of moisture from the CS to GB which is also associated with the intensification of

the contributions to precipitation (fig 8.14.d) whereas the increase of contributions to precipitation from the ETPS occurs despite the transport is reduced for positive PDO (fig 8.14.e). No significant linear trends were found for the transport of moisture and associated precipitation for Nic and HS under the influence of NAO.

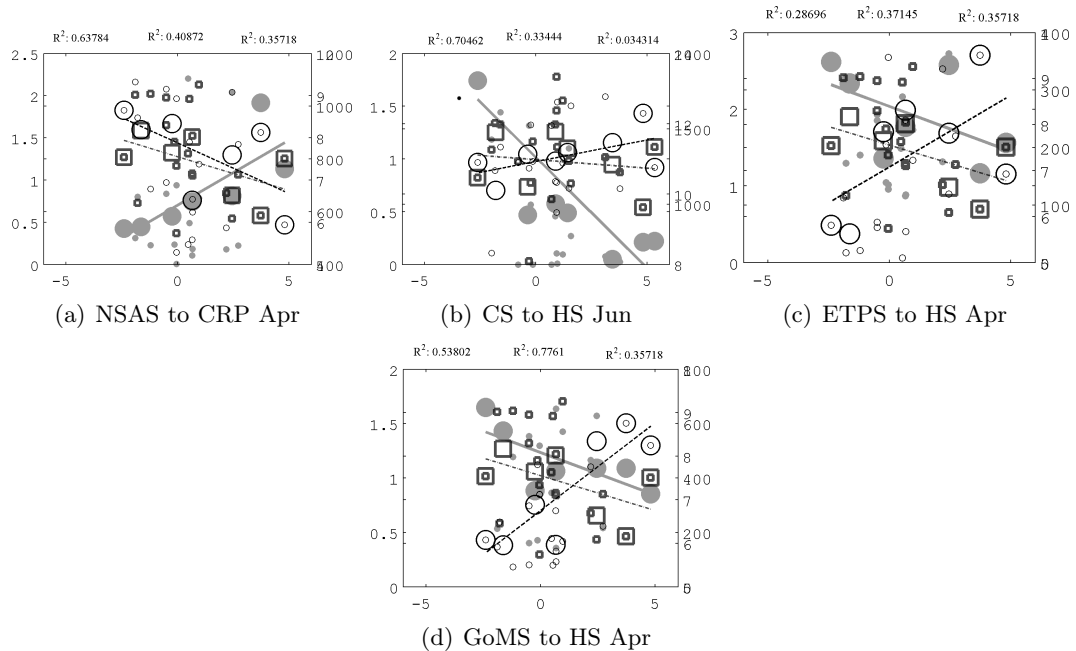


Figure 8.20: Scatter plots for the amount of air particles transported from each remote evaporative source to the target region (open circles), for the relative contributions to precipitation from the source to the target (filled gray circles) and the CLLJ index (open squares) .

In the case of the WHWP, the wind flow is found to be decreased during Spring for the positive phase and the transport of air particles from NSAS is found to be reduced whereas contributions to precipitation from this source are found to increase (fig 8.16.a), suggesting uptake of moisture to be enhanced. Eventhough no simple linear relationship between moisture transport, precipitation and easterly wind flow was found for Nic and GB, the HS region exhibits a varied response to the forcing of the WHWP. For April, transport of moisture from the ETPS is increased as the easterly flow is reduced however, contributions to precipitation are decreased (figure 8.16.b). Meanwhile the transport from the GoMS is increased as a result of the reduction of the easterlies at the same time that contributions to precipitation from this source are reduced (fig 8.16.c).

## 8.5 Chapter highlights

In the present chapter the role of the CLLJ as an structure of particular importance for moisture transport and modulation associated with precipitation has been analysed. Due to the local features, the CLLJ interacts with different systems so that its role for regional modulation of precipitations ranges from evaporation enhancement over the ocean to forcing of topographic precipitation. A simplified conceptual model of the conditions that enhance/inhibit the moisture from the CS to account for precipitation was proposed with the aim of improving the understanding on how the different regional mechanisms interact to favour determined conditions of transport, therefore associated precipitation. The objective is to consider this simplification as start point for considering more complex interactions and build up a more integral view of climate processes that affect Central America, but that can be also of importance for other regions<sup>3</sup>. The Lagrangian analysis allowed not only a good identification of the three dimensional structure of the CLLJ but also of the moisture it transports. The agreement between the core where the peaks of intensity occur and the major uptake of moisture shows that besides of transporting moisture, the CLLJ is important for the enhancement of evaporation. Moreover the accuracy of the trajectories method for capturing both the seasonal cycle of the CLLJ and its variability allows us to consider this methodology for more complex studies in which the information extracted from mean fields is not good enough.

The CLLJ has been found to be extremely important in the modulation of the transport of moisture from the Caribbean to Central America and therefore of the precipitation over the region. Moreover, the CLLJ is indicated as the most important feature of the regional hydrological cycle, since it is involved in the complete cycle at different levels. Figure 8.16 presents an schematic representation of the processes in which the CLLJ is important. The intensification of the easterly flow associated to the maximum of the CLLJ is related to the increase of evaporation due to the drag exerted by the wind over the ocean surface. In addition, the convergence/divergence patterns forced by the jet structure at the right and left of the core of the jet modulate the regional distribution of precipitation over the Caribbean Isles and the Caribbean

---

<sup>3</sup>a discussion of the importance of the CS as a source of moisture for the NAMS is included in appendix.

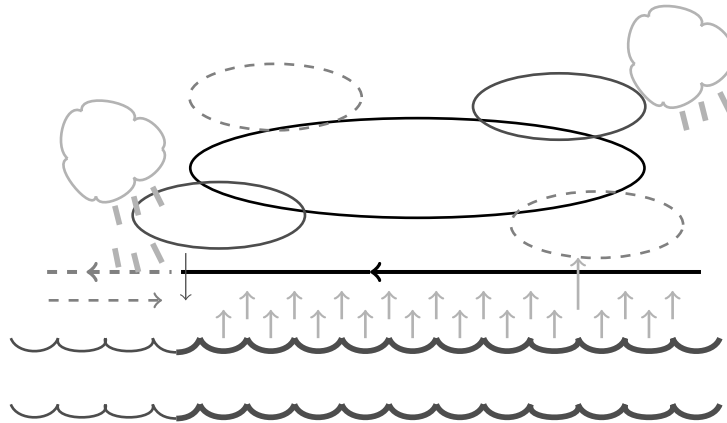


Figure 8.21: Sketch of the mechanisms in which the CLLJ plays a role for the regional water cycle .

coast of Central America where the main centers of convergence/divergence are located when the CLLJ is active. Finally, the intense easterly flow modulates the transport of the moisture from the Caribbean to Central America. Part of the moisture from the Caribbean reaches the Pacific side, while some other precipitates over Central America when the strength of the wind is favourable. Moreover, the CLLJ interacts with local topography to enhance orographic precipitation and at the same time, the interaction between the Caribbean and ETPac via SST gradients results in the modulation of the intensity of the CLLJ and therefore of the regional transport of moisture.





## Part III

# Final remarks



# 9

## Conclusions

Through this work different aspects of the problem of moisture availability, transport of moisture and precipitation in a component of the IAS region to be Central America have been addressed. Being Central America a region poorly studied in comparison to other locations in the tropics, this kind of study was a need in order to provide further details on processes that even when can be considered as simple are of great importance for the region. The assessment of estimating precipitation in Central America presents the issue of the scarcity of data to calibrate the estimates. Whereas numerical models developed for tropical studies fail in the estimation of precipitation by large biases. The study presented was based on a Lagrangian methodology which is far a good alternative to the traditional Eulerian treatment for studying processes within the water cycle. Using this approach, the identification of the main sources of moisture for a region poorly studied was possible. Moreover, an integral analysis of the regional hydrological cycle was performed, providing useful information on the process of the transport of moisture in the region in terms of the key regional climate features.

## 9.1 Lagrangian approach

The skills of the method applied were found to be fairly good in the representation of the processes that occur in the IAS region, which is not always easy to obtain with numerical models even when have being designed for tropical studies. Considering that the FLEXPART model has a simple set up and parametrisations compared to different numerical models used for climate modelling, its ability to capture the most important features of climate in the IAS is good. It is important to mention that the ERA40 analysis used as input may have some part of the credits of FLEXPART representing the mean climate conditions with an excellent accuracy. As the model was used for a preliminar study in which it captured the mean patterns, the time span used was too short to determine if the model could be able to handle variability. The simplicity of the model in terms of processes and parametrisations can be considered as a constraint, however it also has the advantage of not introducing noise due to parametrisations that may be not well suited. Here we are not exactly interested in using a model that copes well with every single process but in using a model that represents well the main climate features (which will depend on the input data) and represented with good accuracy the changes in moisture along the trajectory of air parcels as we are interested in precipitation. The conclusion on the performance of the model and dataset used is that the setup used enabled the representation of the main features of climate in the IAS which was essential for the study that was proposed.

## 9.2 Sources of moisture and contributions to precipitation

In agreement with previous studies, two oceanic regions were found to be of importance as the major sources of moisture for precipitation over Central America. The Caribbean Sea (CS) is the main source of moisture, it provides the basis of the seasonal cycle of precipitation and is associated with the larger high frequency variability. The ETPS, was found to be important for providing moisture mainly to the west coast of Central America and was associated with a region of strong evaporation in the ETPac. Three sources that were not considered in the exploratory analysis were considered in the present work, the Gulf of Mexico even when is not featured as a very important source in terms of contributions, the sum of small contributions was found to be considerably

important. The latter mainly for northern Central America. Local recycling, on the other hand, was found to be of importance during the rainy season as expected and to account for precipitation in a short temporal scale but also to have a lagged effect on precipitation by surface processes due to soil and vegetation. A remarkable result in terms of innovation compared to other studies is the identification of a source of moisture over northern South America which provided evidence on the coupling between precipitation over northern South America, low level winds and precipitation over Central America, which was found to be of importance for determining the seasonal cycle of precipitation. The variability of the sources of moisture was also analysed and an important response of the main variability modes in terms of intensity and horizontal extension of the sources was found, being particularly important ENSO. A relationship between the sources and the easterly wind flow over the Caribbean suggested the variability of the sources may be somehow related with the variability of this wind flow. Up to a 70% of the variability of the sources can be explained using 5 modes of an EOF pattern, from which three of the modes are related with the easterly flow. Being the first mode associated with the 'ground' signal of the easterlies that defined the mean state of the sources and an additional mode which accounts for the anomalies associated to the strengthen of the easterlies (the CLLJ). A third mode was associated with the horizontal extent and variations of the CS. Implying the importance of the zonal wind in determining the availability of moisture and the scale of transport.

Using a simple method that considers the rate change of specific humidity previous to the arrival of an air particle to a target region as an estimate of precipitation, estimates of precipitation due to the contribution from the identifies sources were computed. These estimates provide a quantitative basis for the analysis of the importance of the sources of moisture. By adding the relative contributions from each source, an estimate of the relative contribution from the sources of moisture to the total precipitation over the region was computed. Using a set of stations, quality control was performed to the data and a fraction of the total of stations was determined to be adequate to be used. However, as it corresponded to individual countries, a proper evaluation over Central America could not be performed and the correlation between the precipitation averaged for the stations and the estimated from the Lagrangian model was used instead. Even when this may not be considered as a complete evaluation of the method, it provides

at list information on how reliable is the information obtained. The bias between estimated and observed precipitation ranges between 23 and 46%, which was considered to be reasonable<sup>1</sup>. The underestimation of precipitation that features the estimated from the Lagrangian approach is 'normal' considering that the approximation does not consider microphysical processes which account for part of the observed precipitation. The estimates were then considered as relative contributions to precipitation and not the total precipitation to be correct. The analysis of the estimates revealed that the contributions from the sources accounts for the major part of observed precipitation (up to an 80%). This result suggests that most of the precipitation that falls over Central America comes from remote sources, which implies that the external export of moisture is determinant for precipitation over the region. More interesting is the time series for the contributions to precipitation from individual sources, which shows the different behaviour of each source. The contributions from the CS can be decomposed in two parts, a signal of the mean background signal of precipitation and a component of the variability of the Caribbean. Conversely, the ETPS does not have that background component and is more associated with a seasonal component of the observed precipitation and low frequency variability. The analysis of the time series revealed that the major variability occurs for the 2-8 years band which is actually ENSO band. However, the variability of the ETPS was found to be also probably linked to the effect of a lower frequency variability to be the PDO. Unfortunately, the series are not long enough to prove this result despite the analysis performed reveals some influence of the PDO on the signal of the contributions from the ETPS (accounting for that low frequency variability mentioned). In general, the oceanic sources were found to be more sensitive to the interannual forcing of the variability modes analysed. Moreover, the effect of the variability modes was found to trigger a lagged response from precipitation. This result is importance since the earlier/delayed begin of a dry or wet season is determinant for hydroelectricity and agricultural planning. Which is of great importance in the region since most of the electricity is generated by hydropower and the former countries of Central America have a historical economic dependence on agriculture, both for exportation and local consume. A better understanding on the response of precipitation

---

<sup>1</sup>this compared to the biases of several numerical models

to the variability modes can provide useful information to improve the planning of different economic activities.

### **9.3 Moisture transport and associated mechanisms**

From the results and discussions presented in chapter 7, the most important result is the interaction between the mechanisms involved in the transport of moisture. The use of the backward trajectories enabled the reconstruction of the mean history of the air parcels prior to their arrival to Central America where they 'precipitated'. The applied method allowed us to obtain the complete three-dimensional structure of the transport of moisture. From which was determined that the main component of the transport is not only constrained to the troposphere but also below the boundary layer, as predicted from the theory (more than the 90% of the air particles that contribute to precipitation over Central America have travelled below 2000m). This allowed us to obtain an accurate representation, by using clustering, of the features of the mean climatological flow that is responsible for part of the precipitation observed over Central America. In addition, the clustering algorithm used provided a good and efficient tool for reducing the large datasets into representative smaller amounts of air parcels, with the advantage that the clusters contain the main signature of the properties in which the study is focused. The method also allowed the identification of those regions where the most significant changes in the moisture content of the air parcels occurred. The latter is important since the identification of the uptake locations can be considered as a correction term of the location of the source of moisture. This means that even when air can be identified to come from a determined location, it can be dry air that increases its moisture content over other region. Therefore the contribution of moisture to precipitation from that trajectory is more realistic to be considered to come from the region where the uptake occurred rather than from the region when the air parcel 'started' to move towards the receptor region. Uptake locations were found to be associated with increases of evaporation due to local heating (mainly over the ETPac). But the forcing of low level winds over the Caribbean when the CLLJ is active was also important for the enhancement of evaporation. This result suggests the importance of studying the air-sea interaction that lays beneath the marine boundary layer under the CLLJ, since the forcing for uptake was found to be large and to increase in phase with

the strengthen of the jet. Two structures were determined to exert the main influence in the modulation of the transport of moisture, the low level winds (both the easterly and the southeasterly flows from the Caribbean and the ETPac respectively) and the seasonal movement of the ITCZ which modulates the arrival of moisture from the ETPS to Central America. These two structures explain completely the seasonal cycle of the transport of moisture. As indicated in chapter 5, the first EOF pattern of the sources of moisture, that corresponds basically to the CS is strongly related with the forcing of the easterly flow. The variations in the extension and intensity of the CS described by the third EOF pattern (shown in figure number) are related with the variability in the scale of the transport from the Caribbean. In which long (short) range transport is associated with contributions from the outern (inner) Caribbean. The low level convergence of the winds that transport moisture during spring explains not only the intensification of precipitation but also remarks the importance of the interaction between the Caribbean and ETPac through Central America. As a summary of the mechanisms involved in the transport of moisture, the diagrams of figures provides a good schematic representation of the regional transport of moisture. The application of the Lagrangian approach was satisfying, however we are concerned of the importance of improving the representation of the estimation of precipitation as has been also stated by Sodemann (2008). This because the Lagrangian approach used present a big potential to be used for analysis in specific region, for which the estimates of precipitation may be more accurate. Despite the issue of the uncertainties in the estimation of precipitation, the method provides a good tool jointly with the generated dataset for this analysis to be applied in the study of case analysis, from which we are particularly interested in severe drought conditions in determined locations of Central America.

#### **9.4 Role of the CLLJ in moisture transport and distribution of precipitation**

The importance of the CLLJ was introduced in the second chapter and the first evidence of its role on the modulation of the intensity of the sources of moisture was given, in terms of our results, in chapter 5. Where the influence of the easterly flow was found to be present in three of the main modes of the EOF of the (E-P)-6 field. Accounting up to a 30% of the variability of the field. The analysis of the backward trajectories, as already



mentioned, enable the reconstruction of the path followed by the air particles and the changes in the properties they undergo. This is extremely useful in the identification of specific structures, which using basic dynamic assumptions can be isolated for individual analysis. In the case of the CLLJ, the flow is as confined in the period of activity of the jet, that its structure is isolated by basically constraining the mean height of the flow to be below 3000 m. After applying the second condition, which was based on the geopotential height gradient between the trajectories, few variations in the amount of air particles attributed to the CLLJ during the two peaks (February and July). In average, after the second condition was applied to the particles with origin to the east of the targets, variations smaller than 5% in the number of air particles were found compared to those obtained after only constraining the height. This implies a strong coherence of the easterly flow in presence of the CLLJ, which during its activity lead all the processes in the Caribbean Sea. The typical jet-like structure of the CLLJ, in which the convergence pattern is located to the west of the core is related with the increase of precipitation over Central American Caribbean coast. This accounts for the seasonal differences observed in precipitation between southern and northern Central America. This is important since these patterns also modulate precipitation over the Caribbean Isles. In addition, the development of a divergence wind to the right of the core along the axis of the jet is related with the horizontal distribution of the CS.<sup>2</sup> A well developed jet, with the correspondent convergence/divergence patterns is related with the result that during spring the recycling of moisture over Central America is a feature of the sources of moisture as shown by the (E-P)-6 field. Meanwhile during the period in which the jet is active in summer over the east coast of southern Central America there is low level convergence (and associated precipitation) instead. However, during winter the pattern is not the same and the (E-P)-6 field suggests the presence of divergence over the region which may be considered as different from expected following the latter discussion. The reason of this difference is that during winter the convergence pattern is different from that observed during summer. Then, during summer a strong pattern of low level convergence is located all over Central America while during winter divergence is observed over northern Central America, left to the convergence pattern. The reason

---

<sup>2</sup>note that this implies that the second mode of the EOF pattern of the (E-P)-6 field is also related with the CLLJ

for this lies on the features of the wind flow, being this divergence pattern observed during winter associated with the pass of the easterly flow trough Central America enclosed by the Yucatan peninsula since the mostly zonal structure remains. This does not occur during summer since the axis of the jet is dislocated to the north as the CLLJ develops its northward branch. A description of the intensity of the contributions from the CS was given in terms of the properties of the intensity of the CLLJ and the SST gradient between the Caribbean and the Pacific. The proposed conceptual model of the intensity of the contributions aimed to show how these two variables were enough to explain the modulation of the moisture transport from the Caribbean Sea to Central America. The CLLJ index was found to be useful as a measure of the intensity of the jet as described by Wang (2007) but the SST gradient was also found to be useful for analysing the probability of the difference of SST to induce a thermal response from the easterlies. The latter was found to be even more important as it supports the role of the WHWP as a modulator of the transport of moisture, as the  $\Delta SST$  accounts as a measure of the importance of the WHWP. Using composites and analysis the trajectories for selected events (associated with the larger variations of the main variability modes) the model proposed was tested, under the assumption that the selected composites represented the mean variations and the selected cases variations in the sources due to specific conditions. The result was found to be that the model of variations in the intensity of the CLLJ and the SST gradient explain very well the patterns described by the CS (for the composites) and the transport of moisture (for the selected cases). Suggesting that in order to improve the knowledge on the regional patterns of precipitation and the assessment of forecast (and numerical models evaluation), the focus must be put on the interaction between the CLLJ and the AWP. As the model is too simple, it does not account for explaining all the patterns, however it was found that for those cases in which the pattern did not represent the expected result, the vertical structure of the easterly flow provided a partial explanation for the observed differences. This implies that the three dimensional structure of the CLLJ is more important in terms of analysing precipitation than rather just evaluate the horizontal mean fields. The analysis presented enabled a complete study of the regional hydrological cycle of Central America in terms of its components as described in the first chapter. The Lagrangian methodology was found to fulfill the gaps of information that

are often present in the analysis of climate when Eulerian type analysis applied, since the reconstruction of the history of the air particle allows the study of the complete structure of transport and not just only of the mean state. The application of this approach to the case of Central America allowed us to provide an answer to the questions proposed so that the main objective of the work was accomplished. But more importantly, the results obtained encouraged the further study of specific aspects that were found to be of importance, some of which are of common interest with different groups as is the case of the extratropical moisture export and the contributions of the moisture transported from the Caribbean Sea to the NAMS. As well as to other that have not been study up to now as the vertical structure of the moisture of transport and the eventual coupling with the moisture transport through the tropopause, the forcing of evaporation due to the drag of the CLLJ over the ocean surface as well as the response of the CLLJ to forcing from the Atlantic and correspondent influence on the modulation of regional moisture transport and precipitation. Finally, this study provides a complete and detail analysis of the main components of the regional water cycle in the heart of tropical Americas. The main mechanisms involved in the transport of moisture and the modulation of precipitation over Central America have been assessed. The objectives of the proposed work were satisfactorily accomplished and the obtained results provided the input for the proposal of future studies in which some aspects of the regional climate need to be explored.



# 10

## Further research lines

This work constitutes a detailed analysis of the sources of moisture for precipitation over Central America, a region poorly studied and of a great importance for several reasons as already pointed out. Beyond the mere identification of the sources that provide moisture to the region, a quantification of the relative contributions from the sources was presented. The variability of the sources of moisture and related effect on regional precipitation estimates was also considered. Even when the role of some of the sources was at least supposed, this work demonstrates their existence in a quantitative basis rather than a qualitative overview. Which is of importance since also allowed the identification of an additional continental remote source. The structures involved in the transport of moisture and how do they interact as part of a complex regional water cycle were used to explain part of the dynamics of moisture transport in the region. Finally, the role of the CLLJ as the main moisture transport (and precipitation) modulator was analysed in terms of the results obtained from the Lagrangian analysis and the basic concepts of atmospheric balance. It can be said that even when one must think that a bunch of questions were properly answered, some others came out from the work developed. This is how this work has opened different associated research lines that may be considered for further work (some which are already being explored):

## 10.1 Transport of moisture to and from additional structures

### Moisture transport processes related with the South Pacific Convergence Zone

The convergence regions in the tropics is also of interested in terms of the transport of moisture and other tracers. As a cooperation with the University of Rutgers, the study of the moisture imports and exports from the South Pacific Convergence is in progress. In this case, a backward trajectories dataset based on ERA Interim Reanalysis data for an extended tropical channel has been prepared. The aim is this joint research activity is to provide a novel interpretation of the processes take take place in the SPCZ, not only regarding precipitation but the transport of different The first exploring analysis have consisted of studying the trajectories features for different configurations of the SPCZ, based on the high frequency displacements of the SPCZ. Based on the results obtained in the work herein presented, an improved clustering algorithm was used for computing the average clusters of air particles associated with the SPCZ in order to evaluate its structure under variable magnitude low level wind flow. The next steps are the analysis of the variability of the SPCZ structure under ENSO and the establishment of a relationship between trajectories characteristics and vertical moisture variability statistics. Additional, we are also interested and looking forward to study the tracer constituent transport nearby the SPCZ for which additional backward datasets have been generated using several tracers rather than water vapour.

### Monsoon-like circulations

The methodology applied is in a review and improvement process in order to adapt it for further applications in the study of the transport of moisture associated with the global monsoon-like circulations. In the case of this structures the main interest is to explain in detail how the development of the monsoon is fed by the moisture inflow and at the same time the moisture within the system contributes with intense heavy rainfall when the monsoon is in the active phase. This would allow a deep analysis on the moist structure of the monsoon system from the seasonal to the interannual time scales. Note that a first attempt to show the advantages of the methodology for this problem has been included

in chapter . Moreover, it would be interesting to study how does the transport of moisture changes in a region when the monsoon shifts as is the case if the Asian monsoon. In the very specific case of the NAMS, the Lagrangian trajectories analysis may help in the improvement of conceptual models for the understanding of the interaction between regional low level jets and the life cycle of the monsoon circulation. In order to make use of the campaign fields in the NAMS, a new set of backward trajectories for the periods in which the campaigns were held is being prepared using ERA-Interim Reanalysis data with 91 vertical levels. The latter with the aim of providing a detailed analysis using the backward trajectories method that may be contrasted with in situ observations, for which the NAME and MESA experiments provide a great research and method validation opportunity.

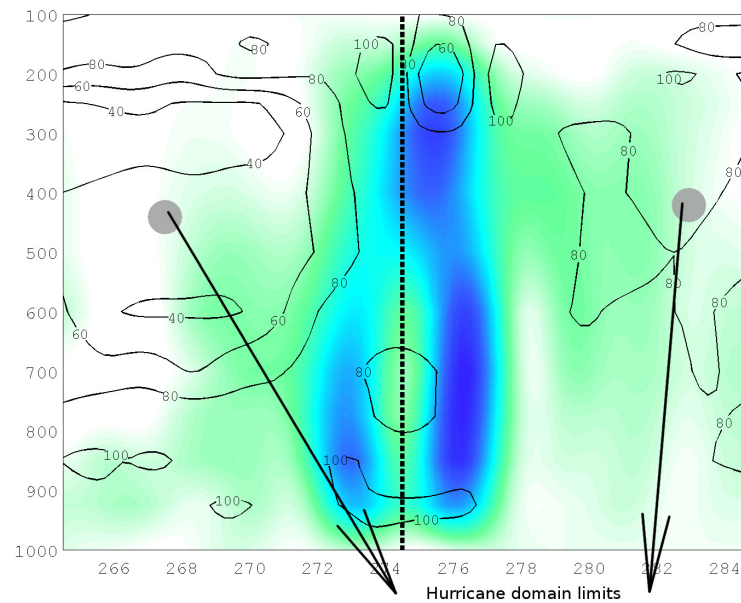
### **Transport of moisture associated to cyclonic structures**

Based on a previous work developed with M.Reboita and A.M. Ramos in which the moisture export associated to selected extra-tropical cyclones in the southern hemisphere an study of the moisture transport processes related with heavy rainfall events in Portugal has been prepared. In the case of the southern hemisphere cyclones the Simmonds et al (2002) method was used to track the cyclones whereas in the latest work a Trigo et al (2006) method was applied. Once the position of the cyclone was determined the evaporative sources of moisture were identified for a one degree box centred in the position of the best track of the cyclone. This allowed us to know where the moisture that feed the cyclone is coming from, then the origin of moist air that contributed to precipitation over Lisbon was determined in order to establish the link between the inflow of moisture into the cyclone and the moisture export to the Iberian Peninsula for the selected case.

### **Moisture and energetics for extreme hurricanes**

Following an analogue reasoning to that of the study of the extra-tropical cyclones, the moisture inflow into selected severe tropical hurricanes was studied. In this case backward Lagrangian trajectories with three hours resolution data were used to explore the moisture import of the hurricanes. As the extension of the hurricanes is very variable, the identification of the associated sources of moisture was carried out by

considering the extension of the section between the eyewall and the border where moisture content was maxima. These two limits were based on the position of the best track of the hurricanes every three hours, the eyewall and maxima relative humidity radii were estimated using ERA-Interim Reanalysis data (see example of Hurricane Mitch limits selection from figure 10.2). The moisture imports and exports for each stage of the life cycle of the hurricanes selected was studied in order to analyse the net moisture conversions inside the hurricane and how they modulate the internal energetics of the cyclone. In addition, forward in time trajectories from the 'hurricane domain' were then computed so the export of moisture could be analysed. Moisture losses from the forward in time trajectories are useful to identify the regions to where the hurricane contributed with heavy rainfall which allows to validate the estimations based on the Lagrangian approach when in situ precipitation observations when available.



(a)

Figure 10.1: Hurricane Mitch vertical velocity (shaded) and relative humidity (line contours) used to approximate the hurricane horizontal extension, as indicated by the gray dots.



## 10.2 Vertical structure of the transport of moisture

Following the results presented in the analysis, the potential of the Lagrangian approach for exploring in more detail the vertical structure of the transport of moisture comes out. The reconstruction of the trajectories air reaching determined receptor regions with information on several variables allows the study of the processes that lead precipitation over the receptor location. What is more important about this application is that this Lagrangian methodology is useful for studying the properties of transport at different spatial scales.

### Short range transport and orographic convection

As mentioned in chapter 8, the easterly flow, due to the presence of a mountainous range system over Central America, presents an important interaction with local topography. The latter is of importance since the lifting of the moist air particles which come from the Caribbean Sea (and even Northern South America) enhance the orographic precipitation over the windward side (as shown in fig 8.2). This has an important implication: vertical structure of the transport of moisture is responsible by the different precipitation regimes in Central America, from which a wetter Caribbean is well known. This reasoning has been several times used to justify the differences in observed precipitation over the Caribbean and Pacific slopes of Central America. However most of the results have been based on the solely assumption while a detailed analysis on the vertical structure of the transport may improve the understanding on the interaction between moist wind flow and topography. Particularly in the cases in which the transport of moisture present important height variations, such an study might be useful to determine how structures like the CLLJ can modify precipitation in other locations rather than the coastal regions. In addition, it could provide further evidences on the impact the transport of moisture towards the Pacific has on precipitation over inner land regions. Finally, a comprehensive analysis on the features of the wind flow (mainly velocity and height) can be useful for identifying locations that might be considered as ideal regions for wind farm development.

### **Long range transport and the extra-tropical connection**

It has been found that the transport of moisture from the Caribbean Sea may have a role in the transport of moisture to extra-tropical regions. A brief evaluation of the sources of moisture for the NAMS (appendix E) show that the Caribbean can contribute with moisture directly to the core of the monsoon as well as transport to the Gulf of Mexico. However, as shown in figure 6.2 the Caribbean Sea also has an important connection with precipitation falling over the US Great Plains. The study of the extra-tropical transport of moisture from the Caribbean would be an interesting problem solved, because in the transport towards the Great Plains via the Gulf of Mexico, moisture from the Caribbean can be separated into two types of flow: a) one going northward to the Great Plains region where it can account for precipitation over e.g the Mississippi basin and b) moist air flow that travels eastward to contribute to the development of synoptic systems in the North Atlantic. For this second type of flow, the regional features of climate may have a remarkable importance, mainly the seasonality that features the WHWP.

### **Vertical transport of moisture to higher altitudes**

Besides the importance of the horizontal transport of moisture due to its role in the forcing of precipitation. An interesting problem for which the use of Lagrangian trajectories can be considered as potentially useful is the vertical transport of moisture in the atmosphere. According to the results of Fueglistaler et al (2005), a region of irreversible transport of moisture across the tropopause is located in the west Pacific Ocean. However, during summer this crossing through the tropopause extends to the east with an important maximum the ETPac and Central America (see figure 10.1). The vertical structure of the wind field during summer averaged in the 10-20 latitude band (see figure 10.2) suggests that the structure of the CLLJ (which reaches upper altitudes during summer) may be associated with the intensification of the vertical transport. This may provide the conditions to create a bridge of transport that links the ETPac with the western Caribbean. This problem is quite interesting since up to know, the potentials of the vertical structure of the CLLJ have not been studied.

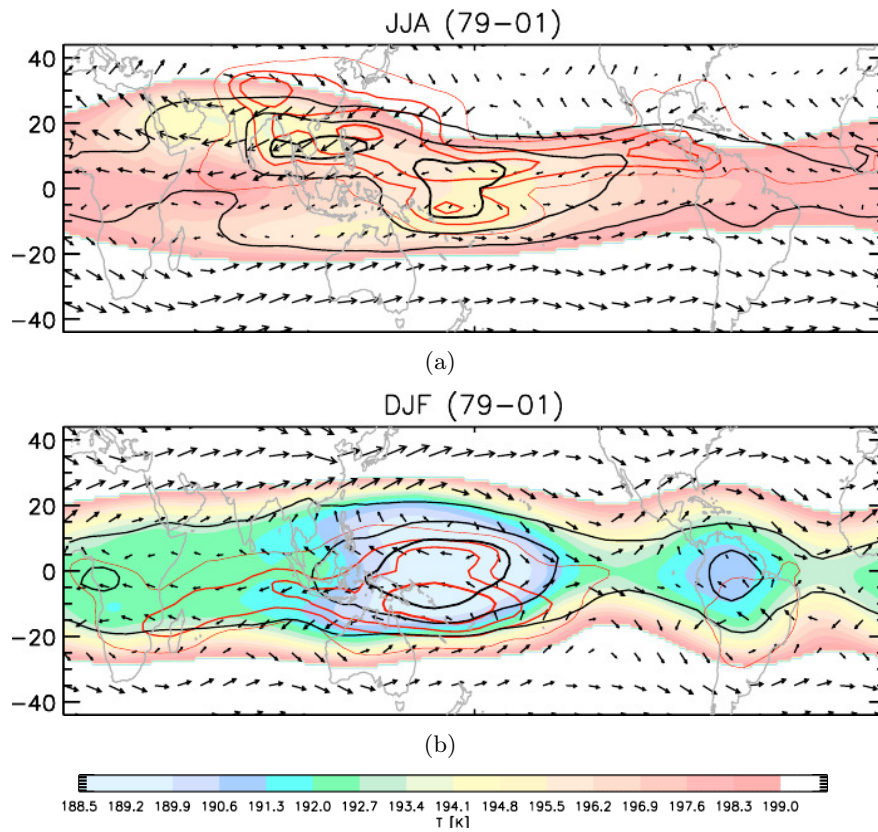


Figure 10.2: Seasonal  $(E - P)^6$  fields for the Caribbean Sea (a) winter, (b) spring, (c) summer and (d) autumn in mm/day.

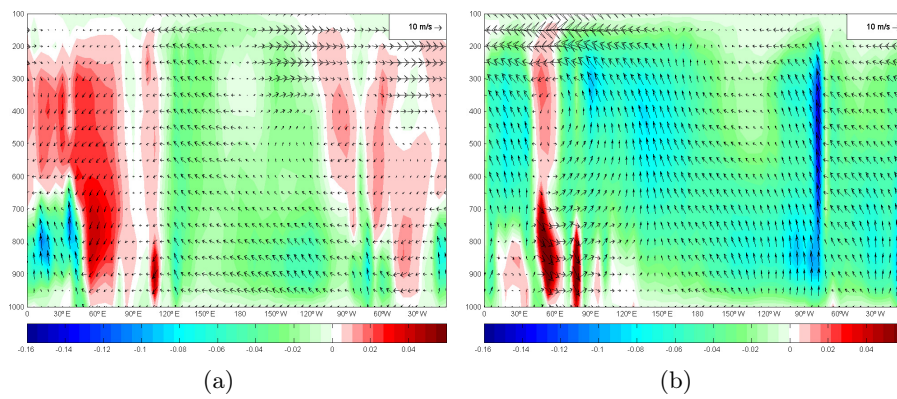


Figure 10.3: Seasonal  $(E - P)^6$  fields for the Caribbean Sea (a) winter, (b) spring, (c) summer and (d) autumn in mm/day.

### 10.3 Response of the sources of moisture to conditional forcing

With the results of this study, in which details on the regional hydrological cycle are given, some additional aspects may be considered of importance.

#### **Warming**

Which may be the response of the sources of moisture to warming? Since the CLLJ is our proposed main moisture conveyor and regional precipitation modulator and some evidence has been found on the circulation being modified under warming, which may be the response of precipitation over Central America to these future conditions. How warming could intensify the marked precipitation patches over Central America. According to the results presented by Trenberth et al (2005), there is a linear trend in the increase of water vapour over the oceans which suggests an increment of 1.2% per decade for the 1988-2004 period (see fig 10.3). As suggested by their results, changes in the runoff may lead to a decrease in regions like Central America. Therefore it might be of importance to consider the results proposed in this study to think ahead on the possible effect of warming on the regional distribution of precipitation.

#### **Atlantic SST forcing**

Finally, a problem that may be of interest and is a potential application of numerical modeling is the influence of variations of SST in the Atlantic in the modulation of the CLLJ. It has been shown that an anomalous heating in the tropical Atlantic presents the typical structure of a Gill-Matsuno-type quadrupole, whose signal is transported by Rossby waves to Central America and the Eastern Tropical Pacific through the Caribbean (Kucharski et al., 2009). As known, the CLLJ is sensitive to these systems and more important it modulates precipitations patterns (see fig 10.4). Which means that any system that may force an anomalous behaviour of the CLLJ can trigger the precipitation patterns over the Caribbean Isles and Central America. How do the CLLJ respond to the signal of this heating and which is the impact it may have on the transport of moisture and associated precipitation?

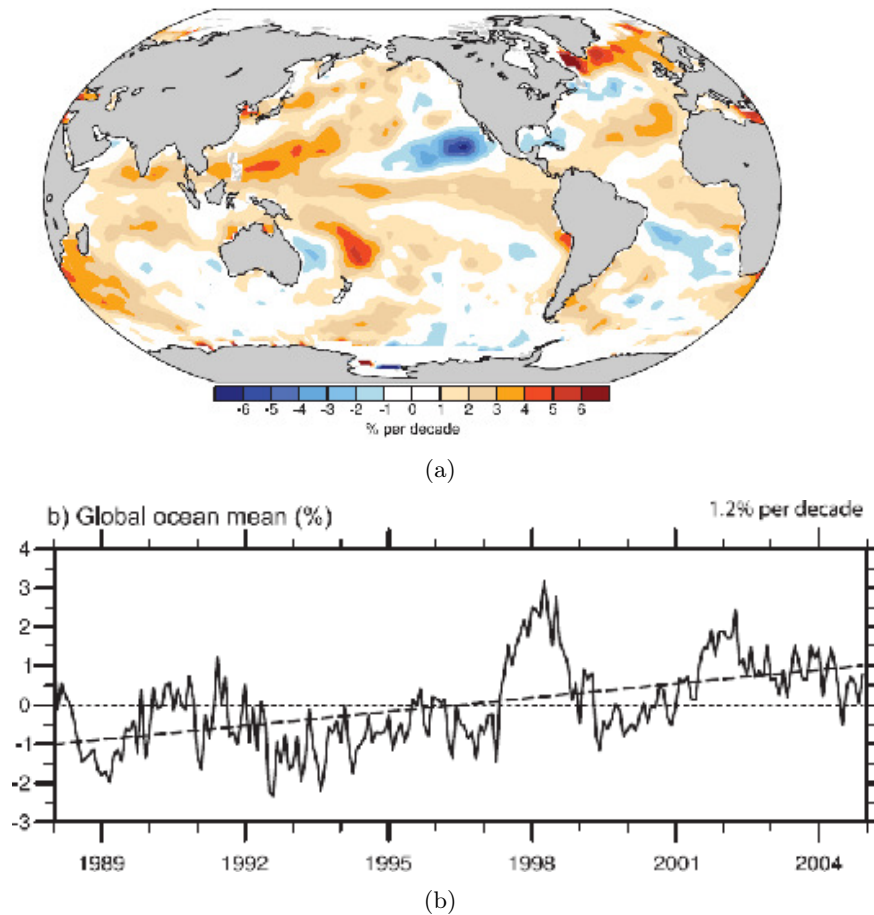


Figure 10.4: Seasonal  $(E - P)^6$  fields for the Caribbean Sea (a) winter, (b) spring, (c) summer and (d) autumn in mm/day.

### Extreme events

Under the premise of the importance of the transport of moisture from the identified sources for precipitation in Central America, and with knowledge on the occurrence of mild to severe drought episodes the region, a detailed study of the transport of moisture during these episodes is important. Such study may improve the understanding of the mechanisms causing drought in the region, but also in other nearby locations. Evidence on the decreases of moisture effective moisture transport were found to be associated with dry events (particularly in Nicaragua). Moreover, as the NSAS was found to have a significant contribution to precipitation, understanding how precipitation vari-

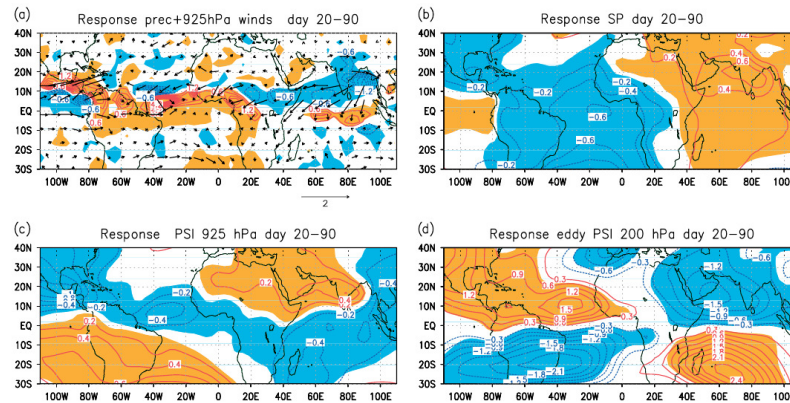


Figure 6. Response to the SST anomaly in Figure 1 (EXP1–EXP2) of (a) precipitation and 925 hPa winds, (b) surface pressure, (c) 925 hPa stream function and (d) 200 hPa eddy streamfunction, averaged from days 20–90. Shading indicates regions of 95% statistically significant anomalies (positive: orange/light grey, negative: blue/dark grey). Contour intervals are 0.6 mm day<sup>-1</sup> for precipitation in (a), 0.2 hPa in (b),  $0.2 \times 10^6 \text{ m}^2 \text{ s}^{-1}$  in (c) and  $0.3 \times 10^6 \text{ m}^2 \text{ s}^{-1}$  in (d). The unit of the wind response in (a) is  $\text{m s}^{-1}$ . This figure is available in colour online at [www.interscience.wiley.com/journal/qj](http://www.interscience.wiley.com/journal/qj)

Figure 10.5: Seasonal  $(E - P)^6$  fields for the Caribbean Sea (a) winter, (b) spring, (c) summer and (d) autumn in mm/day.

ability over northern South America may affect precipitation over Central America is important. An study on this direction may require a longer analysis period because the frequency of sustained extreme dry events (that prolongue dry conditions up to six months) that affect the region were found to be more important outside the analysed period. In addition, a preliminar review of extended drought in Central America has highlighted the importance of the heterogeneity of precipitation. As can be noticed from figures 10.5.a and 10.5.b, the spatial distribution of drought conditions (SPEI6 index Vicente-Serrano et al., 2011) can be featured by two different patterns, generalised drought over the region and drought that affects determined locations. A revision of determined locations (see map in fig 10.6) also remarks that the intensity of the dry episodes has a varied signature in space and time (see fig 10.7).

## 10.4 CLLJ related aspects

Besides the problems related with the regional distribution of precipitation, the problem of the CLLJ and its interactions has not been totally exploited. Several aspects of this structure still need to be analysed in detail. Because of the features of this jet, the processes within the boundary layer in which is involved is of interest.

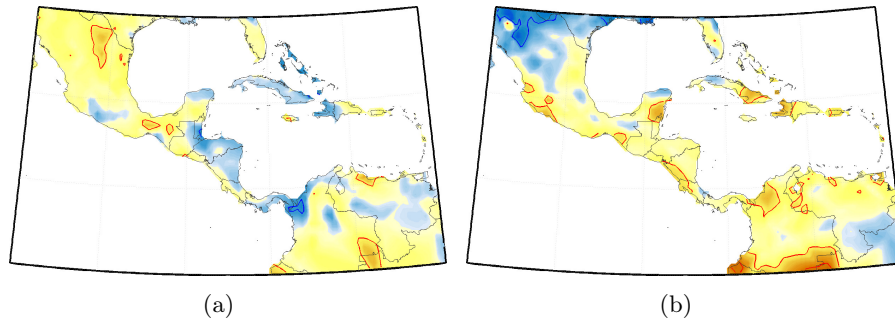


Figure 10.6: Seasonal  $(E - P)^6$  fields for the Caribbean Sea (a) winter, (b) spring, (c) summer and (d) autumn in mm/day.

### air-sea interaction

In the case of the interaction of the CLLJ with the ocean surface, two problems are proposed for further analysis:

#### Associated increase of evaporation

An important region of moisture uptake was found to be located in the vicinity of the CLLJ core, a quantification of the moisture advected to the atmosphere due to the strengthen of the low level winds that provide the other component of the water cycle to which the CLLJ may be related. A quantification of the evaporation forced by the drag of the CLLJ is of interest because it provides further information on the importance the CLLJ has for increasing atmospheric moisture.

#### Associated Langmuir circulation

The intensification of the easterly flow in presence of the peaks of the CLLJ may be associated with a forcing of Langmuir type circulations. This is important because it may have an impact on the mixing in the ocean, therefore on the air-sea fluxes of heat, momentum and also mass (Thorpe, 2004). Moreover, the interaction of the intensified easterly flow and local topography may be related with the forcing of SST variations over the ETPac (Fiedler et al., 2006). Those variations are of biological importance because of their link to the production nutrients, as has been already indicated in the case of the Costa Rica Dome (CRD) (see figure 10.8)

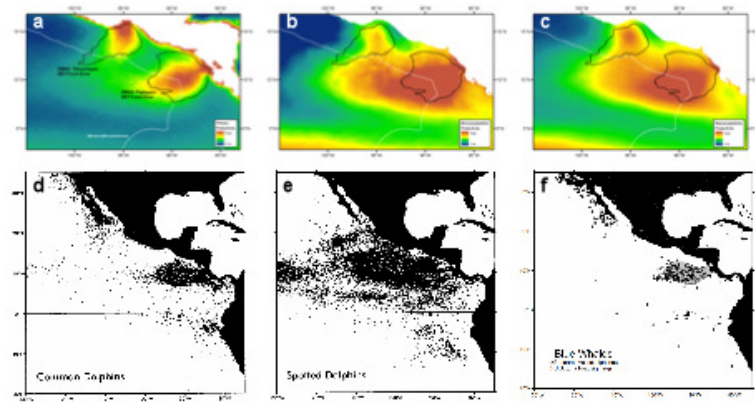


Figure 10.7: Seasonal  $(E - P)^6$  fields for the Caribbean Sea (a) winter, (b) spring, (c) summer and (d) autumn in mm/day.





## Brief introduction to FLEXPART

The advantage of using Lagrangian trajectories analysis in atmospheric studies relies on the possibility of following the air parcels and knowing its properties at each time. A variety of models that enable the computation of such trajectories is available by now e.g HYSPLIT, LAGRANTO and FLEXPART. Due to the requirements of the particular research the Lagrangian model FLEXPART was used. This model was originally developed by Dr. Andreas Stohl during the early nineties as part of his military service in the Austrian Forces. Since then, the model has been improved, new parameterizations have been added and others optimized. Latest updates of the model have derived in an important tool for studying the problems of transport and dispersion of tracers and have been validated during different intercontinental air pollution studies. The FLEXPART model is a freely available Fortran 77 standard code that can be implemented using several compilers and operating systems. This section provides a brief description on some aspects of the version 6.2 of the model as described in the model technical note (Stohl et al., 2005), extra information on aspects of interest for the presented research (specific parameterizations) is added, more information can be found in the FLEXPART homepage (<http://transport.nilu.no/flexpart>).

## A.1 Computing

The FLEXPART model written as a Fortran 77 standard code is a sequential structure in which a list of subroutines are called from a main program. With the previous definition of the configuration of the model for a particular run in the configuration files, data is load and read. A check to determine all required data and paths are correctly set is performed and then the start of the run proceeds with the assignment of the data according to the specific set up. Later on, the set of subroutines containing the physics of the model are implemented to finally generated the output files according to the information asked to be saved. The model was design in a way that each physical parameterization is performed by a single routine that acquires the information from the results of individual smaller subroutines. Similar to the structure followed by the start of a single run of the model in which individual subroutines load the information from the configuration files and then build up the set up of the model in order to proceed with the input data reading and the execution of the model itself.

## A.2 Input data

Data initially in a hybrid coordinate system as retrieved from the ECMWF model is converted to pressure coordinates. Furthermore, vertical wind is calculated to be mass-consistently from the spectral data through a pre-processor. The model requires a set of fields as indicated in the table:

- 
1. Three dimensional fields: horizontal wind components, temperature and specific humidity.
  2. Two dimensional fields: surface pressure, total cloud cover, 10 m horizontal wind components, 2m temperature and dew point temperature, large scale and convective precipitation, sensible heat flux, east/west and north/south surface stress, topography, land-sea mask and subgrid standard deviation of topography.
- 

Table A.1: Input data required to execute the FLEXPART model

### A.3 Physics of the model

A Lagrangian model compute the trajectories for a set of particles in backward or forward mode depending on the specific analysis. The utility of this kind of models is based on the advantage that Lagrangian models are independent of the computational grid, have infinitesimally resolution and unlike the Eulerian methods there is no numerical diffusion (Stohl et al., 2005).

#### Parameterizations

##### Boundary Layer

Boundary Layer parameterization is based on the surface stresses and sensible heat fluxes retrieved from the ECMWF to compute the frictional velocity term as indicated in B.1, in the case data is not available, the computation is performed applying the profile method (Berkowicz & Prahm, 1982).

$$u_* = \sqrt{\frac{\tau}{\rho}} \quad (\text{A.1})$$

in order to obtain the the heat flux term,

$$(\overline{w'\Theta'})_0 = -\rho c_p u_* \Theta_* \quad (\text{A.2})$$

the next set of equations are iteratively solved

$$u_* = \frac{\kappa \Delta u}{\ln(\frac{z_l}{10}) - \Psi_m(\frac{z_l}{L}) + \Psi_m(\frac{10}{L})} \quad (\text{A.3})$$

$$\Theta_* = \frac{\kappa \Delta \Theta}{0.74[\ln(\frac{z_l}{2}) - \Psi_h(\frac{z_l}{L}) + \Psi_h(\frac{2}{L})]} \quad (\text{A.4})$$

$$L = \frac{\bar{T} u_*^2}{g \kappa \Theta_*} \quad (\text{A.5})$$

Note that ABL heights are computed following the critical Richardson number criteria, being  $Ri$  defined as the ratio of buoyancy to shear production of turbulence that provides a measure of the dynamic stability of the flow. The critical  $Ri$  threshold has been set to be 0.25 as defined by Taylor (1931) using perturbation theory. Thus, the ABL height  $h_{mix}$  is set to the height of the first model level  $l$  for  $Ri$  exceeding this value, being  $R_{il}$  defined as

$$R_{il} = \frac{\left(\frac{g}{\Theta_{v1}}\right)(\Theta_{vl} - \Theta_{v1})(z_l - z_1)}{(u_l - u_1)^2 + (v_l - v_1)^2 + 100u_*^2} \quad (\text{A.6})$$

For convective situations, a correction term can be added so that  $\Theta_{vl}$  can be replaced with  $\Theta'_{vl}$  for an improvement of the parameterization.

$$\Theta'_{vl} = \Theta_{vl} + 8.5 \frac{\overline{(w'\Theta'_v)_0}}{w_* c_p} \quad (\text{A.7})$$

where

$$w_* = \left[ \frac{\overline{(w'\Theta'_v)_0} g h_{mix}}{\Theta_{vl} c_p} \right]^{1/3} \quad (\text{A.8})$$

### Moist convection

Convection processes are greatly important moreover dealing with tropical climate issues since significant convection takes place all year round over the region in the form of intense convective systems. Convective transport due to updrafts in convective clouds are not represented by the ECMWF vertical velocity since the transport is grid-scale in the vertical but sub-grid scale horizontally. A redistribution of the particles is the needed to represent this transport and the Emanuel and Živković-Rothman (1999) convection parameterization scheme (hereafter E-ZR scheme) is applied by the model. The current E-ZR scheme is based on a previous parameterization by Emanuel (Emanuel., 1991) with the advantage of offering a good performance in comparison to other schemes in regional modelling. On FLEXPART, the E-ZR scheme has been used in a way that convection is triggered when the virtual temperature of an air parcel lifted to the level above the lifting condensation level (LCL) exceeds a threshold:

$$T_{vp}^{LCL+1} \geq T^{LCL} + 1_v + 0.9K \quad (\text{A.9})$$

Then the net mass flux is determined by using (1) the mixing hypothesis for which increasing buoyancy with height might enhance detrainment and allows an adjustment between the cloud mass fluxes and buoyancy and (2) buoyancy-sorting hypothesis. In FLEXPART, a matrix of unsaturated upward and downward mass fluxes within the clouds is calculated based on the buoyancy-sorting hypothesis by accounting for entrainment and detrainment. The mass fluxes matrix described is used to redistribute the particles in the convective active boxes which fulfilled the criteria given by B.9. The

method has the advantages of eliminating numerical diffusion by calculating subsidence velocity as well as fulfilling the well mixed criterion.

### Wind fluctuations

Wind fluctuations are parametrized following the parametrization scheme proposed by Hanna (1982) based on the boundary layer parameters with a modification applied by Ryall et al. (1997). Turbulence components are estimated taking into consideration the stability following criteria similar to Panofsky et al.(1977) and Hicks (1985). Constant vertical diffusivity is used as described by Legras et al. (2003) in the stratosphere ( $D_z = 0.1m^2s^{-1}$ ) while a horizontal diffusivity is used in the free troposphere ( $D_h = 50m^2s^{-1}$ ). Distinction between troposphere and stratosphere are based on a threshold of 2 *pvu* and diffusivities are converted into velocity scales using  $\sigma_{vi} = \sqrt{\frac{D_i}{dt}}$ . Being  $u$ ,  $v$  and  $w$  the along-wind, cross-and vertical components of turbulent velocity the equations for computing the turbulence terms as indicated by Stohl et al. (2005) for each stability case are:

#### Neutral conditions

$$\frac{\sigma_u}{u_*} = 2.0 \exp(-3f \frac{z}{u_*}) \quad (A.10)$$

$$\frac{\sigma_v}{u_*} = \frac{\sigma_w}{u_*} = 1.3 \exp(-2f \frac{z}{u_*}) \quad (A.11)$$

$$\tau_{L_u} = \tau_{L_v} = \tau_{L_w} = \frac{0.5 \frac{z}{\sigma_w}}{1 + 15f \frac{z}{u_*}} \quad (A.12)$$

#### Stable conditions

$$\frac{\sigma_u}{u_*} = 2.0 \left(1 - \frac{z}{h}\right) \quad (A.13)$$

$$\frac{\sigma_v}{u_*} = \frac{\sigma_w}{u_*} = 1.3 \left(1 - \frac{z}{h}\right) \quad (A.14)$$

$$\tau_{L_{u,v,w}} = 0.15 \frac{h}{\sigma_{u,v,w}} \left(\frac{z}{g}\right)^{0.5} \quad (A.15)$$

### Unstable conditions

$$\frac{\sigma_u}{u_*} = \frac{\sigma_v}{u_*} = \left(12 + \frac{h}{2|L|}\right)^{1/3} \quad (\text{A.16})$$

$$\tau_{L_u} = \tau_{L_v} = 0.15 \frac{h}{\sigma_u} \quad (\text{A.17})$$

$$\frac{\sigma_u}{w_*} = \left[1.2 \left(1 - 0.9 \frac{z}{h}\right) \left(\frac{z}{h}\right)^{2/3} + \left(1.8 - 1.4 \frac{z}{h}\right) u_*^2\right]^{1/2} \quad (\text{A.18})$$

$$\tau_{L_w} = \begin{cases} 0.1 \frac{z}{\sigma_w [0.55 - 0.38(z-z_0)/L]} & \text{if } z/h < 0.1 \text{ and } z - z_0 > -L \\ 0.59 \frac{z}{\sigma_w} & \text{if } z/h < 0.1 \text{ and } z - z_0 < -L \\ 0.15 \frac{h}{\sigma_w} \left[1 - \exp\left(\frac{-5z}{h}\right)\right] & \text{if } z/h > 0.1 \end{cases} \quad (\text{A.19})$$

### Particle transport and diffusion

FLEXPART uses the 'zero acceleration scheme' (B.20) with first order accuracy implementing also a one iteration of the Peterson scheme (1940) for the grid-scale winds as a correction term to the position computed through the 'zero acceleration' under certain conditions (see FLEXPART technical notes for more details).

$$X(t + \Delta t) = X(t) + v(X, t)\Delta t \quad (\text{A.20})$$

A Markov process based on the Langevin equation (Thomson, 1987) was used to parametrize the turbulent motions for the wind components. For long time steps the Langevin equation is considered as in Legg and Raupach (1982) with an additional term for the decrease of air intensity with height from Stohl and Thomson (1999), leading to

$$dw = -w \frac{dt}{\tau_{L_w}} + \frac{\partial \sigma_w^2}{\partial z} dt + \frac{\sigma_w^2}{\rho} \frac{\partial \rho}{\partial z} dt + \left(\frac{2}{\tau_{L_w}}\right)^{1/2} \sigma_w dW \quad (\text{A.21})$$

Otherwise, for short time steps the Langevin equation is considered in terms of  $\frac{w}{\sigma_w}$  following Wilson et al, (1983)

$$d\left(\frac{w}{\sigma_w}\right) = -\frac{w}{\sigma_w} \frac{dt}{\tau_{L_w}} + \frac{\partial \sigma_w}{\partial z} dt + \frac{\sigma_w}{\rho} \frac{\partial \rho}{\partial z} dt + \left(\frac{2}{\tau_{L_w}}\right)^{1/2} dW \quad (\text{A.22})$$

The difference between formulations described by B.21 and B.22 is the fulfillment of the well mixed criterion. Even when B.21 does not meet the criterion for strongly inhomogeneous turbulence the method has been shown to be more robust with increasing integration time step. Discretization of both formulations uses two methods in order to optimize the computational resources usage.

$$\left(\frac{w}{\sigma_w}\right)_{k+a} = \begin{cases} r_w \left(\frac{w}{\sigma_w}\right)_k + \Lambda \frac{\partial \sigma_w}{\partial z} \tau_{Lw} + \Lambda \frac{\sigma_w}{\rho} \frac{\partial \rho}{\partial z} \tau_{Lw} + [\Lambda(1+r_w)]^{1/2} \zeta & \text{if } \frac{\Delta t}{\tau_{Lw}} \geq 0.5 \\ \left(1 - \frac{\Delta t}{\tau_{Lw}}\right) \left(\frac{w}{\sigma_w}\right)_k + \frac{\partial \sigma_w}{\partial z} \Delta t + \frac{\sigma_w}{\rho} \frac{\partial \rho}{\partial z} \Delta t + \left(\frac{2\Delta t}{\tau_{Lw}}\right)^{1/2} \zeta & \text{if } \frac{\Delta t}{\tau_{Lw}} < 0.5 \end{cases} \quad (\text{A.23})$$

where  $\Lambda$  is  $(1 - r_w)$  for  $r_w = \exp(-\Delta t/\tau_{Lw})$ , the correlation for the vertical wind. A normally distributed random number with mean zero and unit standard deviation is represented by  $\zeta$  and  $\Delta t$  is the time step between  $k$  and  $k + 1$ .

### More useful information

FLEXPART model can run both forward or backward in time, for the first mode the particles are released from the source(s) and concentrations are determined downwind on a grid while for the latter mode the particles are released from a receptor location, being this mode more suitable for studying source-receptor relationships. A plume trajectories method based on Dorling et al. (1992) cluster analysis is also available in the model. Radioactive decay as well as wet and dry deposition are also considered explicitly in the model.

The model strictly linearity allows the segmentation of a problem into several runs and later combination of the results which optimizes the run-time performance instead of the usage of a parallel code. The design of the code in calculation routines and subroutines containing the parametrizations and control files with the configuration facilitates the use of the model and offers the possibility of modifying single parametrizations if needed. Output is gridded and files are written as compressed binary files in order to optimize the use of space and avoid extremely large output files. The model provides a particle dump option useful for long range runs, in case of FLEXPART terminates the run can be continued with the information of the last run provided by the files header and partposit\_end.





**B**

Monthly march of (E-P)-6

integrates

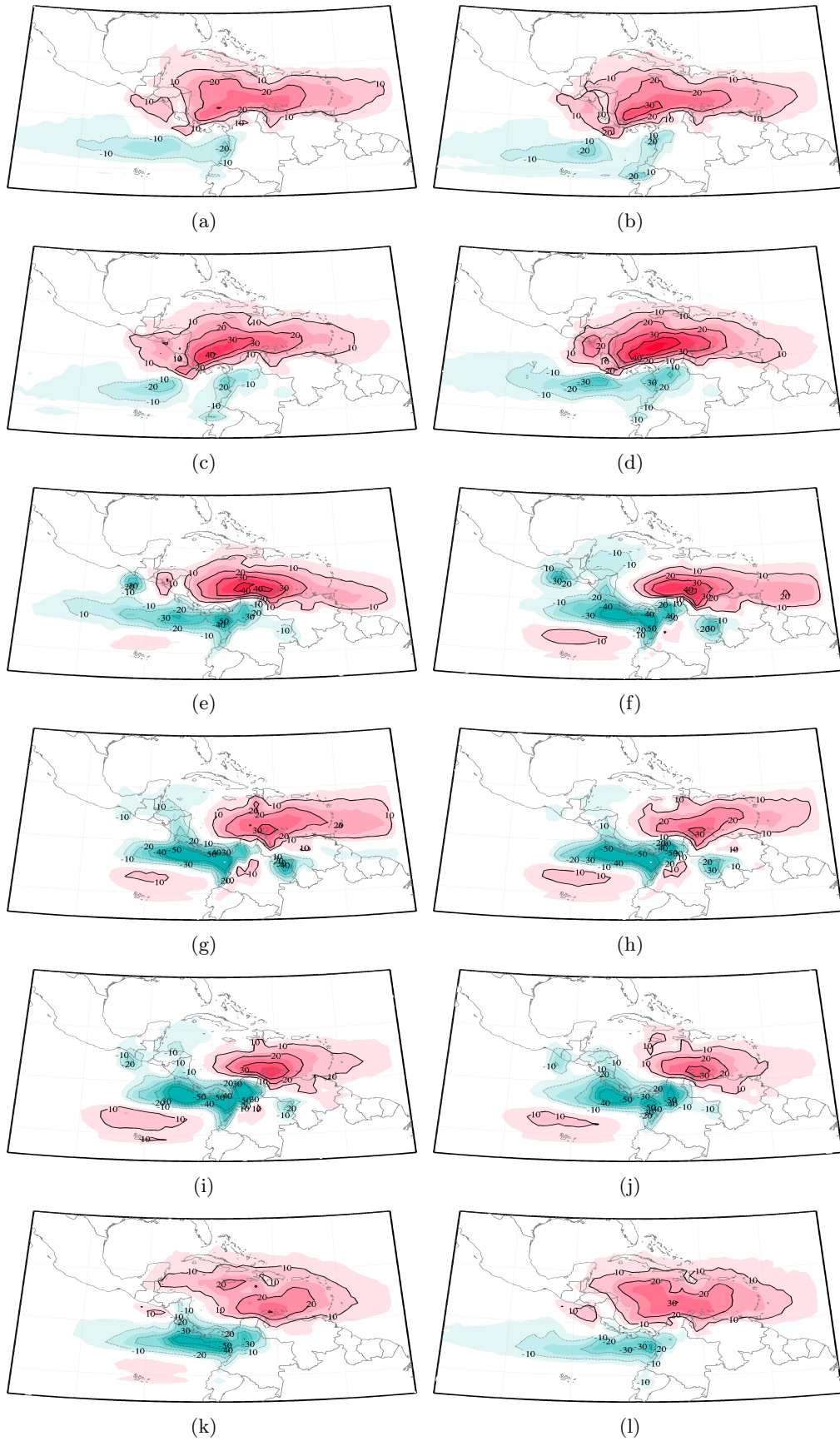


Figure B.1: Mean climatological air streams for the trajectories losing moisture over different locations of Central America.



## Sources of moisture for the NAMS

A monsoon-like anticyclone development near the south of Mexico (at 200hPa) starts at the end of the spring and migrates northward during summer (Ropelewsky et al., 2004). This structure is associated with the intense precipitation observed over north-western Mexico (NWM) and south-western United States of America (SWUS). The seasonal feature, known as the North American Monsoon (NAM) accounts for approximately 40% of the summer local rainfall and even up to 70% in some regions of Mexico (Douglas et al., 1996). The NAM system has an oceanic component (Gulf of California, eastern Pacific Ocean and the Gulf of Mexico) and an overland counterpart (Sierra Madre Mountain Range). Several works have been performed on the dynamics of the NAM, which is under study since a century ago approximately. Several attempts to identify the sources of moisture for the NAM system have been done. Most of those works are based on traditional Eulerian approximations or WVTs (Water Vapour Tracer) (Bosilovich and Schubert, 2001) . Local continental evaporation and transport from adjacent oceanic regions are highlighted as dominant sources of moisture (Castro et al., 2001). Dominguez et al. (2008) show evidence on the importance of local recycling for the supply of moisture to the monsoon. Previous studies (e.g Higgins et al., 1997) suggest that the source of moisture to the NAMS is located eastward, highlighting the Gulf of Mexico as an important source. Recently, Knippertz & Wernli (2010)

indicate the link between the NAMS and the inflow of air masses from the Gulf of Mexico. Furthermore, the regions affected by the NAM are very sensitive to the forcing of different inter-annual signals. There is an increasing interest in understanding the variability of the monsoon precipitation from seasonal to inter-annual scales (see e.g. Liang et al., 2008). This information is valuable not only as a scientific achievement but also for monitoring and forecasting. El Niño-Southern Oscillation (ENSO), the North Atlantic Oscillation (NAO), the Madden-Julian Oscillation (MJO) and the Pacific Decadal Oscillation (PDO) are known to exert an influence over the NAMS and for instance are herein considered. Herein, we provide a study of the summer transport of moist air masses based on backward Lagrangian trajectories. Sources of moisture for a defined NAM core influence region are identified. The evolution of the sources of moisture from the onset to the end of the monsoon is studied. The response of the contribution from the sources of moisture to precipitation over the monsoon core is evaluated for leading signals. The main variations are discussed considering previous results on the analysis of the NAM and key features of the regional circulation.

## C.1 Moisture sources analysed from backward trajectories

A region of moisture flux divergence in the vicinity of the Gulf of Mexico and eastern North Mexico is a signature of the field for southern North America and over the Gulf of California, in contrast with the convergence observed in western Mexico (fig C.1). The moisture flux vector indicates transport of moisture from the IAS (shown by red arrows). From this average fields is not easy to determine with accuracy which region provides most of the moisture for the NAMS. Using the methodology described in chapter 4, an evaluation of the main sources of moisture for the NAM core was performed. Results for summer, when the NAM is active, are provided in figure C.2. Potential sources of moisture were found to present a maximum intensity during the first six backward days. Climatological monthly mean values of the six days integrated net freshwater flux  $(E - P)^{-6}$  from May through September are contoured in figure C.1. Only positive values are shown to highlight the representative evaporative sources of moisture. For NWM a strong excess of evaporation over precipitation is noted to start in May with a higher intensity in the western coast (GoC) . As the time passes by, the presence of a second source over north-eastern Mexico (NEM) merges. During July, when the

monsoon reaches its highest intensity, the source of the Gulf of California and the Baja Peninsula (GoC) has decreased considerably. Meanwhile, the source over NEM has increased three times its intensity for the previous month. In addition, the influence of a third source becomes noticeable over the Caribbean Sea region (Caribbean) and the Gulf of Mexico (GoC).

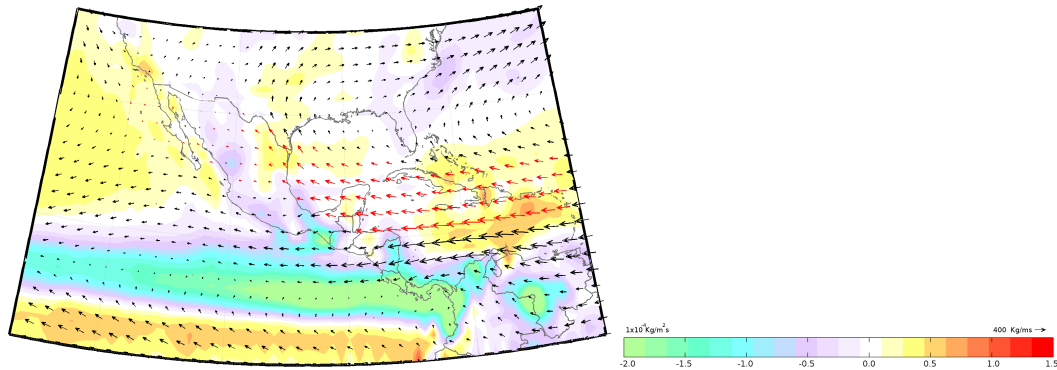


Figure C.1: Long term mean of vertically integrated moisture flux divergence (shaded contours) and vertically integrated moisture flux (vector)

The intensification of the availability of moisture presents the same temporal structure of the precipitation in the monsoon core region (figure C.4). Magnitude of the potential sources of moisture starts to decrease as the end of Summer approaches. While the monsoon season reaches the end, the intensity of the GoC and NEM has decreased. Moreover, the light source in the Caribbean is vanished. The results suggests that the moisture available during the initial stages of the development of the monsoon comes primarily from the GoC. As the monsoon becomes a mature structure, the role of continental sources of moisture strengthens. The role of a remote source of moisture, represented by the Caribbean, is also important during July. The pattern described by this latter source, follows the path of the northward branch developed by low level winds during the maximum intensity of the Caribbean Low level Jet (CLLJ). This result provides additional evidence on the direct role of the CLLJ transporting moisture from the Caribbean Sea to the NAM system. The strong intensification of the NEM source during the active phase of the NAM suggests the intensification of local evaporation and further interaction with the NAM system. Notice that the NEM region is also influenced by an increase in precipitation due to the monsoon (even when the monsoon

core is located westward). Therefore, local evaporation over the NEM becomes very active during the monsoon, which implies an increase of the local recycling of moisture. This result has been analysed by Dominguez et al. (2006) on the importance of continental recycling of moisture during the monsoon. Notice also that the intensification of evaporation over precipitation for NEM during summer is a feature of the presence of the MSD (Magaña et al., 1999). It is important to notice that the role of the GoM is not completely direct, since moisture from this source can reach the NAM core in two ways: a) from direct winds and b) by providing moisture to NEM which is then transported from the NEM.

Estimates of the contributions to precipitation from each source were computed as for the case of Central America (chapter 5) with the result of an important increase of the contributions between May and August. This in agreement with the intensification of precipitation during the monsoon. The annual cycle has been widely explored, and here we are more interested in the variations of the intensity of the monsoon that may be associated with the variability of the transport of moisture. Composites of the contributions were computed in a monthly basis for the positive and negative phases of ENSO, NAO, PDO and MJO (using the table from chapter 4) as well as for the neutral conditions. An 'artificial' annual cycle for each phase was created in order to evaluate the variations that may occur between the active period of the NAM and the rest of the months. Anomalies of the contributions were computed extracting the neutral annual cycle from each phase and signal. Figure C.3 shows the annual cycle of anomalies from which it can be noticed that the larger variations are still observed when the NAM is active. An interesting observation is that it seems that the PDO can be related with the variation of the development of the monsoon, as the peak of contributions to precipitation is shifted to the right for positive PDO.

To study with more detail the contributions to precipitation during summer, the comparison between the composites for positive and negative phases of each signal are presented for June-September in figure C.4. Notice that here we only account for 'direct' contributions, this is, moisture that has been transported directly towards the NAM core and not by any intermediate process, so the contributions from the GoM only consider when moisture has been directly transferred to the NAM core and

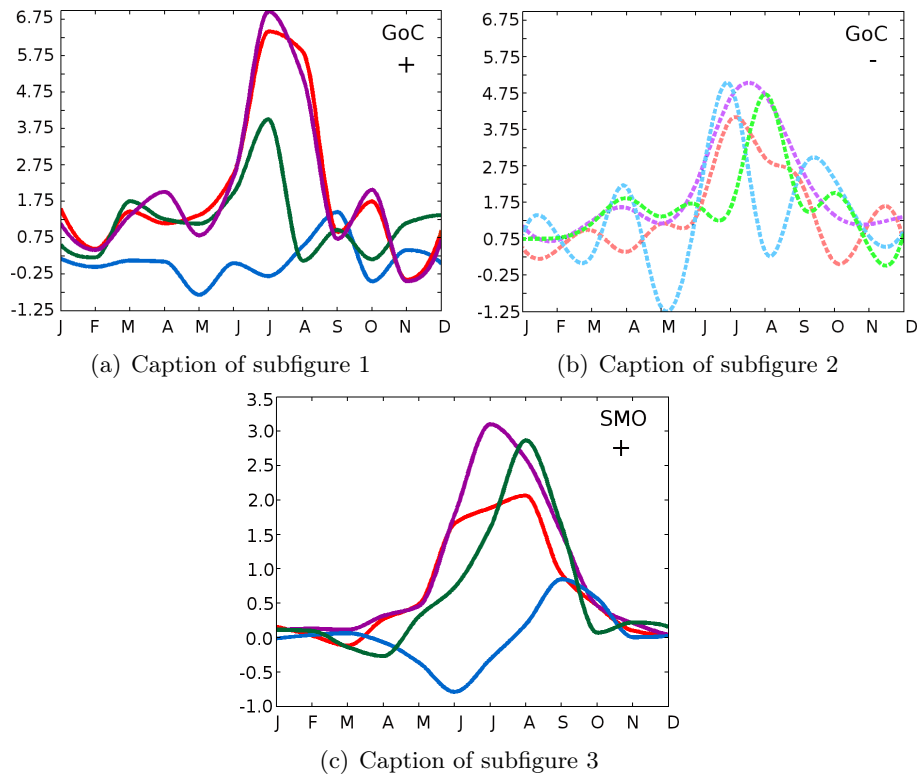


Figure C.2: Caption of subfigures (a), (b) and (c)

contributions from the NEM contain, therefore, an important signature of the moisture from the GoM.

An immediate result is that the GoC and the region of NEM (plus SWUS) are the main sources of the moisture for the NAM. As a result of local circulation, the GoM, the nearest portion of the ETPac and the Caribbean Sea also contribute as sources of moisture. However their role is not strictly direct since due to the transport scales. Their importance is more related to transporting moisture to the main source regions. The ETPac contributes strongly advecting moisture to the GoC and the GoM to eastern Mexico. The Caribbean Sea advects moisture mainly to the GoM and in minor quantities directly to the NAMS core.

Most of the changes in the direction from which low level air masses come to the NAM core region are triggered by changes in the circulation patterns. Mainly variations in the wind field mostly enhanced by changes in the pressure gradient signature. The

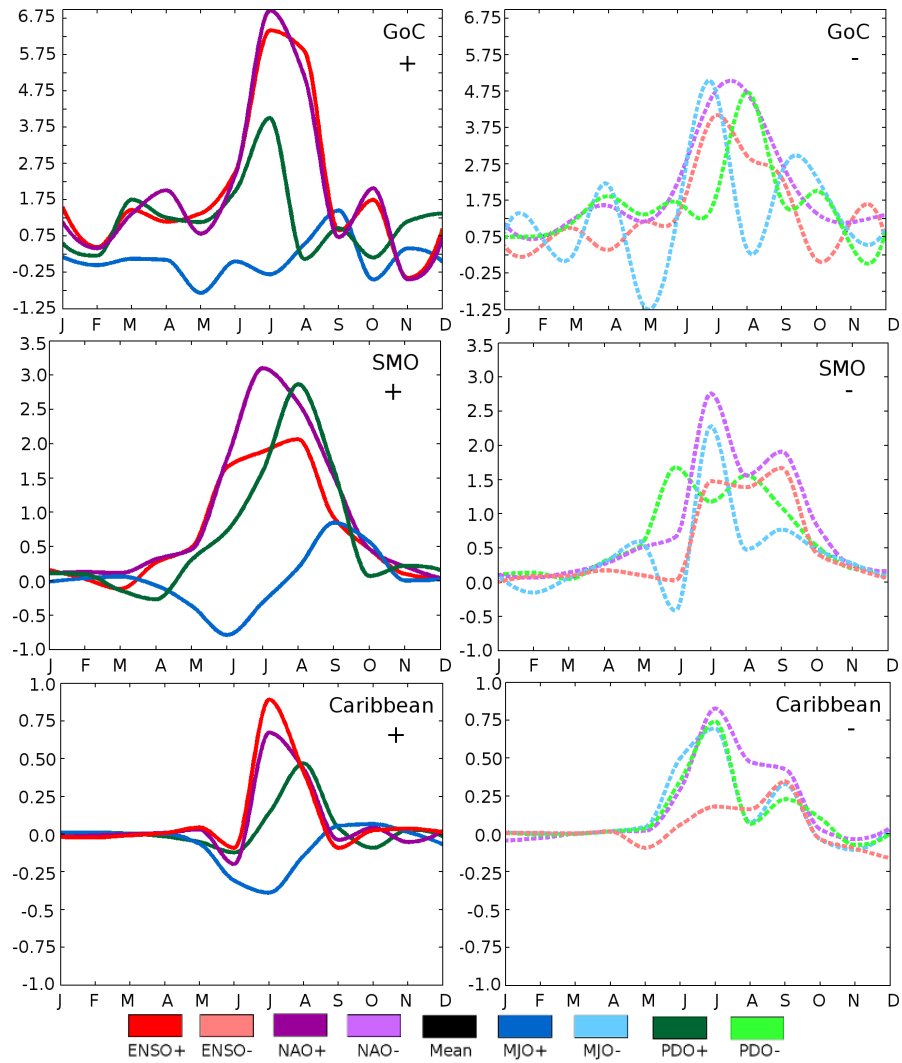


Figure C.3: Mean contributions from each source of moisture (in mm/day) for the composites computed, black presents the mean of the neutral composites.



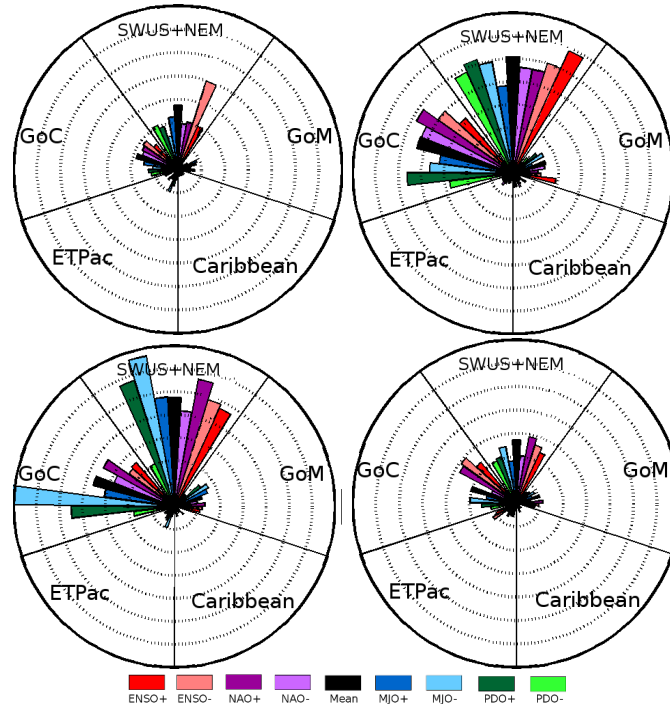


Figure C.4: Mean contributions from each source of moisture (in mm/day) for the composites computed, black presents the mean of the neutral composites.

approximate origin of moisture is explored. The latter provides an overview of the conditions of low level transport, since air masses can be dry or wet, these results may be analysed with caution (more air does not necessarily imply more moisture). Notice that the intrusion of dry air masses affects importantly the transport of moisture and the development of deep convection which is essential for the development and maintenance of the monsoon. In average, air flow coming from all sources during May is relatively dry. By June, moisture content of air flow from the Caribbean increases when travelling over the GoM while air from the GoM experiences an increase of moist content over eastern Mexico. During the monsoon peak, air from the west coast of southern Mexico and the GoC is extremely moist. In the same period (July) air is relatively dry over the outer Caribbean, for this airflow moisture content increases over the western Caribbean and the southern edge of the GoM. Correspondent air stream reaches a peak of moisture over the NEM region and then losses moisture over the NAM core. Conversely for July, air from the SWUS is dry whereas air from northern Mexico is enriched in moist content.

For August the situation is similar to July, with the difference that during this month the influence from the Caribbean has decreased and air flow from the GoM is dry until it enters the continental region. In September air masses are dry in general, except for the air from the west coast of Mexico. Mean relative contributions from the identified sources to precipitation falling over NAM core region were computed in a monthly basis. Composites were computed as already described for positive and negative phases of ENSO, NAO, MJO and PDO. Anomalies reveal important variations under warm ENSO for the GoM and all positive phases for the Caribbean. Negative phases of NAO affect contributions from all sources while negative of PDO does for SUWS-NEM. Negative MJO triggers variations mainly for the contributions from the SWUS-NEM, GoC and Caribbean. A wide variety of studies have been performed regarding the forcing of the NAMS by ENSO (see e.g. Yu and Wallace, 2001; Gutzler, 2002; Brito-Castillo et al., 2002 among others). Composites of monthly relative contributions to precipitation are shown in figure 2 (lower panel, contributions every 2 mm/day from 0 in the origin to 14 in the outer circle) in comparison with the patterns of the percentage of 'air particles' from each source region.

In the case of ENSO, for June, the increase of flow from the SWUS-NEM during the cold phase is followed by a large intensification of the contributions from this region to precipitation over the NAM core. During the peak of the NAM influence of the cold phase is small in comparison to the mean climatology (black) but larger contributions are found during cold (warm) ENSO from the GoC (SWUS-NEM and GoM). During August this pattern is reversed and contributions from the GoM are very small. Contributions decrease in September with larger values for cold ENSO for both main sources. The increase of contributions from the GoC region for cold ENSO (La Niña) is related with wetter conditions associated with the dislocation of the eastern Pacific ITCZ to the north (see Cavazos & Hastenrath, 1990). The results suggest that the total of contributions to precipitation increases during warm ENSO in good agreement with the increase of precipitation during July. Notice a reduced contribution from the GoC and increased contributions from SWUS-NEM and GoM during warm ENSO. The differences between ENSO phases may be associated with the fact that warm (cold) ENSO is characterised by a reduction (increase) of easterly wave activity. Tropical cyclones increase during warm ENSO, which implies an increase of moisture from the GoM, NEM and a little

the CS. On the other hand, surges intensify during cold ENSO, enhancing the increase of contribution of moisture from the GoC. The results are in good agreement with the study of Brito-Castillo et al. (2003) which found wet (dry) monsoons association with ENSO warm (cold) phases. A generalised decrease of contributions from the main sources of moisture occurs during the negative phase of the NAO. Contributions from the GoC increase during positive NAO for July while for August the increase is noticed for the contributions from the GoC and SWUS-NEM region. Positive NAO is known to be related with stronger westerlies favouring the transport of moisture from the GoC into the NAM.

Variations of the contributions triggered by the phases of the MJO are also marked. Higgings & Shi (2001) point out that the importance of the MJO to the NAM is related with the meridional adjustments in precipitation patterns in the ETPac. Their results suggest a strong relation between the MJO and precipitation over western Mexico. For notation, positive (negative) MJO represents the suppression (enhancement) of convection. Then a positive (negative) MJO is associated with an easterly (westerly) phase. Differences are stronger during August rather than July, since for the latter the value of composites for both phases does not exceed the climatological mean values. During August, a strong intensification of the contributions from the main sources is associated with negative MJO. The increment of the contributions to precipitation over the NAM core from the SWUS-NEM and particularly larger from the GoC is in agreement with the observed intensification of precipitation over the NAM during the westerly phase of the MJO. Lorenz & Hartmann (2006) suggest that this intensification of precipitation is triggered by the intensification of easterly waves and the subsequent effect on the ETPac cyclone activity. Both are known to account for the enhancement of gulf surges. Then, if transport of moisture from the GoC is correlated with the surges, negative MJO must be associated with an increase of the contributions to precipitation from this source. The result shown by light blue for July and August confirms this relation, notice also the increase in the contributions from the GoM for negative MJO. Increase from the SWUS-NEM region during August during negative MJO is also related with the enhancement of Mesoscale convective systems (MCSs) in the NAM as pointed by Lorenz & Hartmann (2006).

Brito-Castillo et al. (2003) indicate that the PDO is a modulator of precipitation in western Mexico so that PDO is a good indicator of low frequency variability of the NAM core. The patterns for the phases of the PDO presents a reversed relationship for the NAM peak between the percentage of 'air particles' arriving to the NAM core and the contribution to precipitation. The first implication of this result is that even when there are more air masses being transported to the NAM core region, their moisture content is quite small during negative PDO (suggesting the circulation of dry air). Positive PDO seems to be influenced by a marked increase of the contributions from the GoC during July and even larger for August. Meanwhile, the contributions from the SWUS-NEM region for this phase are just slightly larger for July compared to the negative PDO and much more intense during August. The latter suggest positive (negative) PDO to be linked with wetter (drier) monsoon conditions. For positive PDO, the increase of contributions to precipitation from the SWUS-NEM source region is mainly due to the intensification of the contributions from NEM which are associated with the enhancement of convection over the Sierra Madre Oriental produced by the moist air inflow from the GoM (notice that also direct contributions from the GoM increase for positive PDO). This excess of moisture availability is confirmed by the results of Englehart and Douglas (2001) which show an increase of rainfall over north western Mexico associated with tropical cyclones during positive PDO. Similar, increase of the contributions from the GoC are related also with stronger tropical cyclone activity and more with the warm SST that characterised the ETPac region during positive PDO that influences the intensification of surges in the GoC.

The Lagrangian approach applied results to be very useful for the representation of the variability of the NAM in terms of the contributions to precipitation from the main sources of moisture. The good agreement between the results derived from the Lagrangian estimates and the various studies performed on the variability of the NAM is very encouraging on the application of these methods since the results of the variability of the NAM are supported by a large amount of studies not only based on mean fields and numerical modelling but also on a relative good long term network observations. The next objective regarding Lagrangian based analysis and the NAM is to study the relationship between the transport of moisture form the Caribbean Sea in order to study how does the CLLJ is coupled during the NAM due to the development of its

northward branch. Moreover, it is also important to analyse the transport of moisture from the Caribbean to the Gulf of Mexico and to the Great Plains, in order to study the importance of the CLLJ for the extra-tropics.

